**UNIVERSITAT POLITÈCNICA DE CATALUNYA**
**DEPARTAMENT D'ENGINYERIA DEL TERRENY I CARTOGRÀFICA**
**ESCOLA TÈCNICA SUPERIOR D'ENGINYERS**
**DE**
**CAMINS, CANALS I PORTS**

# *Thermo Hydraulic Behaviour Of Unsaturated Salt Aggregates*

**TESIS DOCTORAL**

PRESENTADA POR:

**SALVATORE CASTAGNA**

DIRIGIDA POR:

**EDUARDO ALONSO PERÉZ DE AGREDA**
**ANTONIO LLORET MORANCHO**
**SEBASTIÀ OLIVELLA PASTALLÉ**

BARCELONA MARZO 2007

*A tutti quelli che mi hanno sempre appoggiato*

# Table of contents

# ABSTRACT

The nuclear energy, which was developed in the last century, is used both in the military and in the civil one. One of the most important application of this type of energy is for the production of electricity for civil use.

The nuclear fuel is long-lasting: a few bars of uranium can produce electrical energy up to a decade. One of the fields of study of nuclear energy is the management of the radioactive waste. This problem emerged and started to be studied in the second half of the last century. This is a very complex aspect of the use of nuclear energy because, although the combustible lasts a decade, its decay takes centuries.

This thesis is a small contribute to this new branch of nuclear science. It studies some aspects of the Geotechnical behaviour of salt aggregates, which can be used as filling material in the final repository of the high level radioactive nuclear waste.

The fundamental rule for a nuclear waste repository is that it must work without human or mechanical help and that the same nature has to protect man against the risk of radiation for centuries. Nowadays, the most widely accepted solution in the world is the disposal in deep repositories in rock formations, often old mines and, including salt mines. It is likely that by the end of the next decade a large number of these repositories will come into operation in the countries where research in this field is more advanced.

In Europe we are making a common effort, under the supervision of the European Union, to study the deep repositories for nuclear waste. Thanks to common research projects granted by the European Union, it is possible to investigate both the behaviour and the development of the high level radioactive waste repositories in all the involved aspects. This facilitates the diffusion of the results of these studies among all the members of the European Union.

This thesis deals with the thermo-hydraulic behaviour of salt aggregates due to the high temperatures produced by the nuclear waste decay. This phenomenon creates effects in the filling materials and in the rock formation around the deposit.

Basically, the thesis has an experimental development. Two main tests were developed in the laboratory: The first one studied the retention curve of compacted salt aggregates. For this one, it was necessary to use the axis translation technique and a special suction plate for salt materials had to be built in order to develop these tests.

This first test allowed to determine the behaviour of a basic property of unsaturated salt materials. And the application of these results was essential for the development of the successive parts of this thesis.

The object of the second laboratory test was to observe and study the porosity variation phenomena in the extremities of the sample due to the presence of a difference of temperature.

This test has a fundamental importance for the deep repositories because radioactive waste is a source of heat lasting centuries and the presence of high temperatures in the canisters leads to flux and transport phenomena in the contact between the waste canister and the filling material. When the filling material is salt aggregates, there is another phenomenon involved: the interchange of salt between the solid and the liquid phase (precipitation/dissolution phenomena).

In order to develop these laboratory tests, an important phase of the research was dedicated to the development and testing of the laboratory equipment, which were unconventional and completely new.

This last laboratory test, in its second phase, was validated through a numeric model (CODE-BRIGHT). The results of the numeric model confirmed the behaviour determined in the experimental phase and the importance of the matrix suction in this phenomena.

Barcelona, March 2007

# RESUMEN

En el siglo pasado se ha desarrollado una nueva energía: la nuclear. Su aplicación comprende tanto el campo militar como el campo civil. Unos de los aspectos más interesantes es el uso de esta energía para la producción de electricidad de uso civil.

El combustible nuclear es de larga duración: unas barras de uranio pueden llegar a producir energía eléctrica durante aproximadamente una década. Sin embargo, a mediados del siglo pasado se planteó el problema de los residuos nucleares. Este problema es muy complejo por que, aunque la duración del combustible sea de una década, el periodo de decaimiento es del orden de siglos.

Esta tesis quiere aportar su granito de arena a esta nueva rama de la ciencia nuclear, estudiando algunos aspectos del comportamiento geotécnico de los agregados de sal, para su uso como material de relleno en los depósitos definitivos de los residuos nucleares de mayor peligrosidad.

La regla fundamental de diseño de dichos depósitos es que su función debe desarrollarse sin la ayuda del hombre o de máquinas y que la misma naturaleza tiene que ser quien proteja al hombre del riesgo de radiaciones durante el transcurso de los siglos.

Parece que al día de hoy la solución mundialmente aceptada es la de un depósito profundo en formaciones rocosas, a veces utilizando antiguas minas, incluso de sal. Se prevé que entre esta década y la próxima entrarán en funcionamiento varios de estos depósitos en los países en que la investigación en este área está más avanzada.

En Europa se está haciendo un esfuerzo común, bajo supervisión de la Unión Europea y por medio de proyectos de investigación, para estudiar el funcionamiento del almacenamiento y la difusión de los resultados de esos estudios entre los miembros de la Unión Europea, a fin de dar el mayor provecho a las diferentes investigaciones que en la actualidad se están desarrollando en todos los centros de investigación de Europa.

Esta tesis trata sobre el comportamiento termo hidráulico de los agregados de sal debido a las altas temperaturas que el decaimiento de los residuos nucleares produce. Este fenómeno crea unos efectos en los materiales de relleno y en la formación de base de alrededor del deposito.

La tesis tiene un desarrollo básicamente experimental. En laboratorio se realizaron fundamentalmente dos ensayos; el primero permitió determinar la curva de retención de los agregados de sal altamente compactados. Para ello se utilizó la técnica de traslación de ejes para aplicar la succión matricial y se construyó una placa de succión apta a los materiales salinos para la realización de estos ensayos.

Este ensayo permitió determinar el comportamiento de una propiedad básica de los materiales salinos no saturados, sus resultados pudieron aplicarse al resto de los trabajos que se realizaron con posterioridad en esta tesis.

El objeto del segundo ensayo de laboratorio fue reproducir los fenómenos de variación de porosidad debidos a la presencia de una diferencia de temperatura en las extremidades de la muestra.

Dicho ensayo tiene una importancia fundamental para los almacenamientos profundos, porque los residuos radiactivos serán una fuente de calor durante varios siglos y la presencia de elevadas temperaturas induce fenómenos de flujo y transporte en el contacto con los contenedores de carburante nuclear agotado. Además, en el caso de los agregados de sal, a estos fenómenos cabe añadir el intercambio de sal entre la fase sólida y la líquida (precipitación /disolución).

Para desarrollar estas pruebas laboratorio se dedicó una parte importante de la investigación al desarrollo y comprobación del equipo de ensayo, siendo éste poco convencional y completamente novedoso.

Este último ensayo, en su segunda fase, fue convalidado mediante un modelo numérico (CODE-BRIGHT). Los resultados del modelo numérico han permitido confirmar todo cuanto se determinó en la fase experimental y la importancia de la succión matricial en estos fenómenos.

Barcelona Marzo 2007

# RIASSUNTO


Nel secolo scorso si è sviluppato un nuovo tipo di energia: quella nucleare. La sua applicazione comprende sia l'ambito militare che quello civile. Uno degli aspetti più interessanti è l'uso di tale energia per la produzione di elettricità per uso civile.

Il combustibile nucleare ha lunga durata: alcune barre d'uranio possono arrivare a produrre energia elettrica per circa un decennio. Senza dubbio, alla metà del secolo scorso si è posto con insistenza il problema dei residui nucleari. Questo problema è molto complesso perché, sebbene la durata del combustibile sia di un decennio, il periodo di smaltimento è nell'ordine di secoli.

Questa tesi intende aggiungere un piccolo contributo a questo nuovo ramo della scienza nucleare, studiando alcuni aspetti del comportamento geotecnico degli aggregati del sale, per un eventuale uso dello stesso come materiale di riempimento dei depositi definitivi dei residui nucleari di maggiore pericolosità.

La principale regola per la progettazione di tali depositi è che il loro funzionamento debba avvenire senza l'aiuto dell'uomo o di macchine e che la stessa natura debba proteggere l'uomo dal rischio di radiazioni nel trascorrere dei secoli.

Ad oggi, la soluzione più accettata a livello mondiale è quella di depositi profondi nelle formazioni rocciose, a volte vengono utilizzate antiche miniere, incluse quelle di sale. Si prevede che tra questo decennio e il prossimo entreranno in funzione diversi depositi di questo tipo nei paesi in cui la ricerca in questo campo è più avanzata.

In Europa si sta facendo uno sforzo comune, grazie anche a progetti di ricerca sotto la supervisione dell'Unione Europea, per studiare il funzionamento di immagazzinamento e per diffondere i risultati di questi studi tra i paesi membri, in modo da dare maggiore circolazione alle differenti ricerche che attualmente sono in fase di svolgimento in molti centri di ricerca.

Questa tesi tratta del comportamento termo-idraulico degli aggregati del sale susseguente alle alte temperature prodotte dallo smaltimento dei residui nucleari. Questo fenomeno crea alcuni effetti nei materiali di riempimento e nella formazione di base intorno al deposito.

La tesi ha uno sviluppo fondamentalmente sperimentale. In laboratorio sono stati realizzati principalmente due esperimenti. Il primo ha permesso di determinare la curva di ritenzione degli aggregati di sale altamente compattati. Per questo è stata utilizzata la tecnica di traslazione di assi per applicare la suzione matriciale e, per la realizzazione di tali esperimenti, è stata appositamente costruita una placca di suzione adatta ai materiali salini.

Questa prova di laboratorio ha permesso di determinare il comportamento di una proprietà basica dei materiali salini non saturi, così che è stato possibile applicare i suoi risultati al resto dei lavori che sono stati realizzati in seguito in questa tesi.

Lo scopo della seconda prova di laboratorio è stato quello di riprodurre i fenomeni di variazione di porosità dovuti alla presenza di una differenza di temperatura alle estremità dei provini.

Tale esperimento ha un'importanza fondamentale per i depositi profondi, perché i residui radioattivi costituiranno una fonte di calore nel corso dei secoli e la presenza di temperature elevate induce fenomeni di flusso e di trasporto nel contatto con i contenitori di carburante nucleare, già utilizzato. Inoltre, nel caso degli aggregati di sale, a questi fenomeni bisogna aggiungere l'interscambio di sale tra la fase solida e quella liquida (precipitazione/dissoluzione).

Per svolgere queste prove di laboratorio è stata dedicata una fase importante della ricerca allo sviluppo e alla verifica degli apparecchi usati per gli esperimenti, essendo questi poco convenzionali e completamente innovativi.

L'ultima prova di laboratorio, nella sua seconda fase, è stata convalidata attraverso un modello numerico (CODE BRIGHT). I risultati di tale modello numerico hanno permesso di confermare tutto ciò che era stato determinato nella fase sperimentale e l'importanza della suzione matriciale in questi fenomeni.

Barcelona, Marzo 2007

# ACKNOWLEDGEMENTS

There are no doubts that this page of the thesis is the most difficult to write. First of all, I would like to thank everybody and I apologise if I forget somebody. These years in Catalunya have been, and I hope will go on being, unforgettable for the richness both of the scientific and the personal experience, especially for the extraordinary personality of the people I had the honour to meet in the Department of Geotechnical Engineering and Geosciences of the Technical School of Civil Engineering (ETSECCP) of the Technical University of Catalonia (UPC)

In the first place, I would like to express my gratitude to the tutors of my thesis, Eduardo Alonso, Antonio Lloret and Sebastià Olivella, who have guided me along the work and whose advice was essential to accomplish this thesis. The scientific help and human support I received from each of them was, even if different, undoubtedly of equal importance.

Eduardo was like a light guiding me along all the thesis, he helped me to make the most important decisions, leading my research when necessary and encouraging me at difficult times; included when I had to work out of the department and it seemed impossible that this thesis could be completed. In fact, when the research was already finished, I had to work out of the department and at the same time I had to proceed to the writing of the thesis.

Sebas's contribution is one I can never forget about. The basis of this thesis is the continuation of one aspect of his. He always backed me, urged me to go on at critical moments and placed all his experience in this field at my disposition. Moreover, I have to thank him, together with Antonio Gens, for taking me with them many times to present this work at other institutions.

Finally, Toni, the last for alphabetical reasons, was my first contact in the department. He was the one who initiated me into the experimental technique with his steady help and who guided me all along the experimental part of my thesis.

I like to remember all of you as very good friends.

I will never forget all the other professors of the in the Department of Geotechnical Engineering and Geosciences of UPC, my thanks go to all the members of this large scientific family, where work gets easier because there's always some one who is ready to help you and support you.

In the second place, I would like to thank all the members of department staff who helped me: Eva, Fernando, José, Mar, who helped me in the final correction of the text of this thesis and that was really important, Mari Carmen and Tomás. Each one of them in their own field was a precious allied making my work easier. Thank you.

I would also like to remember my laboratory and doctorate fellows: Augusto, Betty, Carlos, Clemente, Cristian, Ekaitz, Josep Ramón and his brother Xavi, Jean, Joan, Jordi, Josep Maria, Juan Jorge, Leonardo, Luciano Costa, Mauricio, Roberto, Sandra and Xavi Pintado.

I can't forget about my family. Their backing was fundamental, for they were the ones who incited me to come to Catalunya, to start the doctorate and much more. Special thanks to my parents and my sisters who are always there for me, and especially to my sister Valentina who was always the first to read the chapters of this thesis trying to improve my English.

Last but not least, my dear friends Alessandra with her family, Agustín, Enrique, Juliana, Marcelo with his family, Cristina and Luciano, his wife and his children, whose cheerfulness always made it a pleasure to spend my time with them, making me feel at home.

***Many Thanks to all of you!!!***

# AGRADECIMIENTOS

Esta página de la tesis es seguramente la más difícil de redactar y antes de nada quiero dar las gracias a todo el mundo y pedir disculpas si me olvido de alguien: estos años catalanes han sido, y espero que serán, memorables por la riqueza de las experiencias, no solamente científicas, sino también vitales y por la extraordinaria personalidad de las personas que he tenido el honor de conocer en el Departamento de Ingeniería del Terreno de la Universitat Politècnica de Catalunya.

En primer lugar doy las gracias a los directores de mi tesis Eduardo Alonso, Antonio Lloret y Sebastià Olivella que me han guiado a lo largo de este camino y cuyo consejo ha sido fundamental para que esta tesis llegara a su fin. La ayuda científica y el soporte humano que he recibido de cada uno ellos fue, tal vez, distinto aunque, sin duda, de igual importancia.

Eduardo ha sido como un faro que me guió en toda la tesis ayudándome a tomar las decisiones más importantes, enderezando la investigación cuando fue necesario y dándome animo en los momentos difíciles; incluido cuando, por la necesidad de trabajar fuera del departamento, parecía imposible definir esta tesis, aunque la parte de investigación estuviese ya acabada todavía faltaba la parte formal de la redacción final.

La aportación de Sebas es de las que no se pueden olvidar. La parte fundamental de esta tesis es la continuación de un aspecto de la suya. Él me apoyó en cada momento, me presionó en los momentos difíciles y puso a mi disposición toda su experiencia en este campo. Además, tengo que agradecerle, especialmente a él y a Antonio Gens, el haberme llevado con ellos en muchas ocasiones para presentar este trabajo en otras instituciones que trabajan en este campo.

Finalmente, Toni, último por razones alfabéticas, pero fue mi primer contacto en el departamento y fue él quien con su ayuda constante me inició en el Laboratorio de Geotecnia y me guió a lo largo de la fase experimental de la tesis.

Os quiero recordar a todos como unos muy buenos amigos.

Tampoco, me podré nunca olvidar, del resto de profesores del Departamento de Ingeniería del Terreno de la Universitat Politècnica de Catalunya, mi agradecimiento va para todos los componentes de esta gran familia científica que es el Departamento de Ingeniería del Terreno donde el trabajo se hace más llevadero porque siempre hay alguien dispuesto a ayudarte y apoyarte.

En segundo lugar quiero agradecer a todo el personal del departamento que con su labor me ha ayudado: Eva, Fernando, José, Mar, que ha sido preciosa en la fase de revisión del texto, Mari Carmen y Tomás. Cada uno en su campo fueron unos aliados preciosos para que mi labor fuera más sencilla. Gracias de corazón a todos vosotros. Quisiera también recordar a todos los compañeros del laboratorio y del doctorado: Augusto, Betty, Carlos, Clemente, Cristian, Ekaitz, Josep Ramón y su hermano Xavi, Jean, Joan, Jordi, Josep Maria, Juan Jorge, Leonardo, Luciano Costa, Mauricio, Roberto, Sandra y Xavi Pintado.

No me puedo olvidar de mi familia. Su aportación ha sido fundamental, pues han sido ellos quienes me empujaron a venir a Catalunya, a empezar el doctorado y a mucho más. Un recuerdo especial para mis padres y mis hermanas que siempre están allí en especial a mi hermana Valentina que siempre fue la primera en leer los capítulos de esta tesis para perfeccionar mi inglés.

Last but not the least, mis queridos amigos Alessandra y su familia, Agustín, Enrique y Juliana, Marcelo y su familia, Cristina, Luciano, su mujer y sus hijos, cuya alegría siempre hizo que fuera un placer estar con ellos.

***¡Muchas Gracias a todos vosotros de todo corazón!***

# RINGRAZIAMENTI

Questa pagina della tesi è certamente la più difficile da scrivere e prima di tutto voglio ringraziare tutti e scusarmi se mi dimentico di qualcuno. Questi anni catalani sono stati, e spero che saranno ancora, memorabili per la ricchezza di esperienze non soltanto scientifiche ma anche di vita e per la straordinaria personalità di coloro che ho avuto l'onore di conoscere nel Dipartimento di Ingegneria del Terreno dell'Università Politecnica della Catalunya.

In primo luogo, ringrazio i direttori supervisori della mia tesi, Eduardo Alonso, Antonio Lloret e Sebastià Olivella, che mi hanno guidato lungo questo cammino e il cui consiglio è stato fondamentale affinché questa tesi arrivasse alla conclusione. L'aiuto scientifico e il supporto umano ricevuto da ognuno di loro è stato, sebbene distinto, senza dubbio di uguale importanza.

Eduardo è stato come un faro che mi ha guidato in tutta la tesi aiutandomi a prendere le decisioni più importanti, indirizzando la ricerca quando è stato necessario e dandomi coraggio nei momenti difficili; incluso quando, dovendo lavorare fuori dal dipartimento, sembrava impossibile definire questa tesi. Infatti, sebbene la parte della ricerca fosse già terminata, mancava ancora la parte formale della stesura finale.

L'apporto di Sebas è di quelli che non si possono dimenticare. La parte fondamentale di questa tesi è la continuazione di un aspetto della sua. Inoltre, Sebas mi ha sempre appoggiato, mi ha spinto ad andare avanti nei momenti difficili e ha messo a mia disposizione tutta la sua esperienza in questo campo. Ancora desidero ringraziare sia lui che Antonio Gens per avermi portato con loro in diverse occasioni per presentare questo lavoro presso altre istituzioni che lavorano in questo campo.

Toni, ultimo in ordine alfabetico, che è stato però il mio primo contatto nel dipartimento e colui che con il suo aiuto costante mi ha iniziato al Laboratorio di Geotecnica e mi ha guidato lungo la fase sperimentale della tesi.

Vi voglio ricordare tutti come dei buoni amici.

Né, potrò mai dimenticare il resto dei professori del Dipartimento: il mio ringraziamento va a tutti i componenti di questa grande famiglia scientifica che è il Dipartimento, dove il lavoro si fa più leggero perché c'è sempre qualcuno disposto ad aiutarti e appoggiarti.

In secondo luogo, desidero ringraziare tutto il personale del dipartimento che mi ha aiutato con il proprio lavoro: Eva, Fernando, José, Mar, che è stata preziosa nella fase finale di revisione del testo, Mari Carmen e Tomás. Ciascuno nel proprio campo è stato un alleato prezioso perché il mio lavoro fosse più facile. Grazie di cuore a tutti voi. Vorrei anche ricordare tutti i compagni di laboratorio e di dottorato: Augusto, Betty, Carlos, Clemente, Cristian, Ekaitz, Josep Ramón e suo fratello Xavi, Jean, Joan, Jordi, Josep Maria, Juan Jorge, Leonardo, Luciano Costa, Mauricio, Roberto, Sandra e Xavi Pintado.

Non posso certo dimenticarmi della mia famiglia. Il suo contributo è stato fondamentale: sono stati loro, infatti, che mi hanno spinto a venire in Catalonia, a cominciare il dottorato e molto di più. Un ricordo speciale per i miei genitori e le mie sorelle che sono sempre lì, e in particolare a mia sorella Valentina che è stata sempre la prima a leggere i capitoli di questa tesi per perfezionare il mio inglese.

Last but not least, i miei cari amici Alessandra con la sua famiglia, Agustín, Enrique e Juliana, Marcelo con la sua famiglia, Cristina, Luciano, sua moglie e i suoi figli, la cui allegria ha sempre fatto sì che mi sentissi come in casa.

***Molte Grazie a tutti voi di tutto cuore!***

# PART I

# INTRODUCTION

# CHAPTER 1

# INTRODUCTION

## 1.1 *Background*

In the last years, in all the European Community many research institutions have developed projects about nuclear energy. One of the investigation fields is focused on where and how nuclear waste should be deposited.

One of the options for nuclear waste disposal are old mines. In this case, the waste is placed in bore holes or drift emplacements. The difference between these two systems is shown in Figure 1.1. In the bore hole location, the waste canisters are piled one on top of the other in a vertical hole, and the space between the canister and the host rock is filled up with crushed material. In the second case, the waste is placed in a horizontal position within the existent galleries and, as in the previous case, the space between the canister and the host rock is backfilled with crushed material.

The characteristics of the host rock are essential for the waste deposit to function adequately. The rock must be homogeneous, without cracks, and with a low hydraulic and heating conductivity. The types of host rock considered are:

1. Salt rock;
2. Claystone;
3. Granite.

The use of old mines allows storing the waste material well below the ground reducing thus contamination risks.

A second aspect of the problem consists in preserving the host rock. For this reason, a material fills the space between the canister and the rock walls.

Three types of material are considered:

1. Concrete;
2. Clay or bentonite;
3. Salt aggregates.

It is the author's opinion that the concrete filling is too expensive for underground application, because the gallery is usually located more than 500 m in depth and the fabrication and/or transportation to that quote could be very expensive in comparison with the use of other materials.

Clay and bentonite are both granular materials, although they differ greatly from one another. This thesis will not study the behaviour of these materials. Many papers have been published in the past few years about the use of these materials for waste disposal and clay and bentonite are extensively studied in all the fields of soil mechanics.

The object of this thesis will be then the study of salt aggregates.

Salt materials can be considered from two different points of view: as the host rock and as the crushed material for the backfill between the host rock and the canisters.

Salt is a difficult material to investigate in laboratory because of its characteristics. For example, its extremely corrosive properties do not allow using the usual equipment and each test needs a brand new apparatus specially indicated for salt.

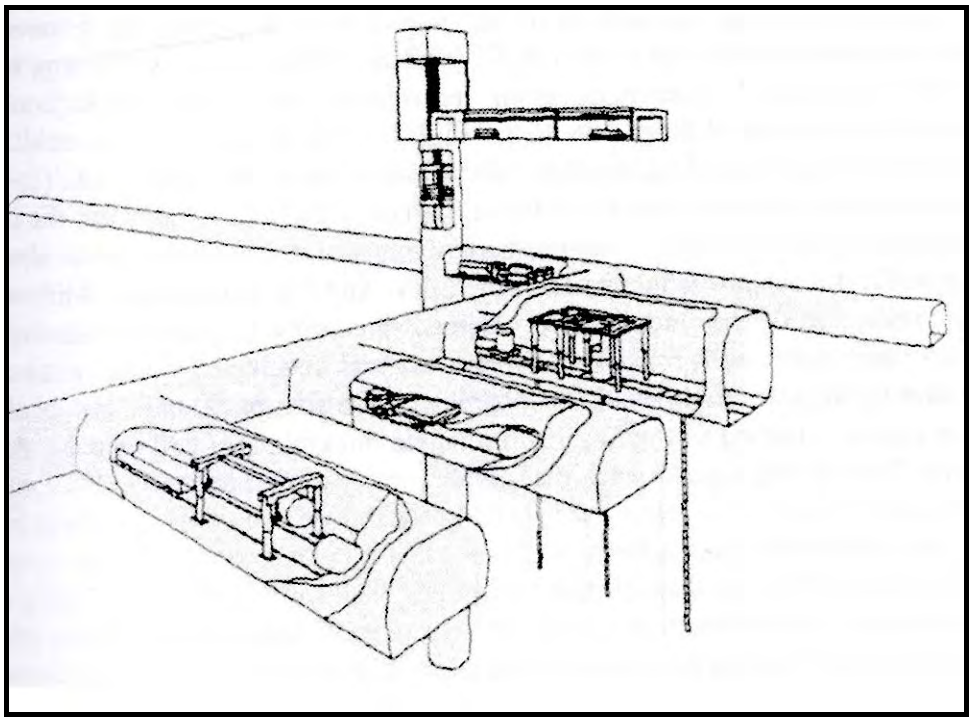

**Fig. 1.1** *Schematic view of drift emplacement and borehole emplacement concepts.* (DBE,1995)

## 1.2 *Scope and Objectives*

When discussing “salt”, the difference between “salt rock” and “crushed salt” must be established, because both of them are used for radioactive waste disposal.

One of the options for waste disposal is to deposit the canisters in old salt mines, where the host rock is salt rock. In this case, due to the salt creep phenomenon, there will be a natural convergence allowing to close the space between the canister and the salt rock. In this type of repositories, the backfill material is crushed salt from that same mine.

One of the phenomena, characteristic of waste deposits, is the heat flow from the radioactive canister to the host rock. Given that salt is liable to dissolution/precipitation phenomena, water would destroy a part of the host rock and the waste radiations could contaminate the environment. Nevertheless, it

must be pointed out that the presence of great amounts of water in mines is not common.

This thesis focuses on the study of the thermo hydraulic behaviour of salt aggregates, in order to determine the real influence of these phenomena on the use of salt for waste disposal purposes.

The work developed is mainly experimental and includes a numerical application of the laboratory results.

Two basic experiments were carried out: the application of matric suction to compacted salt samples to obtain their retention curves and the determination of hydraulic conductivity.

The main laboratory test reproduced the heat flow conditions and its effects on saline media. The test consisted in the study of the porosity changes on crushed salt when a difference in temperature is applied and, due to the presence of brine, the initial porosity changes induced by dissolution/precipitation phenomena and by the flow of gas and liquid phases. Several tests were developed for different initial porosity and saturation degree values and with different test times.

A reference test was established to compare the results of the different tests.

Finally, a numerical analysis of the dissolution/precipitation tests was carried out including the results of matric suction experiments and hydraulic conductivity laboratory data.

The numerical analysis was developed by CODE_BRIGHT, a numerical code developed in the Department of Geotechnical Engineering and Geosciences of the UPC. (Olivella et al., 1996 a)

## 1.3 *Layout*

This thesis is divided into four parts.

The first part being the introduction, is divided into two chapters, the present one and another one in which the general characteristics of salt aggregates are presented to allow the reader to understand the rest of the thesis, where the laboratory and numerical works and its conclusions are shown.

Part II is devoted to the experimental works. Each chapter describes all the aspects of one experiment. The approach for each chapter is usually an introduction and some theoretical notes, the description of the equipment used for the experiment, the presentation of the results and its analysis.

Part III focuses on the numerical work. The results of the numerical analysis give a good qualitative idea of the phenomena. CODE_BRIGHT reproduces the heat flow phenomena including the dissolution/precipitation in salt aggregates studied in the laboratory.

Finally, the general conclusions are presented in the last chapter, where the results for salt are compared to the characteristics and properties of the material that should receive the radioactive waste. The future investigation lines are also illustrated in this part.

# CHAPTER 2

# DEEP REPOSITORY AND GENERAL PROPERTIES OF SALT AGGREGATES

## 2.1 *Introduction*

The main task of this chapter is to introduce the reader to the field object of this thesis.

First of all, there will be a review of the nuclear waste problem, which is the reason that promoted this research.

After that, the material, object of this thesis, is presented: salt aggregates with a special focus on halite. In this part the material used in the experiment is characterized and some general definitions are given.

Finally, some basic experiments are presented in this chapter to characterize salt aggregates.

## 2.2 *The nuclear waste problem*

Safe disposal of radioactive waste and spent nuclear fuel is a major challenge for the present generation, independently from the current and future scenarios of nuclear power use in different countries.

Radioactive waste is produced during the peacetime use of atomic energy to generate electricity, in the fuel cycle of nuclear power stations, through the application of radionuclides in industry, medicine and research, in the closure and dismantling of nuclear systems and, last but not the least, in the mining and milling operations with uranium.

Our generation, as beneficiary and waste producer, has the task of guaranteeing the safe disposal of the radioactive waste produced, which should be permanently excluded from the biosphere to protect mankind and the environment from the damage caused by radioactive radiations. For this purpose, decisive generally recognized basic standards were laid down in the "International convention for the safe handling of spent fuel assemblies and radioactive waste" (September, 1998), in accordance with international laws. (Tonhauser et al., 2006)

It is interesting to remember the cycle of nuclear fuel from the nuclear plant to the final repository. (Fig. 2.1) Nuclear fuel consists of cylindrical pellets of uranium dioxine in ceramic form. The pellets are sealed in rods which are grouped together in clusters, namely the fuel elements. These elements remain in the reactor for five years before being replaced. The nuclear reactions inside the reactor produce new atoms, causing an excess in energy and thus a high-level of radioactivity.

At this stage, when facing the problem of highly radioactive waste disposal, the first step is to put it in an interim storage where man can control the decay of radioactivity. The spent fuel is normally collected in the power plant underground pools and kept there for 30 to 40 years.

The water in the pools provides radiation shielding while cooling, at the same time, the fuel. It is possible to walk around the pools without being exposed to radiation. The water does not become radioactive, but small particles can loosen from the fuel surface and be carried in the water, which should be therefore filtered and the eventual particles removed.

Furthermore, several countries have a first repository in the underground to collect and keep all the material with a high-level of radioactivity for some decades before storing it in the final repository, where it will stay for many centuries reducing its radioactivity without human control.

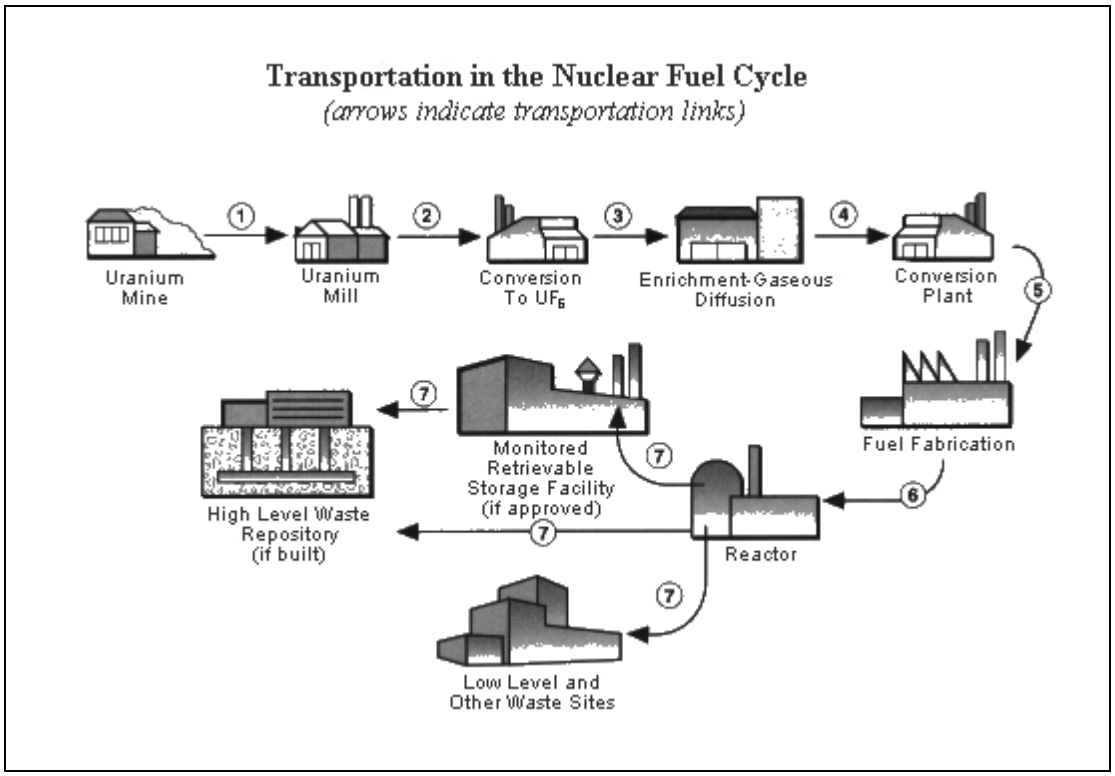


**Fig. 2.1** *The nuclear cycle: From the Uranium mine to the final disposal.*

In general, the classification of radioactive waste is based on the waste's origin, not on the physical and chemical properties that could determine its safe management. One common factor for all the categories of nuclear waste is the presence of, at least, some long-life radio nuclides

Following Astudillo (2002) the IEER (2000) and Beghin (1998), radioactive waste is classified as:

I. "High Level Waste", which is the spent fuel used in the reactors of commercial plants and the reprocessing waste, that is, the liquid waste from solvent extraction cycles in reprocessing. This group also includes the solid, which liquid waste may become. The intensity of its radiation is so high that it lasts for many decades and it releases heat. This kind of waste needs cooling, heavy shielding and remote handling devices. The decay time is over

300 years, and even several centuries. Figure 2.2 shows the high level waste production in a reactor.

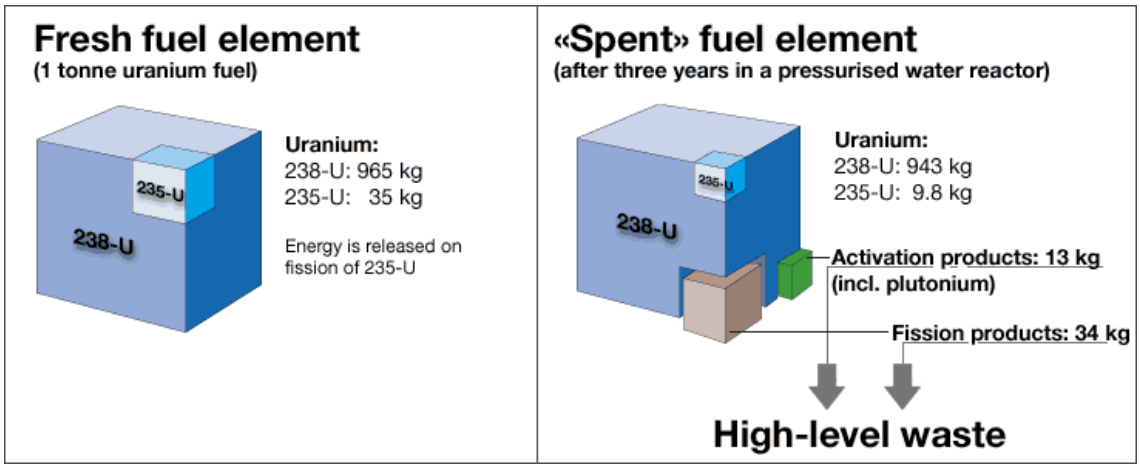


**Fig. 2.2** *Production of high level waste from 1 ton of fresh nuclear fuel.* (NAGRA)

II. "Intermediate Level Waste", which is the waste containing elements with atomic numbers greater than 92, the number for uranium. This category only includes waste material that contains transuranic elements with a half-life greater than 20 years and a concentration greater than 100 nanocuries per gram. Generally speaking, these products come from medicine industry and similar fields of nuclear energy application for civil uses. This kind of waste needs shielding and remote handling devices to protect people managing it.

III. "Low Level Waste", which includes all those sorts of waste not belonging to the first two classes. The value of radiation is low and in thus includes all the things that might have been in contact with radiation, such as the tools of a nuclear plant. It is possible to divide this category into different classes, regarding the average concentration of radiation.

Currently, in Germany, a new classification based only on heat is being used. Nuclear waste is divided into two classes: (Langer M. et al., 1996)

I. Negligible heat developing waste;
II. Heat developing waste.

The heat release per drum for negligible heat developing waste with low-level radioactive contents is in the milliwatt range. The temperature of the encircling rock, the host rock, is not significantly increased by such a small heat release.

In the case of heat developing waste with an accordingly high radioactive content, the heat release is in the kilowatt range, which can lead to a rise in temperature of more than a hundred degrees in the surrounding host rock.

It is clear, from this definition, how important the thermodynamic and thermal problems are in the study of waste final disposal.

Nuclear engineering is a relative new branch of science. It started for military use during the Second World War and was first used for civil purposes in 1950. It is obvious that the problem of waste disposal is quite recent and final solutions are expected for 2010, approximately.

At present, most of the waste is collected in the nuclear plants themselves. But in a few years the storage capacity of these plants will be saturated.

Many final disposal solutions were under study, among which: surface storage, seabed disposal, polar ice cap disposal and space disposal (by rocketing the waste into space).

The more widely accepted solution, right now is to deposit the waste in very deep and stable host rock. Some of the solutions proposed by several countries are shown in the next paragraph.

Nevertheless, the host rock solution is the favourite because the administrator can choose a place with the following characteristics:

- Desert place far from cities; (To reduce contamination problems during transport)
- A homogeneous rock without cracks;
- Absence of water and of any possibility of seepage;
- No problem of stability or earthquake.

Two ways of disposing of waste are possible in deep deposits. In the first one, the bore hole location, the waste canisters are piled one upon the other in a vertical hole, the diameter of the canister is smaller than the diameter of the hole and the space between the canister and the host rock is filled up with crushed material. The vertical holes are drilled for this purpose in existent galleries.

In the second case, the waste is located in horizontal position in already existent galleries and, again, the space between the canister and the host rock is backfilled with crushed material.

The necessary degree of isolation from radiation to the environment is provided by two kinds of barriers:

- The man-made barrier, which is the shield system built by the man including the special container for the waste, the backfill material and the structure of the mines;
- The host rock and all the other formations between the mine galleries and the Earth ground; (Fig. 2.3)

Radionuclides and its radiations should cross all these barriers before reaching, and thus contaminating, life on Earth.

For the purpose of this thesis, our interest is focused on the characteristics of the backfill material and of the host rock when dealing with salt.

**Fig. 2.3** *The excavation of a tunnel in salt rock for nuclear waste disposal*

This study is aimed at determining the physical properties and behaviour of salt aggregates for its use as a sealing material and especially at studying the phenomena of dissolution/precipitation, which can occur in the deposit if water, gases and heat fluxes are present. It is clear that these components are always present in the case of high-level waste, although the water is not present in big quantities.

If the host rock is made of salt, there is also the possibility to dissolve this salt. Note that the disappearance of the natural shield, due to dissolution phenomena, cannot be allowed, because the main task of this barrier is to protect humanity for centuries by natural methods without the intervention of men.

## 2.3 *Review of the final nuclear waste deposits around the world*

In this section the situation of waste disposal in the developed countries is presented. Except for the Waste Isolation Pilot Plant in salt formation, which was applied in USA in 1999, no final repository in deep geology for high-level nuclear waste is currently operative. At present, high level nuclear waste is stored in the nuclear plants themselves in specially cooled and isolated stores. This situation is not expected to change for the next 10 or 20 years.

### USA

USA is the only place in the world where a deep geological repository already works. This installation became operative in 1999 and at the moment it stores the nuclear waste coming from military industry. This plant is called "WASTE ISOLATION PILOT PLANT" and is located in the state of New Mexico, in Carlsbad. The host rock of this plant is a stratiform formation of salt rock, in which the repository of nuclear waste is located 600 m below the ground level.

On the other hand, Yucca Mountain (volcanic tuff rock) is being explored as a final repository location in a deep geological formation. Yucca Mountain is located in the desert of Nevada, where the first nuclear tests were developed. This second installation is in the unsaturated zone of the volcanic rock, because the water table is located 600 below the ground level. Due to this situation, the technicians decided not to use clay as backfill material, because it would be impossible to saturate. The waste will be stored at a temperature of more than 200º C.

The Yucca Mountain installation will start working in a short period of time and it will become the first deep repository for civil nuclear waste operative in the whole world. (Dyer, 1996; Cantlon, 1997; Dublyansky, 2003)

### Germany

As stated above, in Germany radioactive waste is divided into negligible and significant heat developing waste. (Matting, 1997). In order to minimize the costs of final disposal, heat-developing waste is placed in interim storage to cool down over a long period of time.

In the early 1960's, the Federal Government decided that radioactive waste was to be stored exclusively in deep geological formations of the continental crust. The first step towards final disposal in deep geological formations was carried out in 1965, with the construction of the first European underground laboratory in ASSE's salt mine. Till 1978, this installation was also used as an experimental final repository. (Schmidt, 1980)

Whereas the nuclear industry is responsible for waste processing, intermediate disposal and conditioning, the German Government is responsible for final disposal.

In 1982, after extensive studies and exploration, the old iron mine of Konrad was chosen as the most suitable place for the final deposition of all types of radioactive waste.

At that time there were two more sites considered to be used as final repository; the first one is the salt mine of Mosleben in the old DDR, which was used to store the low and medium level waste, but was closed in 1998, after Germany was reunified. The second one is another salt mine in Gorleben.

At first, the German government decided to use the Konrad deposit to store the low and medium level waste (1976) and the Gorleben mine for all kinds of waste.

The Gorleben salt mine was the first choice (1979). Then, the German government decided to use the Konrad mine for all nuclear waste.

In March 2006, the Konrad iron mine was authorized to work with low and medium level waste, but not with high level waste. The use of the salt mine of Gorleben was then reconsidered to analyse some aspects that were not taken into account in 1979, the most important of which being a security problem against human intrusion in the installation. At that moment, high level nuclear waste was temporally being stored in Gorleben. (Langer, 1996; Kaul, 1997).

## Sweden

The Swedish Nuclear Fuel and Waste Management Co (*Svensk Kärnbränslehantering* AB, SKB) is the company in charge of studying the problem of final repositories in Sweden. This company is owned by the four Swedish power companies, whose task is to manage and dispose of Sweden's radioactive waste. They use the common classification into low, medium and high-level nuclear waste.

Sweden was the first country to have a final repository for low and medium level nuclear waste, which they called "SFR" and located in the nuclear power plant of Forsmark. The power plant became operative in 1988, after five years of construction. It consists in an underground deposit with a capacity of 63,000 $m^3$ in four underground caverns. The amount of waste it stores per year is about 1,500 $m^3$.

Another installation that is already working is the CLAB, which is the central interim storage facility for spent nuclear fuel. This plant became operative in 1985 and is located in Oskarshamn, on the Simpevarp peninsula, near Oskarshamn nuclear power station.

The CLAB receives all the spent fuel from the Swedish nuclear plants by ship (the nuclear power plants are close to the Baltic Sea and each plant has its own port). At the end of 2001 (October 2001) the CLAB contained 3,450 t of spent fuel, this fuel is stored in five deep pools of water in an underground cavern, 30 m below the ground surface. Its total capacity is of 5,000 t of uranium, but a second underground cavern is under construction to increase its capacity. Every year the CLAB receives about 300 t of spent fuel. (Grahn, 2005).

Two different lines of investigation are envisaged to determine the final deep repositories. The first one is the selection of probable places for the final repository and the second one is the development of tests in an underground laboratory.

In Sweden the first underground laboratory became operative in 1977 in Bergslagen in the old mine of Stripa. This laboratory worked from 1977 to 1992 in the study of the behaviour of canisters and backfill material.

In 1986, SKB decided to build a new research laboratory: the Äspö Hard Rock Laboratory. Nowadays, this is SKB's central resource for the research on waste disposal in deep repositories. There is still another surface laboratory but with the only aim of developing the technology needed to weld the lid to the copper canister and to check that the weld joints are genuinely tightly sealed.

Äspö Hard Rock Laboratory focuses on the study and development of all the aspects of a deep final repository. Although many of these aspects are out of the field of this thesis, it is interesting to show that the problem of nuclear waste involves many disciplines.

The Äspö Hard Rock Laboratory is in a tunnel, approximately 3,600 m long, which descends to a depth of about 460 m below the ground surface. The laboratories surround the main gallery. This laboratory is located close to the Oskarshamn nuclear power station. (Sjöland, 2005; Sjöland et al., 2006)

In this laboratory many aspects are under study:

- Storage construction method;
- Technology used to blast and drill the canisters holes and tunnels;
- Studies about the security of deep repositories;
- Development, test and demonstration of the technology that will be used in the deep repository;
- Development and testing methods of investigating host rock;
- Development and testing of methods for a deep repository;
- The use of host rock as a barrier against the radioactivity;
- Seepage and transport problems;
- Interaction between host rock and backfill material, on one hand, and interaction between backfill material and the canisters, on the other.

Another line of investigation is the location of sites for the construction of the final repository. At first, eight areas were selected as final deep repositories and two sites were selected to start the first site investigation after the first preliminary studies. The first area is located in Oskarshamn and the first research started in 2002 in two different sites: in an area in the west of Simpevarp and in the Simpevarp peninsula itself. The second area is in the municipality of Osthammar and the site is located in Forsmark. (Andersson et Al., 2005). Both places are located close to other nuclear installations.

In any case, the records from SKB clearly show that there are a lot of possibilities of building the deep repository in the two selected areas, due to the good quality of host rock. Results from the first in-situ investigation are expected in five years. One of the most important aspects is the drilling of bore holes to

characterize the host rock, as the depth to be reached is of 1,000 m below the ground surface. (Ahiström, 1996; Ericsson, 1999)

## Switzerland

Site selection is very much constrained by the small size of Switzerland and by its relatively active tectonic setting.

The current geological consensus is that the orogenesis that formed the Swiss Alps is still alive and that there is still a net uplift in this area of ~1-2 mm/year (which is equivalent to about 1 or 2 km in the million year timescale that must be considered for High-Level Waste).

The fact of excluding alpine areas and other complex geological structures associated with the Jura mountains and the Rhine Graben leaves only a limited area in Northern Switzerland potentially suitable for this purpose. Within this area, two host rock options are considered – either the crystalline basement or one of the overlying, low permeability sediment layers. (McKinley, 1996)

Two deep geological repositories are planned in Switzerland, one for high-level waste, and one for the rest of the waste. The high-level waste repository will receive only the waste from the reprocessing of spent fuel and the spent one. The repository will be operative by the mid 21$^{st}$ century. Currently NAGRA, the Swiss agency for the nuclear waste, is studying the area of Zürcher Weinland for this deposit. The work has just started and there is only a 3D Seismic campaign on the area, the repository will be built in Opalinus Clay (host material). This clay is under study in the underground laboratory of Mont-Terri.

The second emplacement is localized in Wellenberg. This was Nagra's proposal for low and intermediate level waste, but the study of this place has been blocked because of the citizens' negative in September 2002 referendum. That was the second time that people from the Canton voted no to the construction of this structure in this place, so the works have been blocked since 1995.

On the other hand, there are two underground laboratories; the first is located in Grimsel, in a granite formation and the second is in Mt. Terri, in a clay formation (Opalinus Clay). In both cases an international consortium develops the studies.

Grimsel is a rock laboratory. The Grimsel Test Site is located at an altitude of 1730 metres above sea-level in the granite rock of the Aar Massif in central Switzerland. It lies at a depth of around 450 metres beneath the Juchlistock. The Grimsel laboratory consists of a tunnel system, of about one kilometre long and was excavated in 1983. The aim of the research activities in this laboratory is to develop the methods to present the analyses of measurement results and model calculations. This requires sound knowledge on the geological, hydrogeological, geochemical and mechanical properties of the rock. Furthermore, the experiments involve the aspects related to all the disposal concepts. Their objective is to study the behaviour of the disposal

system as a whole, to optimise the various technical procedures involved and to document their safety. (Kickmaier, 2005; Vomvoris, 2004)

On the other hand,, the experiments at the Mont-Terri laboratory are under progress. This laboratory became operative in 1996. The main difference with the former is the kind of hosting formation: Opalinus Clay. (Thury et al., 1999; Thury, 1997)

## Finland

Part of the nuclear technology of Finland comes from Russia and the waste was returned to Russia until 1997.

Finland has only two nuclear power plants, with two reactors each, owned by two different companies. According to the legislation of this country, the responsibility of the whole nuclear process, including waste management, completely lies in these companies.

In 1995, the two companies managing these two power plants, Fortum and TVO, created a joint venture to determine and build a final deep repository, which is under construction at present. This repository will only store the high-level waste from these two power plants and from another one that is under construction. The rest of nuclear installations will be responsible of storing their own waste.

In May 2001, the Finnish Parliament ratified the policy decision, taken by the Government in December 2000, regarding the construction of a final repository in the island of Olkiluoto, close to one of the two power plants. (POSIVA, 2005). The next stage involved the construction of an underground characterization laboratory in Olkiluoto (ONKALO) in 2004. Research activities will be carried out at the final disposal depth, starting in 2007, in order to acquire additional information and verify the present conclusions on the site suitability. The construction of the repository is scheduled for 2010 and it should start operations in 2020. According to the plans, the application for the construction licence for the final disposal facility will be filed to the Government after 2010. (McEwen et al., 2000; Vira, 1996)

**Fig. 2.4 a & b** *Examples of nuclear waste in salt environment*

## 2.4 *The material*

The material used for the laboratory tests was mined from Cardona, Spain. Cardona is located at about 95 km from Barcelona. (Fig.2.5) The material was collected at a depth of 50 m, which corresponds to 350 metres above the sea level, from a mine managed by *Salinera de Cardona SL.*

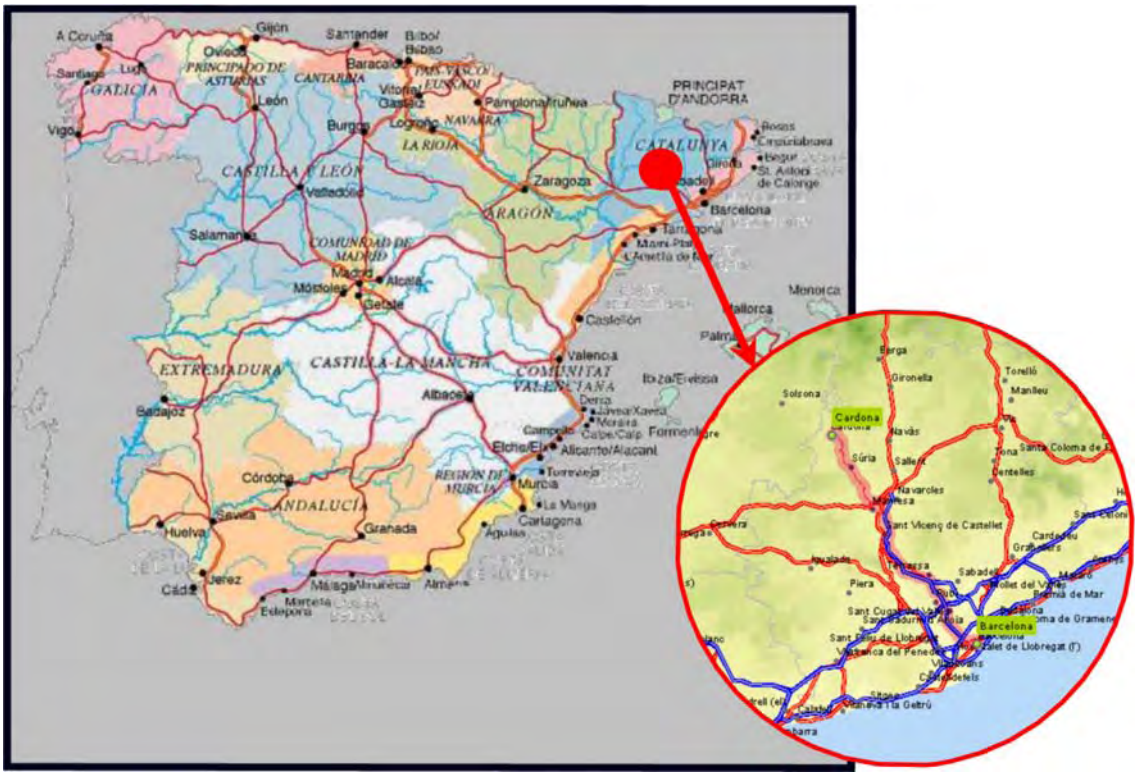


**Fig. 2.5** *Location of the Cardona Mine*

The widely extending Cardona Saline Formation constitutes an evaporitic macrocycle that begins and ends with sulphate facies. This saline formation is formed of rock salt and potashbeds (150-300 m thick). (Ortí et al., 1990). (Fig. 2.6) The Cardona formation is part of the South-Pyrenean Saline Basin, which appears as a narrow and elongated trough, extending from Navarra to Catalunya for about 300 km. Its content in Chloride shows a residual branch of the sea confined by the Pyrenees rising up to the North. Regardless of its intrakratonic position, this basin was related to the evolution of alpine chains and was finally partly covered by the emplacement of the major Pyrenean nappes.

In this evaporitic basin the physiography was inherited from the previous Paleogene evolution. Thus, a wide central zone with salt and sulphates can be distinguished from two smaller marginal basins (the Navarrese and the Catalan), relatively deeper and more subsident, which acted as true collectors for concentrated brines reaching the potash depositional stage.

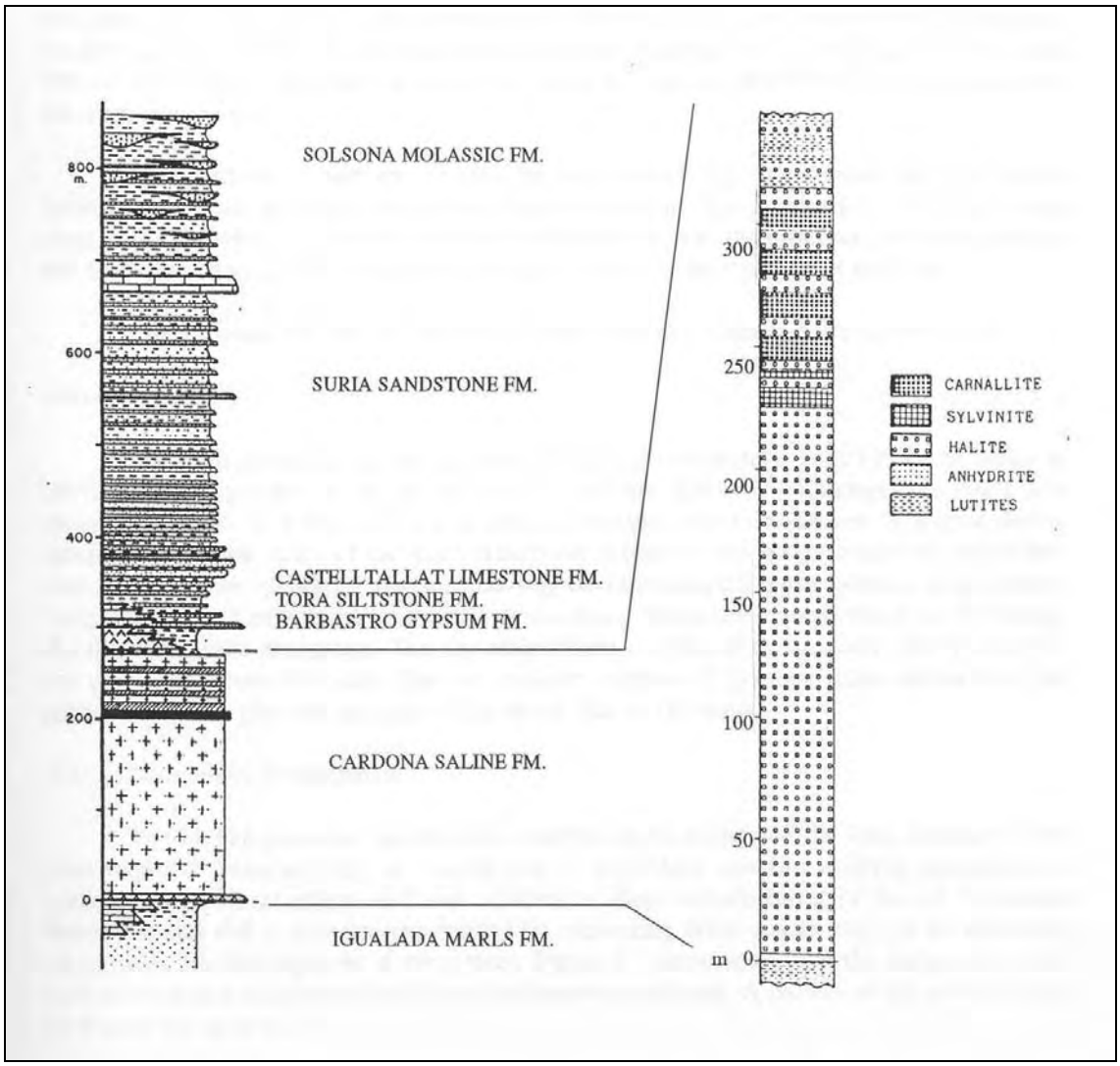


**Fig. 2.6** *Typical disposition of salt strata (Ortí et al., 1990).*

The saline sequence in the centre of both basins is quite similar and represents a complete evaporitic macrocycle characterised by being absolutely impoverished in intermediate magnesium sulphate beds. Only the relative thickness of each saline unit varies from one basin to the other, as well as the total thickness, which is, on average, three times larger in Catalunya than in Navarra.

The material was excavated at a depth of 50 m and the salt rocks were carried directly to the laboratory. Once in the laboratory, the rocks were broken using a hammer to obtain the wished grain size. The chemical analysis of the tested mineral gave the results shown in Table 2.1.

**Table 2.1** *Chemical analysis of the salt aggregates*

| | |
|---|---|
| NaCl | 96.90 % |
| $SO_4^{2-}$ | 1.10 % |
| K | 0.13 % |
| Ca | 0.18 % |
| Mg | 57.14 Ppm |
| Fe | 5.04 Ppm |
| Hg | 0.08 Ppm |
| Pb | 1.34 Ppm |
| As | Not present |
| Cd | Not present |
| $H_2O$ | 0.10 % |

NaCl (halite), whose specific gravity is 2168 kg/m$^3$, is the predominant component of the mineral, about 97%. That is why this thesis will study the salt aggregates taking into account sodium chloride mineral as the only salt component of the material.

The use of salt aggregates in laboratory tests had two different fields of application. Since it is well known that salt aggregates are a highly soluble material, it is obvious that the liquid in the tests could not be pure water but an over saturated solution of water (solvent) with halite (solute). Therefore, the tests were developed in unsaturated salt aggregates ("soil") using brine as liquid. This point is quite significant, because the presence of brine influences the way in which the tests are carried out, due to the properties of saline solution. Thus, in this paragraph some properties of halite, as a porous material, and of brine, as a liquid, will be examined.

Brine is a solution of water and halite, where halite is the solute and water is the solvent. Being an ionic solution, where ions $Na^+$ $Cl^-$ are dispersed in water, this solution is a conductor of electricity.

The concentration of solute in the solvent depends on temperature. The effect of temperature on solubility depends on the kinetic energy of the molecules of solute and solvent, on the stability of the particles of solute and on the reticular energy of halite.

It is possible to dissolve only 36 g of halite at environment temperature. Should more halite be incorporated, the excess would lie at the bottom of the burette. For example, if we put 50 g of NaCl in 100 g of water at environment temperature, only 36 g will dissolve the solution to be saturated. Nevertheless, if we put 50 g of halite in 100 g of water at 100ºC, the quantity that will be dissolved will be 39.8 g. Then, if the excess in solid is removed, and the solution cooled at environment temperature, avoiding precipitation, the solution becomes over saturated. It is possible to distinguish an over saturated solution from a saturated one by adding a small NaCl crystal. The behaviour is different in both cases: the crystal will grow bigger in the over saturated solution, while, in the saturated solution, the crystal will remain at the bottom without change. In order to avoid the phenomena of concentration changes due to variations in

temperature or to sample dissolution, the brine was stored in a tank in which there is more solute lying at the bottom of the container than that strictly necessary to make the solution (Langer et al., 1982).

In this work the concentration of brine is measured in weight percentages. The total density of the brine is 1200 kg/m$^3$ at environment temperature (22ºC).

The presence of a solution of halite and water changes the ebullition and freezing points of the solvent and the reduction of vapour pressure.

The table below shows the relationship between the freezing point of a brine solution and molality.

**Table 2.2** *Freezing point of* NaCl *solutions* (Slabaugh & Parsons, 1966)

| **NaCl molality** | *Freezing Point* [ºC] | *Ideal Freezing Point* [ºC] 100% Ionization | Ionization percentage [%] |
|---|---|---|---|
| **0** | 0.00 | 0.000 | 0 |
| **0.1** | -0.36 | -0.372 | 93 |
| **0.2** | -0.71 | -0.744 | 91 |
| **0.3** | -1.05 | -1.118 | 88 |
| **0.4** | -1.39 | -1.49 | 87 |
| **0.6** | -2.05 | -2.23 | 84 |
| **0.8** | -2.69 | -2.98 | 82 |
| **1.0** | -3.38 | -3.72 | 81 |

## Brine Permeability

At the beginning of the investigation program it was clear that one of the most important variables of the work was hydraulic permeability *k*. As it will be observed in the following chapters of this thesis, this is one of the physical magnitudes involved in all processes. In fact, Chumbe (1996) made several simple tests on saturated halite samples during oedometric tests to determine it.

Another important magnitude of the tests is porosity, whose relationship with brine conductivity should be well known, at least for saturated salt aggregates.

These considerations lead to the decision of making a test campaign to determine several values of hydraulic conductivity for different values of porosity and for different grain sizes under saturated conditions.

The chosen grain sizes are:

- < 0.4 mm;
- 0.4 - 1.2 mm;
- 1.2 - 2 mm;

Porosity varies between 0.25 and 0.45.

The tests were developed with the variable head parameter and constant head parameter. Figures 2.7 and 2.8 show respectively the set-ups for falling head test and constant head test.

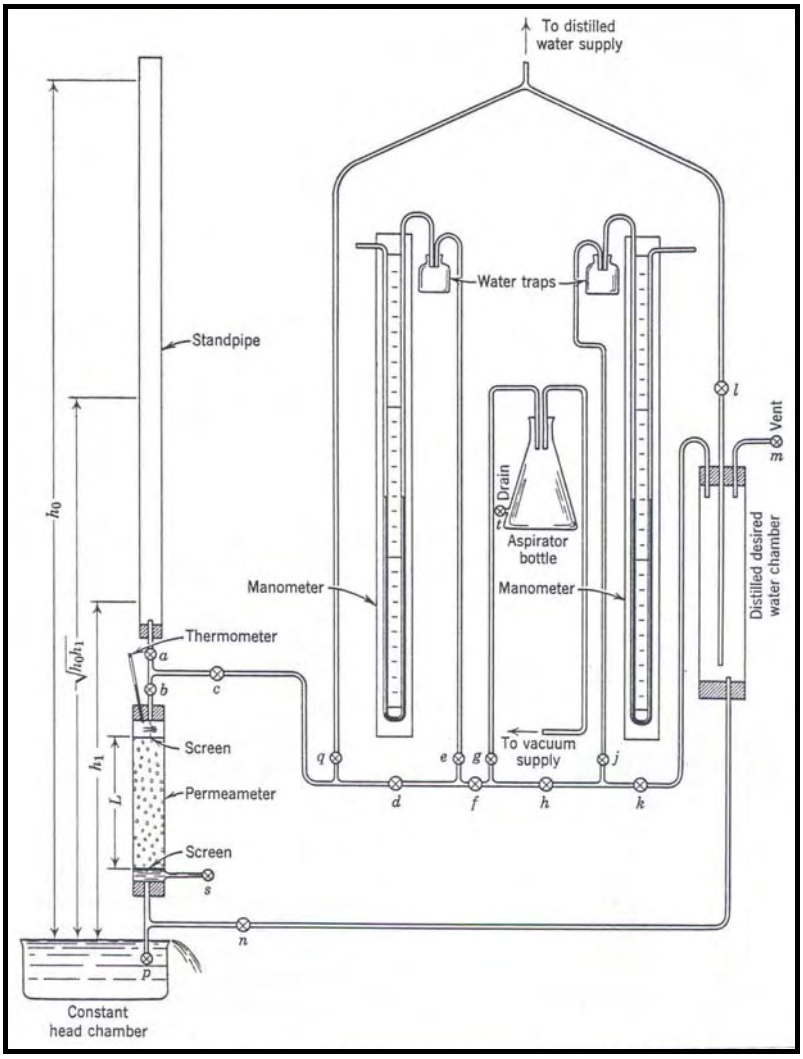


**Fig. 2.7** *Typical installation for a falling head test to determine permeability.* (Lambe & Whitman, 1969).

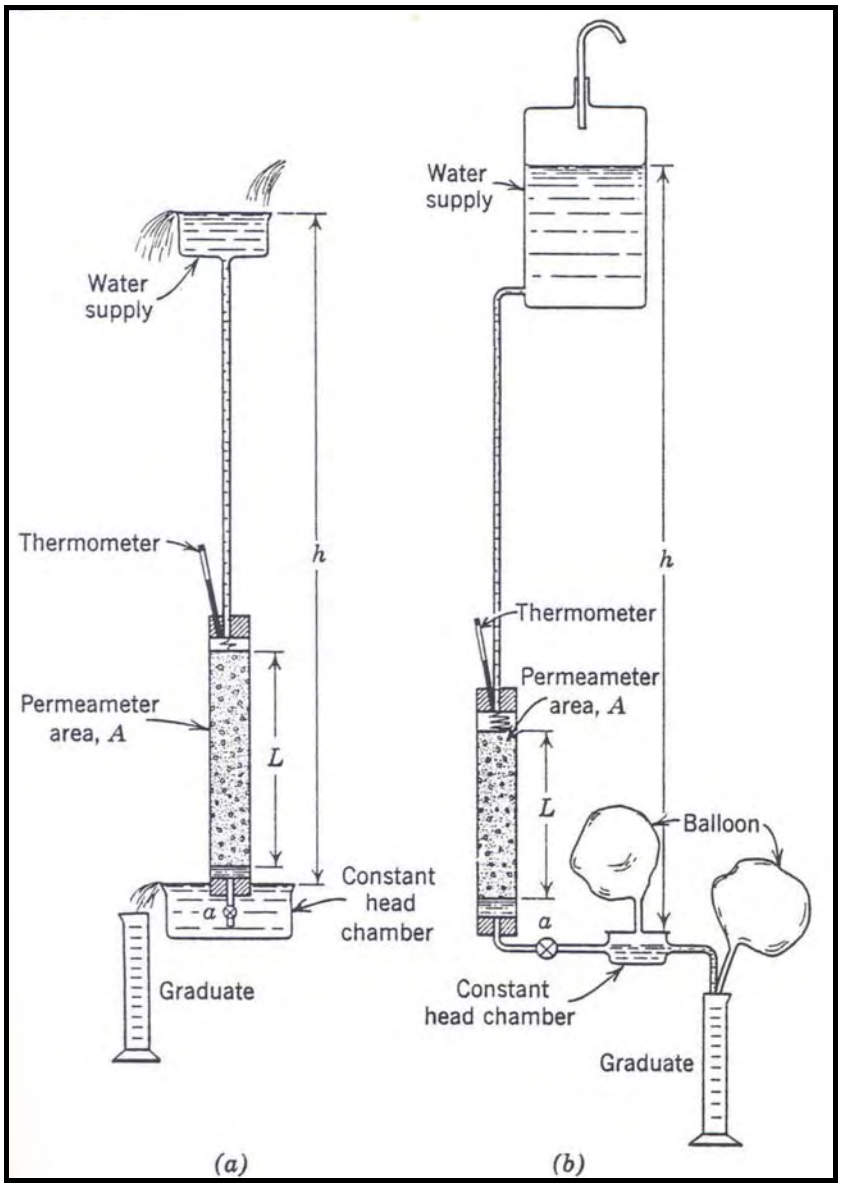


**Fig. 2.8** *Possible set-ups for the constant head test to determine permeability.* (Lambe & Whitman, 1969).

The expression to determine the hydraulic permeability for the variable head test is (Bear,1979):

$$k = \frac{aL}{A(t_1 - t_0)} \ln\left(\frac{h_0}{h_1}\right) \tag{2.1}$$

where:

**a** is the cross-sectional area of the standpipe;
**L** is the length of the porous material sample;

**A** is the cross-sectional area of the sample;
**$h_0$** and **$h_1$** are the heads between which the permeability is determined, and
**$t_0$** and **$t_1$** are the times in which the heads $h_0$ and $h_1$ are measured, respectively.

The expression to determine the hydraulic permeability for the constant head test is:

$$k = \frac{QL}{thA} \tag{2.2}$$

where:
Q is the total quantity of water that flowed through the porous material at elapsed time t;
L is the length of the porous material sample;
h is the fixed head;
A is the cross-sectional area of the sample;
t is the time elapsed during the test;

The scheme used was similar to the one in Figure 2.8.a.

In the following lines the results will be presented in several tables. They will be grouped depending on the grain size. For each value of porosity more tests were developed, and the final value of permeability, presented in this work, was determined applying the minimum square method.

**Table 2.3** *1.2 to 2 mm-diameter grains* (Constant head method)

| **Porosity [%]** | *k* [m/s] | *Number of tests* |
|---|---|---|
| **25.3** | 7.4E-04 | 8 |
| **30.6** | 2.4E-03 | 8 |
| **35.6** | 4.8E-03 | 5 |
| **39.7** | 9.2E-03 | 6 |
| **45.8** | 2.1E-02 | 7 |

**Table 2.4** *0.4 to 1.2 mm-diameter grains* (Constant head method)

| **Porosity [%]** | *k* [m/s] | *Number of tests* |
|---|---|---|
| **24.5** | 3.8E-05 | 15 |
| **29.8** | 1.1E-04 | 10 |
| **34.0** | 4.7E-04 | 8 |
| **40.9** | 2.1E-03 | 4 |

**Table 2.5** *Grains with a diameter inferior to 0.4* (Variable head method)

| **Porosity [%]** | *k* [m/s] | *Number of tests* |
|---|---|---|
| **25.0** | 2.50E-06 | 19 |
| **29.8** | 7.50E-06 | 16 |
| **34.2** | 1.75E-05 | 14 |
| **43.3** | 9.00E-05 | 6 |

The correlation between void ratio (e) and the logarithmic of *k* is plotted in Figure 2.9.

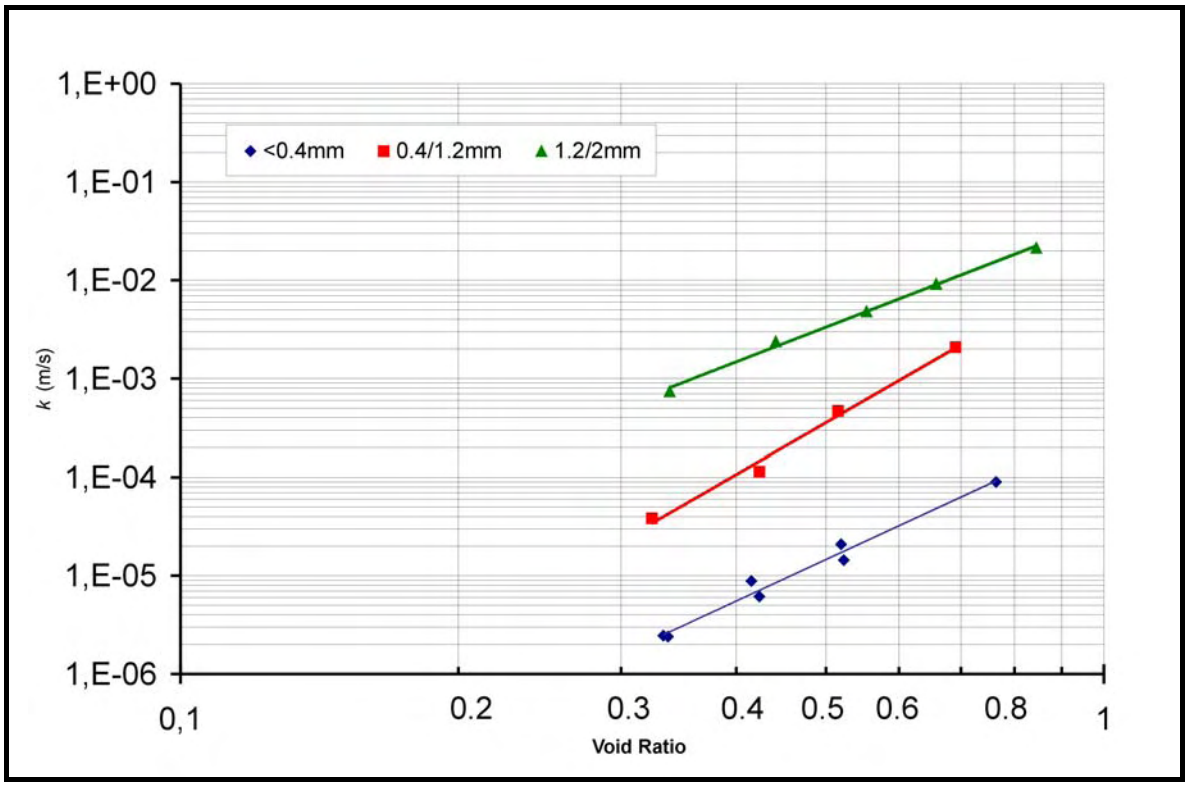


**Fig. 2.9** *Relationship between* log*k and* e*.*

Due to the good correlation between e and log k in all the cases studied, it is possible to find a law for each grain size:

$k$ = 1.15E-04 x $622^{e}$ for grain size between 1.2 and 2 mm;
$k$ = 1.16E-06 x $62790^{e}$ for grain size between 0.4 and 1.2 mm;
$k$ = 1.87E-07 x $4263^{e}$ for grain size inferior to 0.4 mm;

The results of these tests allow determining the relationship between porosity and permeability for saturated salt aggregates.

## Definition of dry sample

At the beginning of the investigation, it was necessary to understand when a salt sample reaches the dry condition, because it is the reference point to evaluate porosities, saturation degrees, volumes, etc.

In common porous material the rule establishes that the dry condition of a material can be usually reached at laboratory when the sample remains at a temperature of 110 ºC for more than 24 hours. Thus, in order to determine when a salt aggregate sample can be defined as dry, three samples were studied. The tests were carried out at the Faculty of Geology of the UB, with the cooperation of Prof. C. De Las Cuevas. The instrument used for this tests allows saving the temperature data and the percentage of loss weight for each time period. The crushed salt was tested at the Universitat de Barcelona.

The aim of the test is to record the loss of weight while the sample is in a chamber at controlled temperature. The temperature value varies progressively up to 450 ºC for 5.400 seconds. Each set of data (t, %W, ºT) represents the weight loss at temperature ºT and at time t.

The weight loss is expressed as:

$$\%W = \frac{\Delta W(t)}{W_0} \tag{2.3}$$

where:

| | |
|---|---|
| %W | is the percentage of loss; |
| $W_0$ | is the initial weight; |
| $\Delta$W(t) | is the difference between the initial weight and weight of a fixed time t, which is a negative number. |

The samples were prepared with the same technique that was used for the samples for the matric suction measurements (see Chapter 3). The three samples are cylindrical, with a diameter of 50 mm and a height of 20 mm. The only difference among samples is the water content. Three cases were considered: a saturated sample, a sample at laboratory humidity conditions and a sample that had previously been in an oven for 48 hours.

The results were automatically presented by the apparatus by means of two curves: variation of weight against time and temperature increase against time. These results were interpreted in a new graph, in which the abscissa represents the temperature in Celsius degrees and the ordinate the percentage of weight loss. Each point was graphically determined from the original graph: firstly the points characterizing the weight loss curve were chosen, and then, entering in the weight loss-time curve the values of t and %W are determined. Once the time is known, the respective value of temperature is determined entering this value of time in the temperature-time curve. Finally, the couple temperature-weight loss is found. These points were plotted in a graph for each of the cases studied.

It is important to underline that, in this case, we are working with salt aggregates and brines, and thus the heating process produces different effects: not only an evaporation of water, but also a precipitation of salt from the brine and a consequent variation in concentration and porosity. The only purpose of this test was to establish a temperature value to ensure that the sample could be considered dry. which is why, all these effects were not taken into account.

The saturated sample shows better the effect (Fig. 2.13) of weight loss (about 8%) that makes it easy to observe the process. The curve can be divided into two parts: one up to 150 ºC and another from 150 to 480 ºC. The former's main loss is about 8% (4.30 g) of the initial weight (53.90 g), whlie the latter's is approximately 0.50% (0.27 g) of the initial weight.

The second sample (Fig. 2.14) was under laboratory conditions, which means that the sample was prepared as described in Chapter 3, but without the presence of brine.

In this case the curve can be divided into five steps. In the first step the weight loss is 0.15%, up to 115 ºC, in the second one (from 115ºC to 175 ºC) the loss equals 0.30%. After this one there is a range of 100 ºC in which the variation is small, only 0.05 %, up to 275ºC, and finally the last two steps, in which the loss is similar, about 0.15% but with two different ranges of temperature, in the first case, from 275º to 325ºC and in the second one, from 325ºC to 450ºC.

The total loss is 0.80% (0.42 g) of the initial weight (52.50 g).

The last sample is the one which had been in an oven for 48 hours before starting the test at a temperature of 110ºC (Fig. 2.15).

The total loss is 0.40% (0.21 g) of the initial weight (53.80 g). In this case the curve can be divided into three parts, a first up to 255ºC, in which the loss is only 0.10% of the initial weight, a second part from 255 to 315ºC, in which the loss is 0.15% and a third one, in which the loss is 0.15% from 315 to 450 ºC. All tests were developed at a time of 5400 s.

The observation of the three tests, taking into account that the test time was short, lead to the final decision to define (for the objectives of this thesis and its laboratory tests) a salt sample under dry conditions as "the specimen which has been in a laboratory oven at 180º C for more than 48 hours". This definition is correct, because the weight losses at more than 180 ºC are negligible: inferior to 0.5%.

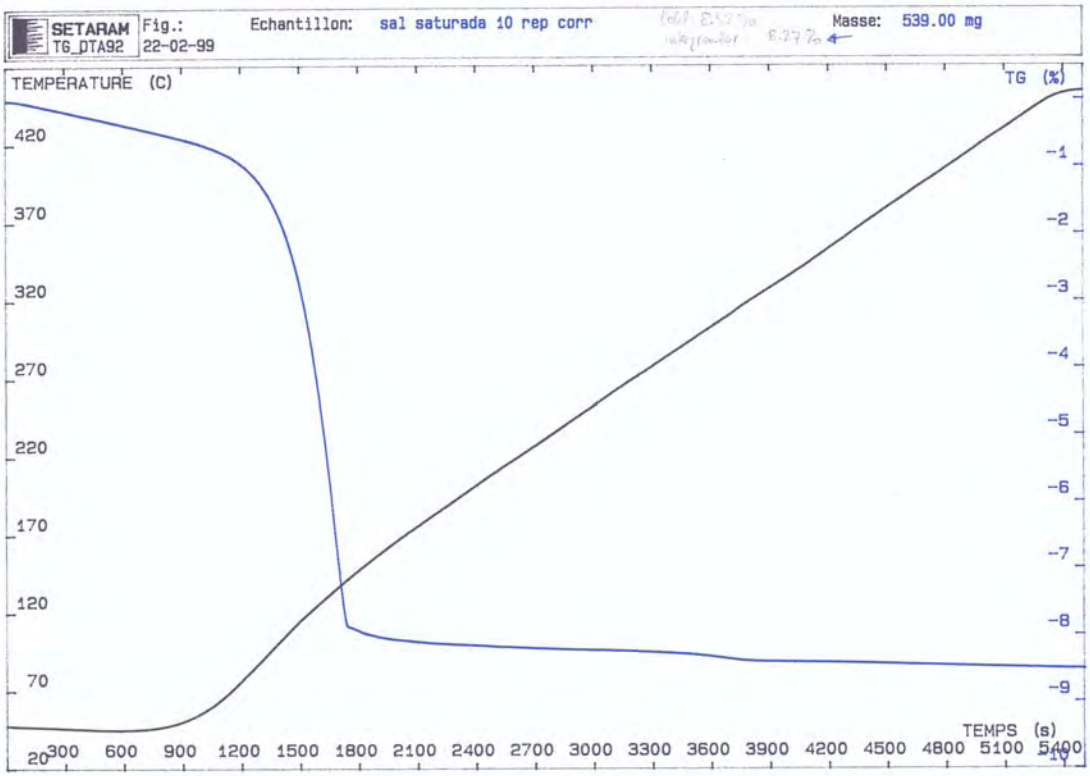


**Fig 2.10** *Apparatus result for the saturated sample.*

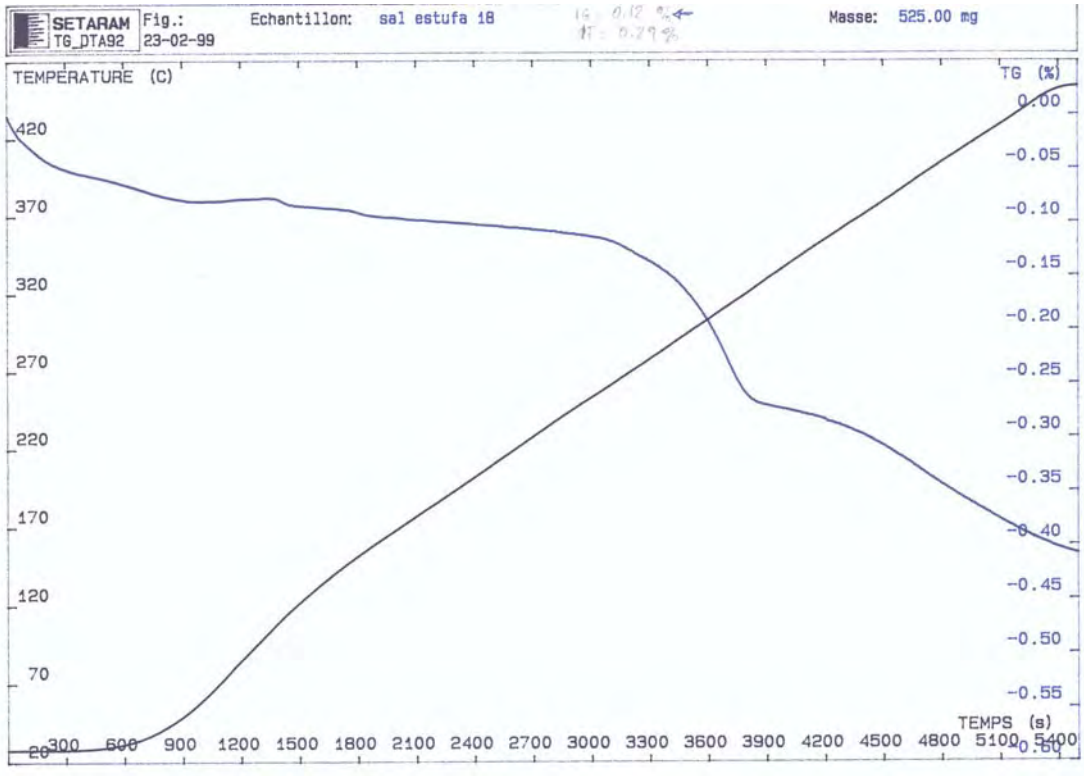


**Fig 2.11** *Apparatus result for the sample that had previously been in an oven at 110 ºC.*

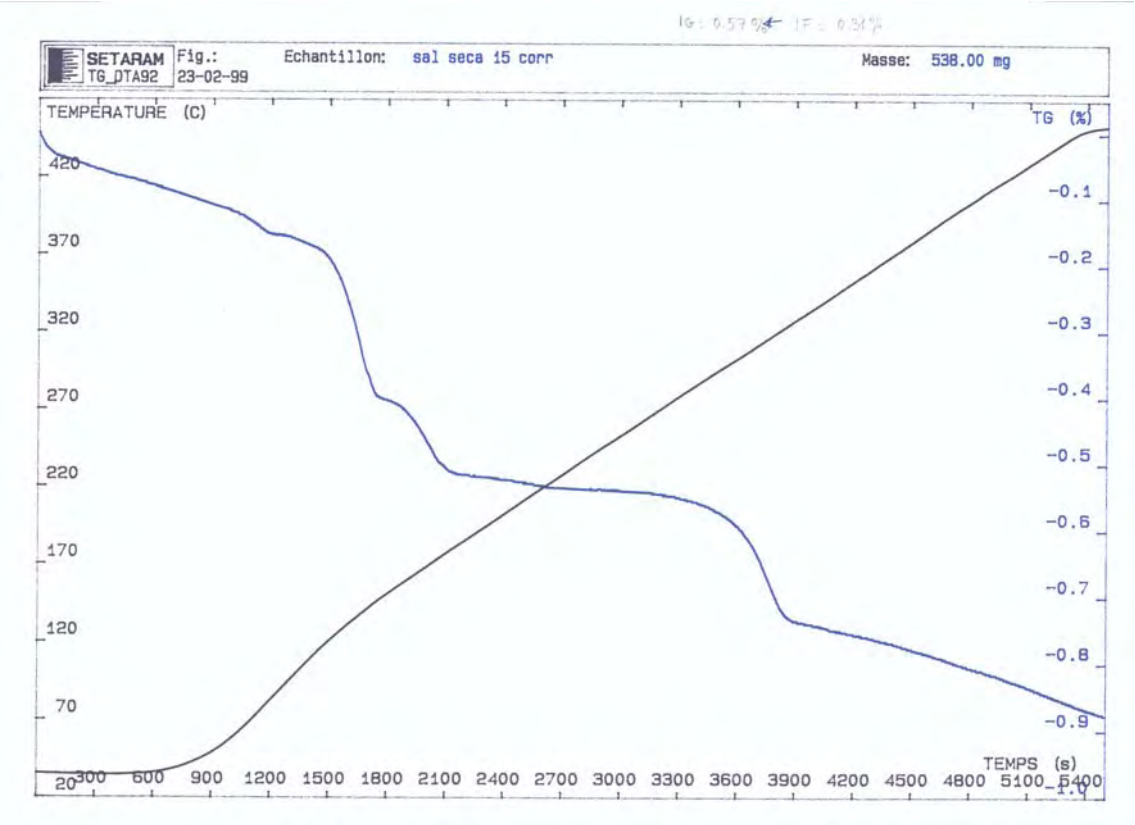


**Fig 2.12** *Apparatus result for the sample that was under intermediate conditions.*

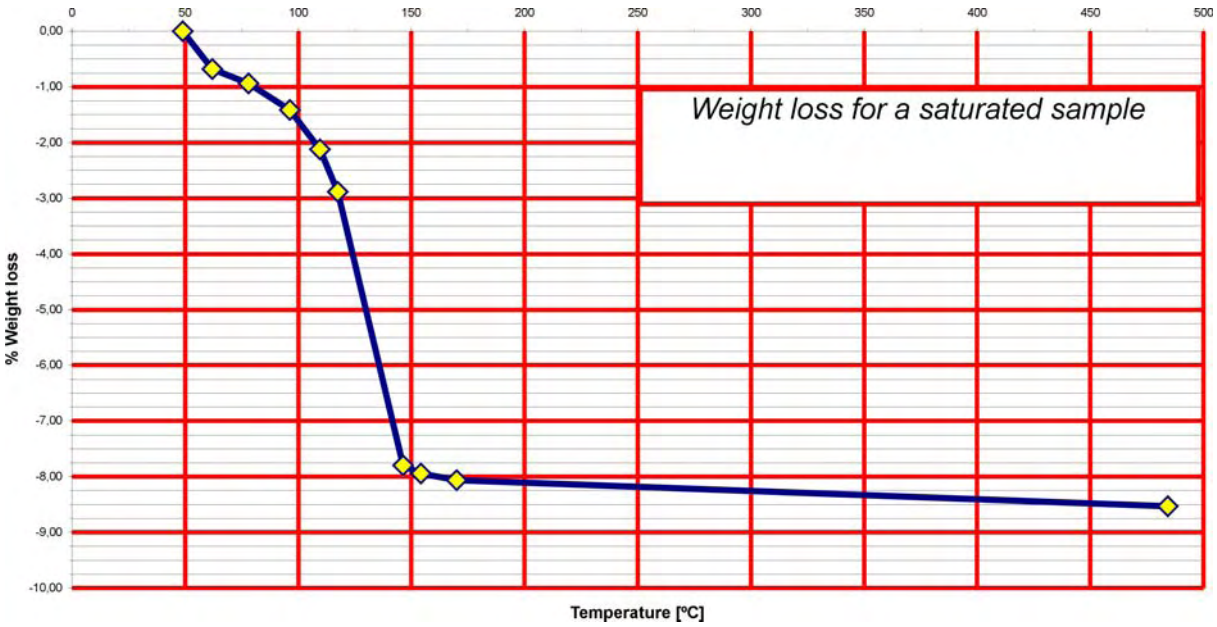


**Fig 2.13** *Weight loss for the saturated sample.*

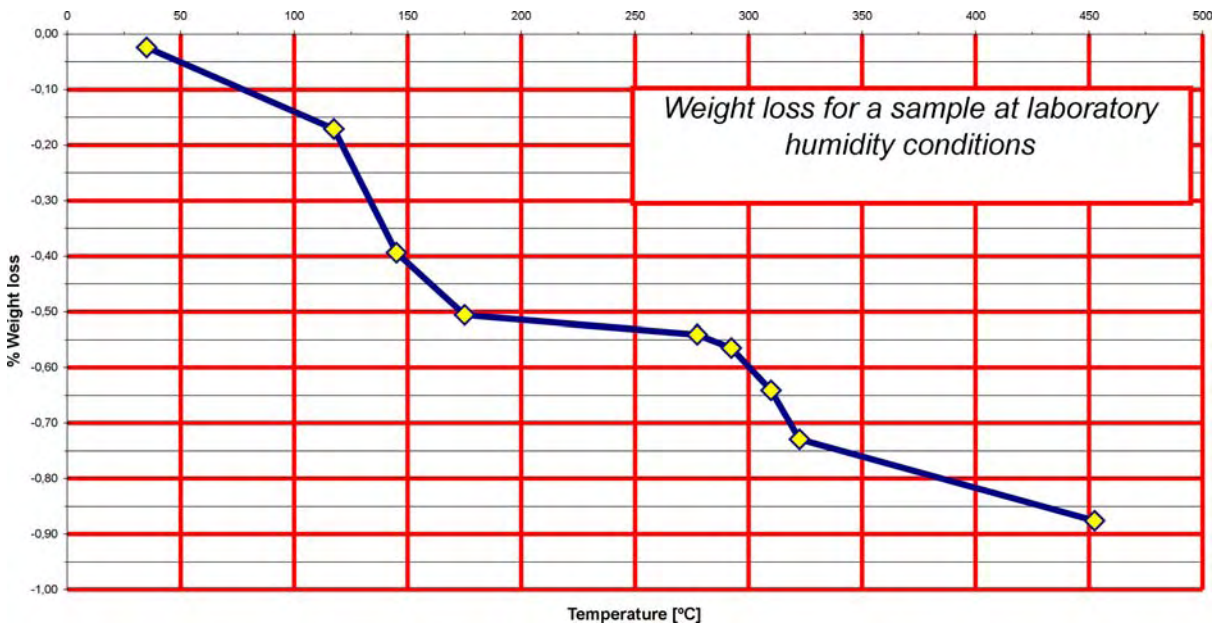


**Fig 2.14** *Weight loss for the sample under laboratory humidity conditions.*

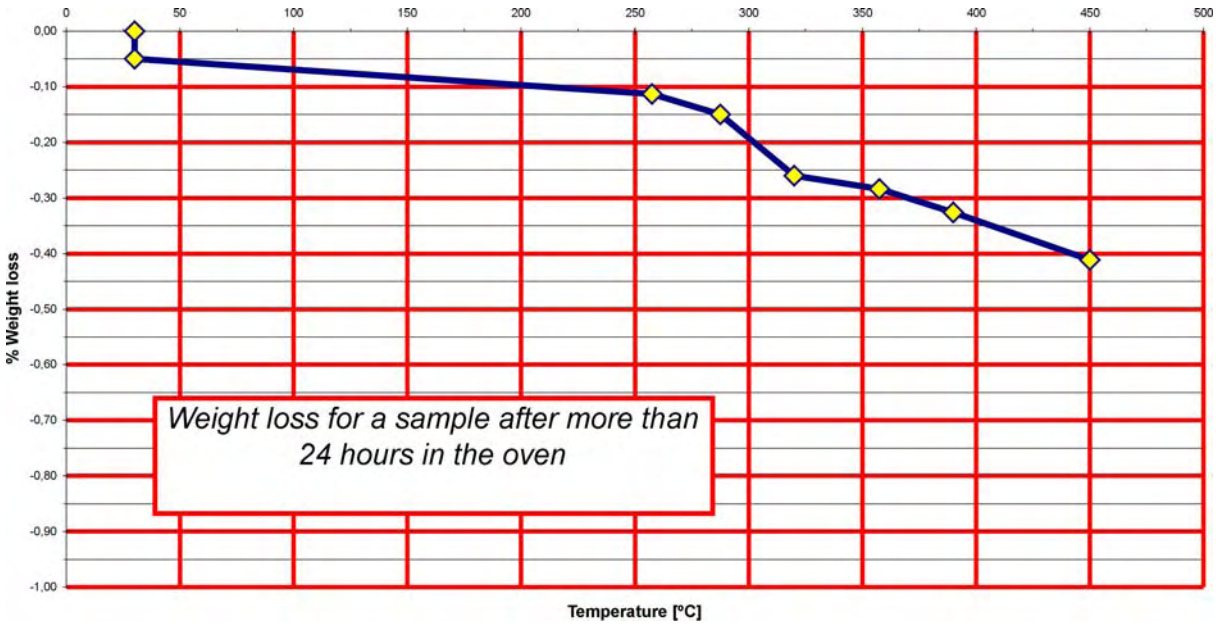


**Fig 2.15** *Weight loss for the sample that had been in an oven at 110 ºC before developing this test.*

# PART II

# EXPERIMENTAL WORKS

# CHAPTER 3

# BRINE RETENTION OF SALT AGGREGATES

## 3.1 *Introduction*

One of the aims of this thesis was to determine the retention curve of a compacted sample of salt aggregates. This task was the first developed because, due to the main significance of matric suction on seepage and the mechanical behaviour of unsaturated porous material, the first step of a laboratory campaign must be the acknowledgement of the role that matric suction plays in this special material.

Salt is a difficult material to investigate in laboratory, and the measurement of matric suction was, probably, the most difficult experiment developed. Many pre-tests were necessary to finally get a “first impression” on how to determine the right way to develop the test. This part took eight months to be completed, and the determination of retention curves, presented in this chapter, took more than one year.

## 3.2 *Review of the suction fundamental concepts*

In the field of unsaturated hydromechanics of porous media, the concept of water held in soil is essential to describe phenomena. On the other hand,it is difficult to describe all suction terms involved in water soil. That is why, the concept of suction may be considered in terms of free energy. In hydraulics, this energy is commonly a specific energy and has the dimensions of pressure.

Three different kinds of suction can be defined (Aitchinson et al., 1965; Ridley, 1993, and Ridley et al. 1996):

1. "Total Suction" or "free energy of the soil water". In suction terms, it is the equivalent suction derived from the measurement of the partial pressure of the water vapour in equilibrium (with a solution identical in composition) with the soil water (interstitial water), relative to the partial pressure of the water vapour in equilibrium with free pure water.
2. "Matric Suction" or "capillary component of free energy". In suction terms, it is the equivalent suction derived from the measurement of the partial pressure of the water vapour in equilibrium with soil water, relative to the partial pressure of the water vapour in equilibrium with a free solution identical in composition with the soil water. (the surface between the liquid and solid phase is plane)
3. "Osmotic Suction" or "solute component of free energy". In suction terms, it is the equivalent suction derived from the measurement of the partial pressure of the water vapour in equilibrium with a free solution identical in composition with the soil water, relative to the partial pressure of the water vapour in equilibrium with free pure water.

Usually, in soil mechanics the symbols representing the three suctions are:

- Total Suction $\Psi$;
- Matric Suction $u_a$-$u_w$;
- Osmotic Suction $\pi$;

The magnitude has the dimensions of pressure and the unit of suction is kPa and its multiples.

In practice, the matric suction concept is strictly linked to the physical phenomenon of capillarity rise (Fig. 3.1). That is, a very small diameter tube is placed in vertical position in a water tank so that a rise in water level above the water table can be observed (Fig. 3.1.a). Obviously, the water pressure will be negative; if we change the tube with another one of different diameter, the height of the rise will be different. The smaller the diameter of the tube is, the higher the water rise above the water table will be (Fig. 3.1.b).

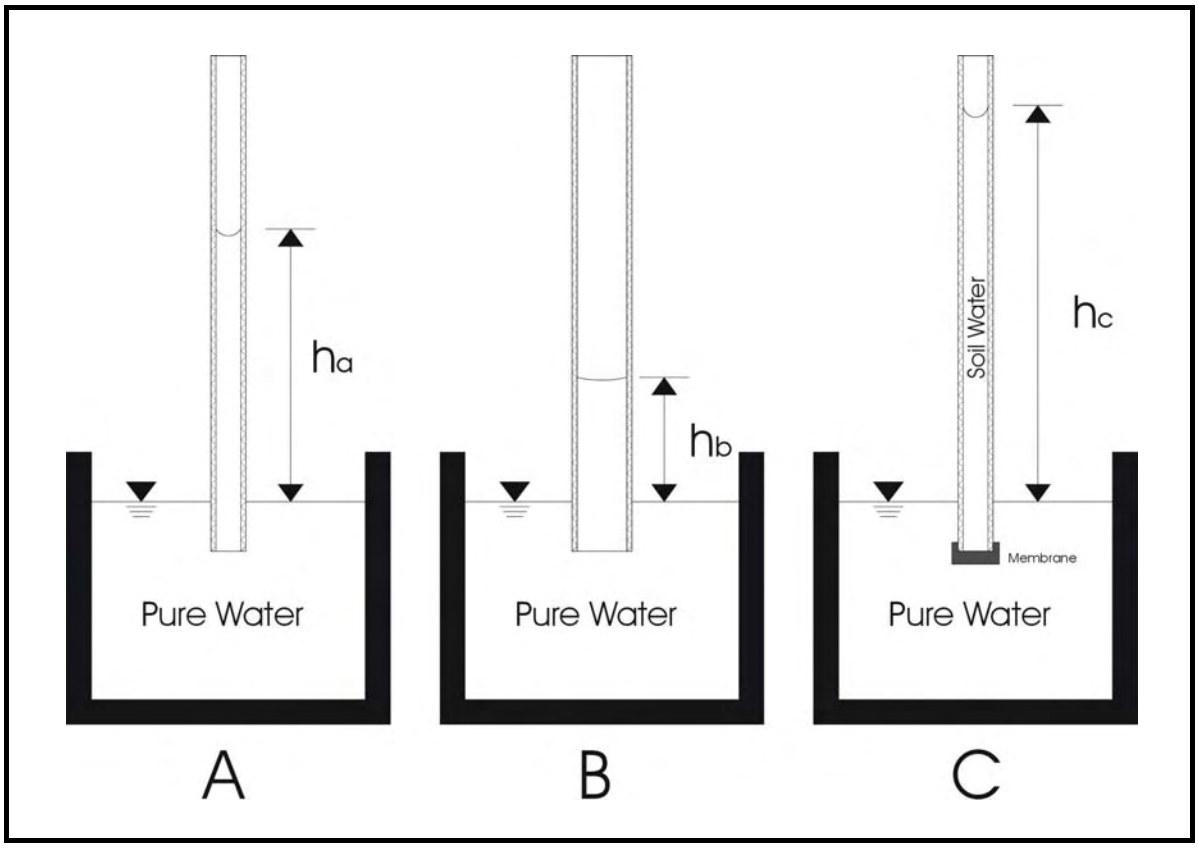


**Fig. 3.1** *The phenomenon of capillarity.*

Another aspect to be considered is the quality of the water: usually, soil water is not free pure water and has some ions of salts dissolved in it, so the vapour pressure is reduced and, thus, the energy of the water.

Therefore, the energy required to reach a determined height will be greater in this case than in the case of pure water, because the presence of salt dissolved in the soil water reduces water potential, due to osmotic suction. Figure 3.1.c reproduces the effects of osmotic suction.

The soil water–air interface is important because it is the place of the points where the forces should be in equilibrium. In this interface the water molecules undergo an unbalanced force towards the liquid side, with a tension along the surface. In order to be in equilibrium, the surface forms a meniscus with a concavity in its upper part (Fig. 3.2). Due to this characteristic, the surface is called "*contractile skin*".

The forces applied on the meniscus depend on:

- air pressure in the upper part;
- water pressure in the lower part, and
- tension surface tangential to the interface water-air.

The value of the tension surface depends on the temperature of the system and on the characteristics of the liquid.

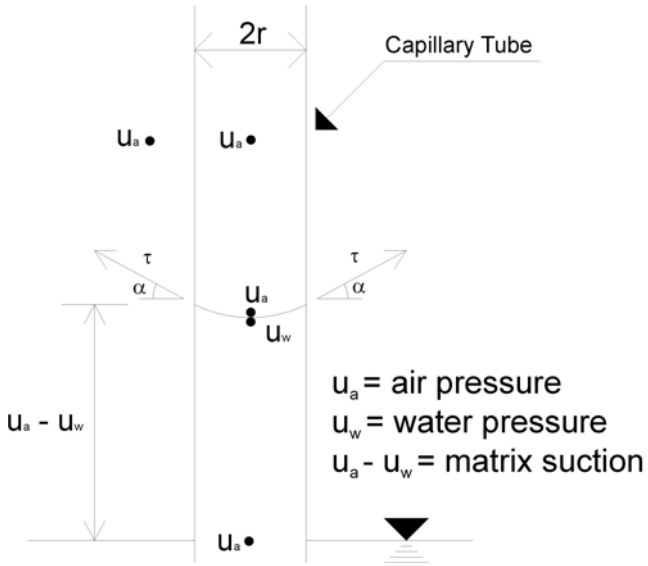


**Fig. 3.2** *Surface tension phenomenon.*

Due to the system symmetry, the horizontal forces are always in equilibrium and so should the vertical forces be to reach equilibrium.

The vertical equilibrium equation is:

$$u_a \pi r^2 = u_w \pi r^2 + 2\pi r \tau \sin\alpha \tag{3.1}$$

where $\tau$ is the surface tension and $\alpha$ is the angle between the water and the tube in the contact point.

The equation can be rewritten as:

$$\left(u_a - u_w\right) = \frac{2\tau \sin\alpha}{r} \tag{3.2}$$

in which the relation between the matric suction and surface tension is quite clear.

If the interface surface is a perfectly spherical meniscus, the angle will be 90º.

From Figure 3.2, it can be observed that:

$$u_a = u_w + \gamma_w h \tag{3.3}$$

so that:

$$u_a - u_w = \gamma_w h \tag{3.4}$$

and (3.4) and (3.2) together equal:

$$\left(u_a - u_w\right) = \frac{2\tau \sin\alpha}{r} = \gamma_w h \tag{3.5}$$

Equation (3.5) demonstrates that matric suction rules capillary rise (h) and that, as it has been previously asserted, this last magnitude depends on tension surface and the diameter of the voids.

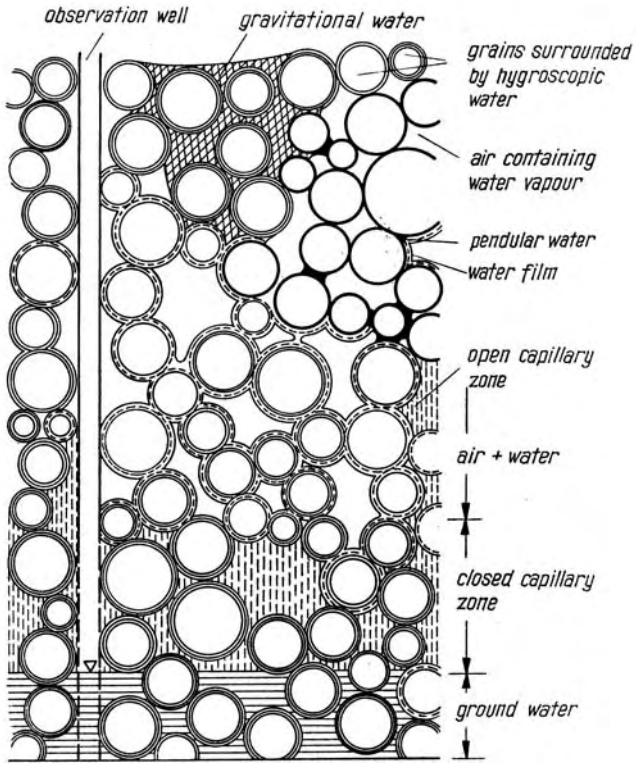


**Fig 3.3** *Various forms of soil moisture above the water table* (Kovacs, 1981).

The behaviour of water in unsaturated media is similar to previous examples. There are four phases: solid, water, air and the interface between water and air.

The voids between solid particles represent the capillarity tube, and the rise of interstitial water depends on the porosity of the medium (**n**) and the

quality of the water (Fig. 3.3).

The water pressure [$\mathbf{u_w}$] will be negative because it is above the water table.

Total suction [$\Psi$] is the rise above the water table under normal conditions and the sum of two effects: matric suction [$\mathbf{u_a}$-$\mathbf{u_w}$] and osmotic suction [$\pi$]:

$$\psi = \left(u_a - u_w\right) + \pi \tag{3.6}$$

The rise depends only on the surface tension and the characteristic diameter of the voids.

Matric suction rules the hydro-mechanical behaviour of porous media; is the rise above the water table, and depends on the mechanical characteristics of the material.

Another way to express total suction is to consider the energy equilibrium of meniscus at a molecular level -*Psychometric law*, which can be written as:

$$\psi = -\frac{RT}{V_{mol}} \ln(RH) \tag{3.7}$$

where:

| | |
|---|---|
| **R** | is the universal gas constant; |
| **T** | is the absolute temperature in Kelvin; |
| $\mathbf{V_{mol}}$ | is the molar volume, and |
| **RH** | is the relative system humidity; |

The values of the osmotic suction of brine are well-known in literature because salt solutions are commonly used to control air relative humidity and to measure suction. For example, Lange published in 1967 the osmotic suction of a NaCl solution, regarding different concentrations and temperatures (Table 3.1). Halite is the object of this work; the tests to determine the points of retention curve were developed in laboratory at controlled temperature (22º C). As it has already been written, total suction is the sum of matric and osmotic suction. In the cases studied in this work, the values of osmotic suction for oversaturated salt solution at 22º C (laboratory temperature) are about 9÷10 MPa (see Table 3.1) and the matric suction values are, at the most, about 100 kPa.

**Table 3.1** *Osmotic suctions* [kPa] *for NaCl solutions* (Lange, 1967)

| | **Temperature** [º C] | | | | |
|---|---|---|---|---|---|
| **NaCl molality** | **0º** | **7.5º** | **15º** | **25º** | **35º** |
| **0** | 0 | 0 | 0 | 0 | 0 |
| **0.2** | 836 | 860 | 884 | 915 | 946 |
| **0.5** | 2070 | 2136 | 2200 | 2281 | 2362 |
| **0.7** | 2901 | 2998 | 3091 | 3210 | 3328 |
| **1.0** | 4169 | 4318 | 4459 | 4640 | 4815 |
| **1.5** | 6359 | 6606 | 6837 | 7134 | 7411 |
| **1.7** | 7260 | 7550 | 7820 | 8170 | 8490 |
| **1.8** | 7730 | 8035 | 8330 | 8700 | 9040 |
| **1.9** | 8190 | 8530 | 8840 | 9240 | 9600 |
| **2.0** | 8670 | 9025 | **9360** | **9780** | 10160 |

In the case of brine and salt aggregates, in case of isothermal conditions, the osmotic suction will be the same at every point of the salt aggregate and the brine movement will be ruled by the matric suction gradient. Likewise, the matric suction is the one governing the mechanical behaviour of salt aggregates. Thus, the investigation efforts had to be addressed to determining the retention curve of salt aggregates in terms of matric suction.

## 3.3 *Suction measurement techniques*

Nowadays, it is possible to measure all kinds of suctions, and, although total and matric suctions are frequently measured in laboratory when dealing with soil studies, osmotic suction is not commonly measured (Romero, 1999).

There are two different approaches to measure total or matric suction. The first one is the *direct* way, in which the suction is directly measured in the soil; and the second one is the *indirect system,* in which several values of suction are applied obtaining then the retention curve.

Suction may be applied in two ways: from a dry condition, and thus the sample increases its water content (*wetting*), or, on the contrary, with a reduction of water content, from a saturated condition (*drying*).

A retention curve is a graph in which suction (y-axis in logarithmic scale) and saturation degree, or water content, (x-axis) are plotted. This curve undergoes a hysteresis phenomenon , which makes the results of a wetting or drying path negligible.

The indirect system is also useful when the investigators want to apply a fixed suction in other apparatus (i.e. oedometers or triaxial equipments). A quick review of the most common apparatus to determine the total or matric suction is given in the next paragraphs.

### The Filter Paper Method

This is the simplest method, as it allows to measure total or matric suction, although it is also the least accurate. The equilibrium time depends on the volume of the sample: about one week for the matric suction, and two weeks for total suction.

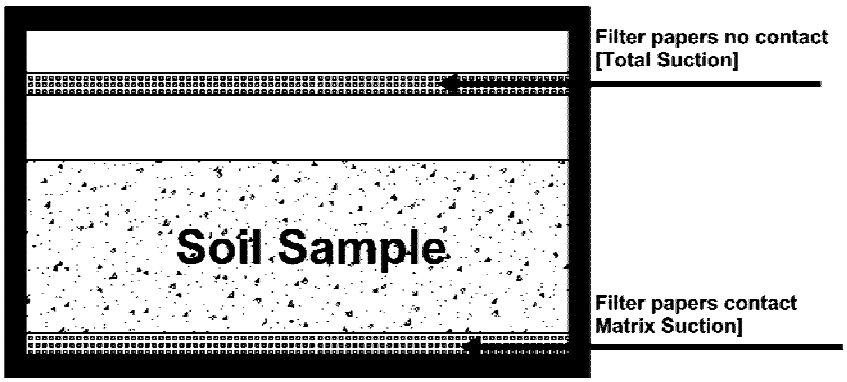


**Fig 3.4** *Scheme of the filter paper method.*

The measure range varies depending on the kind of suction. For total

suction, the range is 400 kPa ÷30 MPa, while for matric suction, it is 30 kPa and 30 MPa (Lloret, 1993).

The difference between matric measure and total measure is that in the former the soil is in contact with the paper, while in the latter there is no contact.

In the case of matric suction a little piece of filter paper is in contact with the soil leading to equilibrium between the suction in the paper filter and the liquid sample. For total suction, the filter paper is suspended in an enclosed container together with the soil,avoiding any contact between soil and paper and reaching equilibrium by vapour movement.

When the system reaches equilibrium, the filter paper and the soil will show the same suction. Therefore, if the relationship between the suction and humidity of the filter paper is already know, it is possible to determine the suction value of the water in the sample by measuring the filter paper's humidity. This is possible only if the water volume absorbed by the filter paper is negligible.

## Porous Block

The porous block is used to measure the matric suction. Its range of application goes from 30 kPa to 3000 kPa. The concept is similar to that of the filter paper: after some days, the system reaches equilibrium and the water content of the porous block is measured. (Lloret, 1993)

The block must have a fixed homogeneous porosity. The most common material used for this kind of blocks is Gypsum, because it can quickly absorb or lose water, that is it is very sensitive, and, finally, it has got a low range of solubility to saline agents. Later, ceramic or synthetic materials have been used.

The water content of the block is calculated by knowing the electrical resistance of the stone. An alternate current is used to keep the water from polarizing.

Before starting the test it is necessary to calibrate the apparatus in order to find out the retention curve of the porous block and the relationship between water content and electrical resistance.

In practice, when the system reaches equilibrium, the electrical resistance is measured to find out the soil matric suction (passing from resistance to suction is possible using a calibration curve).

The presence of salt modifies the electrical resistance values of the porous block. In fact, Ridley (1995) said "*Conversely, the most adverse conditions for the use of blocks are in relatively saline soils subjected to rapid changes of water content."* Its use to determine the retention curve of salt material is not easy, because changes in the concentration of brine or water content should correspond to a different relationship between water content and electrical resistance. Figure 3.5 shows a typical porous block apparatus.

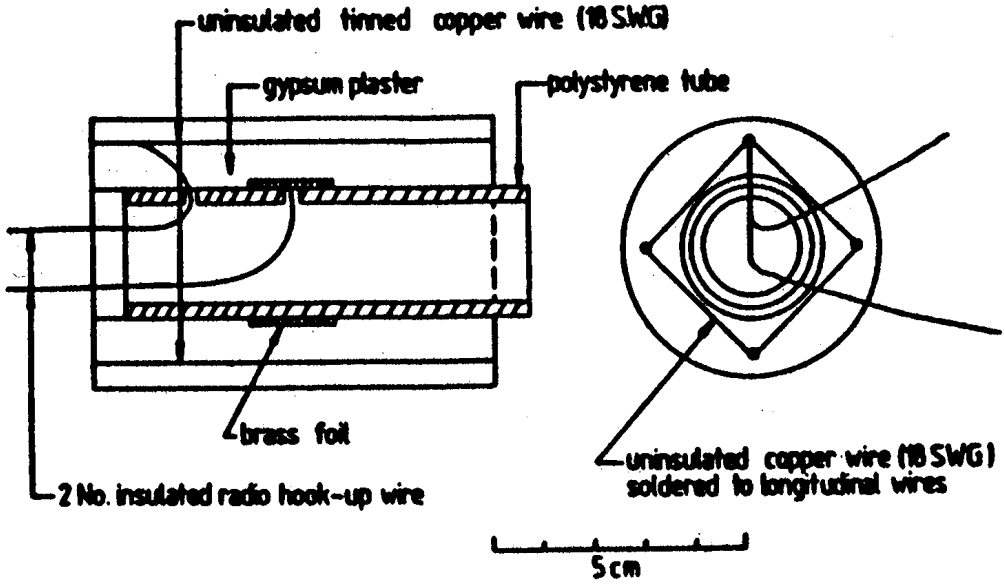


**Fig. 3.5** *Typical porous block* (Ridley, 1995).

## Thermal Conductivity Sensors

This method allows determining the matric suction. The system is the same as in the porous block, the only difference is that the physical variable to be measured, in this case, is the thermal conductivity of a rigid ceramic block.

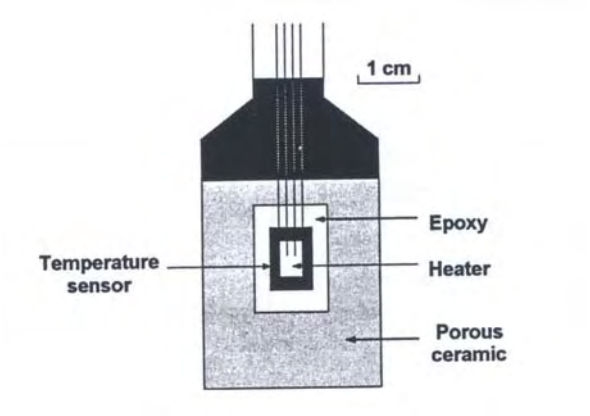


**Fig. 3.6** *Thermal conductivity sensor* (Ridley, 1995).

In practice, inside a ceramic block sensor, there are a temperature sensing element and a heater. The dimensions of the block do not exceed 5 cm and is placed in contact with soil, in an apposite hole. When the system is in equilibrium, the suction of the ceramic stone will be the same as that of the soil. Then, a heat flow is applied in order to measure its thermal conductivity (Ridley,

1993). Figure 3.6 shows the section of a ceramic sensor.

There is a relationship between the thermal conductivity and the water content. Heat dissipation increases with water content, causing the need for the system to be calibrated. In this apparatus the presence of salt does not affect the measurement.

Sattler and Fredlund (1989) presented a thermal conductivity sensor with an application range of 0÷300 kPa. In any case, it is known that using a different ceramic material the application range can change. They stated that, in that case, the calibration curve showed a bi-linearity, the slope changed at about 175 kPa and the equilibrium time varied between 1 day and three weeks.

## Psychrometer

A psychrometer is an instrument to measure directly total suction by applying the pysicometer law (3.7). It determines, then, the value of relative humidity.

The operating principle consists in two thermometers in the same enclosed environment of a soil sample, with identical bulbs but under different conditions (wet vs. dry). The presence of water in the wet bulb generates evaporation, therefore, the temperature of the wet bulb will be lower than that of the dry one. When the ambient reaches equilibrium, its relative humidity will equal that of the soil sample. A relationship exists between this temperature difference and relative humidity. It is possible to calibrate the psychrometer using some salt solutions of known concentration.

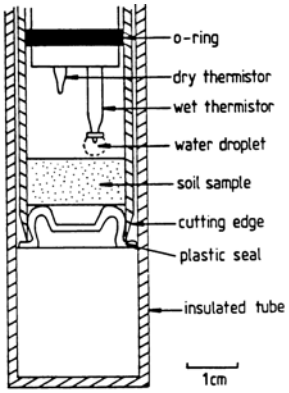


**Fig 3.7** *Thermistor psychrometer* (Ridley, 1995).

There are two types of psychrometers: thermistor and thermocouple. In the thermistor model (Fig. 3.7), there are two thermistors in the same enclosed environment. The two thermistors are identical, but one includes a drop water system (wet bulb) and the other is the dry bulb. The soil sample is enclosed in the same environment. The evaporation of the drop creates an electromotive force (e.m.f) between the two bulbs, once the system reaches equilibrium, the measure of the e.m.f. can be related to relative humidity.

The range of this apparatus is from 100 kPa to 7.5 MPa and it needs a few minutes to reach equilibrium.

In literature there are some examples of the use of this kind of psychrometer to measure total suctions of more than 70 MPa (Woodburn & Lucas, 1995).

The thermocouple psychrometer has similar characteristics to the former type, the equilibrium time and range of application are the same.

The real difference lies in the operating system. In this case, the psychrometer uses the *Peltier Effects* and *Seebeck Effects*. Peltier discovered, in 1834, that if two electrical wires of different material are interconnected, due to the electrical current circulating in the two wires, they will have two different temperatures. The coolest wire will depend on the flow direction of the electrical wires.

Seebeck discovered in 1821 that if in a closed circuit there are two junctions of different metals and a temperature difference in the two cables, there will be an e.m.f. too. This psychrometer is also called Peltier psychrometer, and its scheme is illustrated in Figure 3.8.

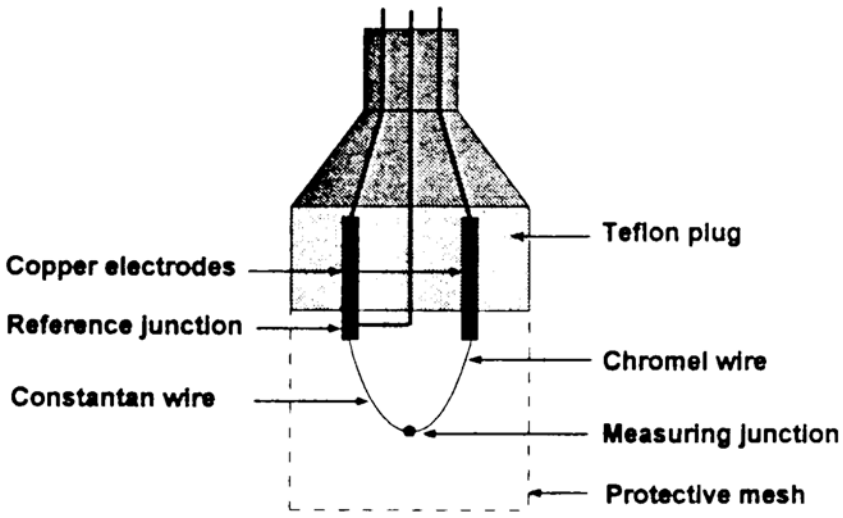


**Fig. 3.8** *Thermocouple psychrometer (Ridley, 1995).*

The psychrometer technique is expensive and the instrument is difficult to calibrate, moreover it is not possible to use it with salt aggregates for the following reasons:

1. matric suction is negligible to osmotic suction, and
2. the high corrosive behaviour of salt aggregates could break the apparatus.

## Tensiometer

The tensiometer is an apparatus that can measure negative water

pressure and is used more in-situ than in laboratory tests. It has an equilibrium time of a few minutes and a very small range of application: no more than 80 kPa.

In fact, investigators from the Imperial Collage of London experimented the use of a tensiometer with a larger range of application (Ridley and Burland, 1993). They found out that it can determine the values of matric suction directly.

The tensiometer consists in a tube with a ceramic head in contact with the soil; and an air entry value of the ceramic piece of 1 atm. The tube is filled with water and when the system is in equilibrium, it is possible to read in a conventional pressure gauge the value of water pressure.

## Axis Translation Technique (Suction and Pressure Plates)

The axis translation technique is a method that may be used to obtain retention curves. It is an indirect measurement, because suction is applied and the water content is measured afterwards. This was the chosen method to determine the retention curve of salt aggregates (see Section 3.4). The bottom of the sample is in contact with a saturated ceramic porous disk. There are different kinds of ceramic disks, whose difference is the *entry air value*.

**Table 3.2** *Properties of ceramic disks from Soilmoisture Equipment.*

| ***Type of disk*** | ***Pore diameter*** **[x $10^{-3}$ mm]** | ***Water permeability*** **[m/s]** | ***Air entry value*** **[kPa]** |
|---|---|---|---|
| ½ bar high flow | 6.0 | 3.110 x $10^{-7}$ | 48÷62 |
| 1 bar | 2.1 | 3.460 x $10^{-9}$ | 138÷207 |
| 1 bar high flow | 2.5 | 8.600 x $10^{-8}$ | 131÷193 |
| 2 bar | 1.2 | 1.730 x $10^{-9}$ | 241÷310 |
| 3 bar | 0.8 | 1.730 x $10^{-9}$ | 317÷483 |
| 5 bar | 0.5 | 1.210 x $10^{-9}$ | >550 |
| 15 bar | 0.16 | 2.59 x $10^{-11}$ | >1520 |

Table 3.2 shows de characteristics of disks from Soilmoisture Equipment Corporation.

A ceramic disk is a permeable material that allows seepage, but, if the air pressure is inferior to the entry value, the air will not pass through the disk. The difference between the suction plate and the pressure plate is that the former works at atmospheric pressure ($\mathbf{u_a}$=0) and that in the latter an air pressure ($\mathbf{u_a}\neq$0) is applied.

The maximum value of matric suction that can be applied depends on the ceramic disk, because the suction must be lower than the air entry value of the

disk, so the maximum absolute value, using ceramic disks, is about 1500 kPa.

If the ceramic disk is changed by a micro membrane of seepage the range of suction measured reaches a valuel of 14 MPa, due to the very small diameter of its pores. Nevertheless, the small thickness of the membrane reduces its life, because it has problem of durability.

Several authors suggest different values for the equilibrium time. It is difficult to give an average value, because the equilibrium time depends on several factors:

- ceramic disk thickness and permeability;
- saturation degree of the soil;
- water conductivity of the soil, and
- contact between soil and ceramic disk.

For example, Ridley (1995) states that the equilibrium is reached after several hours while Lloret (1993) advocates for an equilibrium time of some days.

Finally, it was possible to observe during the development of these tests that the equilibrium time for salt aggregates is more or less three weeks, for the lowest head gradients [$u_a$-$u_w$<50 kPa].

More details about this method will be illustrated below, where the laboratory tests determining the retention curve are described.

## 3.4 *Methodology to measure matric suction on a compacted sample of salt aggregates*

The determination of the retention curve of the salt aggregates was developed in three separated phases. The first part was a pre-investigation campaign in laboratory, in which the first qualitative conclusions were defined and allowed to prepare the lab test programme. After that, the laboratory tests using the axial translation technique were carried out and finally the results interpretation were given.

The suction to be measured was the matric one, because in the pre investigation tests it was clear that the values for matric suction were much smaller than the osmotic ones (see _Table 3.1) and so, if the total suction of salt aggregates were determined, it would not be possible to separate the matric part from the osmotic one.

The order of magnitude of matric suction is of 50 kPa, reaching 100 kPa for low porosity and low saturation degree. In this range of application, the best equipment for salt tests is the axis translation technique.

The test phases are:

1. compaction of salt aggregates to prepare the sample;
2. application of matric suction, and
3. determination of the saturation degree when there is equilibrium.

The granulometry of the grains was between 0.540 and 1 mm.

A known quantity of salt is placed into a compaction apparatus with a saturated quantity of brine (in concentration). The quantity of salt is the one necessary to determine a sample of the prefixed porosity after compaction. The weight of the brine is unknown, because the quantity of brine during the sample preparation process is greater than the one needed to saturate the sample.

To avoid sample dissolution phenomena, especially during the compaction phase, the liquid used in the test was saturated brine of the same mineral (NaCl). Therefore, the brine was stored in a tank in which there is an excess of salt. The concentration value of NaCl is about 36 g per 100 gr of pure water.

Thus, the filling operation of the apparatus is done so that there is not any air surrounding the salt grains. Therefore, it is necessary to wait some minutes, before applying the load to create the sample. The compaction apparatus is a sealed system with a brine exit tube on top of the piston allowing the unnecessary brine to go out during the compaction process (Fig. 3.9 and 3.10).

The sample is cylindrical with a diameter of 50 mm and a height of 20 mm. The sample dimensions were established after trying different sample sizes and shapes and considering that these were the size and shape that allowed finding out the correct total volume and that reduced the measurement errors. The time needed to reach equilibrium also influenced the choice of the sample dimensions and shape.

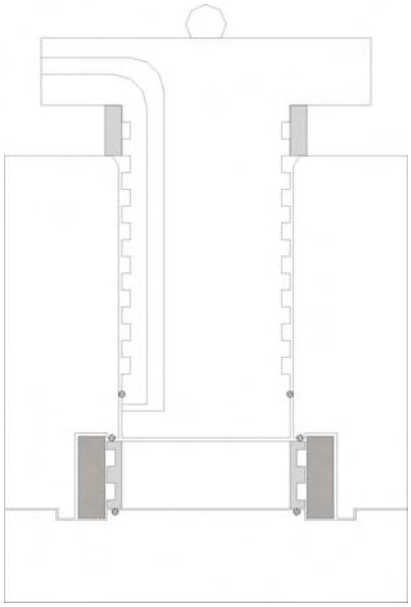

**Fig 3.9** *Diagram of the apparatus to prepare the samples.*

At each step of the experiment the salt sample is contained in an iron retention ring (Fig. 3.11).


**Fig. 3.10** *Compactor during the preparation process.*

Some results presented in this chapter were obtained from a different sample type, which was used at the beginning of the investigation, in the developed suction plate for salt material. In this case, an oedometer of 50 mm

diameter was used to prepare the sample. The sample ring had a conic part on the top of the sample to adjust its shape to the oedometer wall, that system was changed for another one, in which the sample is more regular and the system is more accurate.

The first points were not repeated because it was determined that the error system was little and there was no time convenience. The sample size was the fundamental starting point to design the compaction apparatus and the pressure plate.

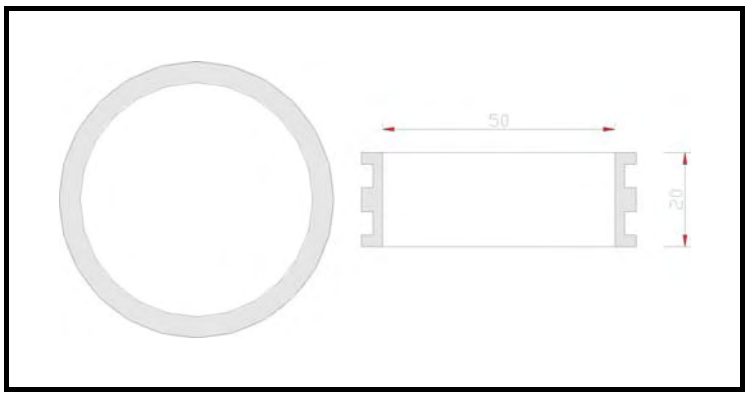


**Fig. 3.11** *Sample ring.*

After the compaction and before being placed on the suction plate, the sample is controlled to check the weight, saturation degree and porosity. Once the sample is placed in the suction plate, a suction value is applied.

**Fig. 3.12** *Sample in the suction plate with coil spring.*

To guarantee the contact between the bottom of the sample and the ceramic disk surface, it is necessary to apply a vertical force. Two methods were used, the first is to apply a weight on the top of the sample. This method is convenient if there are few samples. Nevertheless, if the samples in the apparatus are many it could be less productive than the second method, which consists in applying the force with a coil spring, one for each sample (Fig. 3.12).

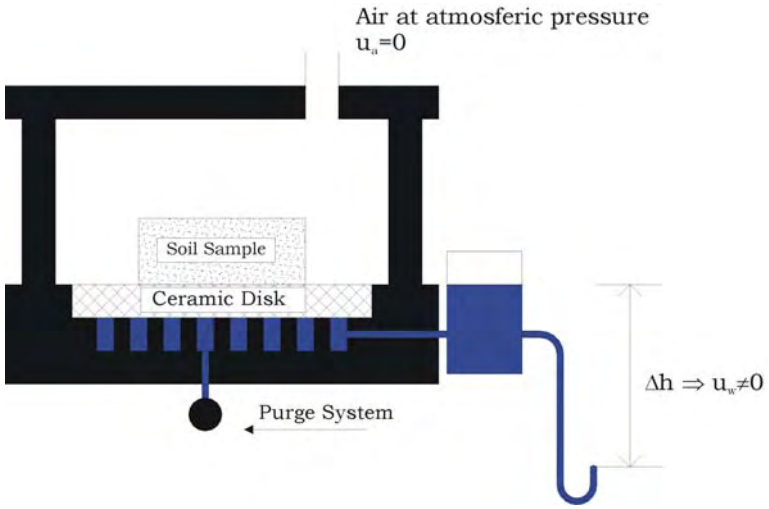


**Fig 3.13** *Working diagram of the suction plate.*

Once the contact between the ceramic disk and the lower side of the sample is established, the matric suction is applied, using two different systems:

1. "Suction Plate": The apparatus is in a room at controlled temperature (23º C), the sample is at atmospheric pressure ($u_a$=0) and the suction is applied putting the brine tube at a fixed height from the upper face of the ceramic disk. This height represents the matric suction applied to the sample (Fig. 3.13).

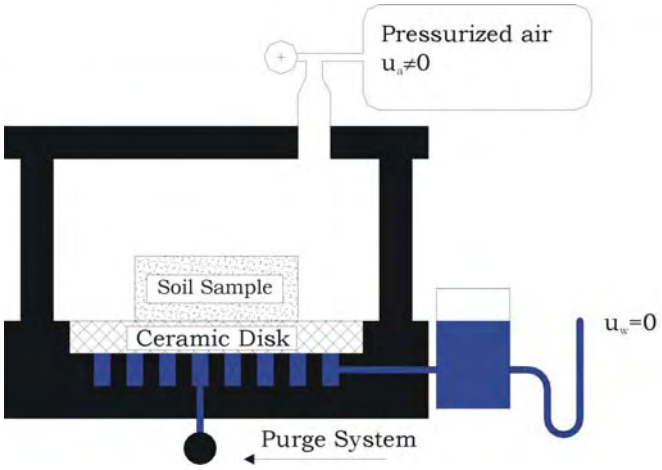


**Fig 3.14** *Working diagram of the pressure plate.*

2. "Pressure Plate": Also in this case the apparatus is in a room at controlled temperature (23º C), but the tube is at the same level of the upper face of the ceramic disk ($u_w$=0) and the matric suction is applied with an air pressure. The value of the air pressure is the matric suction applied to the sample (Fig. 3.14).

In both cases, the brine will keep coming out from the tube, until the equilibrium between the samples and the ceramic disk is reached, which depends on the suction applied and on the permeability of the ceramic disk. In the tests developed, this time varied from three days to three weeks for the lowest values of matric suction.

There are two methods to control if the system is in equilibrium: firstly by observing the seepage it is possible to detect if brine comes out from the tube (visual control). If there is seepage, the concavity of the contact surface is direct downward, while if the system is in equilibrium, the concavity is upward, due to the surface tension.

Then, to be sure that the equilibrium is reached, the operator must check the sample's weight, which should be constant. It is for this reason that two measurements of weight are done, one after twelve hours from the other. If this control is positive, then there is equilibrium and the experiment can pass to the next level.

Finally, in order to find out the saturation degree, the weight under equilibrium conditions is compared to the dry weight of the sample. At this step there are two differences between the salt and the other soils, the first is that there is a quantity of salt that precipitates from the brine when the sample is in the laboratory oven. This quantity must be taken into consideration when determining the porosity and saturation degree. Figure 3.15 shows the salt condition in the various steps of the experiment.

As explained in Chapter 2, to be sure that water evaporates completely, the second difference is that the oven must work at more than 180º C. ("Dry sample" condition).

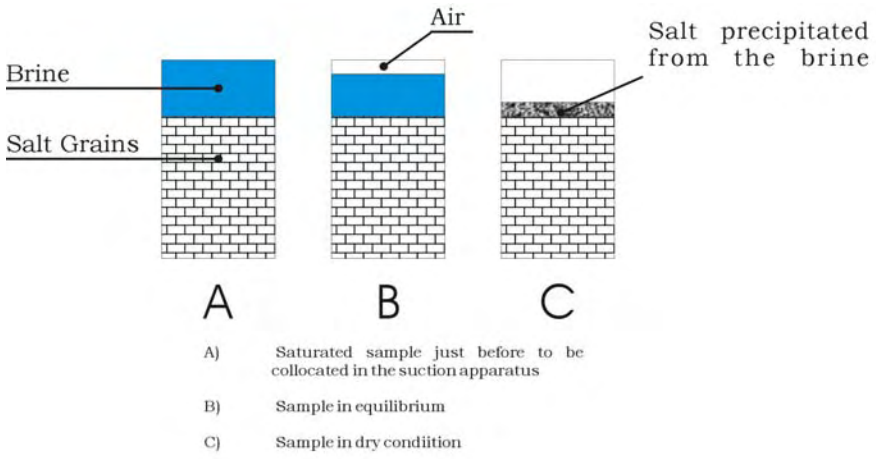


**Fig. 3.15** *Sample condition in the different steps of the suction experiment.*

The suction apparatus (Fig. 3.16) used for the experiment was specially studied to be used with salt samples and brine. Figure 3.19 shows its installation and main details. The apparatus is designed to apply air pressure up to 200 kPa and it is possible to fill in up to 9 samples of 50 mm in diameter. It is

made of AISI 319 iron with special characteristics for corrosion resistance.

The initial design hypotheses were:

- the dimensions of the ceramic disk;
- the forecast of salt retention curves;
- the sample dimensions, and
- all the special characteristics of an experiment with a salt material.

The most important parts of the suction plate are:

1. the ceramic disk;
2. the iron chamber;
3. the spiral channel to distribute the brine uniformly below the ceramic disk;
4. the level tube;
5. the over pressure valve, and
6. the air applying system.

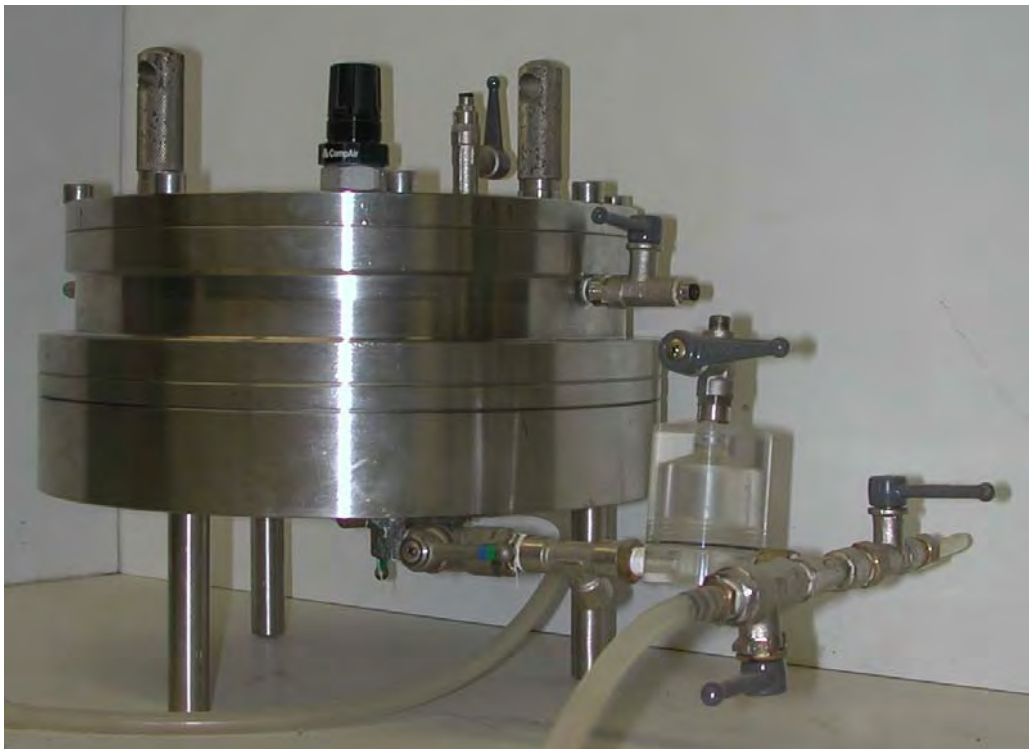

**Fig. 3.16** *The suction plate apparatus*

The ceramic porous disk is a 2-bar type made by Soilmoisture Equipment. The diameter is 140 mm and the thickness, 5 mm.

The firm gave, in its specification sheet (see Table 3.2), a pore diameter of $1.2 \times 10^{-3}$ mm, an air entry value of about 250 kPa and a water permeability of $1.730 \times 10^{-9}$ m/s. Laboratory tests determined a brine permeability between $0.95\ 10^{-7} \div 1.85\ 10^{-7}$ m/s, the permeability and saturation conditions of the porous disk were checked several times during the tests to control its efficiency

and good condition.

The porous stone was lathed to obtain two horizontal surfaces to guarantee a perfect contact between the iron base and the lower face of the disk throughout the surface and to allow the contact between the sample and the upper face of the ceramic disk. The disk is then glued to the iron base.

These two operations are very difficult because of the fragility of the ceramic material.

Three parts constitute the iron chamber:

- the base;
- the wall ring; and
- the cap.

The three parts are connected by pins and the plate is sealed by some o-rings, the cap is opened for normal operations. The pins between the base and the wall ring are twisted off only for special maintenance operations. They also block the porous stone, so it is dangerous to twist them. In fact, should they be twisted, all the preparation operations would have to be repeated.

**Fig.3.17** *Upper side of the base of the suction plate.*

The most important part of the suction plate is the base, (Fig. 3.17), because it should be thick enough to avoid deformations, which could break the ceramic stone, and, at the same time, the spiral where the brine flows is milled in this part of the suction plate. This spiral is a significant part of the system, because it allows the uniform distribution of brine and, at the same time, avoids preferential paths. In the case of brine, the spiral channel must be wider and deeper than usual to avoid saline incrustations that could stop the flow. Actually

this was one of the conclusions of the pre-investigation phase, in which commercial suction plates revealed this problem. In this case, the channel was 8 mm wide and 6 mm deep. Two valves connected the spiral to the exterior. The first one was in the center of the lower face of the base and was used to let brine flow in the spiral to eliminate air bubbles and incrustations. Of course, this was a maintenance operation and was carried out every time it was necessary (at least once every two months). The second valve lead to the brine level; generally speaking, it was always open to keep the brine pressure at a fixed level.

In this circuit, “Brine Circuit”, there are two important pieces: the air trap and the level tube. The pipeline from the valve to the air trap is made of iron and placed in the position required to have a fixed volume of brine in it. The air trap was bigger than usual to allow brine flow, in the upper part of the air trap there is a valve and in the bottom there is a flexible transparent rubber tube connecting the brine level tube.

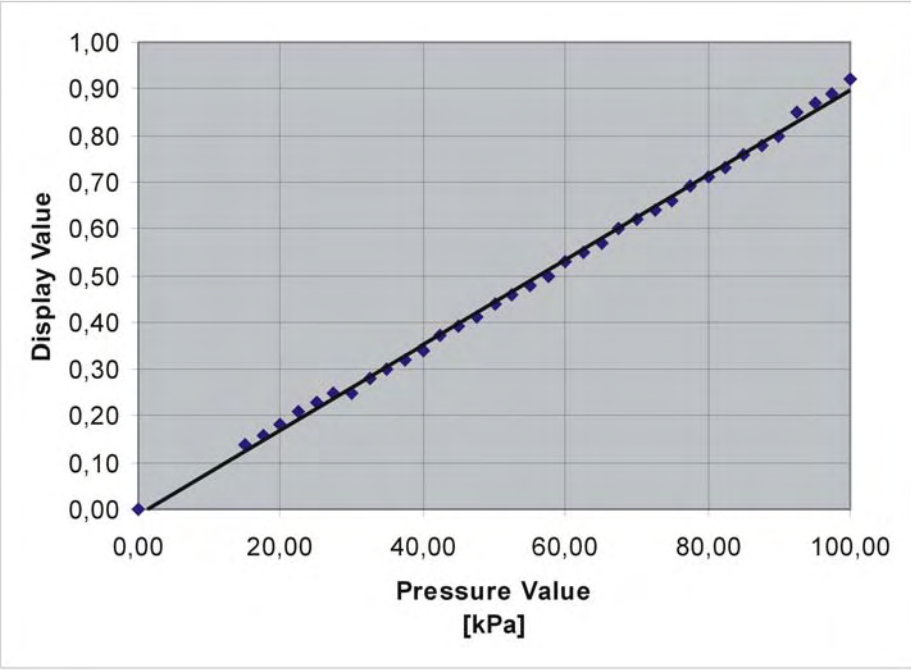


**Fig.3.18** *Calibration graphic of the measurement apparatus of the air pressure system.*

The level tube is a rigid transparent plastic tube. The upper side was put at a fixed level to obtain the requested brine pressure. In the open side of the tube there was some silicon oil to avoid evaporation and a system with a tank to collect the brine that goes out [See details in Figure 3.19].

The wall ring has two spherical valves; which are normally used to connect the chamber to the external ambient in order to keep the atmospheric pressure during suction plate tests or in case of using them as a pressure plate to discharge the air pressure after the tests to move the samples.

All the air pressure applications are in the cap. There are two threads, one including the over pressure valve and another with a spherical valve through which the airflow enters.

The overpressure valve is a COMPAIR model A130-2 and has a maximum air pressure of 700 kPa. In this case, the opening pressure is 175 kPa, because of the ceramic disk air entry value and the apparatus design strength.

The “air circuit” consists of several accesories but basically the most important of its pieces are the air regulator and the air pressure gauge.

The air pressure regulator is a BELLOFRAM type 70 with a maximum air pressure entry value of 1700 kPa and a range of air pressure exit between 0 and 200 kPa. Its resolution is of 1 kPa but, probably, that is a limitation of the digital display (0.00 bar) because the impression is that the sensibility of the air regulator is higher.

The pressure gauge is a TME model PI 103 SC with a maximum pressure value of 200 kPa. A LEXITRON L2 digital meter, which could show variations of 1 kPa, displayed the pressure values.

This measurement system was calibrated with a highly precise analogical air pressure manometer. The calibration graphic is shown in Figure 3.18. The regression coefficient of the envelope line is 0.9981. In any case, the method of application of matric suction reduces the error between the wished matric suction and the displayed value, because it is a direct way: so it is sufficient to know the correspondence for those few air pressure values that will be applied to fix the matric suction. Thus, it was possible to put in a table during the calibration phase the correspondence between these air pressure values and the displayed values.

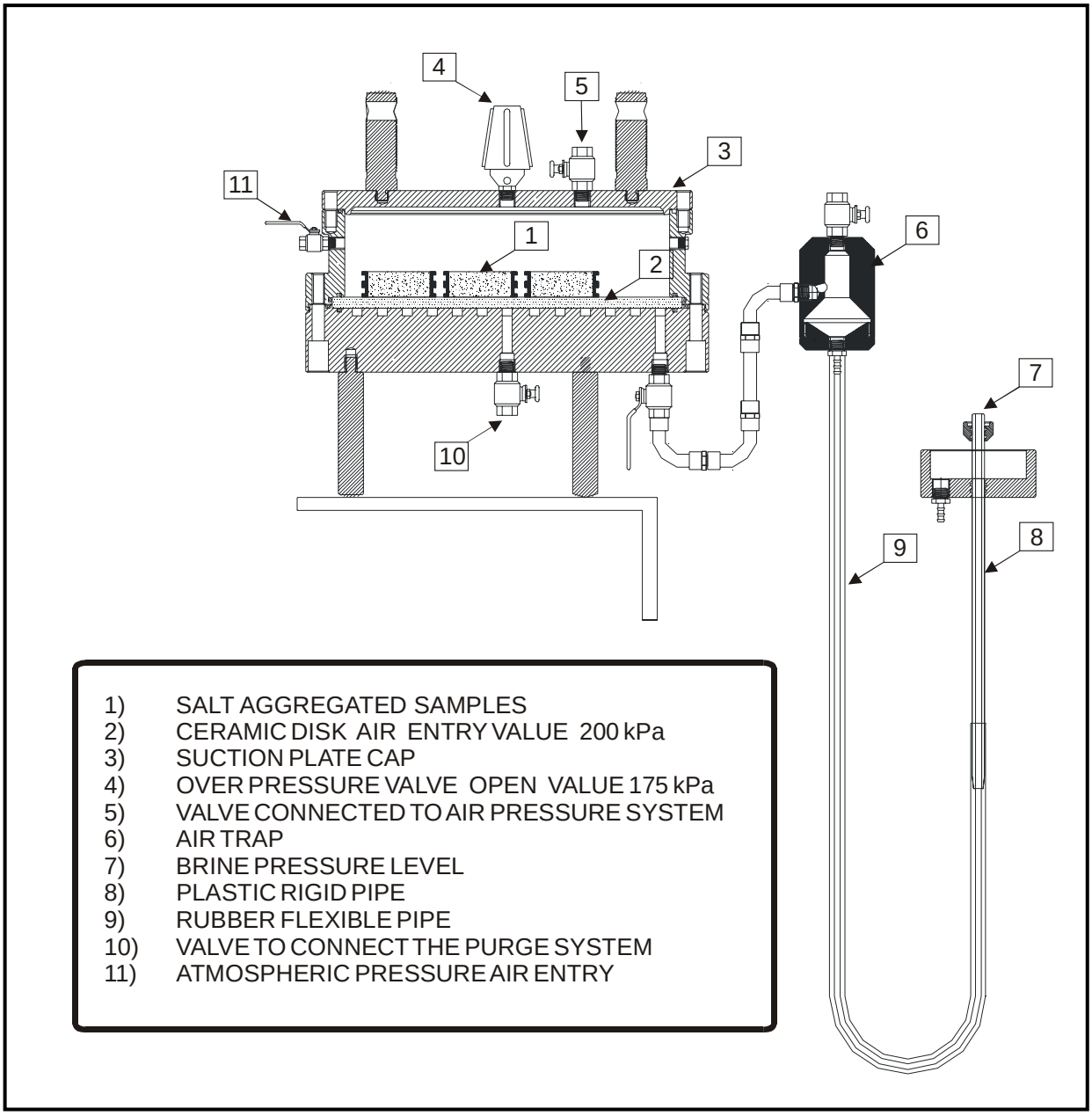


**Fig.3.19** *Suction plate used to determine the retention curves. The picture shows the plate during a suction plate application, in which the matric suction is applied by a brine pressure difference.*

## 3.5 *Experimental results*

The task of this experiment was to determine the retention curve of compacted salt. Two different values of porosity were studied (5% and 10%) in the dry path of the retention curve. For each point of the retention curve at least three different samples were used. To avoid errors three new samples were used for each suction value.

Table 3.3 shows the matric suction values applied for the two values of porosity and the number of samples in each case.

**Table 3.3** *Tests on compacted sample of salt aggregates to determine the retention curve*

| $u_a$-$u_w$ [kPa] | Number of samples for the matric suction fixed value for a sample porosity of 5% | Number of samples for the matric suction fixed value for a sample porosity of 10% |
|---|---|---|
| 0.5 | 4 | 6 |
| 1.0 | 1 | 4 |
| 1.5 | 0 | 5 |
| 2.0 | 3 | 3 |
| 2.5 | 2 | 4 |
| 3.5 | 1 | 4 |
| 4.5 | 3 | 3 |
| 5.5 | 3 | 3 |
| 6.0 | 2 | 4 |
| 7.5 | 4 | 2 |
| 10.0 | 3 | 4 |
| 12.5 | 4 | 4 |
| 15.0 | 3 | 3 |
| 17.5 | 3 | 3 |
| 30.0 | 2 | 4 |
| 50.0 | 1 | 3 |

The experiment can be divided into two steps: in the first one (up to a matric suction value of 12.5 kPa) the suction was applied by a negative brine pressure and a null atmospheric pressure, from there [$u_a$-$u_w$ = 17.5 kPa], the points were determined by the pressure plate method.

As shown in the previous paragraph the points belong to the drying path of the retention curve. The van Genuchten Equation (1980) can be used to fit the measured points to the salt aggregate retention curve:

$$S_e = \frac{S_l - S_{rl}}{S_{ls} - S_{rl}} = \left( 1 + \left( \frac{u_a - u_w}{p_o \dfrac{\sigma}{\sigma_0}} \right)^{\frac{1}{1-\lambda}} \right)^{\lambda} \qquad (3.8)$$

where:

- **$S_l$** is the (brine) saturation degree
- **$S_{rl}$** is the residual saturation degree
- **$S_{ls}$** is the maximum saturation degree, usually $S_{ls}$=1
- **$p_0$** is the air entry value of the soil (in the graph it is the suction value in the inflection point of the retention curve, it has the dimensions of a pressure and it is one of the parameters to be determined)
- **$\sigma_0$** is the surface tension at the temperature in which $p_0$ is measured ($\sigma_0$= 0.072 N/m at 20º C)
- **$\lambda$** is the second parameter to be determined and gives the shape of the retention curve

In the following pages, the experimental results to determine the retention curves are given in some tables. Not all the results of the calculation are presented, but only the most representative, in order to make the relative analysis.

For each experimental step the tables report the porosity values (theoretical and measured), sample height, saturated weight, sample weight when equilibrium is reached, crystal weight and, of course, saturation degree, the object of this investigation work.

The crystal weight is obtained subtracting from the dry weight the salt quantity precipitated during the drying of the sample in the stove (See Fig. 3.15c). In order to know this salt weight, the concentration of salt in brine and the weight in several wet condition (saturated and equilibrium ones) are considered.

The two retention curves for the studied porosities are presented below, each in a separate graph, with its own experimental data. (See Fig. 3.20 and 3.21)

Table 3.4 $u_a$-$u_w$ = 0.5 kPa

| Porosity | | Sample height | Weight [g] | | | Saturation Degree |
|---|---|---|---|---|---|---|
| *Theoretical* | *Laboratory* | [mm] | *Saturated* | *Equilibrium* | *Crystal* | |
| **5 %** | 6.73% | 15.06 | 51.9999 | 51.8509 | 50.02171 | 96.77% |
| | 6.91% | 15 | 51.7098 | 51.5188 | 49.68863 | 94.85% |
| | 7.61% | 15.17 | 52.2373 | 52.0323 | 49.98116 | 95.21% |
| | 7.90% | 15 | 51.4716 | 51.3086 | 49.16181 | 97.24% |
| **10 %** | 10.16% | 14.93 | 50.7181 | 50.5661 | 47.76063 | 99.16% |
| | 11.61% | 14.88 | 50.2204 | 50.1054 | 46.84827 | 99.89% |
| | 11.86% | 15.09 | 50.8774 | 50.7084 | 47.38489 | 99.46% |
| | 11.95% | 15.03 | 50.6148 | 50.4008 | 47.1126 | 98.19% |
| | 12.33% | 14.95 | 50.2549 | 49.9109 | 46.66058 | 94.73% |
| | 15.30% | 15.5 | 51.6608 | 51.3278 | 47.00934 | 97.14% |

Table 3.5 $u_a$-$u_w$ = 1.0 kPa

| Porosity | | Sample height | Weight [g] | | | Saturation Degree |
|---|---|---|---|---|---|---|
| *Theoretical* | *Laboratory* | [mm] | *Saturated* | *Equilibrium* | *Crystal* | |
| **5%** | 8.52% | 15.05 | 51.5266 | 51.1706 | 49.02635 | 90.06% |
| **10 %** | 10.40% | 15.37 | 52.3653 | 51.9203 | 49.23589 | 90.08% |
| | 10.98% | 14.98 | 50.6678 | 50.1648 | 47.46006 | 88.62% |
| | 12.87% | 14.9 | 49.9774 | 49.4381 | 46.2356 | 89.89% |
| | 14.07% | 14.88 | 49.6306 | 49.253 | 45.54384 | 95.06% |

Table 3.6 $u_a$-$u_w$ = 1.5 kPa

| Porosity | | Sample height | Weight [g] | | | Saturation Degree |
|---|---|---|---|---|---|---|
| *Theoretical* | *Laboratory* | [mm] | *Saturated* | *Equilibrium* | *Crystal* | |
| **10 %** | 9.31% | 15.12 | 51.6188 | 51.2268 | 48.87035 | 90.04% |
| | 9.84% | 15.16 | 51.6524 | 51.2294 | 48.73898 | 89.78% |
| | 11.26% | 14.87 | 50.2764 | 49.6714 | 47.00968 | 85.78% |
| | 11.45% | 14.9 | 50.3172 | 49.8732 | 46.98711 | 90.97% |
| | 12.00% | 14.85 | 50.0386 | 49.5818 | 46.55876 | 91.17% |

Table 3.7 $u_a$-$u_w$ = 2.0 kPa

| Porosity | | Sample height | Weight [g] | | | Saturation Degree |
|---|---|---|---|---|---|---|
| *Theoretical* | *Laboratory* | [mm] | *Saturated* | *Equilibrium* | *Crystal* | |
| **5 %** | 6.75% | 15 | 51.7483 | 51.3813 | 49.77377 | 85.71% |
| | 7.65% | 15.25 | 52.555 | 52.291 | 50.27246 | 92.73% |
| | 8.02% | 15.25 | 52.4656 | 52.1496 | 50.07474 | 91.08% |
| **10 %** | 13.27% | 15.04 | 50.3341 | 49.8715 | 46.44037 | 92.42% |
| | 15.34% | 15 | 49.6746 | 49.3369 | 45.18746 | 96.77% |
| | 16.16% | 15.01 | 49.5174 | 49.1303 | 44.78837 | 96.11% |

Table 3.8 $u_a$-$u_w$ = 2.5 kPa

| Porosity | | Sample height | Weight [g] | | | Saturation Degree |
|---|---|---|---|---|---|---|
| *Theoretical* | *Laboratory* | [mm] | *Saturated* | *Equilibrium* | *Crystal* | |
| **5 %** | 7.02% | 15.05 | 51.8881 | 51.5381 | 49.82586 | 87.33% |
| | 7.04% | 15.09 | 52.4943 | 51.9413 | 50.421 | 83.89% |
| **10 %** | 9.76% | 14.85 | 50.5757 | 50.2957 | 47.74664 | 94.40% |
| | 10.09% | 15.2 | 51.5996 | 51.1376 | 48.61125 | 88.84% |
| | 11.74% | 15.15 | 51.148 | 50.772 | 47.67484 | 93.47% |
| | 14.20% | 15.07 | 50.2289 | 49.9339 | 46.05344 | 97.23% |

Table 3.9 $u_a$-$u_w$ = 3.5 kPa

| Porosity | | Sample height | Weight [g] | | | Saturation Degree |
|---|---|---|---|---|---|---|
| *Theoretical* | *Laboratory* | [mm] | *Saturated* | *Equilibrium* | *Crystal* | |
| **5 %** | 6.13% | 15 | 51.8982 | 51.6232 | 50.1053 | 88.96% |
| **10 %** | 8.39% | 14.73 | 50.5477 | 50.2467 | 48.13177 | 91.84% |
| | 8.66% | 14.87 | 50.8975 | 50.5005 | 48.38334 | 88.51% |
| | 10.14% | 14.83 | 50.4262 | 50.1742 | 47.49087 | 95.71% |
| | 10.91% | 15.34 | 52.1174 | 52.0814 | 48.84186 | 98.90% |

Table 3.10 $u_a$-$u_w$ = 4.5 kPa

| Porosity | | Sample height | Weight [g] | | | Saturation Degree |
|---|---|---|---|---|---|---|
| *Theoretical* | *Laboratory* | [mm] | *Saturated* | *Equilibrium* | *Crystal* | |
| **5 %** | 4.72% | 14.94 | 52.054 | 51.48 | 50.67739 | 84.33% |
| | 5.43% | 15.09 | 52.4405 | 51.9835 | 50.84193 | 75.71% |
| | 6.22% | 14.93 | 51.665 | 51.129 | 49.85485 | 74.69% |
| **10 %** | 10.25% | 14.73 | 50.1058 | 49.3819 | 47.15444 | 79.77% |
| | 10.64% | 14.91 | 50.5425 | 49.8001 | 47.44772 | 80.31% |
| | 10.68% | 14.76 | 50.0915 | 49.4067 | 47.01153 | 82.07% |

Table 3.11 $u_a$-$u_w$ = 5.5 kPa

| Porosity | | Sample height | Weight [g] | | | Saturation Degree |
|---|---|---|---|---|---|---|
| *Theoretical* | *Laboratory* | [mm] | *Saturated* | *Equilibrium* | *Crystal* | |
| **5 %** | 3.81% | 14.87 | 52.3251 | 52.0151 | 51.21978 | 76.25% |
| | 5.04% | 14.98 | 52.7389 | 52.3739 | 51.26542 | 79.53% |
| | 5.06% | 14.89 | 51.8216 | 51.3286 | 50.35197 | 83.09% |
| **10 %** | 8.13% | 14.77 | 50.7293 | 50.2992 | 48.38497 | 85.95% |
| | 11.01% | 14.85 | 50.2754 | 49.7124 | 47.08248 | 86.67% |
| | 12.78% | 14.78 | 49.6495 | 49.1055 | 45.9596 | 89.56% |

Table 3.12 $u_a$-$u_w$ = 6.0 kPa

| Porosity | | Sample height | Weight [g] | | | Saturation Degree |
|---|---|---|---|---|---|---|
| *Theoretical* | *Laboratory* | [mm] | *Saturated* | *Equilibrium* | *Crystal* | |
| **5 %** | 7.61% | 20.22 | 82.922 | 81.419 | 79.34378 | 62.30% |
| | 8.33% | 20.2 | 82.5606 | 81.3826 | 78.64741 | 74.20% |
| **10 %** | 9.87% | 20.33 | 82.488 | 81.605 | 77.81787 | 85.39% |
| | 13.46% | 20.19 | 80.53 | 78.367 | 74.20788 | 70.09% |
| | 13.83% | 20.22 | 80.504 | 78.256 | 73.996 | 69.76% |
| | 14.85% | 20.2 | 80.0287 | 78.3077 | 73.04772 | 79.65% |

Table 3.13 $u_a$-$u_w$ = 7.5 kPa

| Porosity | | Sample height | Weight [g] | | | Saturation Degree |
|---|---|---|---|---|---|---|
| *Theoretical* | *Laboratory* | [mm] | *Saturated* | *Equilibrium* | *Crystal* | |
| **5 %** | 4.17% | 15 | 52.3713 | 51.5513 | 51.15164 | 37.07% |
| | 5.63% | 15.02 | 52.1028 | 51.4898 | 50.45497 | 80.26% |
| | 7.20% | 14.68 | 50.6847 | 49.8463 | 48.61951 | 63.70% |
| | 7.35% | 15.03 | 51.7272 | 51.0682 | 49.57285 | 73.71% |
| **10 %** | 8.06% | 14.8 | 50.834 | 49.8827 | 48.50483 | 63.46% |
| | 13.84% | 14.99 | 50.0075 | 49.1292 | 45.96172 | 82.59% |

Table 3.14 $u_a$-$u_w$ = 10.0 kPa

| Porosity | | Sample height | Weight [g] | | | Saturation Degree |
|---|---|---|---|---|---|---|
| *Theoretical* | *Laboratory* | [mm] | *Saturated* | *Equilibrium* | *Crystal* | |
| **5 %** | 4.69% | 14.88 | 52.3975 | 52.1375 | 51.02105 | 85.41% |
| | 5.74% | 15.03 | 52.1162 | 51.8252 | 50.43318 | 87.01% |
| | 7.32% | 20.65 | 84.187 | 83.338 | 79.92877 | 80.16% |
| **10 %** | 8.30% | 20.25 | 80.291 | 78.463 | 73.37053 | 57.54% |
| | 9.31% | 14.98 | 51.0715 | 49.714 | 48.3529 | 54.37% |
| | 10.09% | 20.6 | 81.2365 | 79.2195 | 73.66057 | 62.60% |
| | 10.33% | 20.5 | 81.3001 | 79.1561 | 74.31583 | 60.77% |

Table 3.15 $u_a$-$u_w$ = 12.5 kPa

| Porosity | | Sample height | Weight [g] | | | Saturation Degree |
|---|---|---|---|---|---|---|
| *Theoretical* | *Laboratory* | [mm] | *Saturated* | *Equilibrium* | *Crystal* | |
| **5 %** | 3.65% | 14.86 | 49.2562 | 48.9433 | 44.79088 | 74.74% |
| | 6.32% | 14.47 | 49.6034 | 49.173 | 46.9946 | 80.29% |
| | 7.79% | 20.32 | 83.26 | 81.855 | 79.57673 | 66.15% |
| | 7.83% | 20.33 | 83.286 | 82.523 | 79.58277 | 83.70% |
| **10 %** | 8.95% | 20.4 | 83.135 | 81.564 | 78.8886 | 67.30% |
| | 12.70% | 20.22 | 80.9438 | 77.9198 | 74.96868 | 53.69% |
| | 12.88% | 20.22 | 80.874 | 77.466 | 74.81431 | 48.06% |
| | 13.01% | 20.3 | 81.144 | 78.597 | 74.99978 | 62.85% |

Table 3.16 $u_a$-$u_w$ = 15.0 kPa

| Porosity | | Sample height | Weight [g] | | | Saturation Degree |
|---|---|---|---|---|---|---|
| *Theoretical* | *Laboratory* | [mm] | *Saturated* | *Equilibrium* | *Crystal* | |
| **5 %** | 5.42% | 20.31 | 82.49 | 81.10 | 79.19 | 49.93% |
| | 7.31% | 20.21 | 83.37 | 80.67 | 79.22 | 25.80% |
| | 7.40% | 20.31 | 83.46 | 81.13 | 79.47 | 37.75% |
| **10 %** | 9.04% | 20.13 | 79.86 | 76.66 | 75.17 | 28.68% |
| | 10.65% | 20.16 | 80.67 | 76.59 | 75.26 | 22.66% |
| | 11.67% | 20.11 | 81.12 | 76.62 | 74.97 | 21.98% |

Table 3.17 $u_a$-$u_w$ = 17.5 kPa

| Porosity | | Sample height | Weight [g] | | | Saturation Degree |
|---|---|---|---|---|---|---|
| *Theoretical* | *Laboratory* | [mm] | *Saturated* | *Equilibrium* | *Crystal* | |
| **5 %** | 6.53% | 20.5 | 84.4934 | 83.0904 | 81.37831 | 24.47% |
| | 6.90% | 20.34 | 83.9107 | 82.8527 | 80.643 | 19.50% |
| | 7.79% | 20.35 | 83.385 | 81.963 | 79.69881 | 26.39% |
| **10 %** | 11.14% | 20.2 | 81.468 | 80.626 | 76.23095 | 16.17% |
| | 12.34% | 20.22 | 81.082 | 77.844 | 75.27433 | 14.17% |
| | 15.93% | 20.18 | 79.5334 | 79.0594 | 72.0552 | 16.60% |

Table 3.18 $u_a$-$u_w$ = 30.0 kPa

| Porosity | | Sample height | Weight [g] | | | Saturation Degree |
|---|---|---|---|---|---|---|
| *Theoretical* | *Laboratory* | [mm] | *Saturated* | *Equilibrium* | *Crystal* | |
| **5 %** | 8.25% | 20.4 | 83.9113 | 80.4213 | 79.49017 | 15.20% |
| | 8.73% | 20.35 | 82.936 | 79.547 | 78.88049 | 22.33% |
| **10 %** | 9.09% | 20.4 | 82.817 | 78.765 | 78.76475 | 10.36% |
| | 10.30% | 20.16 | 81.3552 | 77.0692 | 75.4423 | 15.60% |
| | 11.78% | 20.3 | 81.157 | 77.155 | 75.4989 | 32.37% |
| | 12.35% | 20.3 | 81.107 | 76.672 | 75.4619 | 28.25% |

Table 3.19 $u_a$-$u_w$ = 50.0 kPa

| Porosity | | Sample height | Weight [g] | | | Saturation Degree |
|---|---|---|---|---|---|---|
| *Theoretical* | *Laboratory* | [mm] | *Saturated* | *Equilibrium* | *Crystal* | |
| **5%** | 7.58% | 20.32 | 83.3421 | 80.2411 | 79.75831 | 17.77% |
| **10 %** | 11.35% | 20.2 | 81.3885 | 76.7295 | 76.05513 | 16.94% |
| | 11.76% | 20.15 | 81.028 | 76.346 | 75.51513 | 19.37% |
| | 11.99% | 20.2 | 81.14 | 76.263 | 75.50553 | 17.74% |

**Tables from 3.4 to 3.19** *Experimental results of the axis translation technique for salt aggregates with a porosity of 5% and 10%. Each table reproduces the experimental data for a fixed value of matric suction.*

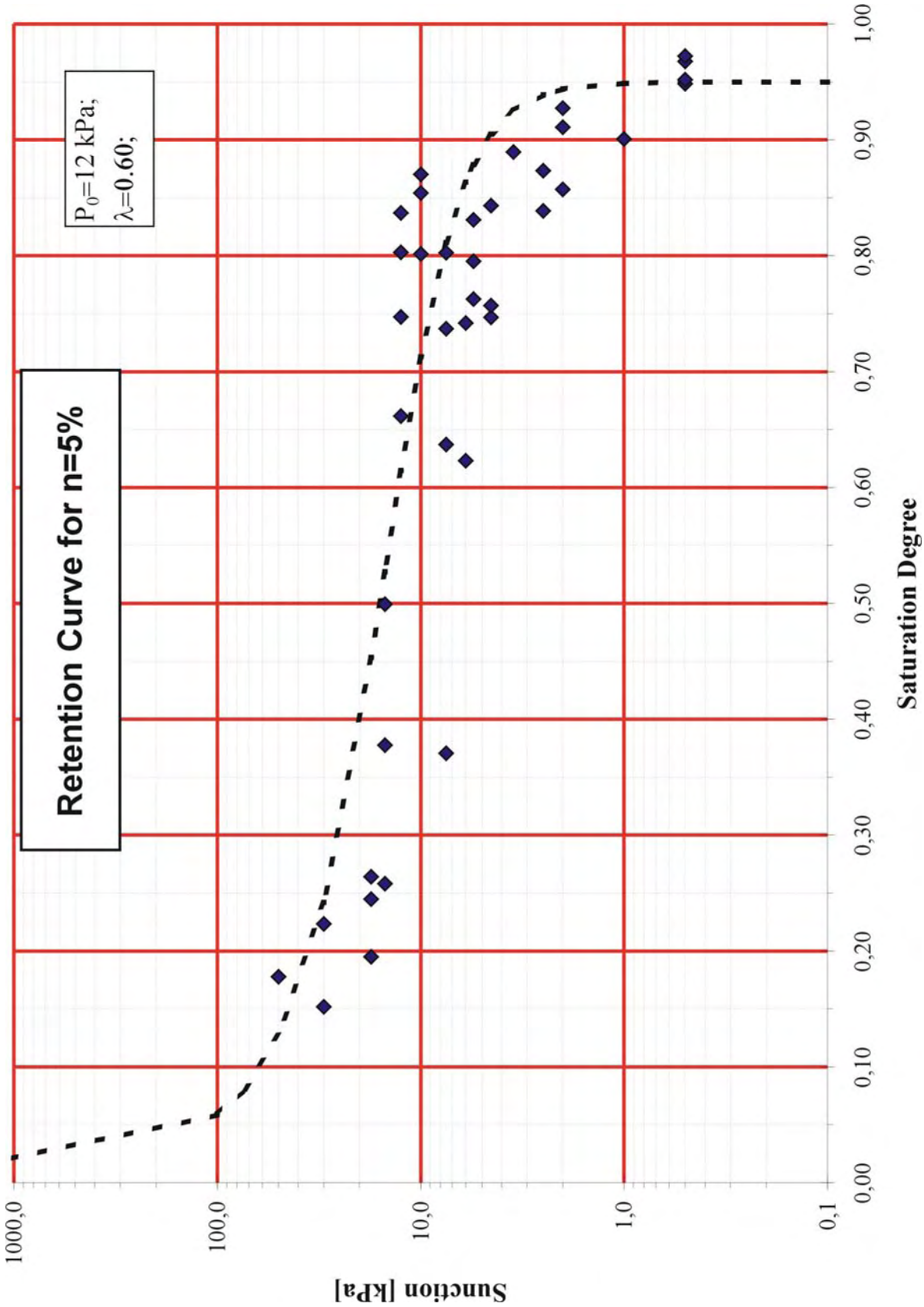


**Fig 3.20** *Retention curve for n=5%*

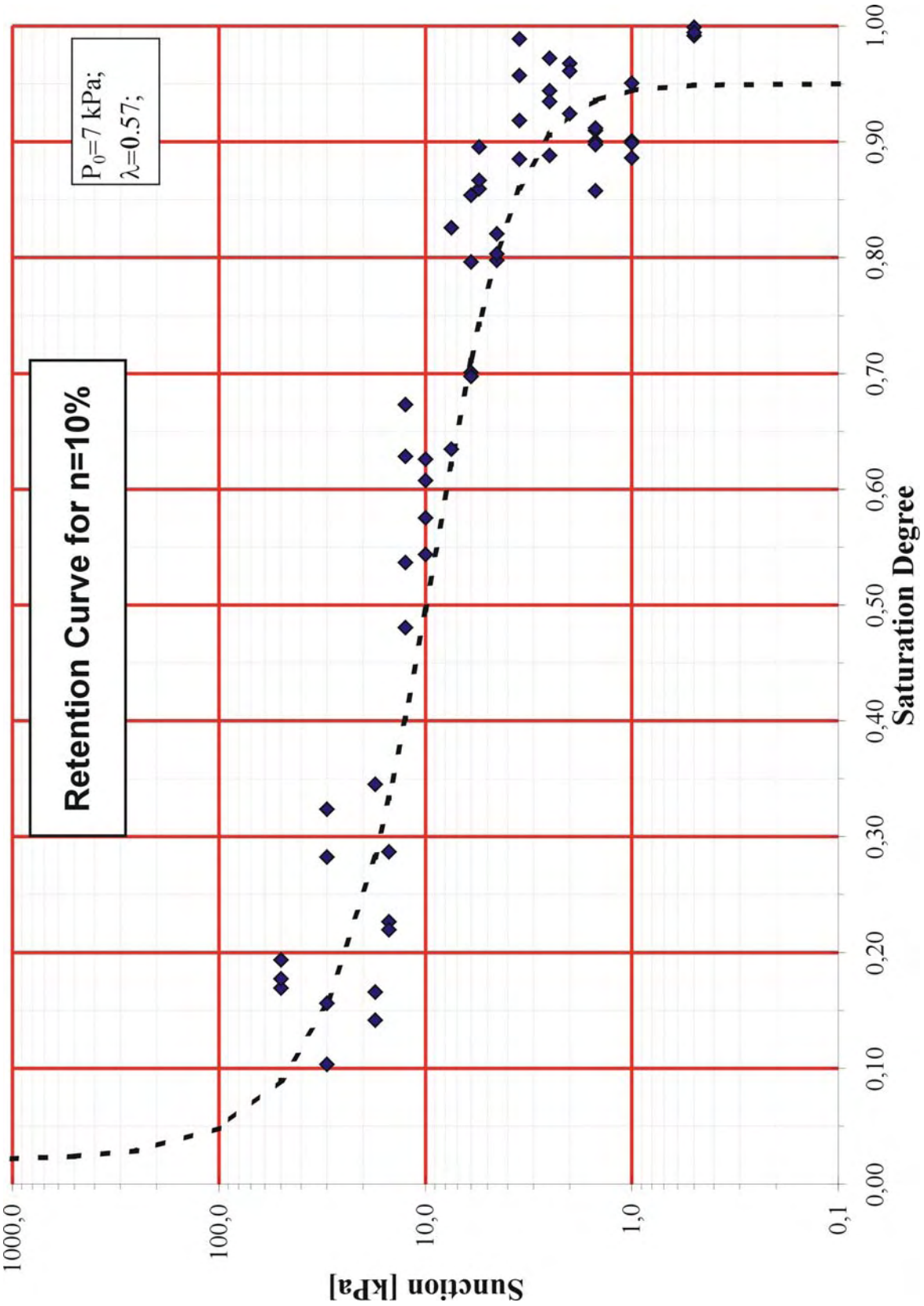


**Fig 3.21** *Retention curve for n=10%*

## 3.6 *Result analysis*

At the beginning of this experimental campaign the idea was to use the same sample for all matric suction points, but the results were not so satisfactory, because they gave a saturation degree of about 15÷30% less with respect to the case in which a sample is used for each measured suction point. This error is due to the continuous manipulation of the sample that loses brine and grains during the translation from the plate to the balance. Furthermore, it is not possible to know the development of the test until the end, after many months, because the measurement of the dry weight is only done at the end of the application of all matric suction values. This is a situation to avoid, because if something went wrong it could not be noticed until the end, in many cases, well before a year had passed there is no control on the test. For this reason those results were not taken into consideration and the tests were developed using the following method: "three new samples for each matric suction value".

The result of the obtained porosity clearly shows that it had a deviation from the theoretical values of n= 5% and n=10%.

For the sample of a nominal 5% porosity the average value is 6.67% with a minimum value of 3.65%, a maximum one of 8.73% and maximum deviation values of –1.35% and 3.73%.

For the second group of samples, theoretical porosity equals 10% and the average value is 11.45% with a minimum value of 8.06%, a maximum one of 16.16% and maximum deviation values of –1.94% and 6.16%.

This deviation from the theoretical and real porosity is due to three different causes:

1. Mistakes in the total sample volume measurements;
2. Environmental humidity of the salt when the sample was prepared. The material was kept in a laboratory at fixed temperature in a sealed container, but it could have variations of the dry weight;
3. The Creep phenomena. The compaction pressure is much higher (>15 MPa) than the pressure that could be applied by the weight on the top side of the sample during the application of the matric suction, moreover the sample is not loaded, at least in the phase in which it is translated from the compactor to the suction plate.

To reduce these effects several precautions were taken. To avoid total volume error during the campaign the sample shape and dimensions were changed, from a composed shape to a new sample: a regular cylinder with a bigger total volume. In Figure 3.22 the two samples are reproduced without the correspondent iron ring.

The difference between theoretical and obtained porosity had a very important effect on the experiment for two reasons.

The first is that the same suction point had to be repeated many times to obtain a laboratory value close to the fixed porosity.

The second one, which was not possible to detect at beginning of the campaign, is that, due to the shape of the retention curves for salt materials, very small variations of porosity (< 1%) will give completely different results, in

terms of saturation degree, for matric suction values of the central part of the retention curve path, the sub-horizontal part, because they belong to different curves.

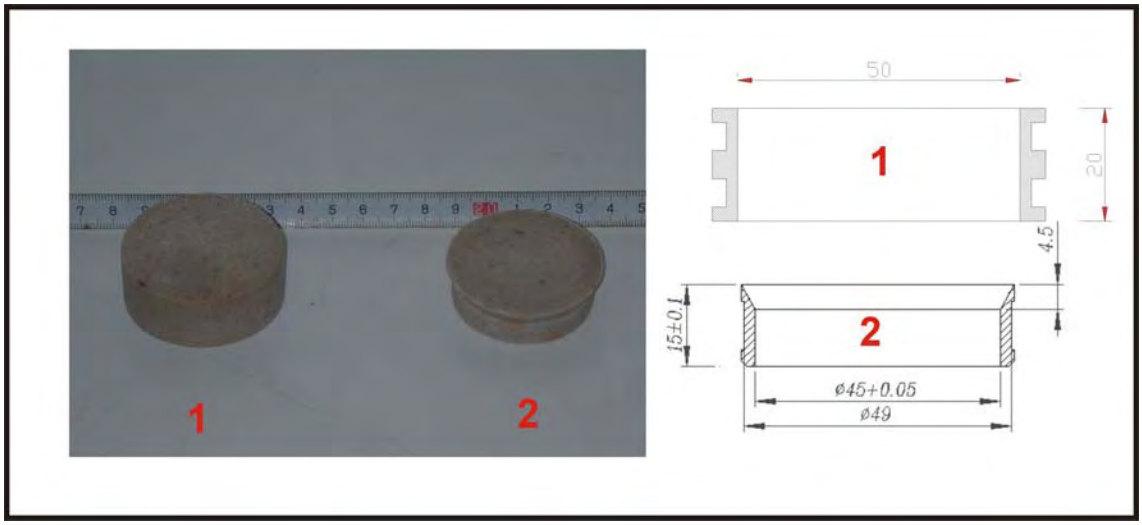


**Fig. 3.22** *Sample types used to determine the retention curves.*

It can be observed in the retention table results that the saturation degree can vary a lot for small variations of porosity and for a fixed matric suction value. For example, this is the case for matric suction ($u_a$-$u_w$) fixed at 15.0 kPa in 3 samples with a theoretical porosity n=5% and whose saturation degree and real porosity were:

- ✓ $S_1$=49.93% $n_1$=5.42%;
- ✓ $S_2$=25.80% $n_2$=7.31%;
- ✓ $S_3$=37.75% $n_3$=7.40%.

The interpolation of the result by the van Genuchten equation shows for both cases some peculiarity. The initial porosity value of 5% gives heavily compacted samples with very low values of matric suction. The air entry value ($p_0$) is 12 kPa for n=5% and 7 kPa for n=10%, and the curve can be easily divided into three different parts.

The most important characteristics of the first sub-vertical part are the air entry value and the intersection with the Saturation Degree axis. In both cases, n=5% and n=10%, the intersection the value is inferior to $S_l$=100%, about 95%.

The second part has a sub-horizontal shape and it is possible to predict that for higher values of porosity this part is practically horizontal, showing great variations of the saturation degree for small changes in porosity.

For example, it can be observed in the n=10% curve how the saturation degree goes from S=0.90 to S=0.50 with a matric suction variation of only 7 kPa.

The last part of the curve is asymptotic to the matric suction axis and the curve change is tangent from sub-horizontal to sub-vertical between 10 and 100 kPa approximately for both curves.

The fact that salt aggregates are a “non conventional” material difficults its comparison to other soil mechanics most common materials.

It is well known in literature that the mechanical behaviour of salt materials is different from other soil mechanics materials. For instance, Chumbe et al. (1996) studied creep phenomena on salt aggregates by means of oedometric tests, and it is also well known that, depending on load conditions, the aggregates can be compared to the behaviour of sand or clays indistinctly.

In the case of the determination of the retention curve of strongly compacted salt aggregates, the comparisons are not that clear.

On the one hand, it can be observed how the sample preparation is that of a soil, while on the other, the sample is a strongly compacted soil (See Fig. 3.22). Thus, the comparison can be done either with a soil or with a rock.

If the path of the retention curves of salt aggregates and that of sand were compared, it would be observed that the two materials have the same type of retention curve path. (Fig. 3.23)

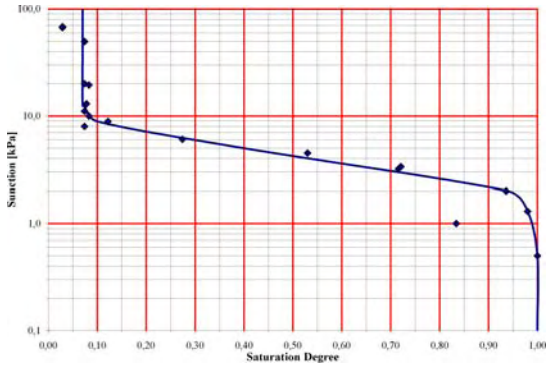


**Fig. 3.23** *Retention curve of the Fontaineblau sand*

In this work this comparison is done with the Fontaineblau sand from Paris (Soeiro, 1964), we used the data from this work and we plotted the data on a new graph to have the same units for matric suction and saturation degree. Dr. Soeiro studied the retention curve during the drying and wetting phases of the two different sands. Only this one was taken into account, because the porosity value was similar to our case. The porosity is about 15% (it was not possible to determine it more accurately). The data on Fig. 3.23 belong to the drying path. The observation of this retention curve shows how close the two cases are, it can be observed that in this curve salt aggregates behave in the same way and that the air entry value is also similar (about 10 kPa).

If we compare the salt retention curves to a rock retention curve, we find that the two curves have very different parameters.

For example, Fig. 3.24 shows the retention curve of a slate stone from Rio Pancrudo (L.A. Oldecop et E.E. Alonso, 2001) with an average porosity of n=8%. It can be observed that the air entry value of this rock is much higher than the heavily compacted salt.

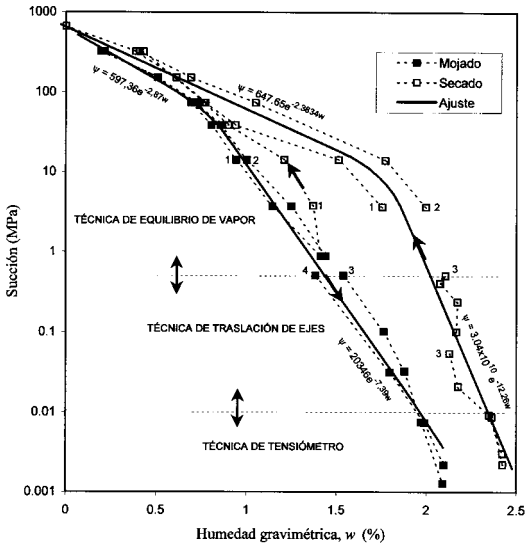


**Fig. 3.24** *Rio Pancrudo Slate Stone retention curve* (L.A. Oldecop & E.E. Alonso, 2001)

Therefore, it is possible to confirm that, in the case of retention curves, the behaviour of salt aggregates is similar to the behaviour of sands.

Due to the high pressure applied to make the sample, it was not possible to reach lower porosity values to find higher values for air entry values. In the pre-campaign works, higher porosity values were tested up to 25%, but these samples showed some problems, because often the sample is destroyed because of low cohesion, during the sample preparation phase or when the sample is raised from the suction plate (because the contact forces between the lower side and the ceramic disk are higher than the cohesion forces).

To study a higher value than n=15% a new apparatus should be prepared to allow researchers to make all the operation of the experiment, from the preparation to the control of the weight, always keeping the contact between the porous stone and the sample. The main object of this part of the experimental program was successfully reached, now the retention curve characteristics of the salt aggregates are well known.

Due to the long laboratory time, it is considered that more analysis in this field are not strictly necessary, but to study in depth the retention curves behavior a new experimental program curve could be done. Our work may give the layout for further studies in which the wetting curves, the influence of grain size and other bigger values of porosity might be investigated. It is easy to foresee that all these new analysis will lead to lower retention curves and lower values of the matric suction. Furthermore in the next chapters we will take a look at the importance of matric suction in the rest of this thesis. In the chapter on numerical simulation, an interpolation of air entry values will be presented to describe its variation regarding porosity.

# CHAPTER 4

# THE POROSITY VARIATION ON SALT AGGREGATES WHEN A TEMPERATURE DIFFERENCE IS APPLIED TO AN UNSATURATED SAMPLE

## 4.1 *Introduction*

The main object of this thesis is to study the sealing/unsealing phenomena caused by the precipitation of the salt transported through the liquid phase.

A quite extensive work has been performed, in the past, in the field of crushed salt compaction (e.g. Spiers et al., 1990: Korthaus, 1996; Olivella et al., 2002) while less effort was made to investigate its hydro-thermal behaviour. Although saline media remain apparently dry, small contents of moisture are the cause of several processes.

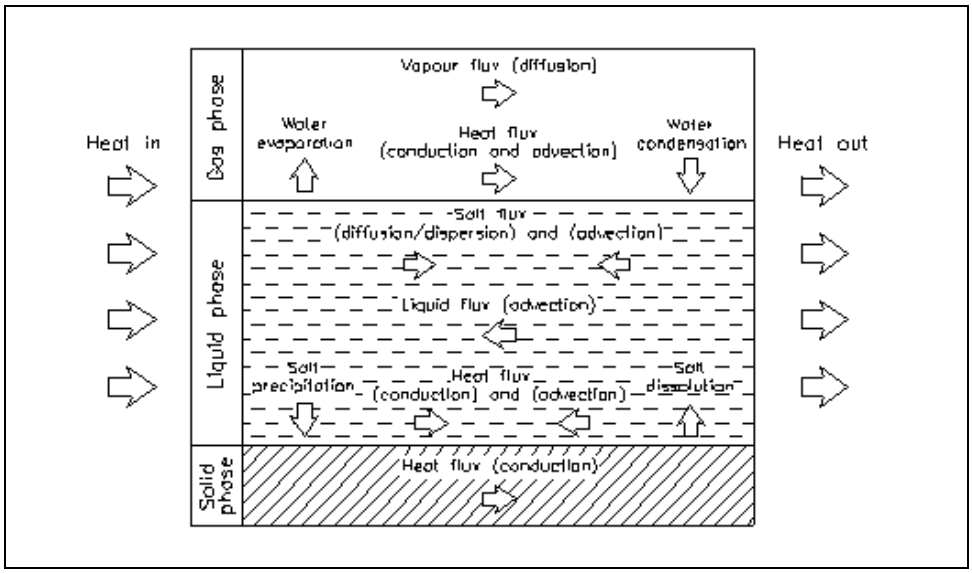


**Fig. 4.1** *Coupled phenomena induced by a temperature gradient (from Olivella, 1995).*

Figure 4.1 (Olivella, 1995) shows a schematic representation of the phenomena involved in a horizontal one-dimensional sample subjected to a temperature gradient. In this problem the medium is assumed to be rigid to avoid the effect of the deformability on porosity changes.

The solubility of salt in water is a function of several variables: one of the most important ones being temperature. The migration of brine inclusions in the solid phase may be caused by temperature gradients. In addition, temperature

gradients may induce important healing phenomena in wet unsaturated saline media.

Firstly, solubility dependence on temperature originates salt concentration gradients. Secondly, temperature-induced vapour concentration originates is the cause of vapour pressure and, consequently, of the migration of water vapour. When water evaporates from saturated brine, the concentration of solute increases above equilibrium solubility and salt precipitates. Likewise water condensation leads to dissolution of salt. The vapour, transferred from a hot region to a cold one, generates a brine motion. The motion of salt in dissolution may be advective (liquid tends to flow in order to compensate for vapour migration) or non-advective (diffusion plus dispersion), induced by gradients of salt concentration.

Under unsaturated conditions, it seems that the second mechanism of solute transfer (i.e. caused by vapour migration) would be dominant with respect to the other one (i.e. induced by temperature-concentration differences). Of course, this relative importance of transport mechanisms depends on the transport properties of the medium. Nevertheless, note that the diffusion of vapour in air is much more effective than the diffusion of salt in brine. The dominance of solute migration induced by concentration differences would take place in saturated conditions because vapour migration is not possible in such a case.

The study of this problem was developed in two different manners: firstly, laboratory tests were carried out, which is the argument of this chapter, and then the results were compared (see the next part of the thesis) by a numerical approach using CODE_BRIGHT, a finite element program developed by S. Olivella to solve the thermo hydro mechanical problems of salt materials. (Olivella et al. 1996 a; Olivella et al. 1996 b)

In this chapter the experimental campaign will be presented and its results will be analysed. It is important, now, to describe briefly the main apparatus used in the experiment in order to understand the theoretical hypothesis and the numerical model used.

The experiment campaign wants to reproduce the phenomena induced in the backfill saline aggregates of a deep nuclear waste deposit when a temperature difference occurs. The laboratory tests reproduced the phenomena at a small scale. Once these results are known, the second phase is the confirmation of the model proposed by Olivella et al. (1994 b) comparing the numerical results to the experimental results. After that, the numerical model will be applied to reproduce the conditions of a deep repository in saline media. At this point, the mechanical conditions will be also introduced to allow predicting the behaviour of the repository during the decay time (centuries).

## 4.2 *Representation of the multi phase flow phenomena in laboratory*

Figure 4.2 shows a scheme of the use of crushed salt as a filling material to give continuity to the system from the waste nuclear canisters to the host rock. The decay time of this waste is very long, the order of magnitude is of some hundreds of years, and during this period the canisters are subjected to high temperatures: more than 250º C.

The presence of a temperature difference between the canister and the host rock generates a heat flux from the canister to the host rock. In the case of salt, this flux is very important because there are two effects: the first one is the liquid (brine) flux, which is common to all kinds of soils used to fill this space, while the second one is only for crushed salt. Furthermore, the concentration of salt dissolved in the brine is different in each point, due to the temperature difference, and there are phenomena of precipitation and of dissolution in the medium thanks to brine flow. It is important to highlight that the water presence in the waste nuclear deposit is limited, but the presence of cracks in the filling material could be a way to create an important seepage.

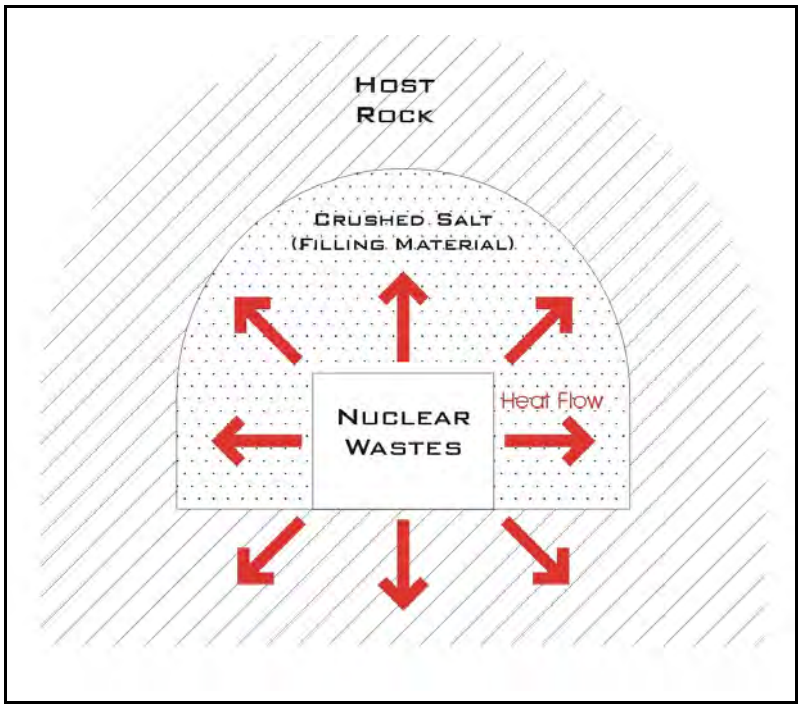


**Fig. 4.2** *Scheme of a gallery used for nuclear waste deposits with a heat flow phenomenon.*

The dissolution of salts in a waste deposit is a phenomenon that should be absolutely avoided, because the loss of salt would mean the loss of one of

the main characteristic of a waste deposit: the waste wouldn't have a proper sealing system.

The effort was focused on the development of a brand new equipment to simulate these phenomena in laboratory (this chapter), and then to simulate it by a numerical approach (Chapter 5). In the next paragraphs, the details of this laboratory equipment will be presented, but before this, it is important to explain the characteristics of the test.

The idea is to create the same conditions as in Figure 4.2. Thus, the main characteristics of the apparatus simulating the phenomena are:

1. Two systems able to keep the temperature constant during the experiment
2. A crushed salt sample with an initial porosity suitable to show the changes of porosity during the test
3. A not very high initial brine saturation degree
4. A geotechnical shape suitable to prepare the sample, to do the test and to be reproduced by a mesh for the numerical studies
5. A test time that must be long enough to show the phenomena and short enough to perform a large number of tests.
6. A sample container that should allow watching the interior to check the dissolution/precipitation during the test

Olivella et al. (1996 b) presented a paper about this problem from a numerical point of view: that work was considered as the starting point for these laboratory tests.

The numerical analysis was 1-D.

In that case the sample (the mesh) was cylindrical, with a horizontal main axis and a diameter of about 1 cm.

The initial porosity was n=30%.

Several saturation degrees and times were used.

Thus, the first point of this work was to establish a "*reference test"* and to determine the right system to carry out the experiments.

Castagna et al. (1998) presented the preliminary results in a paper and from that moment on the *"reference test"* and the test procedure were fixed.

The "*reference test*" had then the following characteristics:

| | |
|---|---|
| Sample | cylindrical with horizontal axis |
| Diameter | 50 mm |
| Length | 100 mm |
| Initial porosity | 30% |
| Initial saturation degree | 40% |
| Grain size | 1÷2 mm |
| Hot side temperature | 85º C |
| Cold side temperature | 5º C |
| Test time | 15 days |

The test method will be explained in Section 4.4.

The sample shape was cylindrical, because it was easy to prepare the sample and the sample size allowed doing all the operation of the test with limited errors. Furthermore, it was easy to prepare a mesh in 3-D to reproduce the phenomenon.

The initial porosity was fixed at n= 30%, because the sample case was of Plexiglas and this value allows compacting the sample with no risks of container failure and, at the same time, it was possible to study a lower value of porosity. Moreover this was also Olivella's initial porosity value.

The grain size was chosen ranging 1÷2 mm, because it was observed that during the preparation of the sample the compaction pressures are lower than in the case of smaller grain size. This effect is very important due to the characteristics of the case, because the PVC container can break if the compacting pressures are higher.

The two temperatures were chosen close to limits of evaporation and freezing values to apply the maximum temperature difference possible.

The test time was 15 days, because, as it will become clear once the results are presented, a test time of 7 days was too short to find differences among cases, and more than 15 days could be too long to develop a complete experimental campaign. For this reason, the test time was established in 15 days. It was decided that three experiments would be carried out at the same time to develop a larger and complete campaign.

## 4.3 *Experimental campaign programme*

The experimental campaign should be large enough to cover many aspects of the phenomena and to validate the results.

For this reason each test was performed at least three times, while the "*reference tests*" was repeated five times to secure the results.

It is believed that this was the first time that the multiphase flow, due to the temperature difference coupled to a dissolution-precipitation phenomenon that leads to porosity variations, was studied in a laboratory. No similar examples were found in the literature. Thus, the experimental campaign must be as complete as possible to establish a first knowledge of the problem. In the test programme we tried to consider all the main parameters involved in this phenomenon. For this reason the test programme was formed of:

a) Five experiments of the reference test
b) Ten experiments with different test times
   - ✓ Four with a test time of 7 days
   - ✓ Three with a test time of 30 days
   - ✓ Three with a test time of 65 days
c) Six experiments with different saturation degrees
   - ✓ Three with a saturation degree of 10%
   - ✓ Three with a saturation degree of 30%
d) Seven experiments with different initial porosites
   - ✓ Three with a initial porosity of 40%
   - ✓ Four with a initial porosity of 20%
e) One experiment with a longer sample (L= 160 mm)

The total number of tests is 29 with a total test time of 598 days. Three more tests were developed to verify the initial condition after the compaction.

It is unnecessary to say that there are more tests of the initial phase that are not presented in this work. These ones were used to determine and fit the apparatus characteristics and to establish the reference conditions of the test. These tests did not follow the standard procedure and it is difficult to compare them with the standard tests. Performing these initial tests was useful to carry out the rest of the campaign following a standard method.

## 4.4 *Experimental procedure and test apparatus*

A testing equipment has been specifically developed at the Department of Geotechnical Engineering and Geosciences of the UPC for this research work.

Each one of the experiments is divided into three main parts:

1. Sample preparation
2. Application of the temperature difference
3. Determination of the variables values when the test is finished

Even if the second part is the one that reproduces the phenomenon, and needs a special study to determine the correct way to proceed in order to determine the parameters with little error, each part is important,.

The first part of the test consists in sample preparation: the initial conditions of the experiment are fixed in this step and the sample is generated.

This is a process that should be repetitive because the porosity distribution of the sample at a given time is obtained by a destructive technique. Therefore, it is necessary to repeat the experiment several times in order to obtain different isocrones of porosity and brine content, so the initial condition must be guaranteed in this part for all the samples.

If this condition is not respected, the experimental campaign cannot be considered valid because it will be impossible to compare the results.

The variables, measured before starting the test, are porosity and degree of saturation.

Also, another basic condition of the sample is its homogeneity, because, if heterogeneity were present, this fact should be known and there would be implications in the analysis of results.

The previous considerations led to two different aspects of the problem: the first one is that the method used to prepare the sample should be the most accurate and the second one is that the procedure should be normalized.

A length of 100 mm was established to have, at the end of the test, 8 slices of about 10 mm in thickness (8 experimental points for each sample) and with a diameter of 50 mm to determine the distribution of the porosity along the sample axis.

In order to improve the homogeneity of the sample, the compaction operation is performed using two pistons, one for each side of the sample.

Figure 4.3 shows the compaction operation and the equipment.

The sample case is made of PVC, because it is heat insulating material and because it seemed interesting the possibility it offered of watching the salt aggregates during the temperature application and observing its effects on the sample.

The use of a PVC material allows reaching these results, but, at the same time, the compactor equipment should be designed to hold the stresses that are generated during the compaction phase.

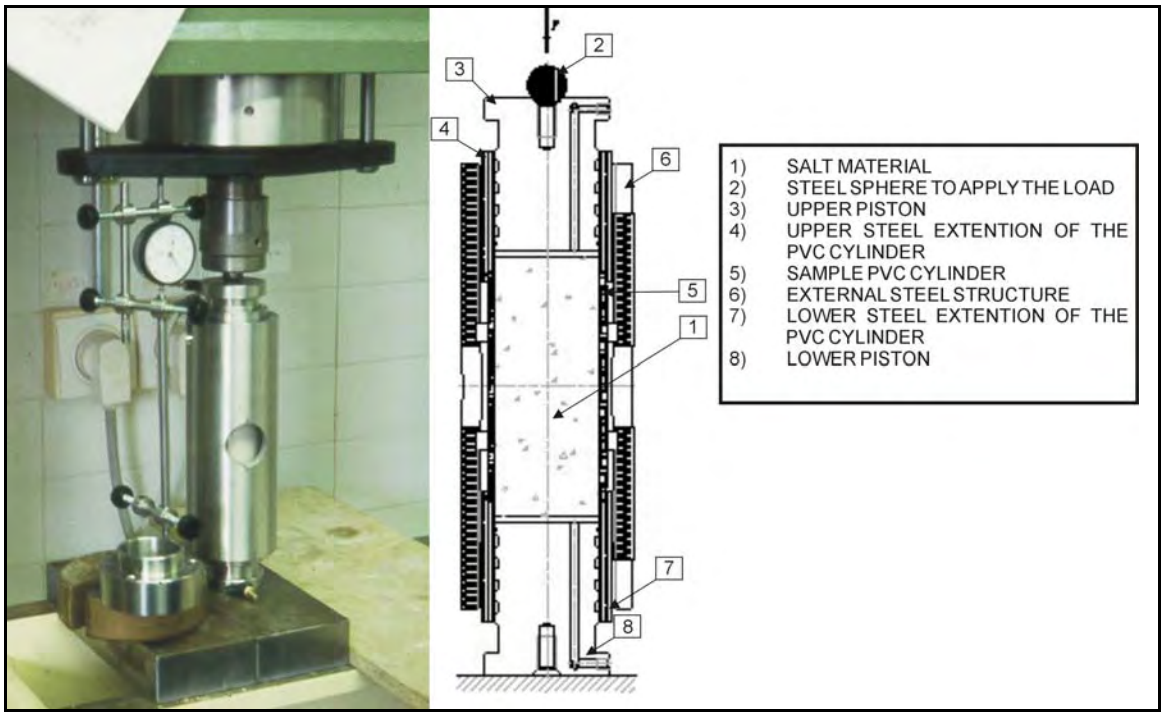


**Fig. 4.3** *Sample preparation.*

Moreover the equipment should allow the preparation of samples of different lengths, even if the effect of this parameter was not studied in detail during the campaign.

The result was a new compactor system in which three main components can be recognised:

1. "The PVC cylinder sample": the main property of this part is to give a geometric form to the sample, the choice was a cylindrical one. In the first part of the investigation there was the idea to use samples of different length and the intermediate size (the one of the reference test) was of 100 mm. This size allows obtaining eight slices that are enough to draw the porosity variation in a graph as a function of the sample's length. The PVC cylinder was lathed from a PVC tube 6mm in thickness to have a regular cylinder with an inner diameter of 50 mm. After the preparation of the sample, there is a free space of about 2 mm in depth at each side to locate the "Heat transmitters" in contact with the salt sample.
2. "The steel external structure": this structure has many tasks, the main one is to bear the effort applied by the press during the compaction. This structure is composed of three pieces, the central one is a steel cylinder with a bigger diameter than the PVC one. This transmits the efforts from one side to the other and protects the operator from the possibility of explosion of the plastic

cylinder. This occurrence is not common, but it happened several times during the test campaign; and it depends on the pressing velocity and pressure. This central part is connected by thread to the two steel cylinders of the edges of the compacting machine, being its inner diameter equal to the inner diameter of the PVC cylinder. The group of the PVC container and the two steel extension already gives a container good enough to receive the salt material, but there will not be strength enough without the central steel cylinder, and the alignment of the three pieces will not be guaranteed. The result would be the sure failure of the compaction operation without the central steel cylinder: the threads allow them being aligned and they transmit the effort from one side to the other reducing the effort on the PVC cylinder. Last but not least, thanks to this system, it is possible to prepare samples with different lengths. The two steel cylinders have two main functions, the first is to drive the pistons and the second one is to hold the salt before the sample is pressed.

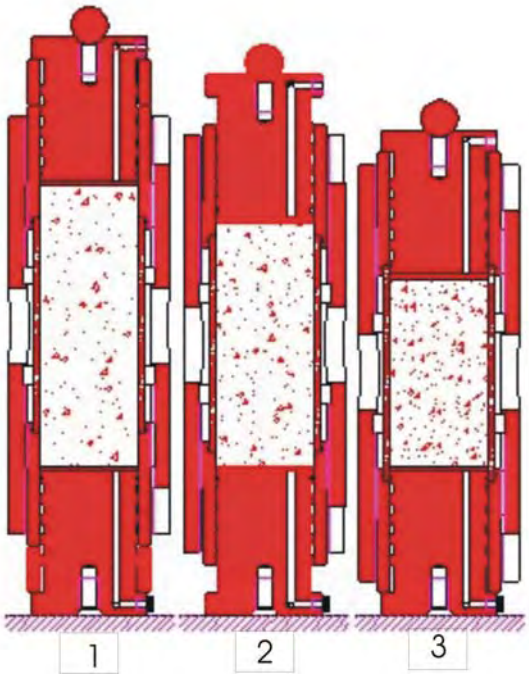


**Fig. 4.4** *Scheme of the sample preparation.* 1) The salt is in the compacting apparatus; 2) Pressure is applied; 3) The sample is ready for the next step.

3. “The pistons”: the two pistons are made in steel. They have got an o-ring, a bronze filter, an exit to let the fluids (air and brine) flow and, finally, the piston is designed to reduce the friction in the

contact between its surface and the cylinder wall: the piston is built in one lathed piece but the piston has two different diameter sizes, one is the same as the cylinder diameter and a second one is a bit smaller, 4 mm. These two “rings” are alternated and, of course, the last ring in contact with the filter is the bigger one.

The sample preparation method is different from the one described in Chapter 3 for the sample used to determine the matric suction, because they have different sample geometries and initial conditions.

In this case, the sample is unsaturated and its height is bigger than its diameter and, finally, in this case the sample ring is of plastic material.

The salt and the over-saturated brine are mixed in a bowl and, then, this material is introduced in the compacting apparatus that was already prepared (Fig. 4.4).

Of course both material and sample are checked to verify the sample’s initial conditions: saturation degree, porosity and total density. The initial conditions of the sample- initial porosity and degree of saturation- are checked twice. The first time the weights of salt, brine and PVC container are checked before compacting operation. The total weight and the length of the sample are measured after the pressing operation to verify the initial conditions.

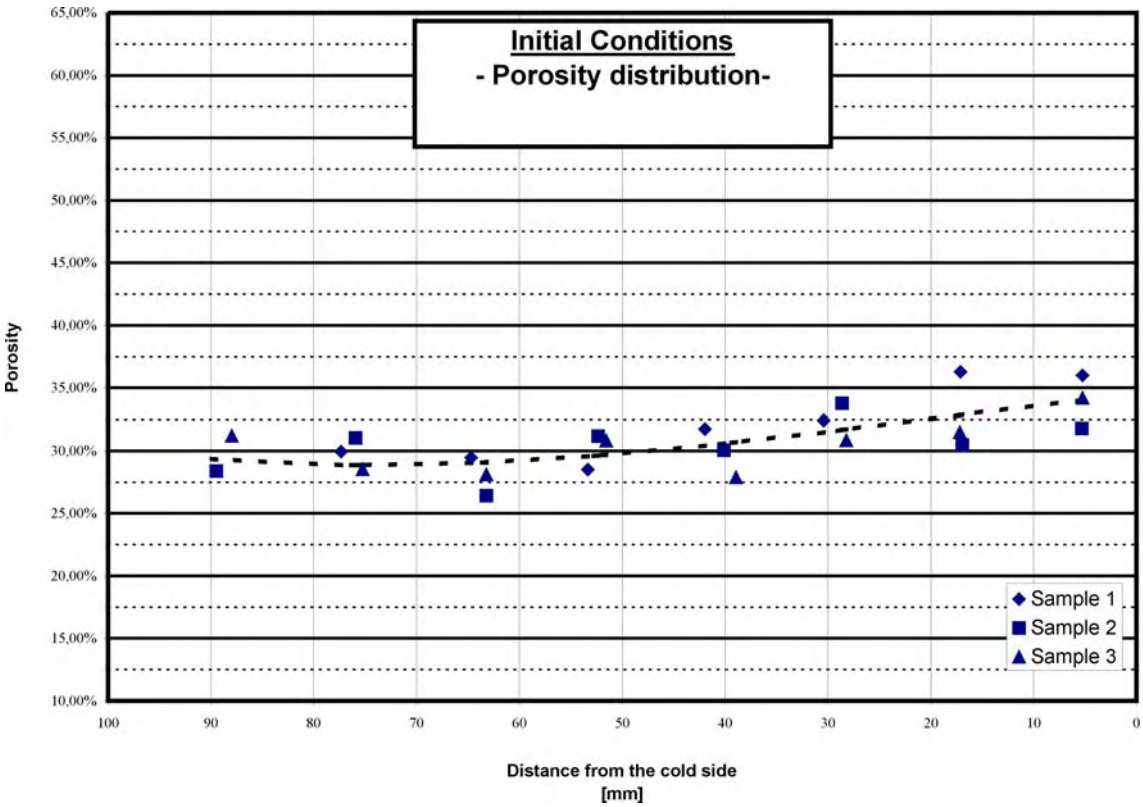


**Fig. 4.5a** *Compaction tests results in terms of porosity.*

As it will seen afterwards, there is the possibility of making three temperature tests at the same time, so the samples are numbered to recognize them and, at the same time, the upper part during the compaction is marked with the word “hot” because it is the part where the higher temperature transmitter is located.

Figure 4.5a reproduces the results of three different compaction tests with a theoretical porosity of n=30%.

The temperature difference was not applied in this test. The procedure of sample preparation is the same as the one in the cases in which a temperature difference is applied afterwards. So, although it would be more adequate to consider the upper side and lower side of the sample in this analysis, it is better to analyse this test speaking of hot and cold sides to have a clear reference with the following tests in which the temperature is applied.

The three samples gave similar results and there is not evidence of a real different behaviour among the samples. The porosity values were determined by a destructive method that will be described in the following pages.

The tests clearly show that the porosity is not constant in the entire sample length and that in the cold side (x=0; it corresponds to the lower part during the sample preparation) the porosity reaches a value of more than 35% in two points, 35.99% and 36.28%.

From the hot side there is one point that reaches a porosity value of 26.41%.

Figure 4.5a shows how the distribution of porosity value for the same value of x is random for the three samples, but it is possible to observe a tendency in the compaction test in which the cold side (x=0) has got porosity values of more than n= 30% and where the porosity in the hot side (x=100 mm) is less than n=30%.

Moreover the majority of points, 81%, have a ±2.5% deviation from the theoretical value of 30%.

**Table 4.1** *Porosity values of the samples.*

| SAMPLE | Calculated Porosity before the cut | Average Porosity of the sample slices | Δ |
|---|---|---|---|
| 1 | 28.39% | 32.05% | 3.66% |
| 2 | 28.01% | 30.19% | 2.18% |
| 3 | 26.35% | 29.84% | 3.49% |
| Average Value | 27.6% | 30.7% | 3.1% |

Table 4.1 shows the difference between the porosity values immediately after the sample preparation and the average porosity of the slices of the same sample. There is a difference of about 3% and the two values of porosity are

different from the fixed initial value (n=30.00%), but the average porosity of the slices is very close to this value for two samples (n=30.19% and 29.84%). There is no mass transfer, namely the system is sealed, so it can be asserted that the initial porosity is the target value with some small variations caused by the system errors.

The difference of average porosities between the initial porosity and one of the slices (Table 4.1) is due to grain losses during the cut.

Porosity (n) is the ratio from void volume ($V_{void}$) to total volume ($V_{total}$):

$$n = \frac{V_{void}}{V_{total}} = \frac{V_{total} - V_{salt}}{V_{total}} \tag{4.1}$$

where:

$$V_{total} = h \times \frac{\pi D^2}{4}$$
$$V_{salt} = \frac{W_{salt}}{\gamma_{salt}} \tag{4.1.a}$$

so:

$$n = \frac{\left( h \times \frac{\pi D^2}{4} \right) - \frac{W_{salt}}{\gamma_{salt}}}{h \times \frac{\pi D^2}{4}} \tag{4.1.b}$$

where:

| | |
|---|---|
| h | is the sample height |
| D | is the sample diameter |
| $W_{salt}$ | is the salt (solid) weight |
| $\gamma_{salt}$ | is the unit weight of the salt |

The only parameter that can be variable is the weight of the salt. In the case of sample 1 we have:

D= 52.29 mm;
h= 95.50 mm;
$V_{total}$= 204979,444 $mm^3$

$W_{sal}$= 317.51 g; (Initial value, this being the amount of solid added to the sample during compaction).

$n_0$= 28.39% (Initial value, which is calculated after the preparation of the sample)

Likewise, the porosities of the 8 slices where calculated after the 7 band saw cuts (see the following pages), and the average porosity was n= 30.7%.

Now, to obtain an initial porosity of 30.7%, it is necessary a weight loss of 10 g, that is $\frac{10}{7}\frac{[gr]}{slices}=1.43gr$. This stands for the small amount of salt grains that come off during the cut. This is a systematic error of the test method that is impossible to eliminate.

The hypothesis will then be that the samples have got a constant initial porosity in the next analysis, because the small variations found in this test are negligible with respect to the results that will be illustrated in the next section. This argument will be brought again when the results of the reference test are presented in order to compare the two results.

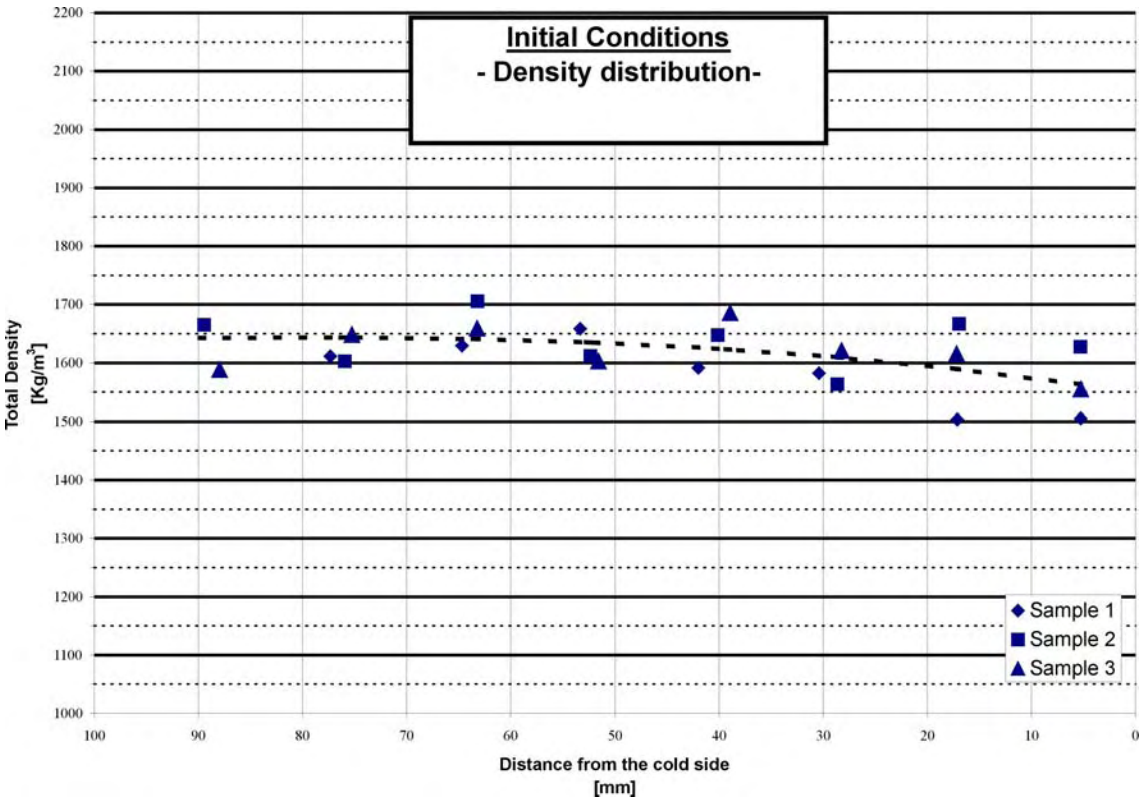


**Fig. 4.5.b** *Total density initial distribution.*

Figure 4.5.b shows the initial total density distribution. The average value of total density is about 1,600 kg/m$^3$. Observations similar to the ones of porosity after compactation can be done for the initial total density of the sample, due to the relationship between porosity and total density:

$$\left.\begin{aligned} n &= \frac{V_{voids}}{V_{total}} \\ \rho &= \frac{W}{V_{total}} \end{aligned}\right\} \Rightarrow n = \rho \frac{V_{void}}{W} \qquad (4.2)$$

Once the sample is ready, it is placed in the apparatus that applies the temperature difference.

In this case, the procedure is quite simple:

1. Placing of the sample (Fig. 4.6)
2. Sealing of the sample from the external environment
3. Keeping the chosen temperature difference during the test time

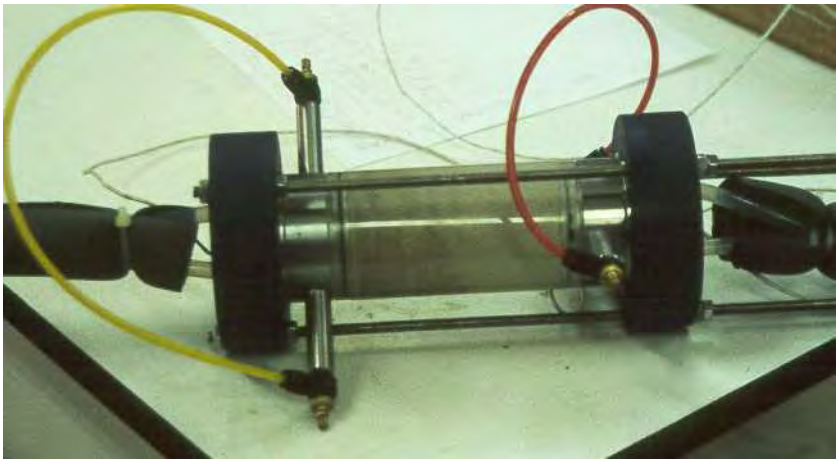

**Fig. 4.6** *The sample is placed in the test apparatus after its preparation.*

The controls during the tests are: the temperature of the two transmitters, which must be checked several times a day, and a visual control of the sample conditions.

The development of the apparatus took a great part of the thesis, because the apparatus was a new concept, it had to reproduce a new phenomenon and, at the same time, the project had to take into account the salt characteristics.

One of the first points to be fixed was the test duration. After some preliminary tests, this aspect was clear: the minimum time to reproduce something interesting is 15 days. This consideration involves another one: only one sample every 15 days is not enough to have a sufficient number of data to gather enough analysis results in such a short period of time as a doctorate thesis. It was obvious from the beginning that, to be sure of the results, the same test had to be developed several times and that the minimum amount of repetitions should be three, because it was possible to make a comparative analysis between three different results and to understand the behaviour of the phenomenon in case of different results for the same test conditions.

These two last considerations lead to the result that the optimum number of tests to be developed simultaneously is three. This number allows verifying immediately the test success and, in case of doubt, it is possible to repeat the tests in a short time and thus to obtain a clear description of the phenomenon.

Another aspect was the sample position during the application of temperature; two positions were considered: the vertical solution and the horizontal one.

The difference between one and the other consists in two aspects: the influence of gravity and the mesh type in the subsequent numerical analysis.

The choice, finally, was for the horizontal position, because the benefits are greater than the disadvantages. The most important benefit of the horizontal position remains in porosity variation being so big, which will be shown afterwards, and that allows salt grains not to fall down.

The disadvantages are the presence of preferential paths for the fluid flows and a more complicate numerical analysis.

The initial conditions and campaign programme were discussed in the previous paragraphs.

The scheme of the apparatus is shown in Figure 4.7.

In this picture several main elements can be recognized:

1. The heat transmitters
2. The samples
3. The sealing components
4. The temperature measurement system
5. The cooling system
6. The heating system
7. The hydraulic circuit

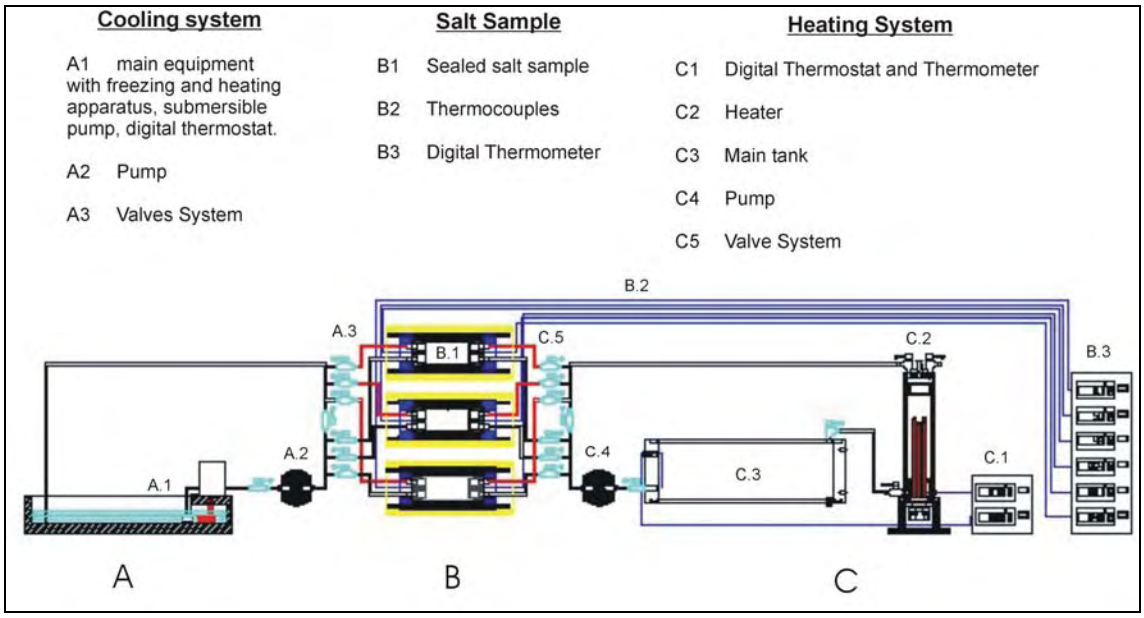


**Fig 4.7** *Apparatus used to apply the temperature difference on salt samples to determine the porosity variations.*

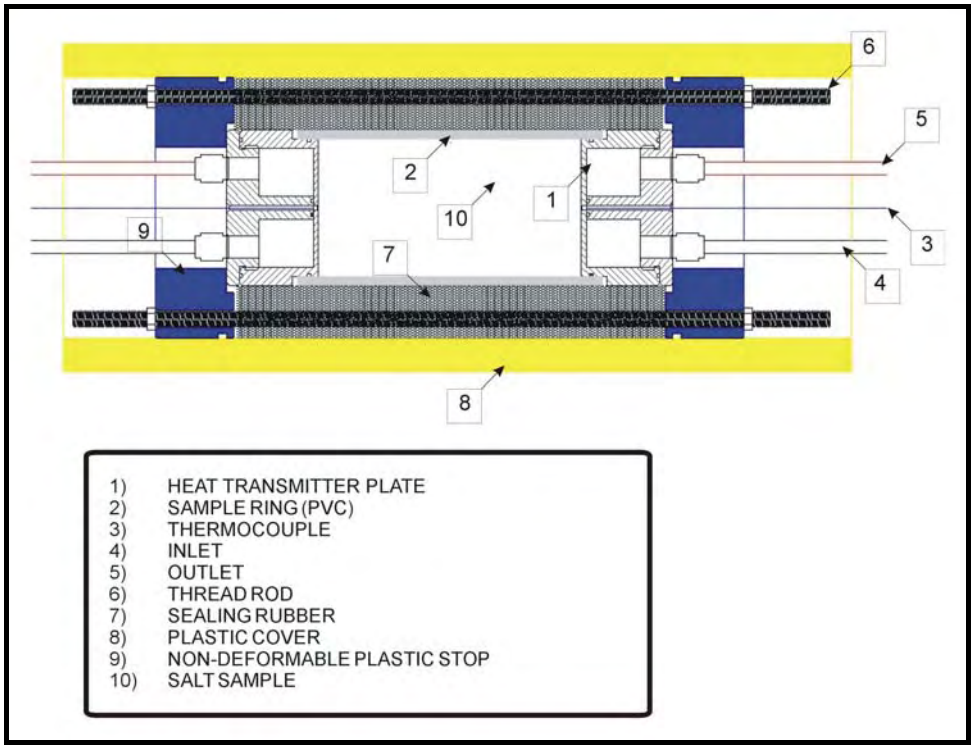


**Fig. 4.8** *Salt sample during the application of the temperature difference.*

Figure 4.8 shows the scheme of the salt cell sample during the application of the temperature difference.

The salt sample is placed in direct contact with the two heat transmitter plates, the plates are made of AISI 319 steel to avoid the corrosion effects, which could be very important in this case, due to the presence of a wet and saline environment for many days.

The two plates are the only metal parts in contact with salt in this installation. The temperature is kept constant by heat transfer from the liquid flowing in the interior of the transmitters to the salt sample faces. The liquid is kept at constant temperature thanks to the cooling and heating systems.

The sample is sealed, completely insulated from the external agents by o-rings, so there can be no mass transfer and no deformation except for the deformability of the container.

The temperature of the salt sample is measured in the two faces, hot and cold side, by two thermocouples, one for each side, which are in contact with the interior side of the plate, just in the middle.

The non-deformable plastic stops, together with three rods, guarantee the initial contact between the salt faces and the two plates.

The sample is insulated against the external environment by two different layers: the first one is a soft sealing rubber that envelops the sample and the second one is a rigid plastic cover 12 mm in thickness.

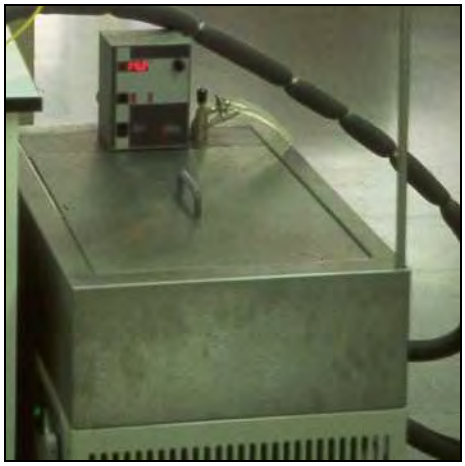

**Fig. 4.9** *Equipment from the HETO model "**DT 1 CB 8-30 e"** to keep the temperature constant in the cold side.*

The cooling system is a cooling bath from HETO, model DT 1 CB 8-30 e. It is possible to regulate the temperature between –30º C and 110º C (Fig. 4.9). There are two separate equipments in the same tank: a refrigerator and a heater. The cooling supply is continuous with the temperature controlled by a constant pressure valve: this means that the compressor pressure regulates the temperature of the cooler. The power of the refrigerator is 630 W. The refrigerator coil is located in the walls of the tank in contact with the liquid. The

heater has a power of 1200 W and it has a digital thermostat with a precision of ±0.005% and a resolution of 0.1 ºC. In the same heater there is a submersible pump with a flow rate of 14 l/min, but it was insufficient to provide with the flow rate necessary to keep the temperature in the heat transmitters constant. This pump is used to create a flow in the bath to have a uniform temperature in the entire bath (Table 4.2) and to pump the fluid into a bigger pump whose main task is pumping the liquid in the temperature transmitters at a sufficient flow rate to keep the temperature in the sample cold side constant.

**Table 4.2** *Study of the temperatures of the cooling bath. Two points are measured by a calibrated thermometer, one adjacent to the apparatus thermostat* (DT-1) *and one in the opposite side of the bath. The points are compared with the* DT-1 *display value.*

| Temperatures [ºC] | | |
|---|---|---|
| Bath Thermostat DT-1 | Adjacent to DT-1 | Far from DT-1 |
| 15.5 | 15.3 | 15.5 |
| 20.0 | 19.0 | 19.2 |
| 25.0 | 23.8 | 23.7 |
| 30.0 | 28.8 | 29.1 |
| 47.7 | 45.1 | 43.0 |
| 54.6 | 52.6 | 49.9 |
| 59.6 | 57.7 | 55.2 |
| 70.6 | 68.4 | 65.0 |
| 80.0 | 80.3 | 80.3 |

It was observed that the temperature of samples was affected by environment temperature without the use of the second pump. At the beginning, during the preliminary tests, this pump was not necessary, because the tests were developed with only one sample installation.

The bath capacity is 8 litres and the filling liquid was a mixture of water and ethylenglycol good to be used at 5º C without undergoing any freezing phenomena.

On the surface of the liquid, a layer of floating spheres avoids the evaporation of liquid.

The test was developed for more than one year and during this time the bath worked non-stop. There is a valve system that diverts the flow and when there are not samples, it is possible to close the flow in the temperature transmitters and let the liquid flow in another circuit not to stop the bath. This is important, because the bath needs about two hours to reach the temperature.

All the pipelines are insulated against the loss of heat.

The temperature variations were studied and the behaviour of the bath was good during all tests, the temperature had been constant for many months with a maximum variation of ±0.1º C.

The bath could be used as a heater too, but it was not used in this way in this test, all the test equipment is prepared to work in the entire range of temperature: between –45º and 110º C.

The heating system working principle is similar to the cooling one. The system is identical in the valve system and pump: it can be defined as a "symmetric system". The heater was developed at the Department of Geotechnical Engineering and Geosciences of the UPC.

The heating system works under pressure. The same fluid (mixture of water and ethylenglycol) was also used in the heating system.

The main components are:

1. The heater (Fig. 4.7 C2)
2. The liquid tank (Fig. 4.7 C3)
3. The temperature control system (Fig. 4.7 C1)

The heater is an electric resistance with a maximum power of 1500 W, The resistance is located within a stainless cylinder with a volume of 0.55 litres. In the heater there is a security pressure valve, a thermometer to check the liquid temperature near the resistance and the necessary valves to make the normal operations.

The electric resistance works at half power.

The main tank is separated from the heater. Its volume is of 6.5 litres. A pipeline connects the heater and the main tank.

The necessity of this tank emerged during the preliminary phase: the heater volume was not enough to keep the temperature constant, the average value was the established one but the variations were than more than 4º C from the average. This behaviour was due to the proximity of the thermocouple of the thermostat to the electric resistance and to the small liquid volume in the circuit.

The experience gained during the preparation of the cooling system led to build a bigger tank of 6,5 litres, the material for this tank was plastic with a low heat dilatation coefficient. The effect of this tank was immediate: the heating system had the same efficiency of the cooling one. To reach this result the thermocouple of the thermostat is placed in proximity of the exit that goes to the heat side temperature transmitters.

For security reasons, the heating system has two LEXITRON digital thermometers (models DPM 2 and L3 T), equipped with a K-type thermocouple. The two instruments have the possibility to control the resistance. In normal conditions one works as a thermostat at the exit of the main tank to control the temperature of the heat transmitters and the second one works as a thermometer in proximity of the electric resistance to check temperature variations in that zone. In case of failure it is possible to interchange one with the other and to continue the test.

This is the temperature control system for the two heaters. The possibilities of these two instruments are much more than what it is necessary for the test. These instruments did not need calibration because each temperature transmitter has its thermocouple and they needed to be calibrated. The difference between model DPM 2 and model L3 T is that the first has an output to a computer to save the data, although this characteristic was not used in this case.

Point B.3 in Figure 4.7 shows the temperature control system of the three samples. This system is formed by six k-type thermocouples and a TESTO 922 digital thermometer. This kind of thermometer has a temperature range between –50 and 1,000º C, a precision of 0.5% (from –40º to 900º C) and a resolution of 0.1ºC (up to 200º C). This thermometer can be connected to two different thermocouples at the same time.

The thermocouples arrived from the manufacture with a calibration certificate, but their efficiency was tested before installing them in the apparatus. At the same time the DPM-2 and DT1 were tested to study their behaviour.

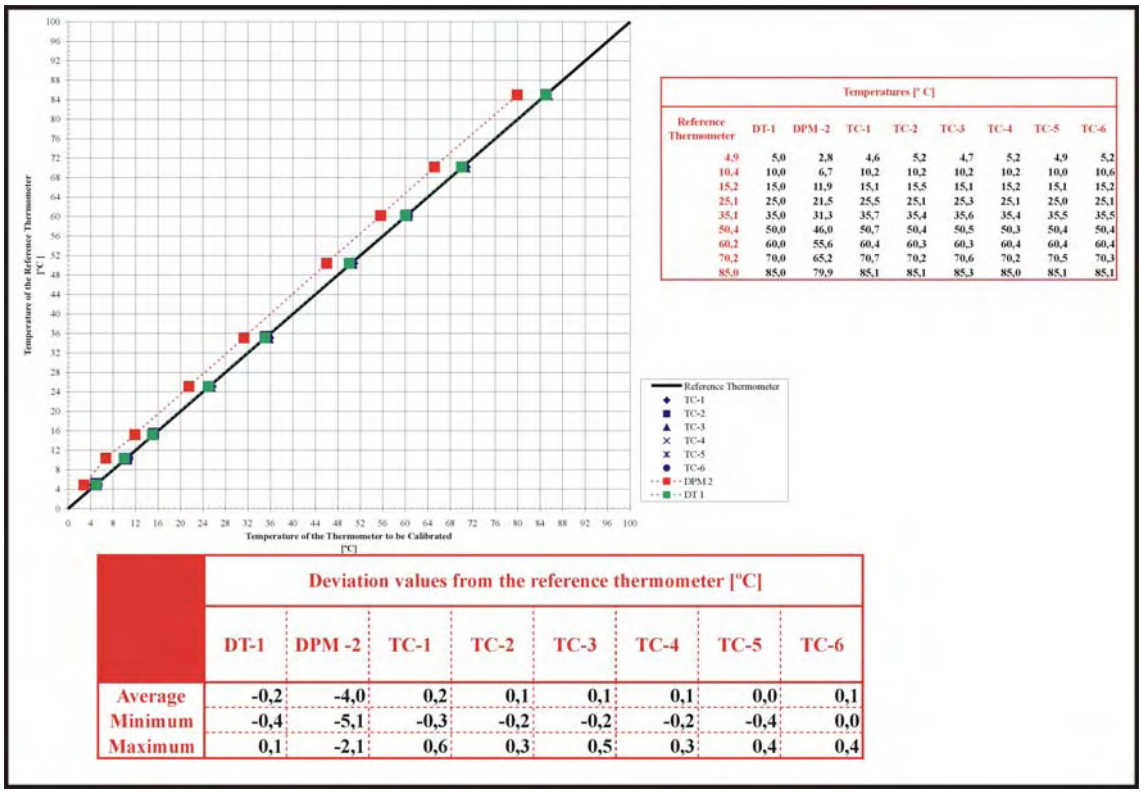


Temperatures [° C]

| Reference Thermometer | DT-1 | DPM -2 | TC-1 | TC-2 | TC-3 | TC-4 | TC-5 | TC-6 |
|---|---|---|---|---|---|---|---|---|
| 4,9 | 5,0 | 2,8 | 4,6 | 5,2 | 4,7 | 5,2 | 4,9 | 5,2 |
| 10,4 | 10,0 | 6,7 | 10,2 | 10,2 | 10,2 | 10,2 | 10,0 | 10,6 |
| 15,2 | 15,0 | 11,9 | 15,1 | 15,5 | 15,1 | 15,2 | 15,1 | 15,2 |
| 25,1 | 25,0 | 21,5 | 25,5 | 25,1 | 25,3 | 25,1 | 25,0 | 25,1 |
| 35,1 | 35,0 | 31,3 | 35,7 | 35,4 | 35,6 | 35,4 | 35,5 | 35,5 |
| 50,4 | 50,0 | 46,0 | 50,7 | 50,4 | 50,5 | 50,3 | 50,4 | 50,4 |
| 60,2 | 60,0 | 55,6 | 60,4 | 60,3 | 60,3 | 60,4 | 60,4 | 60,4 |
| 70,2 | 70,0 | 65,2 | 70,7 | 70,2 | 70,6 | 70,2 | 70,5 | 70,3 |
| 85,0 | 85,0 | 79,9 | 85,1 | 85,1 | 85,3 | 85,0 | 85,1 | 85,1 |

| | Deviation values from the reference thermometer [°C] | | | | | | | |
|---|---|---|---|---|---|---|---|---|
| | DT-1 | DPM -2 | TC-1 | TC-2 | TC-3 | TC-4 | TC-5 | TC-6 |
| Average | -0,2 | -4,0 | 0,2 | 0,1 | 0,1 | 0,1 | 0,0 | 0,1 |
| Minimum | -0,4 | -5,1 | -0,3 | -0,2 | -0,2 | -0,2 | -0,4 | 0,0 |
| Maximum | 0,1 | -2,1 | 0,6 | 0,3 | 0,5 | 0,3 | 0,4 | 0,4 |

**Fig. 4.10** *Results of the calibration of the thermocouples.*

All the thermocouples were submerged in the “DT 1 CB 8-30 e” bath and were fixed in a point close to the DT-1 temperature sensor. After that, several temperatures values were fixed by DT-1 thermostat and, when the established

temperature was reached and stable, the temperatures of a calibration thermometer and of all the thermocouples were compared.

The results are presented in Figure 4.10.

The results are good with the exception of DPM-2, which is the instrument of the heating system, but as it was pointed out previously, the important results were only the ones of the thermocouples applied at the sample (TC-*n*), so these results have no importance for the test development.

Likewise, note the precision of the cooling bath thermostat in which the results are similar to the heat transmitter thermocouples.

With regards to the transmitter thermocouples, it is possible to observe that the average deviations from the reference thermometer are very small: inferior to 0.2º C, and that the absolute variations are in the range –0.4ºC - 0.6ºC.

These values can be accepted as normal, because they are in the equipment error range and, moreover, the test duration is very large and, in this lapse of time, there are little variations of temperature: ±0.3ºC.

Temperature data were recorded, at least, three times a day. Since they don't give further information about the tests, they are not shown here.

The last part of the laboratory tests is the determination of porosity values and of the other variables in several sample sections.

This aspect was studied in detail because the methodology of the test and the subsequent analysis depended on it.

Three different forms of determination were considered:

- ✓ Tomography
- ✓ Image processing
- ✓ Destructive methods by an electrical band saw

The only method, as well as the fastest, that allows determining total density and saturation degree is the destructive method.

Several preliminary tests were done with the other two methods, but the results were not satisfactory.

Firstly, the image processing method was tried. The sample voids were filled with epoxy resin and then the sample was cut in several fine slices and the image processed by computer analysis to determine the percentage of resin in the slice. Unfortunately, calibration was impossible and it was found out that both operator and software could give very different results for the same slice. In one occasion, the same sample was given to the same operator. The first result was a porosity of about 10%; the second, one of about 45%. This method could not be considered correct!!! (Fig. 4.11)

The tomography method had the apparent advantage that it was possible to use the same sample for different time steps, but the UPC does not have this costly equipment. Therefore, this option was discarded because the use of an external laboratory forced to change the sample in order not to stop the rest of laboratory tests.

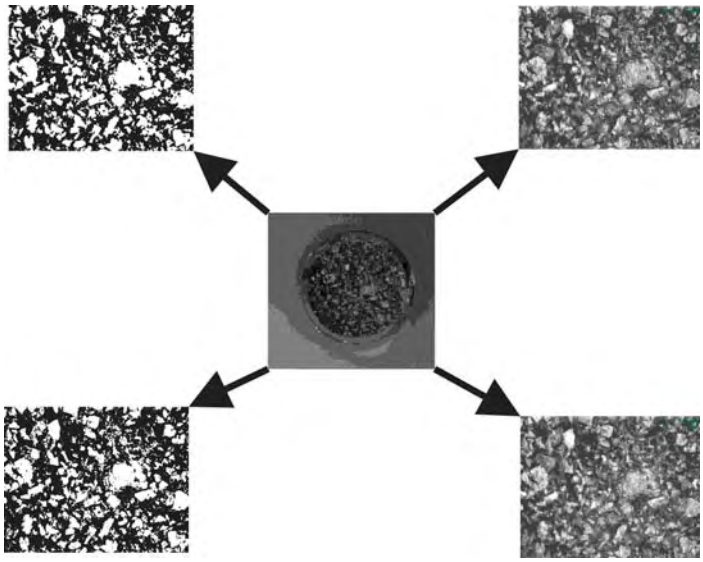

**Fig. 4.11** *Sample slice and its images. Each image gives different porosity results!!!*

Several laboratories were contacted in Spain, France, Italy, Holland and Belgium to make the job. In all the cases the first negative result was that to study the sample, they had to fill the sample with a liquid that could destroy the sample, because it could displace the grains from their original position. Moreover the transport time did not guarantee accurate results due to the variation that the sample can undergo during this period.

Most of these laboratories did not have an apparatus suitable for such a big sample.

Only the laboratory of the Faculty of Geology of the Katholieke Universiteit Leuven (Belgium) (van Geet et al., 2000) was able to make the tomography, but they could only supply images and they needed a calibration sample to provide porosity results. (Fig. 4.28) The same happened with the image processing and the idea of using tomography for salt samples had to be reconsidered.

The destructive method of cutting is the most interesting among all the methods considered, even if the preliminary study shows some problems. At the beginning the idea was to proceed with the cutting in an external laboratory or workshop, but the final decision was different: an electrical band saw was installed close to the equipment used to apply the temperature difference (Fig. 4.12).

The saw is a normal workshop model slightly modified for this use: a V-frame was installed to keep the cylindrical sample in the right position and to reduce the blade vibrations (Fig. 4.13).

The cutting is done under dry conditions and the two sides are covered with a plastic sheet to avoid evaporation. The blade thickness is about 4 mm and each cut is of about 5 mm.

The cut is fast, in about 45 minutes the whole sample is divided into slices; the number of slices for the reference tests is eight.

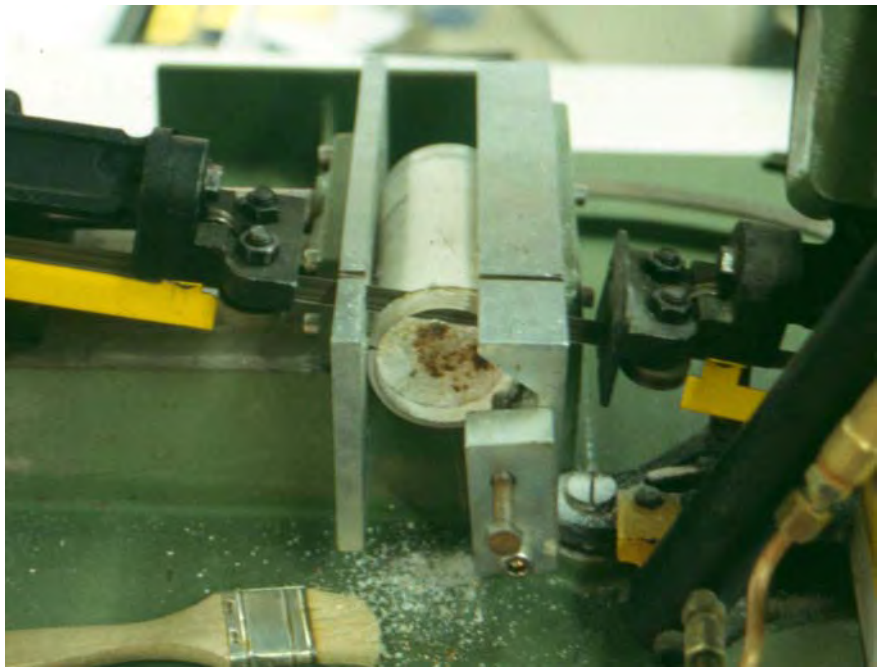

**Fig. 4.12** *Sample cut in progress.*

**Fig. 4.13** *Another view of the cutting operation.*

The salt material of each slice is kept in a different container and its weight is checked: first the wet weight is measured before being put in a stove to determine then its dry weight. (See Chapter 2 for the definition of dry weight)

The quantity of salt precipitated from the brine during the period in the oven must be subtracted to find out the dry weight. The process was already explained in Chapter 3 for laboratory test to determine the retention curves of salt aggregates (See Fig. 3.15).

This allows determining the porosity, total density, humidity and saturation degree of each slice.

## 4.5 *Analysis of results*

In this paragraph the results will be presented.

This part of the thesis can be divided into two parts.

The first one shows the behaviour of crushed salt. To develop this part the photos of the 30-day and 65-day test are presented because in these cases the effects of temperature difference are more evident than in the reference test.

In the second part the results of each test are presented, first those of the reference test and then the others.

The results are divided into groups:

- ✓ Time variation (7, 30, 65 days)
- ✓ Initial porosity variation (n=20%, 40%)
- ✓ Initial saturation degree variation (S=10%, 30%)
- ✓ Sample with an increased length (L=160 mm)

The results of each group follow the same layout. First the analysis of the results of each test and then the comparison of the results as a function of the correspondent variable (i.e. the porosity variation in function of the test time).

The results are presented only as a graph; the worksheet will not be presented.

### The behaviour of crushed salt due to temperature difference

To describe the crushed salt behaviour when a temperature difference is applied to the sample, the photos of the 30-day and 65-day tests are presented, because the effects of temperature difference are clearer than after the 15-day reference test.

Figure 4.14 shows two samples after a 30-day test of just after being removed from the apparatus.

The first remark is that the two samples are in similar conditions and they can be divided into two zones: one of low density in the cold side and another of high total density in the hot side. This observation is clearer in Figure 4.15 where the hot and cold ends are shown.

Besides, in Sample 2 of Figure 4.14 two dotted lines have been plotted. The green line limits a zone where there is no salt (see also Fig. 4.16). The red one shows the zone in which it is possible to distinguish the difference in density between the cold side and the hot one.

Another aspect that can be observed in Figure 4.14 is the presence of flow paths. These paths are preferential, there are some lines following the generatrices of the cylinder in the internal surface of the sample ring. In Figure 4.15, it can be observed that the gravitational forces affect these paths; in the lower part of the cold side there are two zones where the porosity is higher than in the contours of the same zones. The first zone is close to the lowest generatrix, and here it is possible to notice how low the density is in a small

area and this behaviour depends on a preferential path for the brine flow (liquid flow in the lower part). Likewise (Figs. 4.15 and 4.16), there is a zone near the highest generatrix in which there is no material because there is no contact between the grains, and/or the frictional angle is very low and the grains fall down because of the gravitational forces towards the lower part of the sample.

This effect affects half of the sample in the case of the 65-day sample and a sort of half cone wedge can be observed, in which the vertex is at about 50 mm from the sample cold side (see pictures in Fig. 4.17).

The presence of these large voids represents a problem to determine the porosity values because the porosity was calculated by weight measurements in a circular 10-mm thick slice, so there are some sections in which the deviation from the average value is significant.

It is important to underline that this problem is present only for an elapsed test time of more than 30 days, because before that, there are not any macro voids in the slices.

Figure 4.15 shows the two ends of the sample. The hot side is brown due to the burnt salt. This effect was observed in all the tests performed and since the contact between hot face and the heat transmitter is strong, it was necessary to use a tool to break it because it was impossible to do it by hand.

The mark in the middle of the hot ends corresponds to the thermocouple.

It is possible to observe how the sample looks like a rock on this side.

The appearance of the cold end is the opposite: the grains can be recognized and there is no thermocouple mark. In this case, the heat transmitter can be removed by hand and there is no contact between the heat transmitter surface and the sample at the end of the test.

In Figure 4.17 the effect of dissolution in the 65-day test is quite clear in the cold end, as it is possible to see that there is not salt material in the lower part of the sample: after more than 2 months of tests the results of the dissolution and transport processes are evident: the sample lost at least 50% of its original section. It is implied that, although the presence of water could destroy a barrier of salt aggregates, laboratory results should be checked against large scale phenomena to confirm the behaviour for the deep waste repository.

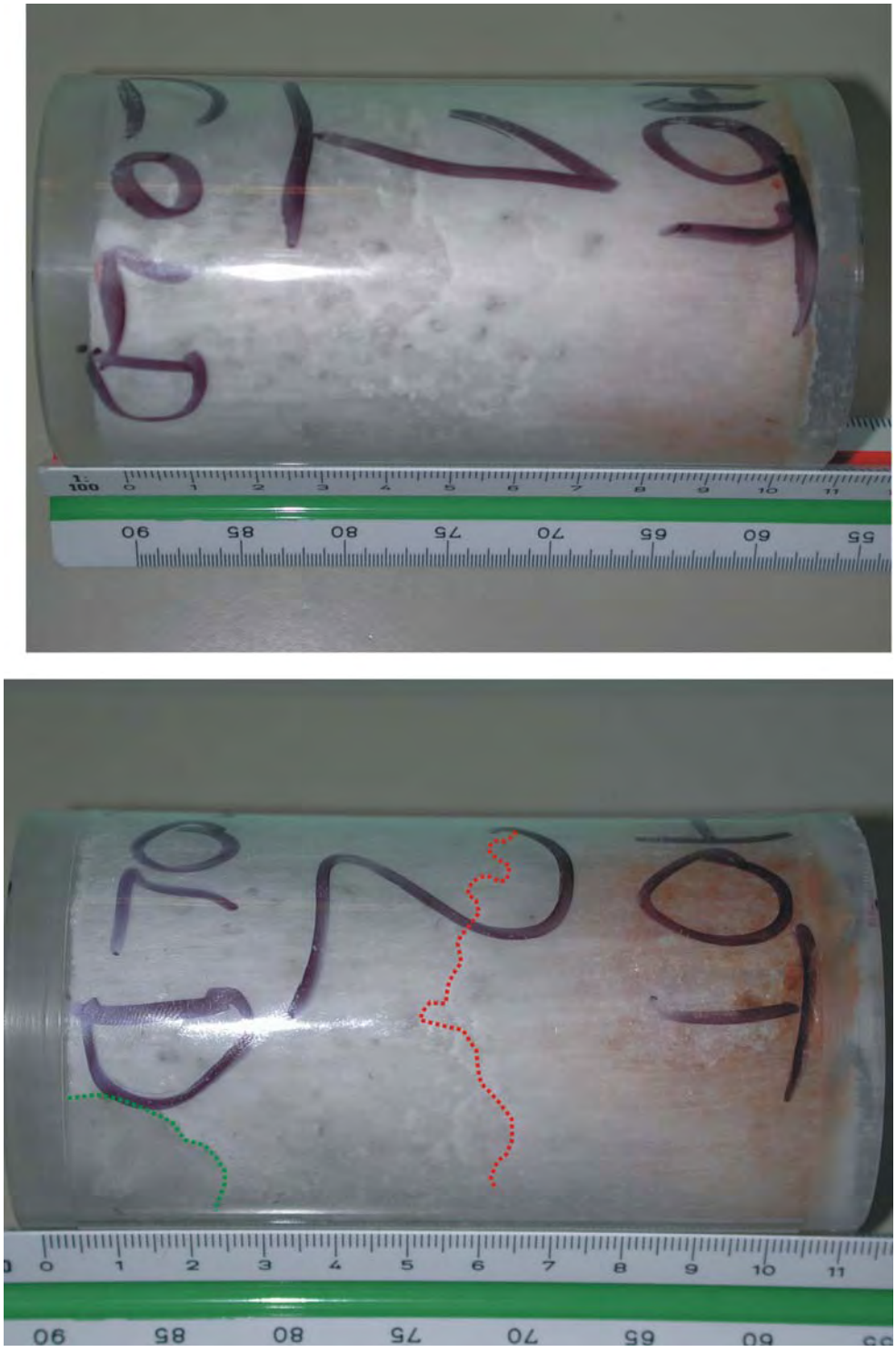

**Fig. 4.14** *Two samples after 30 days of application of the temperature difference. Hot and cold ends are marked in the sample holder. The upper generatrix corresponds to the number in the middle of the sample.*

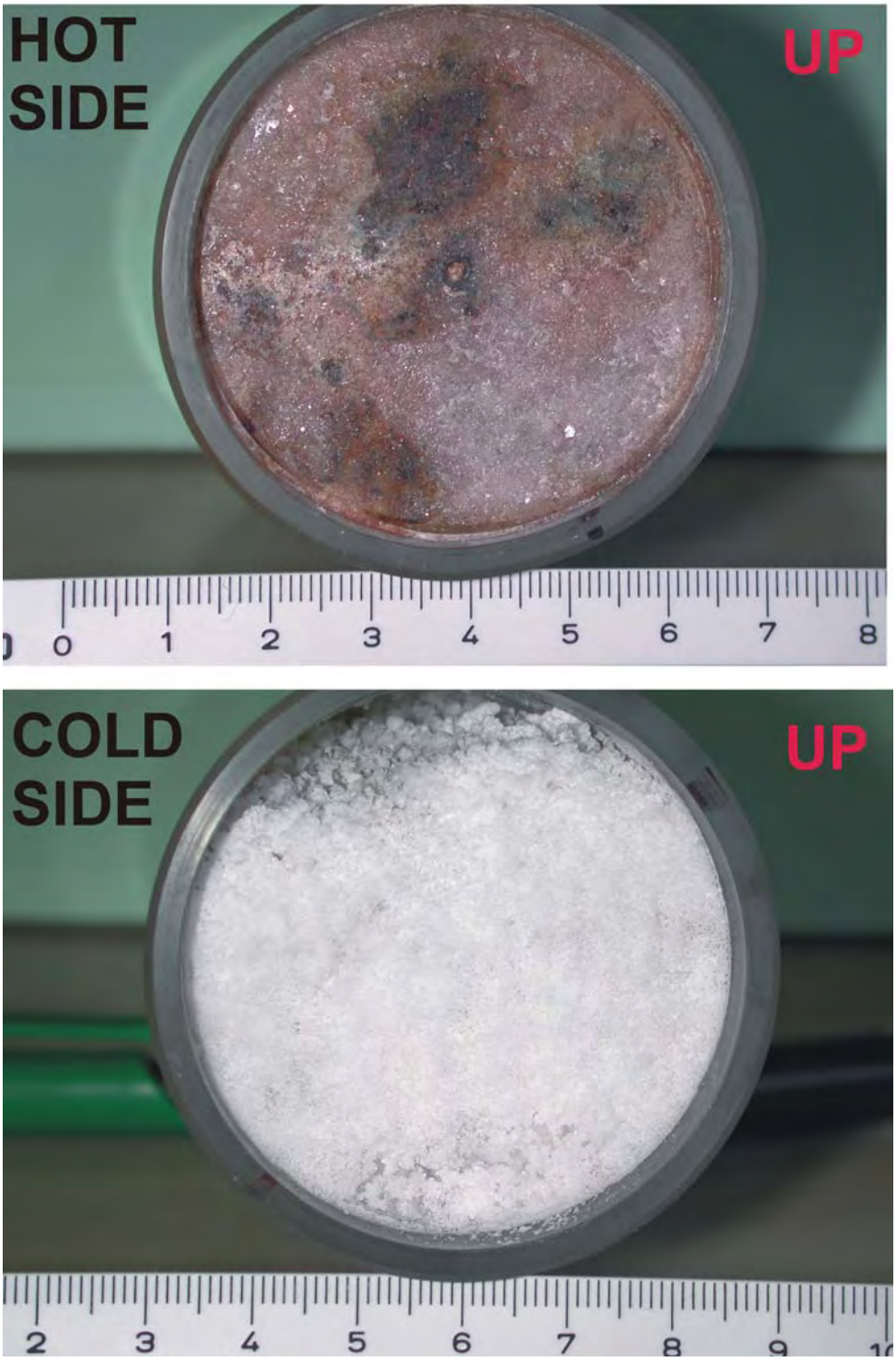


**Fig. 4.15** *The hot side and the cold one of a sample after 30 days of application of the temperature difference.*

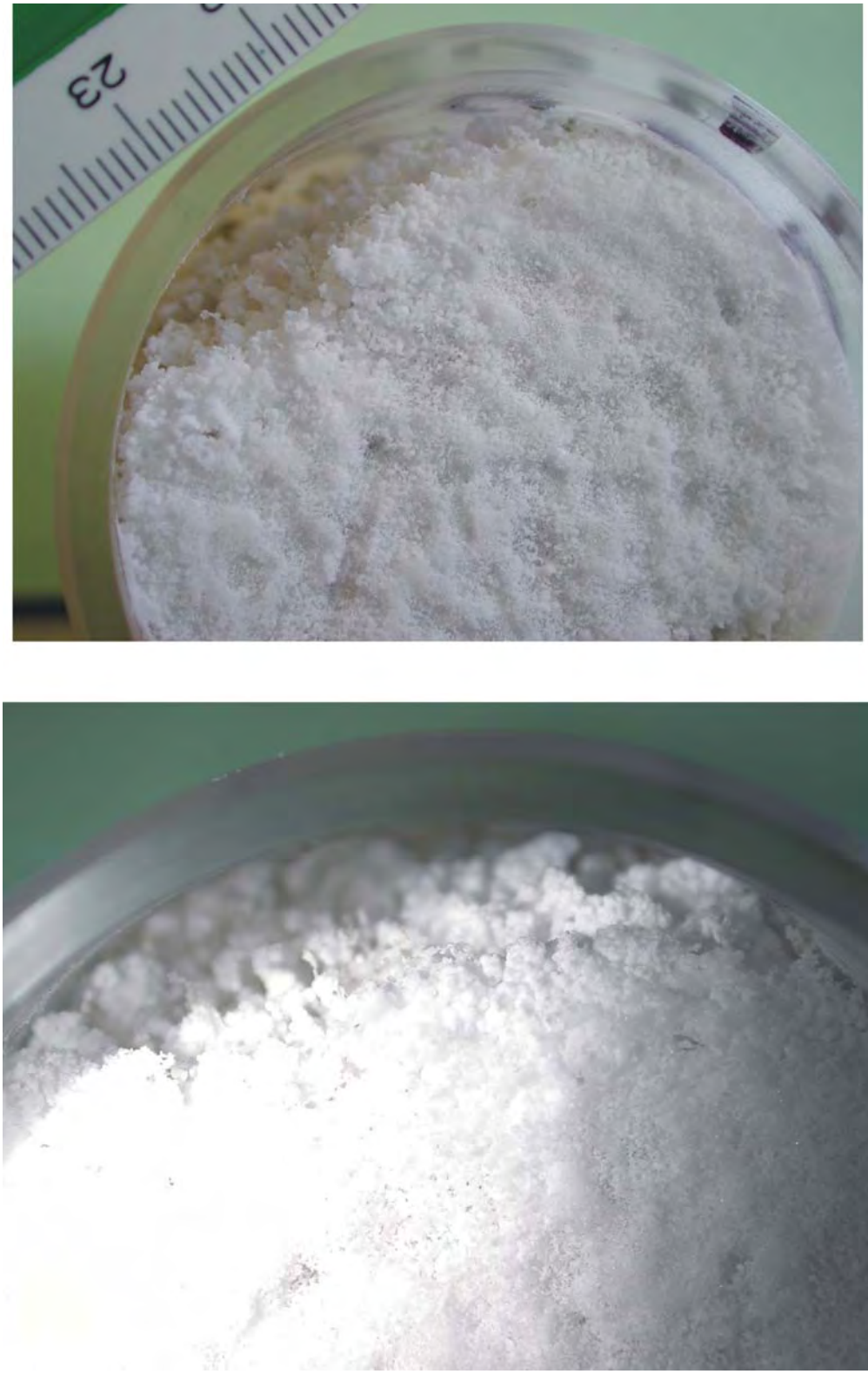

**Fig. 4.16** *Details of the cold end in the top of a sample after 30 days of application of the temperature difference.*

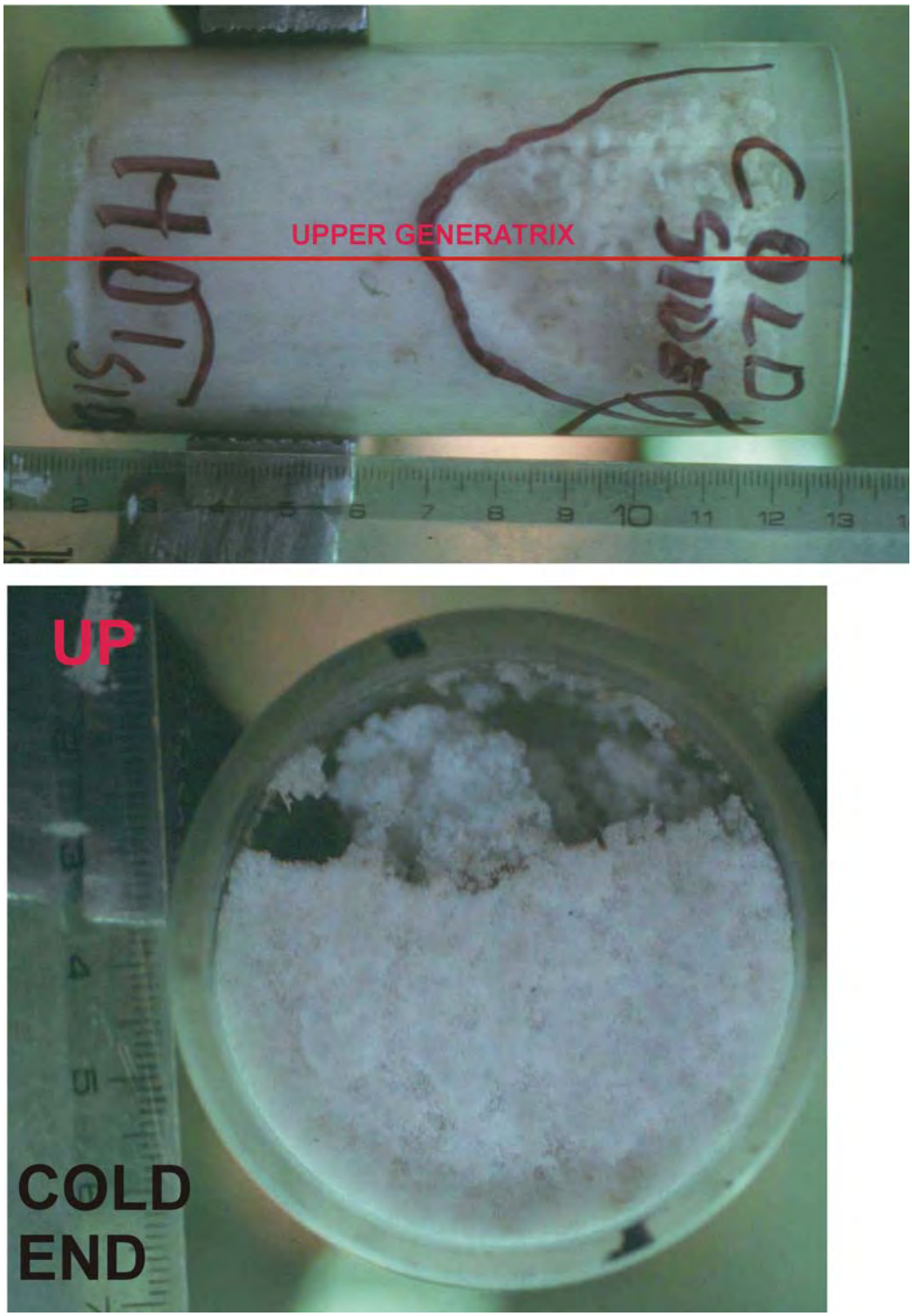


**Fig. 4.17** *Details of the sample after 65 days of application of the temperature difference. The effects of the temperature difference are quite clear!*

## Reference test

The characteristics of the reference test are:

| | |
|---|---|
| Length | 100 mm |
| Initial porosity | 30% |
| Initial saturation degree | 40% |
| Test time | 15 days |
| Grain size | 1÷2 mm |
| Hot side temperature | 85º C |
| Cold side temperature | 5º C |

The first four properties will vary in the other tests while the last three are fixed for all the experiments.

Due to its *reference* characteristic, this test was repeated five times to ensure the results.

**Table 4.3** *Comparison between the sample total weight before and after the application of the temperature difference.*

| Sample | Initial Weight $W_0$ [g] | Final Weight $W_f$ [g] | Weight Loss $\Delta = W_0 - W_f$ [g] | $\frac{\Delta}{W_0}$ [%] | Brine Weight $W_b$ [g] | $\frac{\Delta}{W_b}$ [%] | Salt Weight $W_{NaCl}$ [g] | $\frac{\Delta}{W_{NaCl}}$ [%] |
|---|---|---|---|---|---|---|---|---|
| 1 | 428.37 | 427.23 | 1.14 | 0.27 | 31.41 | 3.63 | 317.48 | 0.36 |
| 2 | 427.58 | 425.26 | 2.32 | 0.54 | 30.53 | 7.60 | 317.48 | 0.73 |
| 3 | 426.76 | 424.95 | 1.81 | 0.42 | 30.45 | 5.94 | 317.49 | 0.57 |
| 4 | 428.22 | 424.40 | 3.82 | 0.89 | 30.93 | 12.35 | 317.49 | 1.20 |
| 5 | 425.17 | 423.70 | 1.47 | 0.35 | 30.26 | 4.86 | 317.51 | 0.46 |

Table 4.3 shows the difference between the total initial weight and the final one. The “Initial weight” is the weight of the sample after its preparation and before the installation in the apparatus for the application of the temperature difference and includes, sample ring, salt aggregates and brine. The “final weight” is the total weight of the same components immediately after the test and before the specimen is cut in slices. The weight loss is the difference between the initial and final weight. The losses are represented in percentage terms and the comparison is done with the initial, brine and salt aggregates weights, too.

The results are satisfactory since losses are small, less than 2.50 g in all the cases with the exception of sample 4, in which is higher: 3.82 g (probably there was a small loss during the transport from the apparatus to the scale).

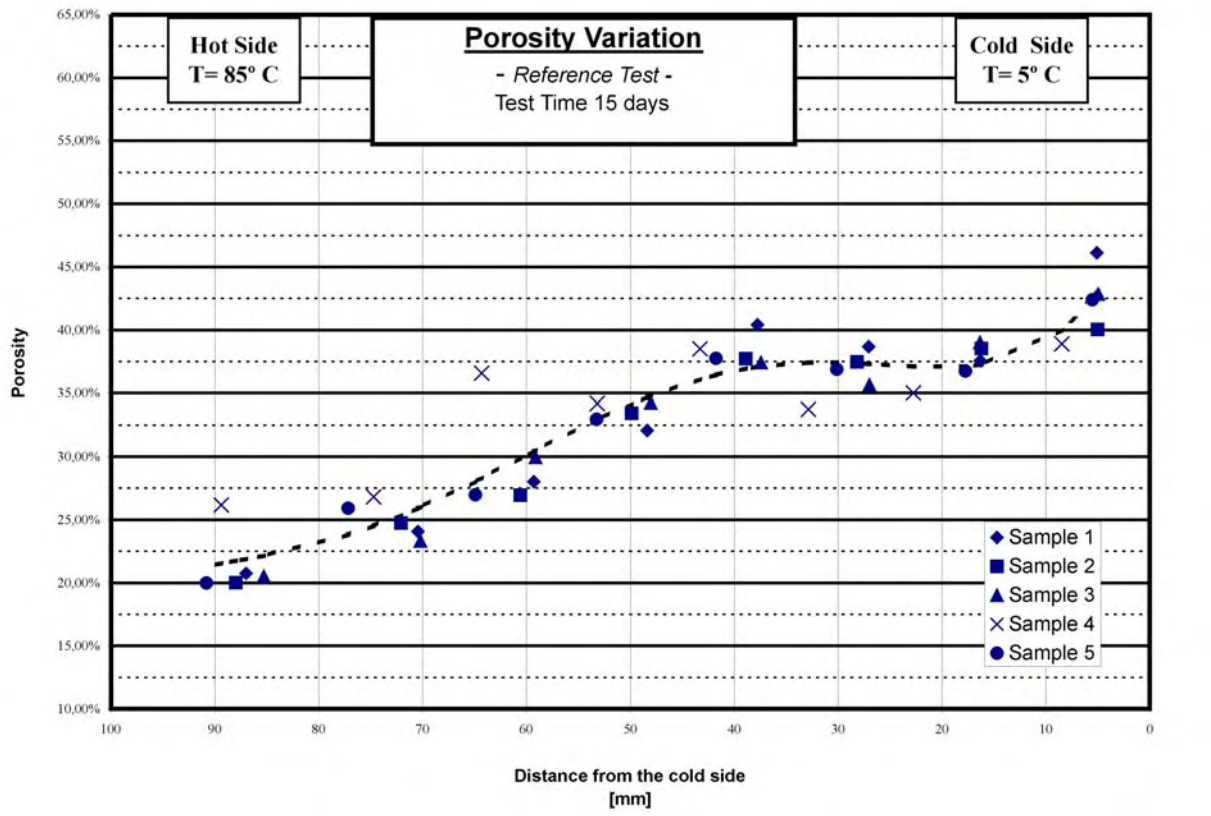


**Fig. 4.18** *Porosity variation of the reference test.*

The first result to be presented is the porosity variation (Fig. 4.18);

The results show that the behaviour of the five samples is similar. Differences in porosity for the same abscissa are small. There are only two points of sample 4 that have a difference of more than 7% from the others, all the other points have a difference in porosity of only 2.5%. This is a good result, because the five samples are completely independent and two of them, samples 4 and 5, were tested after the other ones. These results add confidence in the test method and apparatus, due to the repeatability of the test.

Before concluding the treatment of this first aspect of the reference test analysis, it is necessary to compare the porosity variation in the reference test with the initial values of porosity of each slice after the preparation of the sample.

The results are presented in the same graph in terms of porosity (Fig. 4.19). The red colour is used for the slice porosity before the application of the temperature difference and the blue one is used for the porosity of the reference test. Two coloured lines show the minimum square method for both cases. The curve represents an interpolated curve using a $5^{th}$ degree polynomial function.

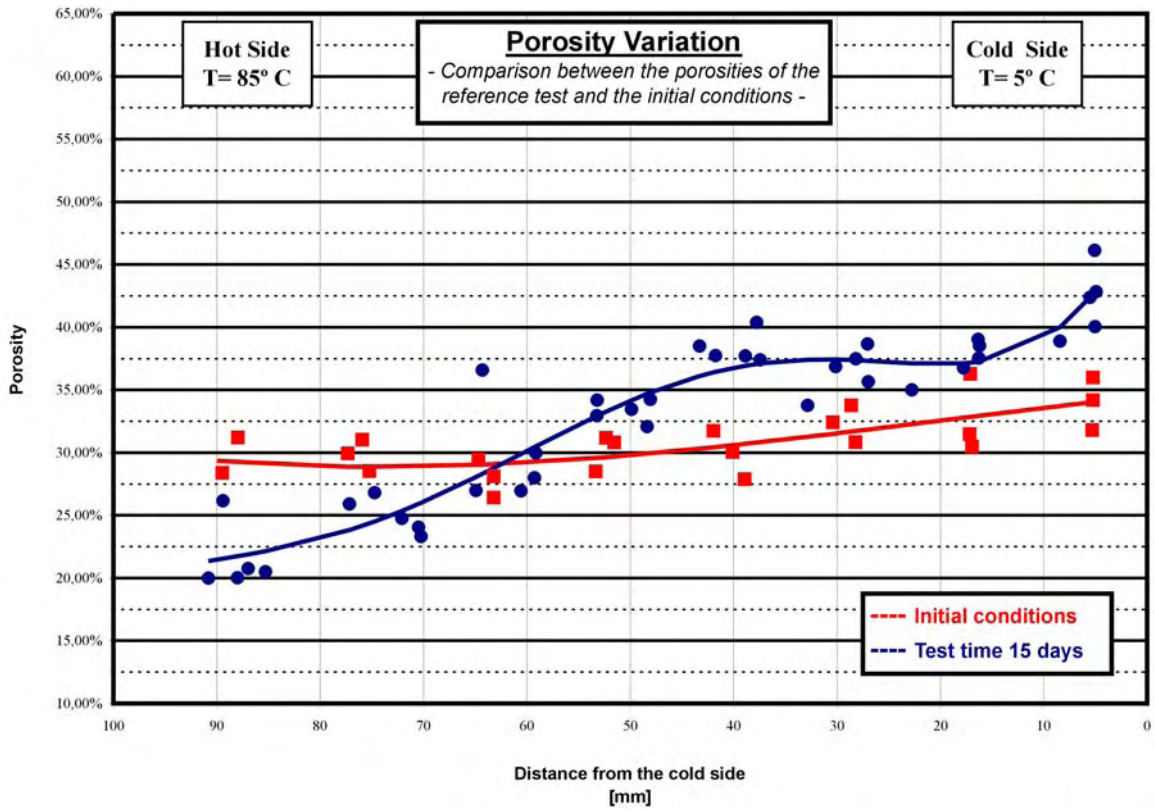


**Fig. 4.19** *Comparison between the porosity values of the slices in two different conditions: before the application of the temperature difference and after a test time of 15 days (Reference Test).*

The porosity after the application of the temperature difference is different from the initial conditions. The two sample groups, the reference test samples and initial condition, are completely separated, with the exception of the zone where the reference test line crosses the initial condition one. The maximum change in porosity is 15÷20%. This maximum corresponds to values of porosity in the sample extremities.

These observations allow confirming that the small difference between samples and/or the little different values of porosity in the same sample before the application of the temperature difference do not affect the phenomenon examined.

Table 4.4 shows the difference between the porosity values immediately after the sample preparation and the average porosity of the slices of the same sample after the application of the temperature difference.

As it has been already mentioned in the previous paragraphs, for the purpose of the analysis, the initial value of the porosity will be considered as constant in the entire sample with a value n=30%.

**Table 4.4** *Porosity values of the samples.*

| SAMPLE | Calculated Porosity in the entire sample before the application of temperature difference | Average Porosity of the sample slices after the application of the temperature difference | Δ |
|---|---|---|---|
| 1 | 29.56% | 33.45% | 3.89% |
| 2 | 30.33% | 32.37% | 2.04% |
| 3 | 29.05% | 32.87% | 3.82% |
| 4 | 29.23% | 33.74% | 4.51% |
| 5 | 29.65% | 32.45% | 2.80% |
| Average Value | 29.56% | 32.98% | 3.41% |

The difference of average porosities between the initial porosity and the one of the slices (Table 4.4) is due to grain losses during the cut, as it was explained before.

It is possible to observe that the hypothesis of no mass transfer is verified: if we consider the two surfaces, that the hot and the cold side form with an ideal initial porosity line for n=33 %, the envelope curve, the vertical limit line and another vertical line in the crossing point, these two surfaces have identical area.

The curve that describes the porosity variation has a different behaviour in the hot side and in the cold side, respectively. Starting from the hot side the curve has a constant slope up to the point in which it crosses the initial condition line (from n=20% to n=30%) (Hot side).

The crossing point is an inflection point and is located at about 60 mm from the cold side (60% of the length). From this point the curve reduces its slope and there is a smooth path of about 20 mm in which there is a maximum point (n=37.50%), and then there is a minimum point and after that the porosity increases up to its maximum value of more than 40%. (Cold Side)

The path can be divided into three parts. Starting from the hot side, the first part of the path (about the 40% of sample length) has got a constant variation of the porosity and after there is the second one where the porosity changes are small, the curve is smooth and, finally, in the last part of the path close to the cold extremity the porosity variations are bigger.

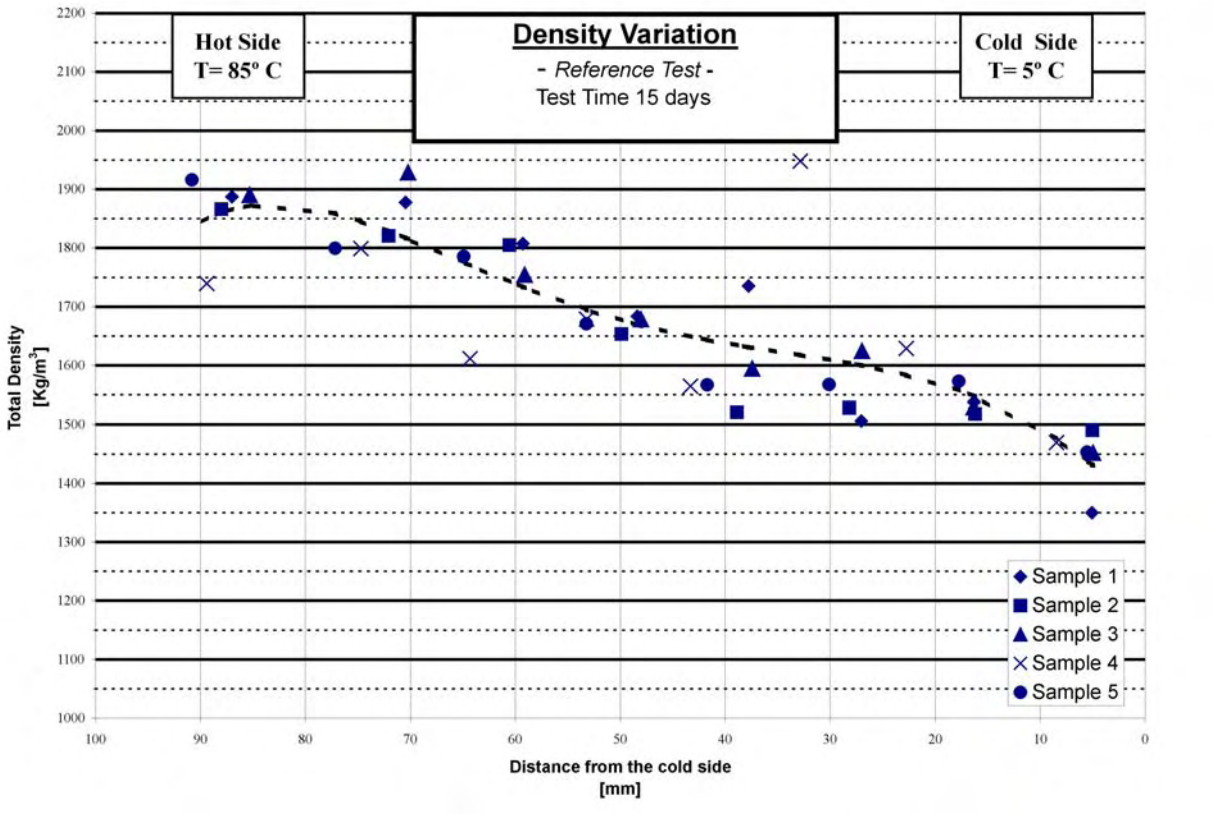


**Fig. 4.20** *Variation of total density for the reference test.*

Figure 4.20 shows the total density variation for the reference test.

The results and the observations are the same as those of the porosity variation (see paragraph on sample preparation), but it is interesting to enclose also this graph because total density is a physical magnitude that civil engineers are more familiar with rather than porosity.

It is interesting to notice that the total density varies from a maximum value of 1,900 kg/m$^3$ in the hot side to a minimum of 1,400 kg/m$^3$ in the cold side.

Figure 4.21 represents the water content for the five samples of the reference test. Water content is the ratio of the water weight in the liquid phase to the salt weight of the solid phase. The water in the liquid phase was determined by the difference between the weight after the cut of the slice and the dry weight of the same slice. The weight of the salt in the solid phase was determined deducting the weight of salt precipitated from the brine in the oven.

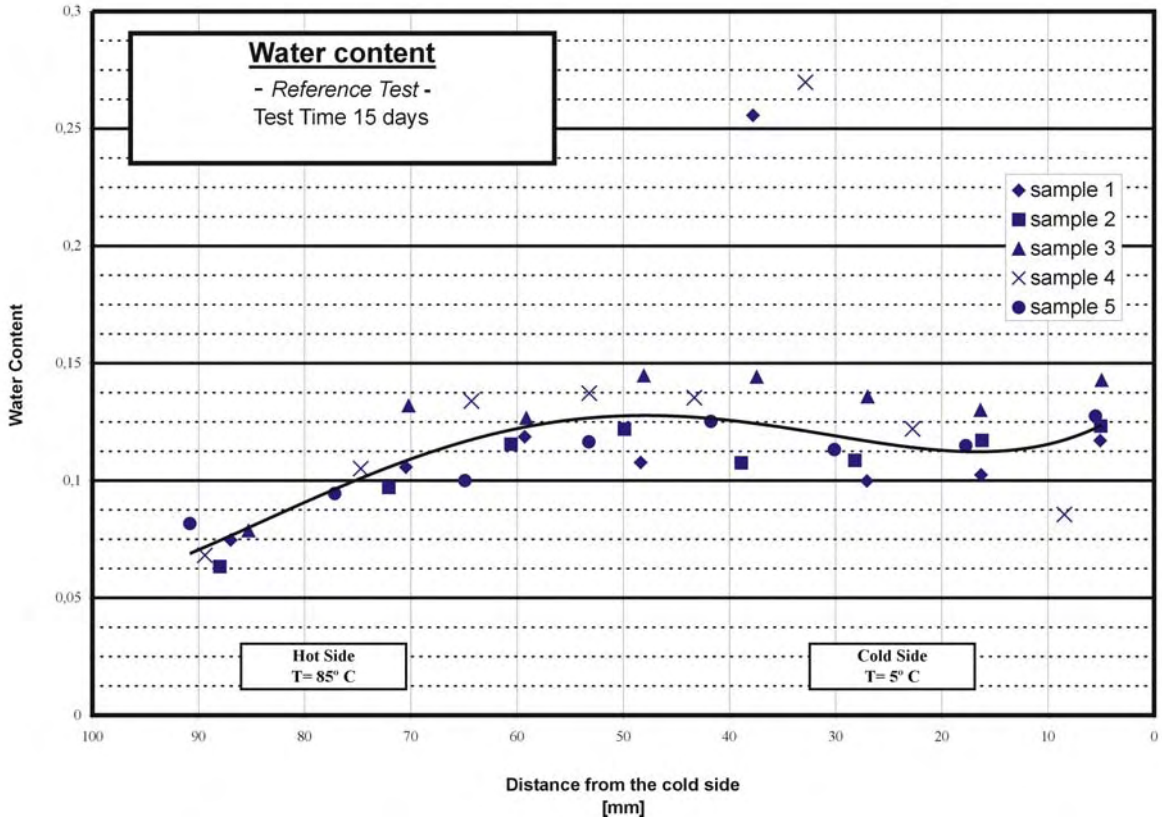


**Fig. 4.21** *Water content after 15 days of application of temperature difference.*

The water content is smaller in the hot side and has got higher values in the cold side. The difference between the two sides is about 0.10 (0.05 in the hot side and 0.15 in the cold side), it seems that the maximum values are located in the middle of the sample and in the cold extremity. The observation of the path of each sample shows that there is a similar behaviour for everyone: from the hot extremity to middle the variation is quasi linear and after there is a second section with upwards concavity, finally the last part in correspondence of the cold side there is a downwards concavity.

## 7-day test

The characteristics of the 7-day test are the same as in the reference test, the only difference is the period of time during which the temperature is applied: 7 days.

The test was repeated four times, one more than the minimum established, because there is a certain deviation in the results of the cold side.

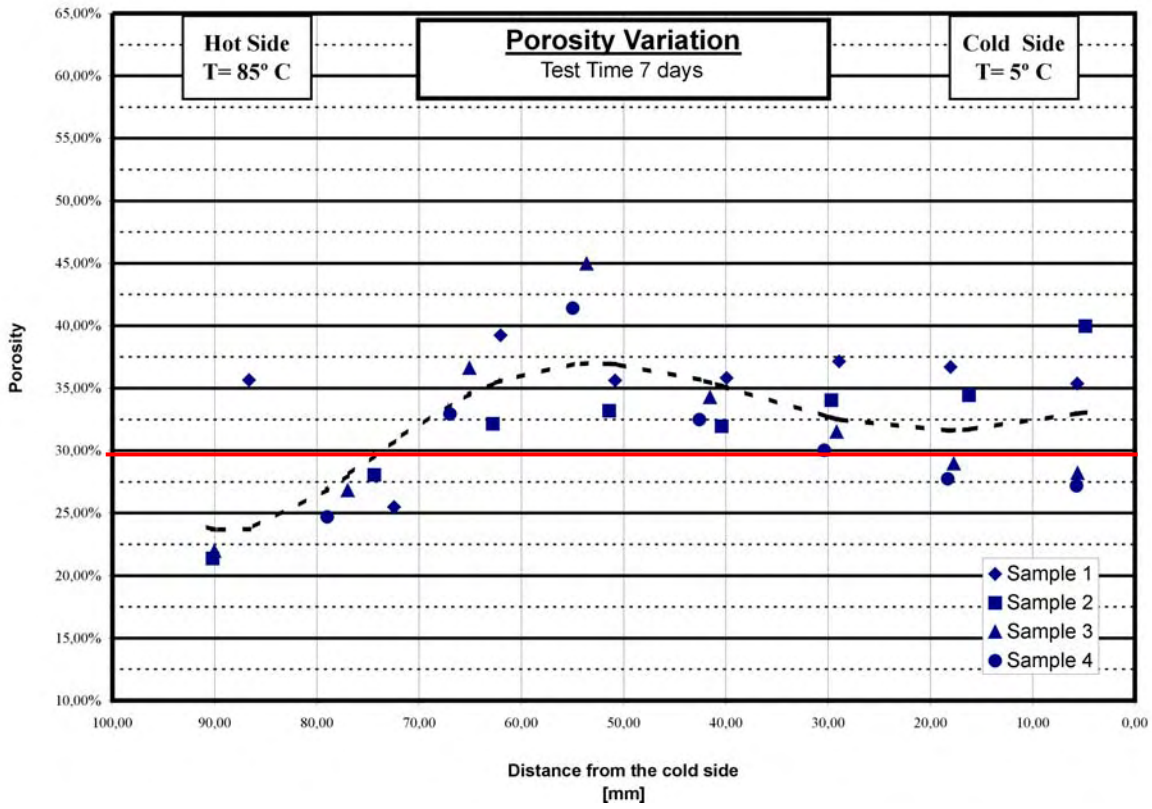


**Fig. 4.22** *Porosity variation when the temperature difference is applied for seven days.*

The first aspect to be pointed out is this indetermination in the results.

The path of the curve is similar to the one of the reference test. The changes of porosity in the specimen are small. It is difficult to make a correct observation, because the porosity values are affected by the initial condition of the sample. Two paths can be identified after crossing the ideal line of initial porosity: one where the porosity is higher than the initial one, about 35% and the second one in which it is exactly the opposite, the porosity value is lower than the initial value, approximately n=27.50%. In both cases the length of the

path is similar, about 30 mm from the cold side, and the porosity is quite constant (see Fig. 4.22).

Moreover, it is difficult to recognize the two surfaces in which the area of the cold side is equal to the one of the hot side, as it was done for the reference test.

The only explanation for this indetermination lies in the real porosity average for the first 30 mm from the cold side: the porosity of these slices is similar to the initial porosity and the phenomenon needs more time to reach this part of the sample, so this part of the sample is affected by the compaction and measurement errors, but at the same time the same behaviour as in the reference test can be recognized.

Thus, it is not appropriate to extend more on the 7-day test now, because the variations are so small that any type of affirmation can be wrong. Only when all the time tests are presented more details about this test will be observed.

The results of total density are presented in Figure 4.23.

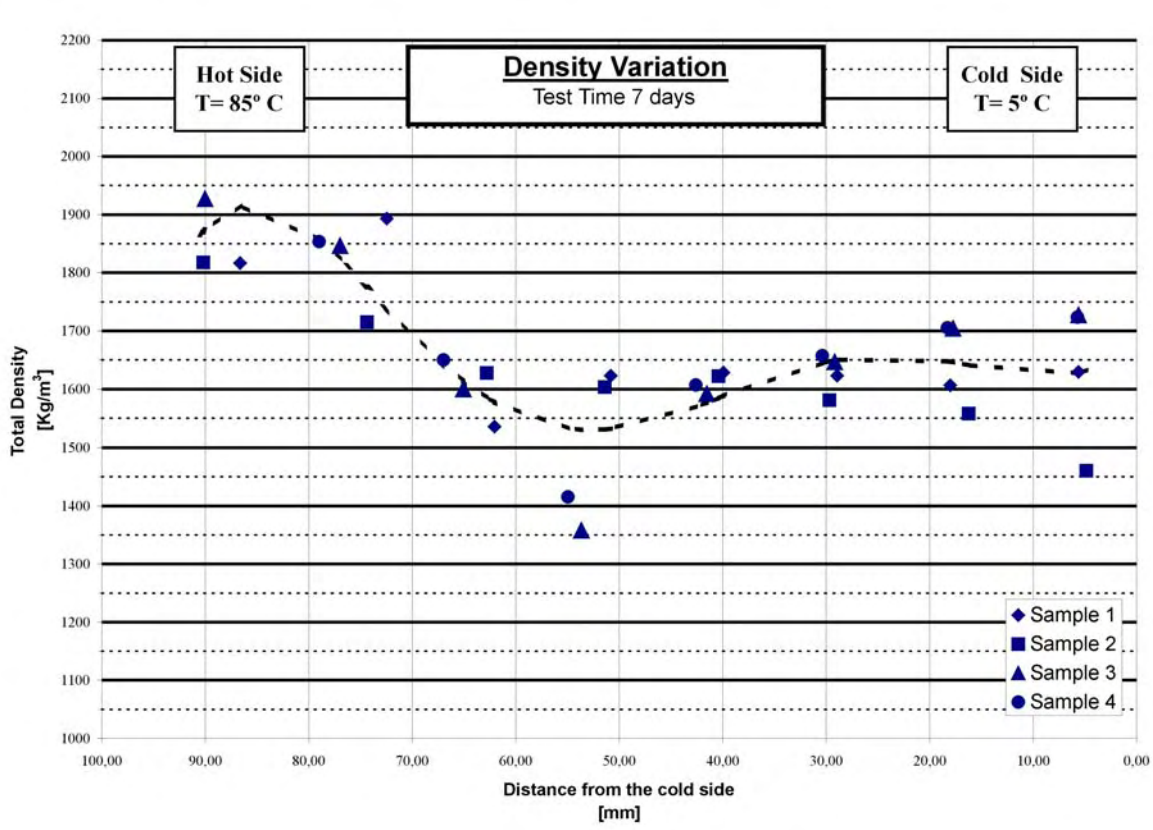


**Fig. 4.23** *Total density variations for a temperature difference application of 7 days.*

## 30-day test

Figure 4.24 shows the results of the 30-day test. As observed in the above-case, the porosity value of each slice is in the y-axis and the distance from the cold side is in the x-axis. In this case there are three samples and the line indicates the behaviour of the phenomenon for this period of application of the temperature difference.

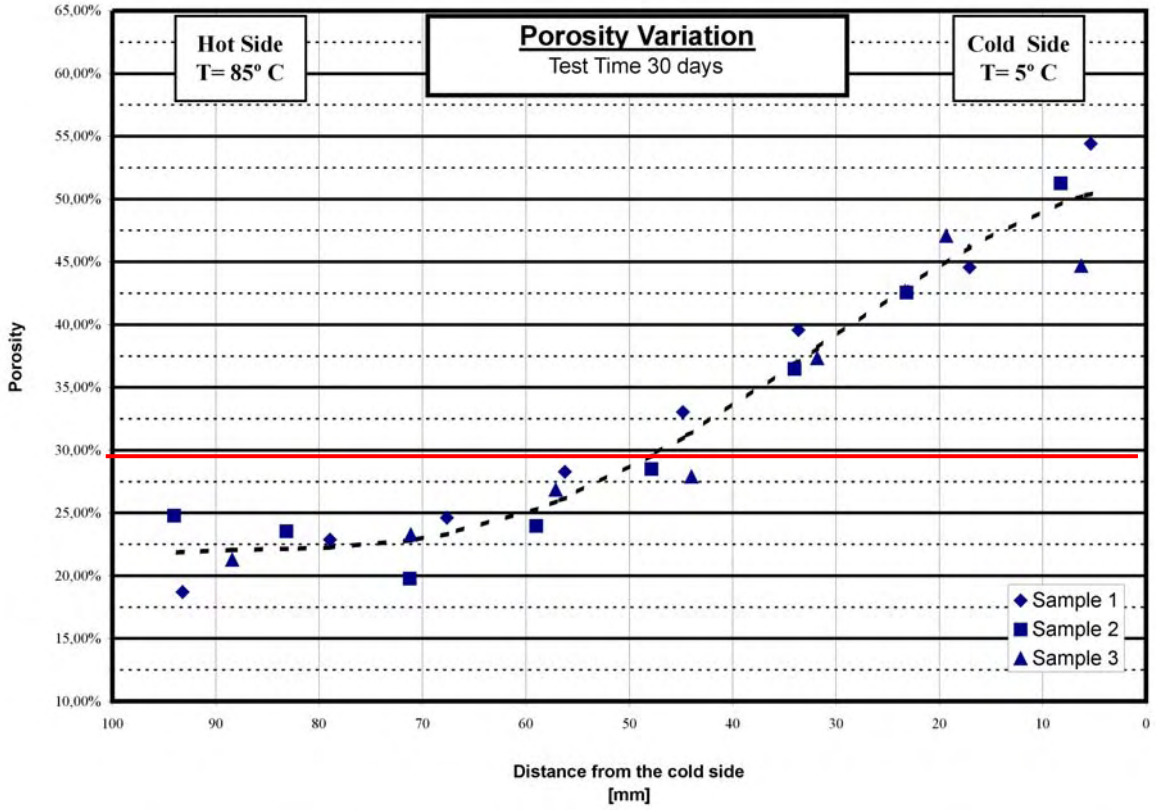


**Fig. 4.24** *Porosity variations for a temperature difference application of 30 days.*

The three points of similar abscissa have got close porosity values with a variation of about 2.50%; only the two groups of points of the extremities have stronger differences.

The difference between the three porosity values is about 7.50% in the hot extremity and is more than 15% in the case of the cold extremity. Nevertheless, in this case this can be considered “normal” because the 30-day samples presented the aspect shown in Figures 4.15 and 4.16, namely the porosity values are high and in a small portion of the sample macro voids can be observed.

The shape of the n(x) of this curve is different from the other cases analysed formerly. It is possible to distinguish three parts of constant slope in the curve. Starting from the hot side, firstly, there is a sub horizontal part for about 30% of the sample length, where the porosity is 22.50%. Then, there is a second linear part up to the crossing point, with the ideal initial porosity line (x=47.50mm; n=30%), and from this point there is an increasing of the slope up to the cold side. The maximum value of porosity is n=55.00%.

This variation of porosity is quite important, and it is reflected in Figure 4.25, where the variation in total density is presented.

It is important to note that it seems that n=20% represents an absolute minimum value: the system cannot reduce its porosity more.

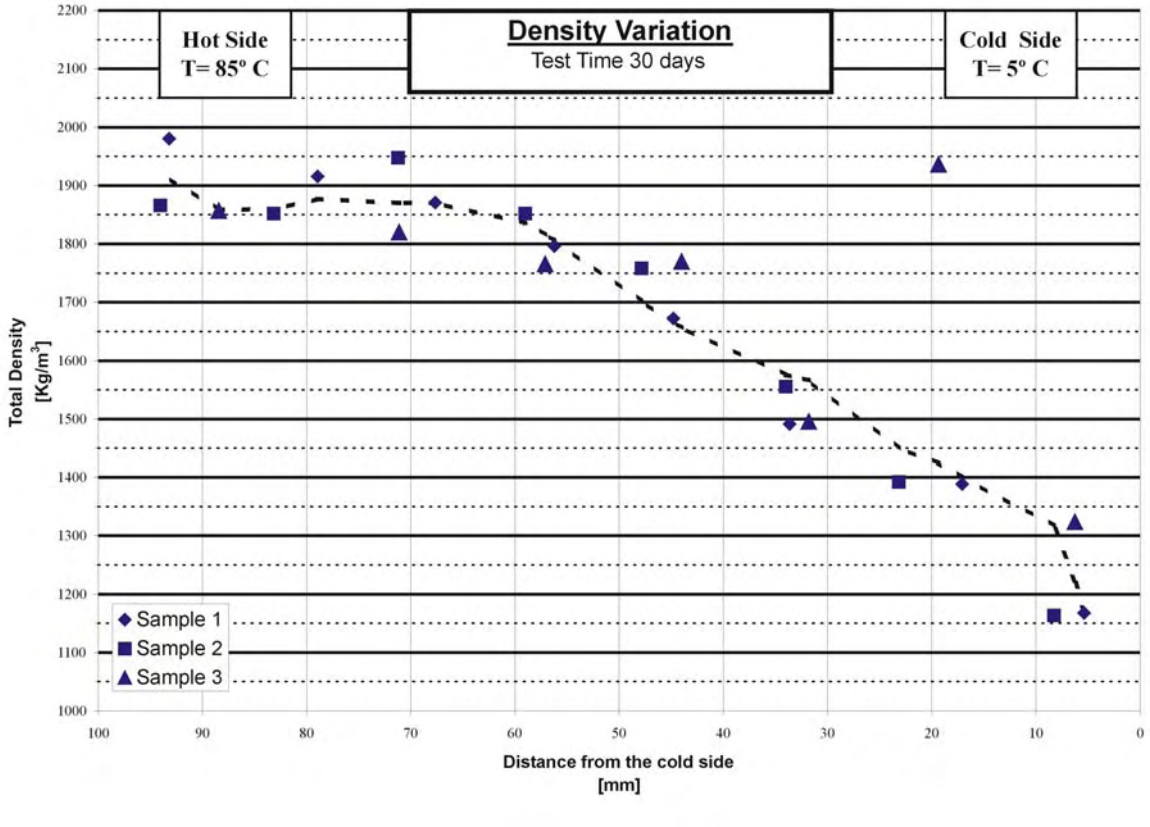


**Fig. 4.25** *Total density variation when the temperature difference is applied for 30 days.*

The total density curve (Fig. 4.25) is more representative of the effects of a temperature difference in a salt sample after 30 days of application: the difference between the cold and the hot side in density terms is of more than 750 kg/m$^3$.

The maximum value is about 1900 kg/m$^3$ and the minimum one is only 1150 kg/m$^3$.

## 65-day test

The 65-day test has already been mentioned to explain the qualitative aspects of the phenomenon in the former chapter.

Figures 4.26 and 4.27 show the porosity and total density variation respectively.

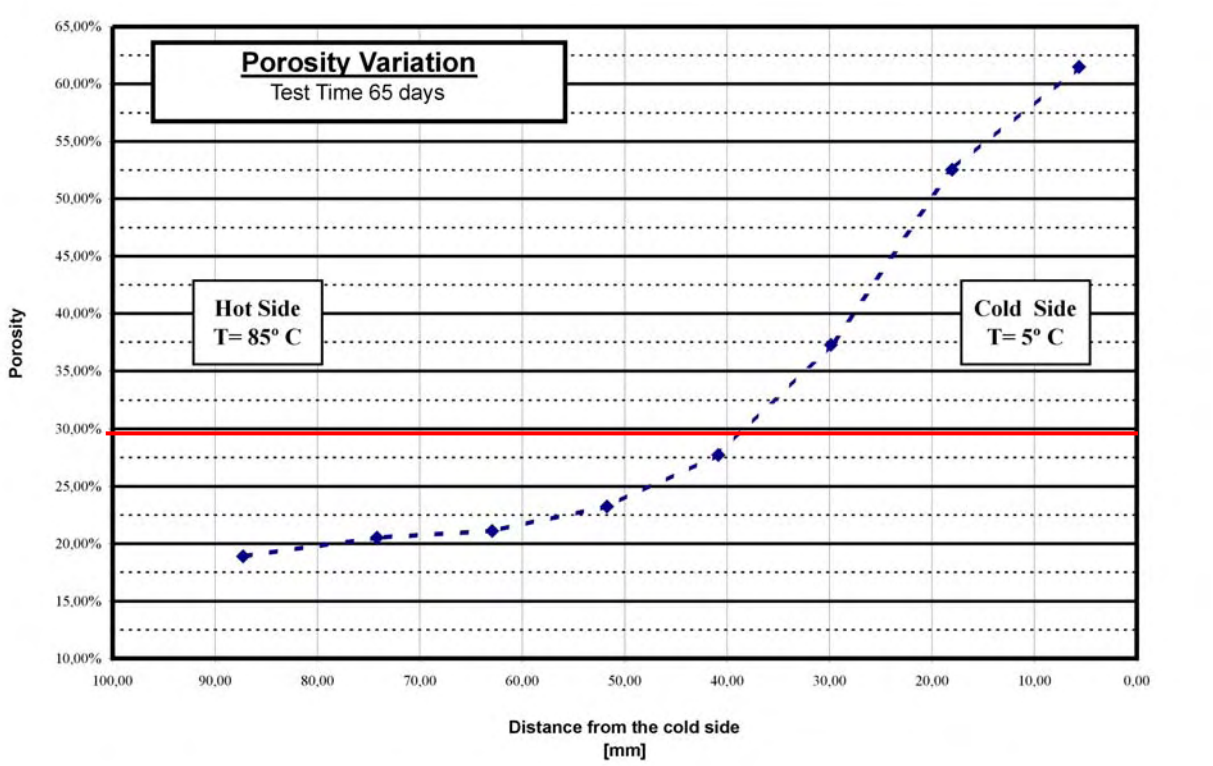


**Fig. 4.26** *Porosity variation for a temperature difference application of 65 days.*

The porosity and total density graphs present only the results of one sample because the other two samples were used to take photos, which does not allow to cut them: there was a brine leak and the cold side lost some grains.

The description of the sample appearance after the application of a temperature difference was shown in the former paragraph and it is useful to remind that there was an important volume in which, due to the dissolution and transport phenomena, the salt material had completely disappeared near the cold extremity. This volume had the shape of a half cone and its vertex was at about 40 mm from the cold extremity.

It was not possible to establish the geometry of this void space more accurately, but this space has a special importance because the plotted graphs represent the average porosity, or total density, of a 10-mm thick slice. That is why, in the evaluation of the total volume, this void space is taken into account. It would be better if the considered total volume for each slice could be divided into two parts, one with infinite porosity and another one with a lower porosity than the one calculated for the entire slice. Unfortunately, this kind of manipulation cannot be done because of the fragility of the samples, and especially from the first two slices from the cold side. This problem concerns approximately only the part from the cold extremity up to the middle of the sample, the rest (hot extremity) has the consistence of a rock.

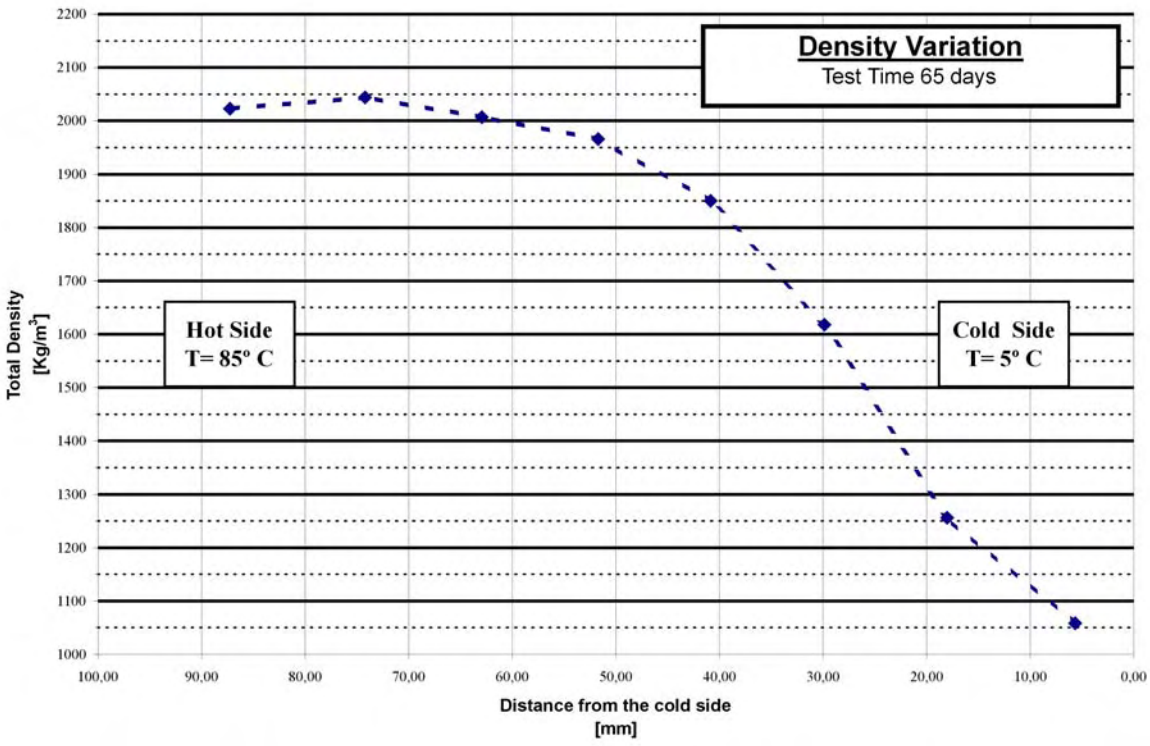


**Fig. 4.27** *Total density variation for a temperature difference application of 65 days.*

The curves are similar to the curves of the 30-day tests. The curve that describes the porosity variations can be divided into three parts as the previous case. In this case, the sub-horizontal segment has a length of about 30mm and, as in the 30-day test, the porosity is about 20% in this part.

The *average* total density of the slice is interesting because it is easy to notice how big the difference is between the cold extremity and the hot one, namely 1000 kg/m$^3$.

Finally Figure 4.28 shows a tomography image of a section of the sample in the hot side. The laboratory delivered the result and made the test five

months after they received the samples. There is a central crack probably due to this waiting time but it can be observed how homogeneous the sample is.

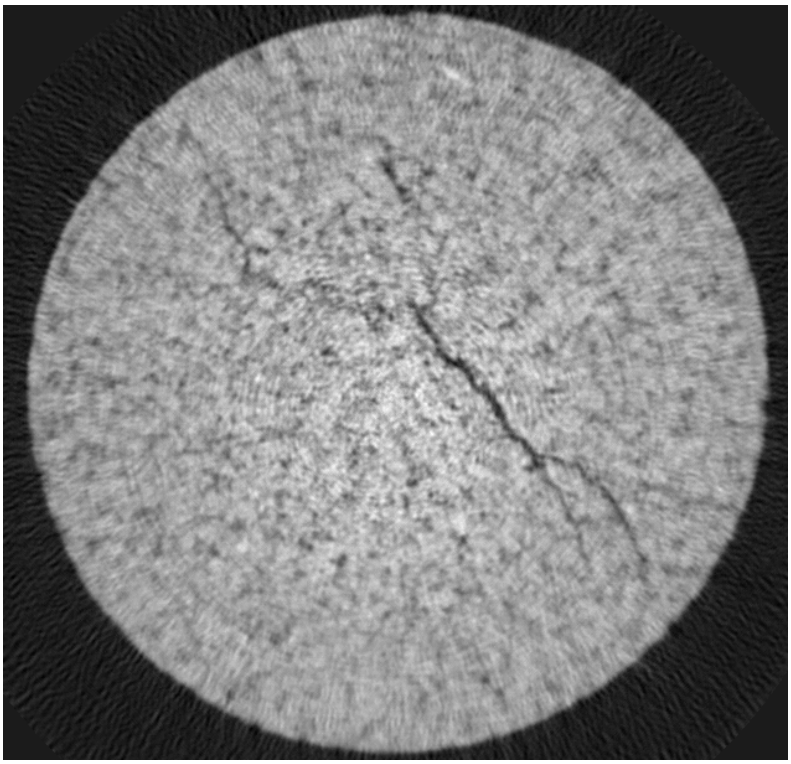

**Fig. 4.28** *Tomography image of the hot side of the 65-day sample.*

## Effect of time

Figure 4.29 shows the porosity variation due to a temperature difference found in all the tests already presented. This graph represents the time development of the phenomena in terms of porosity variation.

The results are represented by five different colours: one for each test time. In this case there is not a different symbol for samples of the same test time: the sample symbols are different only for the test time and a continuous line represents a $5^{th}$ degree polynomial function calculated by the minimum square method.

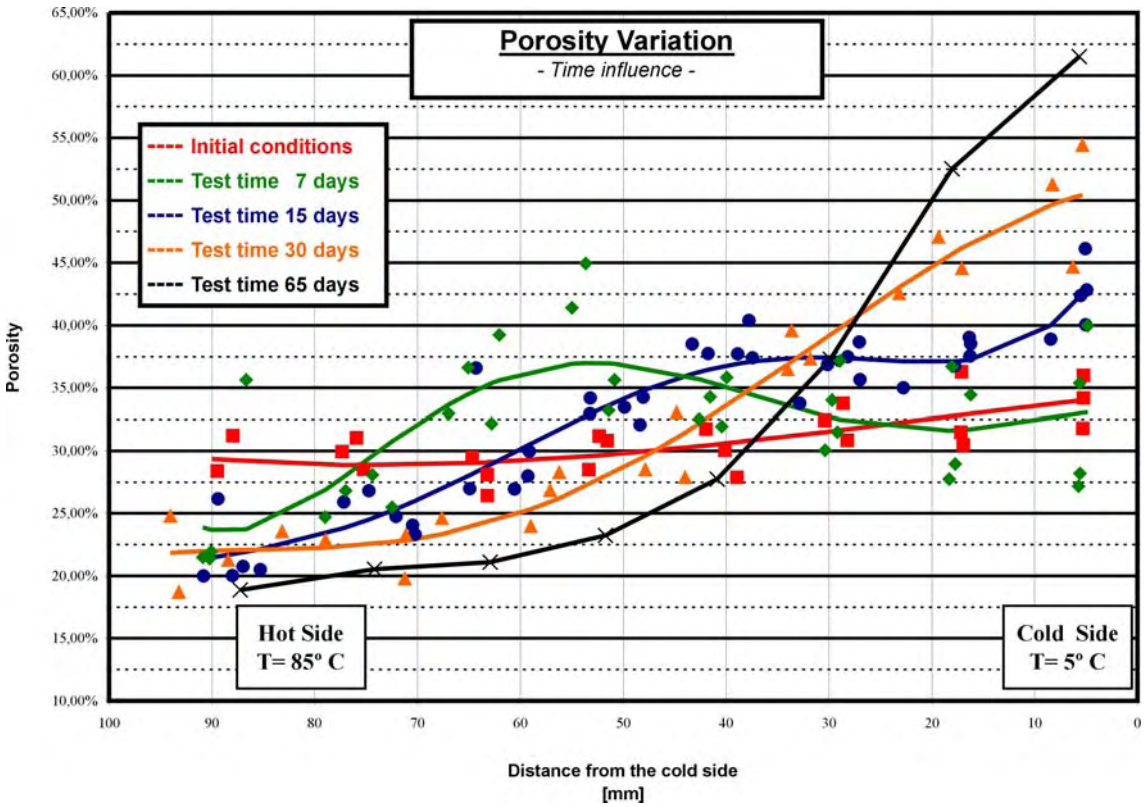


**Fig. 4.29** *Time development of the phenomena in terms of porosity variation.*

The first observation to be done is that these phenomena do not allow clearly defining the boundaries among a test times. There is a superposition between the points of a test time and the points of another test time because, while the larger the time of application of the temperature gets, the higher porosity gets in the cold extremity and the lower, in the hot one. Thus, the points must cross the ideal line of initial porosity. The envelope lines and the study of each test in its own help to solve this problem.

These lines allow determining the development of the phenomenon and understanding it.

In the graph, the initial condition data are also present and it could be noticed how the green line of the 7-day tests is below the red line, belonging to the initial conditions in the cold extremity (0<x<20 mm), although they are also parallel. When the 7-day test was presented it was observed that there was an indetermination in this test and that the points of these samples in this region had two different behaviours. Note that the upper group is between the initial condition points and the 15-day tests and thus, respects its “chronological” position. Although the low porosity variation of the 7-day points from the initial conditions leads to think that, in the first 20 mm, the samples are little or not affected by porosity variation phenomena and that those are (approximately) the initial values, the parallelism with initial condition confirms it.

Moreover, these reasons confirm that seven days could not be considered a significant period of testing to know the behaviour of salt aggregates when the temperature gradient is applied.

Despite these considerations, the evolution of average lines follows its natural and chronological order. In the cold extremity the development is quite clear. There is a direct proportionality between the slope of the curves and the time of application of temperature difference. With regards to the concavity change it is better not to give statements because it could be only an effect of the few points available in a zone in which the changes of porosity are extremely high.

The point where the envelope line crosses the initial condition ideal line (n=30%) varies its position with time: the point moves from the hot side to the cold one.

The behaviour of the curves in proximity of the hot extremity calls for a special analysis. The average lines respect the time chronology but the observation of the points of the different test time shows a peculiarity: there is a minimum value in the system, about n=20%, and there is a sub-horizontal segment in all the cases. For the highest values of time, 30 and 65 days, this trend can be immediately discovered. In the case of the reference test (15-day) it can be pointed out that there are several points (4) in a range of 5 mm with the same value of porosity, about n=20%.

The difference between a case and another is the length of the sub-horizontal segment. As time increases, this sub-horizontal section of the curve lengthens, in the same way the point in which the envelope curve crosses the initial condition line moves trough the cold extremity.

The phenomena induced by a temperature difference in the cases studied lead to reduce, at the same time, the porosity and the length of the sample. It is possible that, in the same test conditions, when $t \rightarrow \infty$, the sample has a new uniform porosity, lower than the former one and, at the same time, the sample length should be reduced because of the absence of mass transfer.

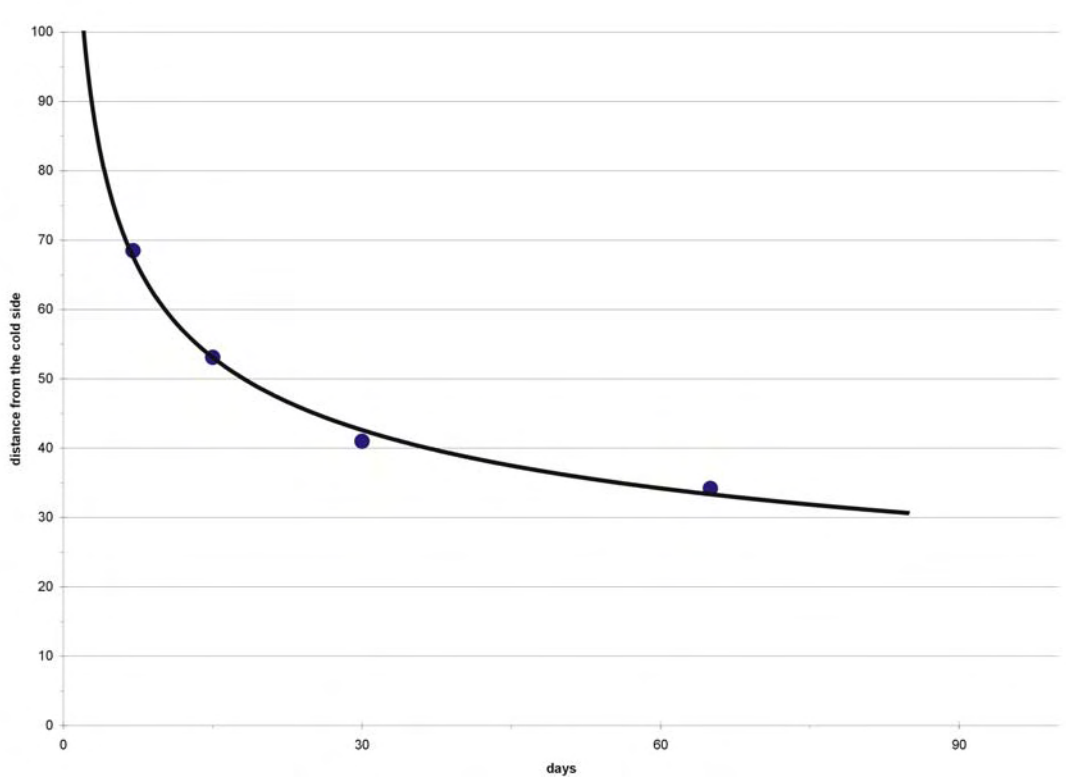


**Fig. 4.30** *Position of the intersection point between the initial porosity value (n=30%) and the average curve of porosity variations as a function of testing time.*

Furthermore, Fig. 4.29 allows understanding the phenomena explained at the beginning of this chapter (See Fig. 4.1). It is now clear that the temperature difference induces several different effects in the sample. These phenomena can be divided in three categories: evaporation/condensation, precipitation/dissolution and fluxes. The development of these phenomena in time shows (Fig. 4.29) that evaporation/condensation and dissolution/precipitation move from the extremities of the sample to the centre: the intersection of the envelope lines and the initial porosity line move from the hot side to the cold side.

Fig. 4.30 confirms these statements, it represents the displacement of the interception point between the initial porosity line value (n=30%) and the envelope curves of the performed tests. Four experimental points are represented in the graph and its envelope curve. The equation of the curve is:

$$d = 125.27t^{-0.317} \tag{4.3}$$

where d is the distance from the cold side and t is the test time, the regression coefficient of the curve is $R^2$=0.9917.

The curve describes the displacement of the precipitation phenomena from the hot side to the cold side. The obsrevation of the path of the curve leads to the statement that for $t \rightarrow \infty$ the precipitation phenomenon could, theoretically, reach the cold side (d=0). This effect was already determined in Figure 4.29 and confirms the behaviour based on the phenomena under study: there is a smaller porosity value, about n=20%, than the initial n value (n=30%) for which the hydraulic conductivity is too low and there is no brine flow in this part of the hot side. Therefore, this zone is dry and the precipitation of salt from brine is not possible, thus the phenomena move in the direction of the cold side. Meanwhile the sample reduces its length in this zone for the dissolution of the salt aggregates (solid phase) in the pure water because of the condensed vapour arriving from the hot side.

It is possible to observe in Figure 4.29 that the hypothesis of “no mass transfer” is valid for all times studied.

The phenomena are very important in the case studied because, if the behaviour of the barrier were similar to the one observed in the laboratory experiments, the canisters of nuclear deposits should have a stronger barrier close around them but, at the same time, with no maintenance, there would be a zone without contact between the host rock and the filling material.

Figure 4.31 represents the water content results for all samples tested with different duration, a different colour represents a tested time. The points represent the experimental results and the lines are the envelope for each time. The envelope line is a $5^{th}$ degree polynomial function calculated by the minimum square method.

The experimental points confirm the tendency of the porosity graph, namely the result has got small deviation and it is possible to recognize a clear behaviour induced by the elapsed time.

The lowest values of water content are localized in the hot side and the higher values, in the cold side.

The tendency of the lines respects the chronological order of the lines and the no-mass balance transfer hypothesis is confirmed, too, even if the dispersion of experimental water content points is much higher then the porosity experimental points dispersion and it is quite difficult to observe it.

The dispersion is high and for this reason it was not possible to represent the initial condition for the water content. In any case, the average value of the water content at initial condition is 9,60%; this value was obtained by the average of the three samples used to study the initial conditions.

It must be pointed out that the dispersion of the points and the difficulty of interpretation of the graph of the water content is caused by the new equilibrium that the sample reaches at the moment that the two heat transmitters are disassembled. Then the high suction present in the sample disappears and all flows stop, the system reaches a new equilibrium and the water content tends to be the same at all points. Furthermore the cutting operation by saw took about 45 minutes for each sample and this time is sufficient to reach a new equilibrium. Prior and post-investigation confirm (Olivella et al. 1996 b) that there is a dying process in the hot side, so that the water content in Figure 4.31

does not represent the actual situation when the temperature difference is applied.

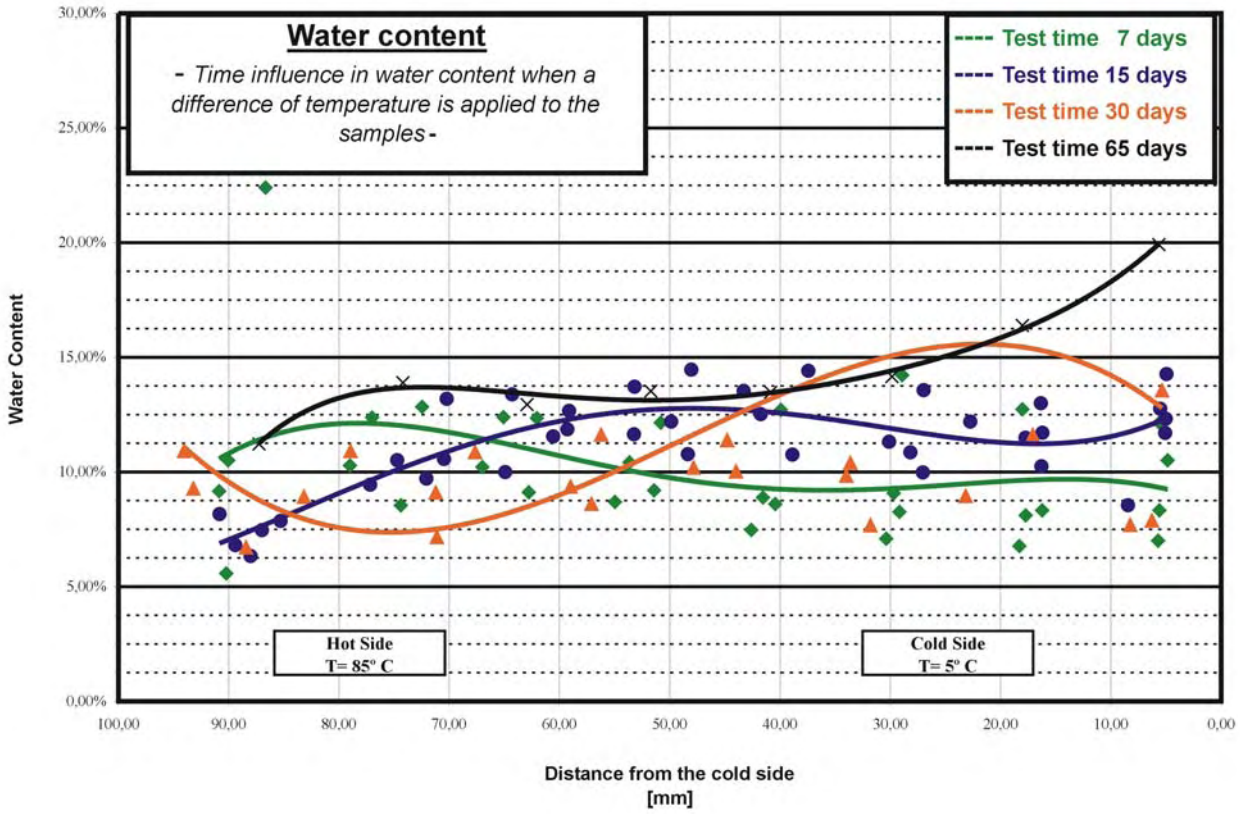


**Fig. 4.31** *Water content variation in the samples.*

Table 4.5 reproduces the weight losses in the sample, this values is obtained, as in Table 4.3, by subtracting the initial weight of the sample before performing the test and the final weight of the sample immediately after the test is stopped.

**Table 4.5** *Weight loss in the sample during test performance.*

| | Test duration | | | |
|---|---|---|---|---|
| | 7 days | 15 days | 30 days | 65 days |
| Sample 1 | 1.53 | 1.14 | 3.48 | 10.18 |
| Sample 2 | 1.24 | 2.32 | 5.63 | *** |
| Sample 3 | 0.38 | 1.81 | 4.80 | *** |
| Sample 4 | 0.77 | 3.82 | *** | *** |
| Sample 5 | *** | 1.47 | *** | *** |
| Average | 0.98 | 2.11 | 4.64 | 10.18 |

The loss increases by time, it is very small in the case of 7-day test, while significant for the 65-day test, but it must be pointed out that in the last two cases (30 and 65-day tests) there is a possibility of grain loss in the cold side during the phases between the disconnection of the heat transmitter and weighing.

## Effect of Initial porosity

The second effect to be studied is how the behaviour of the phenomena involved in this case can vary when initial porosity changes.

This influence can be considered the second in order of importance, being time influence the first one, as it rises the following question: “which is the optimum density of salt aggregates, if there is one, to reduce the dissolution phenomena and protect the environment from nuclear pollution?”

As usual, the results are presented and analysed in terms of porosity variation but, in this case, the total density values are also taken into account.

The reference test has a porosity of 30%, so considering the constraints of the apparatus and the method, the choice of the new values of initial porosity was compulsory. In order to be effective, the initial porosity should be higher or lower than at least ten percentage points. Moreover, the plastic ring cannot resist the efforts of the sample preparation when the wished initial porosity is lower than n=20%. Finally a porosity of more than n=40% does not guarantee the requested uniformity, and there is a very high risk to lose the sample before the test can start. So there are only two possibilities: n=20% and n=40%.

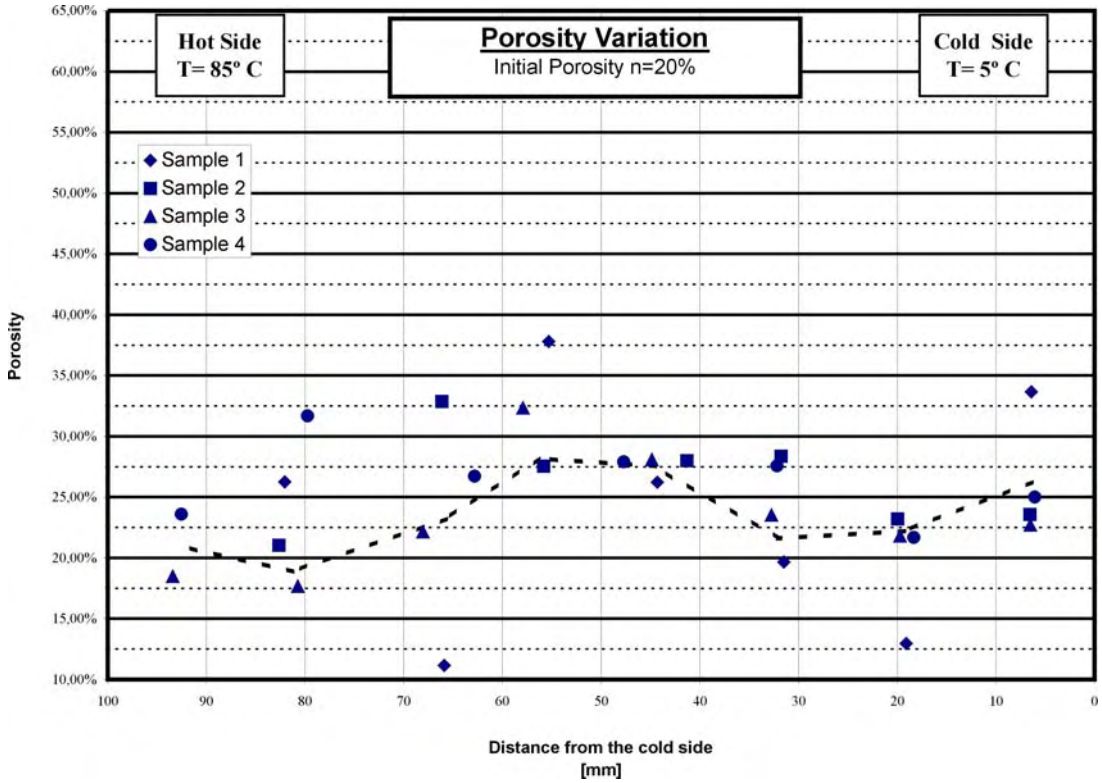


**Fig. 4.32** *Porosity variation when the initial value of porosity is n=20%.*

Both cases were tested and the results are presented here. The rest of parameters are those of the reference test, including the duration of the test: 15

days. Figures 4.32 and 4.33 show the porosity and total density variation due to the temperature difference when the initial average porosity value is n=20%.

The results of n=20% are the worst of the entire test campaign, there is a big dispersion of the points with the same x-value, more than 10% in many cases, thus any further comment is not justified. The envelope line was calculated excluding several points to recreate a curve with a path similar to the other cases, but the curve does not verify the absence of mass transfer.

The test was repeated six times. To reach a better result, the way to obtain the porosity variation was changed and two different methods were used. The first sample was sent to a tomography laboratory and in the second case, the determination of total volume was done by immersion in mercury. The two methods did not give significant results, so they were not included in the graph.

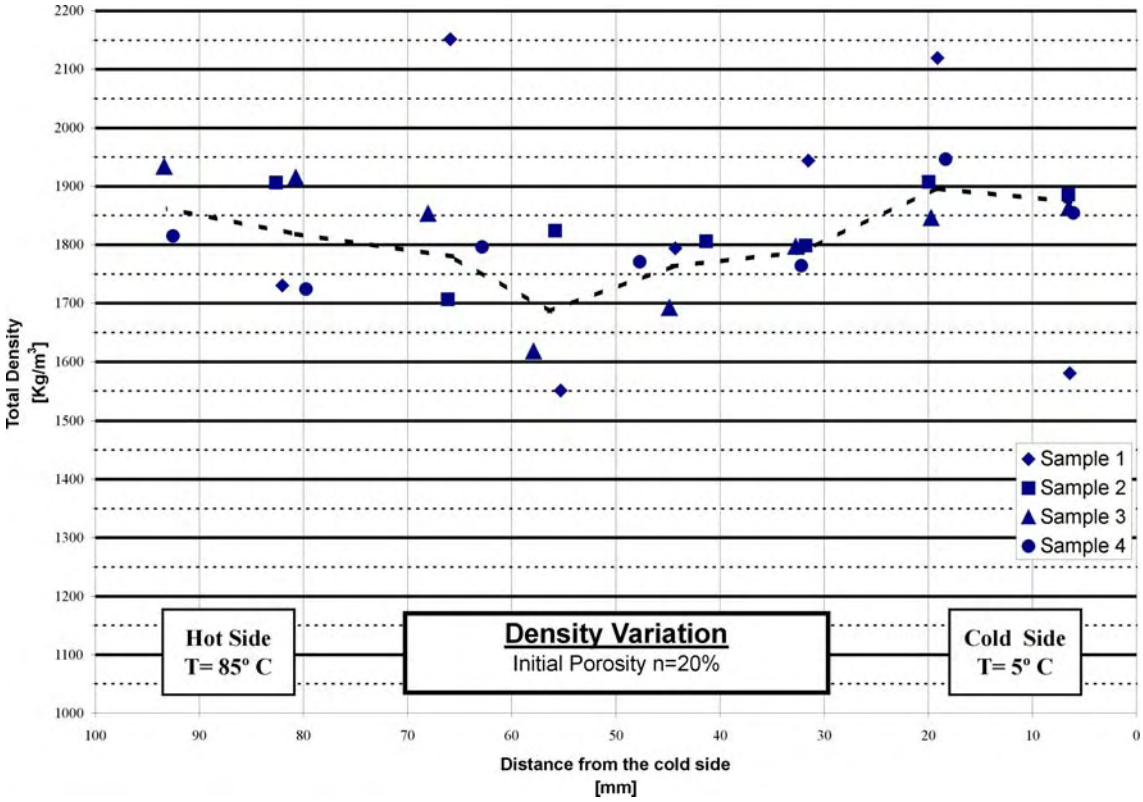


**Fig. 4.33** *Total density variation when the initial value of porosity is n=20%*

Table 4.6 shows the difference between the porosity values immediately after the sample preparation and before applying the temperature difference, and the average porosity of the slices of the same sample after the application of the temperature for 15 days.

The data in Table 4.6 could be the answer to this bad result although it is not clear enough because the deviation from the theoretical value is quite big for the average porosity of slices in three out of the four samples (about 5.5% from the measured initial value of the total sample) and this deviation could be

caused by several effects: one being the creep phenomenon. In this case, the compaction load is much higher than in the reference test (n=30%) and it is possible that, while the samples were installed in the apparatus for the application of the temperature difference, there was a creep effect.

**Table 4.6** *Porosity values of the samples* [n=20%].

| Sample | Calculated Porosity before the application of temperature difference | Average Porosity of the sample slices | Δ |
|---|---|---|---|
| 1 | 19.47% | 23.96% | 4.49% |
| 2 | 19.71% | 26.37% | 6.66% |
| 3 | 21.65% | 23.34% | 1.69% |
| 4 | 20.72% | 26.32% | 5.60% |

The second test was developed with an average initial porosity of 40%, and the results are much better than in the previous case. Three samples were enough to determine the behaviour of this case. There are some points with a deviation of more than 5%, but in this case the envelope curve path is quite clear.

**Table 4.7** *Porosity values of the samples* [n=40%].

| Sample | Calculated Porosity before the application of temperature difference | Average Porosity of the sample slices | Δ |
|---|---|---|---|
| 1 | 38.98% | 40.70% | 1.72% |
| 2 | 37.69% | 40.41% | 2.72% |
| 3 | 38.52% | 41.29% | 2.77% |

Table 4.7 shows the difference between the porosity values immediately after the sample preparation and the average porosity of the slices of the same sample. In this case, the values have a deviation similar to that found for the reference case. Moreover, the average value of porosity of the slices is close to the wished value n=40%.

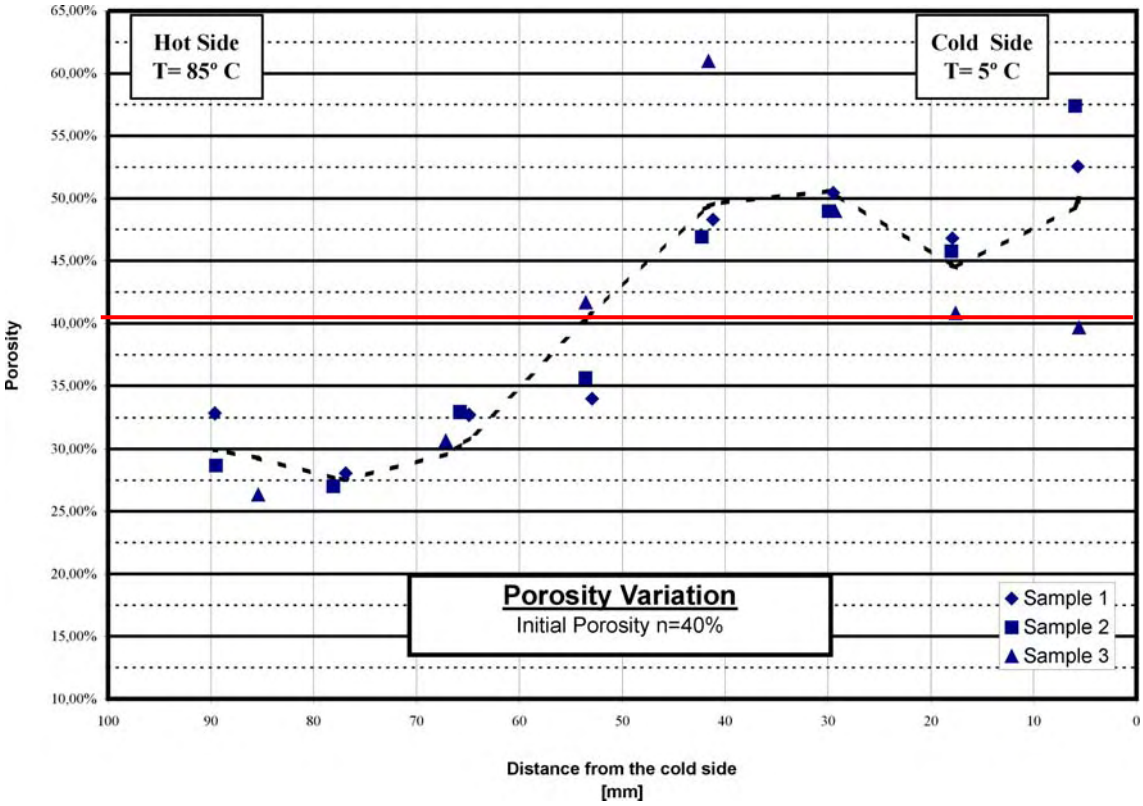


**Fig. 4.34** *Porosity variation for an initial value of porosity* n=40%.

The compaction of these samples needed very low load capacity. This was possible to do in the press by manually fixing the screw of the top head of the equipment.

Figure 4.34 reproduces the porosity variation induced by temperature difference when the initial porosity is n=40%. The curve presents a maximum value of porosity in the cold side (x=30 mm; n=50%) and a minimum one in the hot side (x=78 mm; n=27.50%).

Figure 4.35 shows the results in terms of total density. In this case the absolute values of density are similar to the ones obtained in the case of the 65-day test.

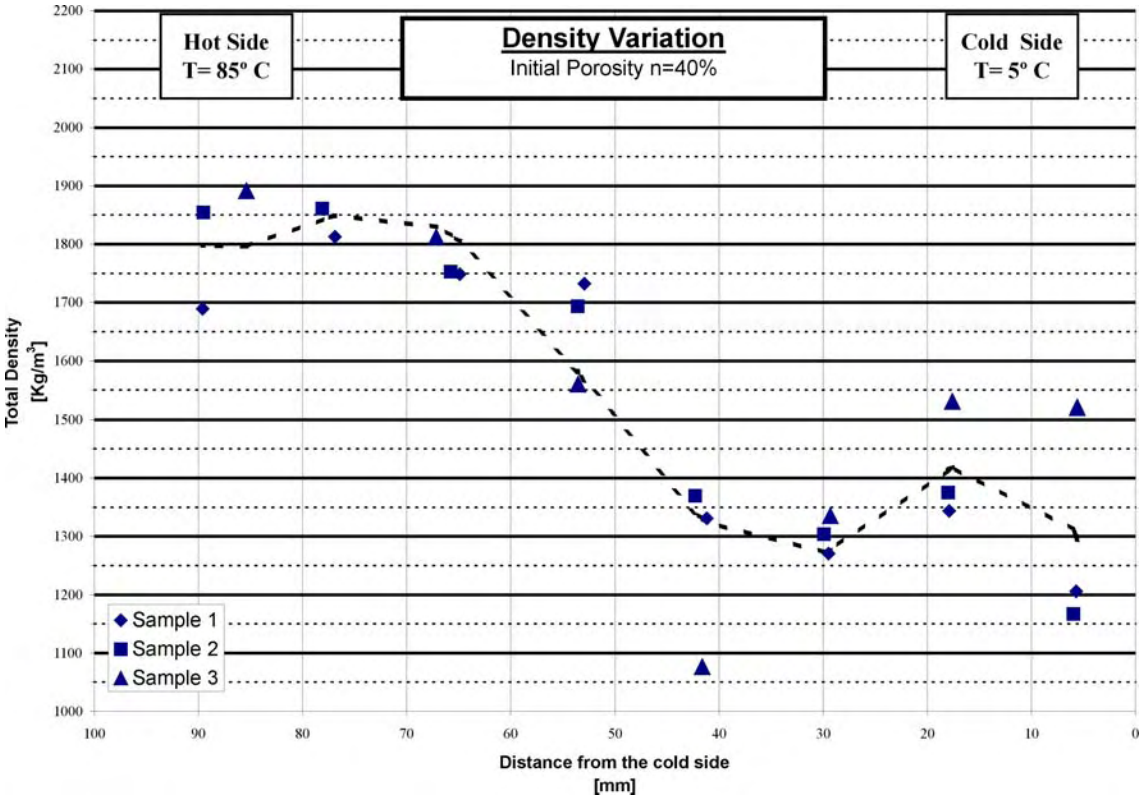


**Fig. 4.35** *Total density variation for an initial value of porosity n=40%*

Finally, Figure 4.36 reproduces the influence of the initial porosity in the behaviour of the sample when a temperature difference is applied.

First of all, it is important to say that the envelope curve for initial porosity n=20% test seems not so bad because it had the same behaviour of the other and more or less there is a symmetry, what is bad are the points because there are many that are out of range.

In the same way is important to notice that the points of the reference test are well separated from the ones of the n=40% initial porosity-tests.

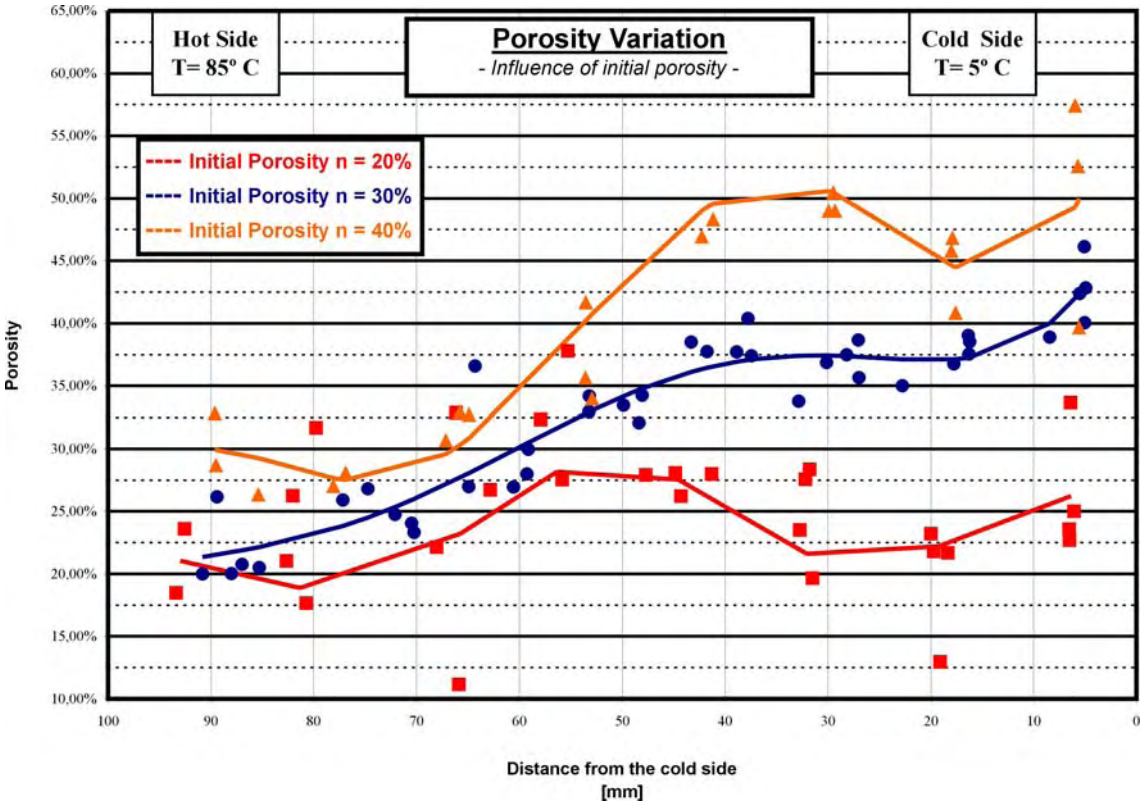


**Fig. 4.36** *Initial porosity influence. Testing time: 15 days.*

The final result of this part of investigation is evident: there is a direct proportionality between the speed of the phenomena of precipitation/dissolution and the average initial porosity. The porosity distribution for n=20% is similar to the one founded for the 7-day test. In the same way, the porosity distribution for n=40% is similar to the 30-day test, although in the case of n=40% it is easy determining the surfaces to verify the hypothesis of no mass transfer. Furthermore, the final porosity of the hot side is directly connected to the initial porosity: the observation of the n=40% graph demonstrates that the precipitation stopped at n=27,50% in this case.

**Table 4.8** *Weight loss in the sample during the test performance.*

| | Initial test porosity | | |
|---|---|---|---|
| | n=20% | n=30 % | n=40% |
| Sample 1 | 1.02 | 1.14 | 2.08 |
| Sample 2 | 0.83 | 2.32 | 2.13 |
| Sample 3 | 0.42 | 1.81 | 7.07 |
| Sample 4 | 0.23 | 3.82 | *** |
| Sample 5 | 1.28 | 1.47 | *** |
| Sample 6 | 0.42 | *** | *** |
| Average | 0.70 | 2.11 | 3.76 |

Table 4.8 reproduces the weight losses in the sample, this number is obtained, as in Table 4.3, by subtracting the initial weight of the sample, before performing the test, and the final weight of the sample, immediately after the test ends. The results for n=20% include the two samples used to determine the porosity variation by other methods: Sample 5 by immersion in mercury and Sample 6 by tomography. Sample 3 for n=40% was affected by grain loss in the cold side (final porosity is n≈55%) during the displacement from the apparatus to apply temperature difference to the weighing. Excluding the result of Sample 3 for n=40%, the results are similar in all tests, that is satisfactory.

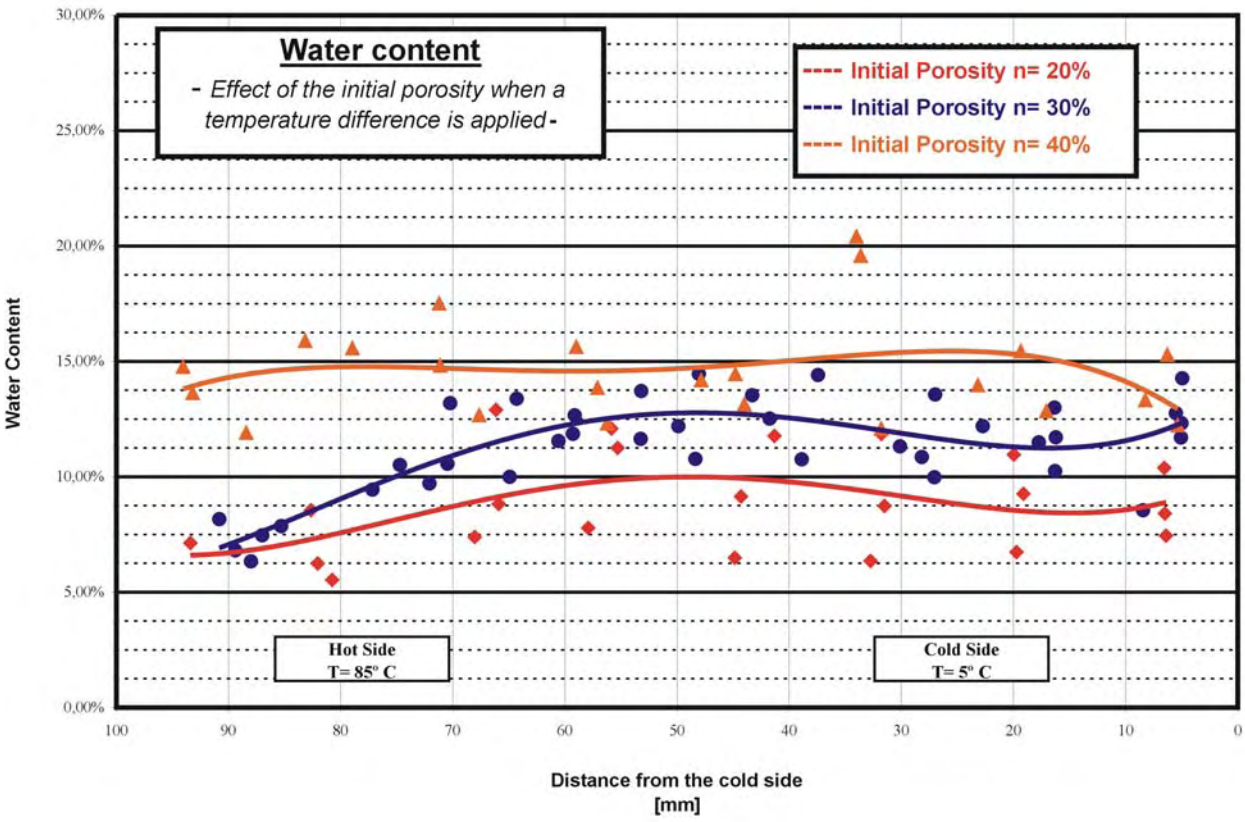


**Fig. 4.37** *Effect of initial porosity on the water content when the temperature difference is applied in the salt aggregates.*

The effect of initial porosity on water content is represented in Figure 4.37. The representation is done by the usual convention used in this work, in this case the envelope curves are a 4$^{th}$ degree polynomial function calculated by the minimum square method. It is possible to appreciate a clear separation among the experimental points of the three different initial porosities considered for this study. Lower values of water content correspond to lower values of initial porosity; the water content is always lower in the hot side and higher in the cold one. Furthermore, the values of water content for n=40% show small variations

with respect to its average value. In any case, this result depends on the dependency between the water content and initial porosity. The points represent the new equilibrium reached after disconnecting the heat transmitter.

## Influence of the saturation degree

The last parameter of the sample that could be changed is the saturation degree. The saturation degree has got an influence in the process of dissolution/precipitation because it is trivial to say that the presence of brine is one of the essential components to start the phenomena object of this study.

To study the importance of the influence of saturation degree in the phenomena, two values of saturation degree are considered, S=10% and S=30%, both of them are lower than the one of the reference test, S=40%, this choice is motivated by the former consideration about the real brine content of the mines.

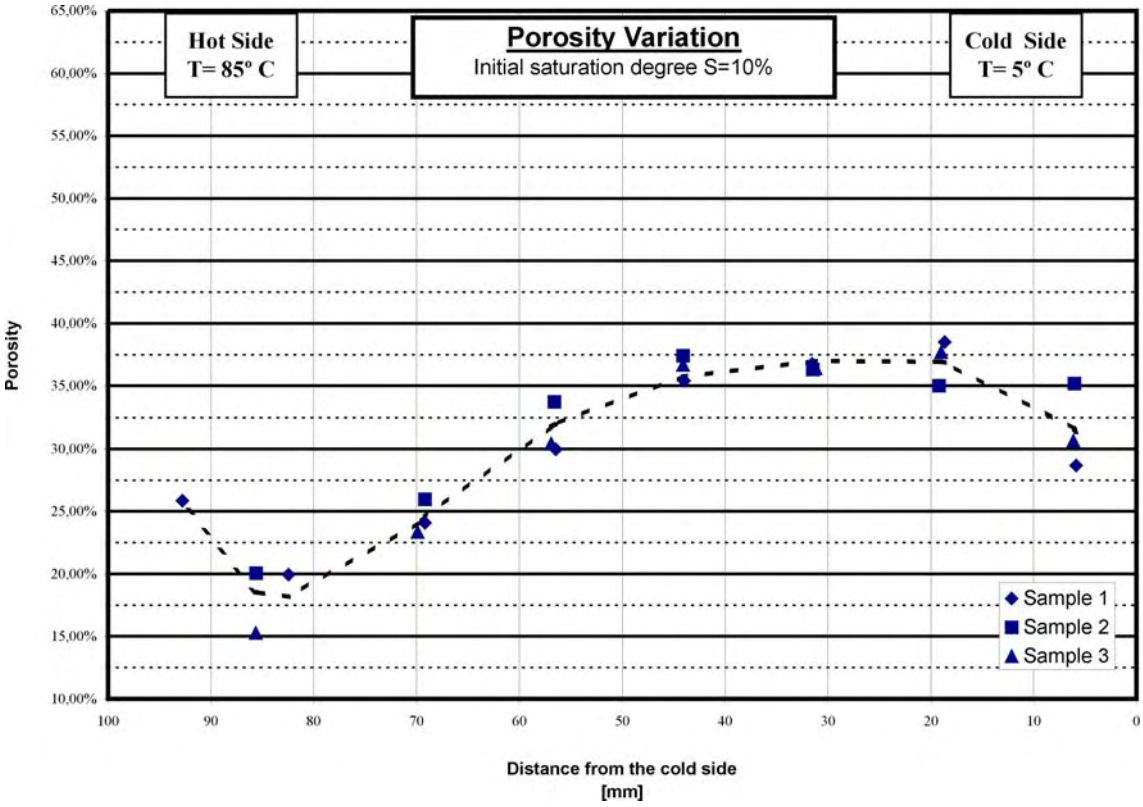


**Fig. 4.38** *Porosity variation for an initial value of saturation degree* S=10%.

Following the usual representation system, Figures 4.38 and 4.39 show the results for the case of initial saturation degree S=10% in terms of porosity and total density, respectively.

Three samples were tested and the three give very similar results, thus, making it possible to determine the curve of the path.

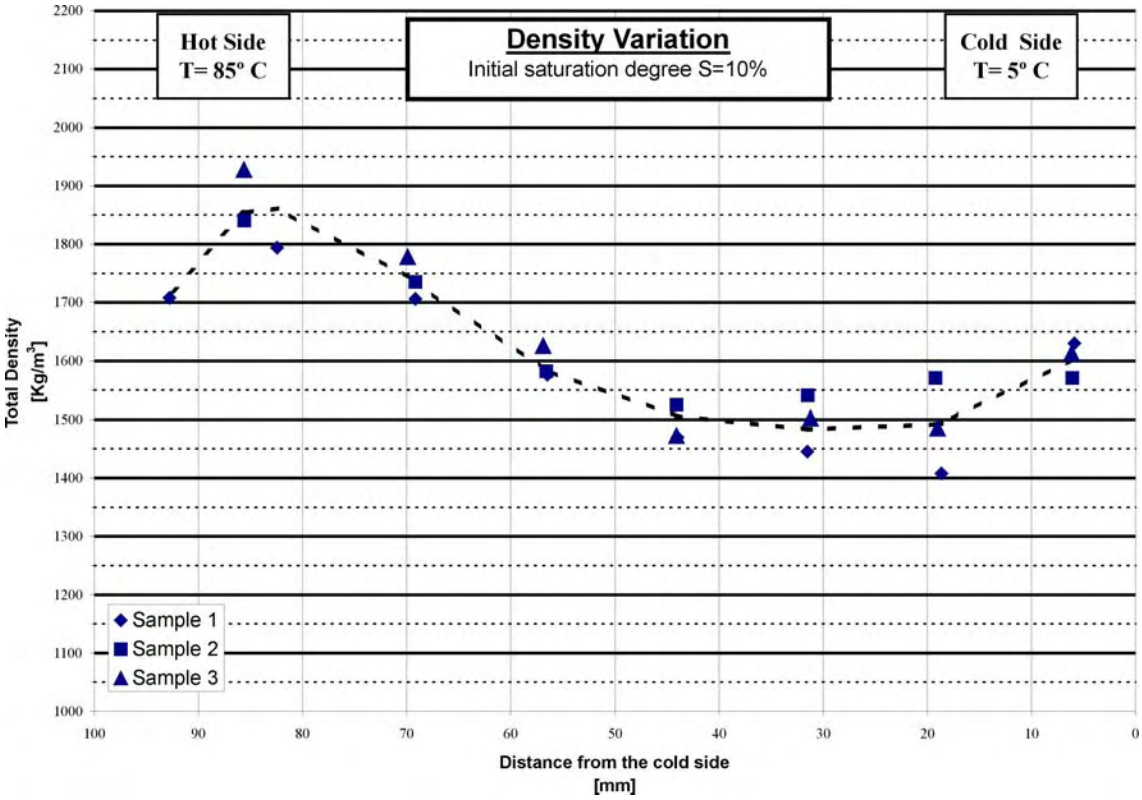


**Fig. 4.39** *Total density variation for an initial value of saturation degree* S=10%.

The results of S=30% are presented in Figure 4.40a and b. In this case, three tests were also performed. The results of the three tests are also quite good. The difference of values for the same value of x is very little in all the cases.

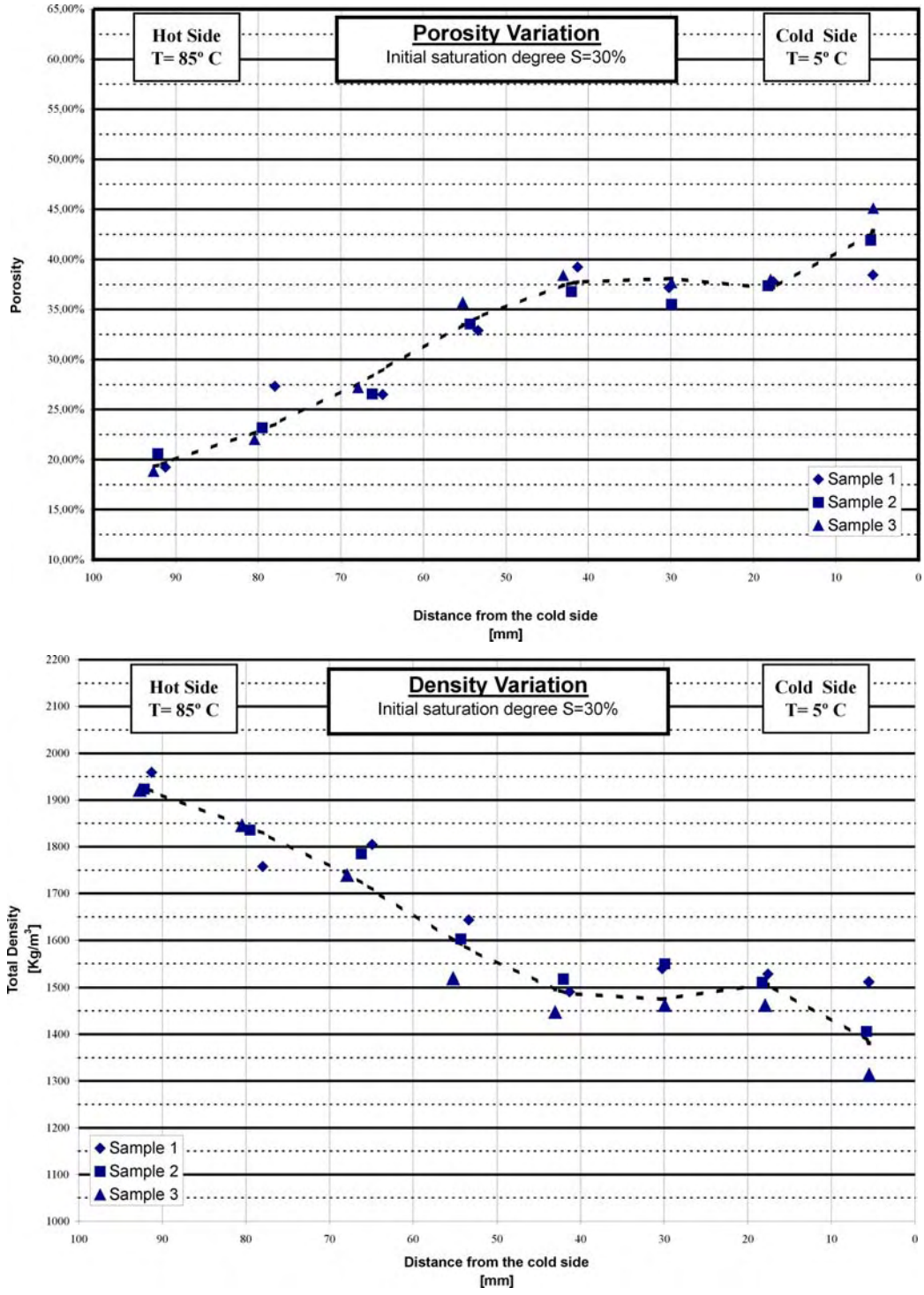


**Fig. 4.40 a.b** *Porosity and total density variation for an initial value of saturation degree* S=30%.

To better describe the influence of initial saturation degree, the tests are plotted in the same graph, together with the ones of the reference test, following the established convention of a colour for each case.

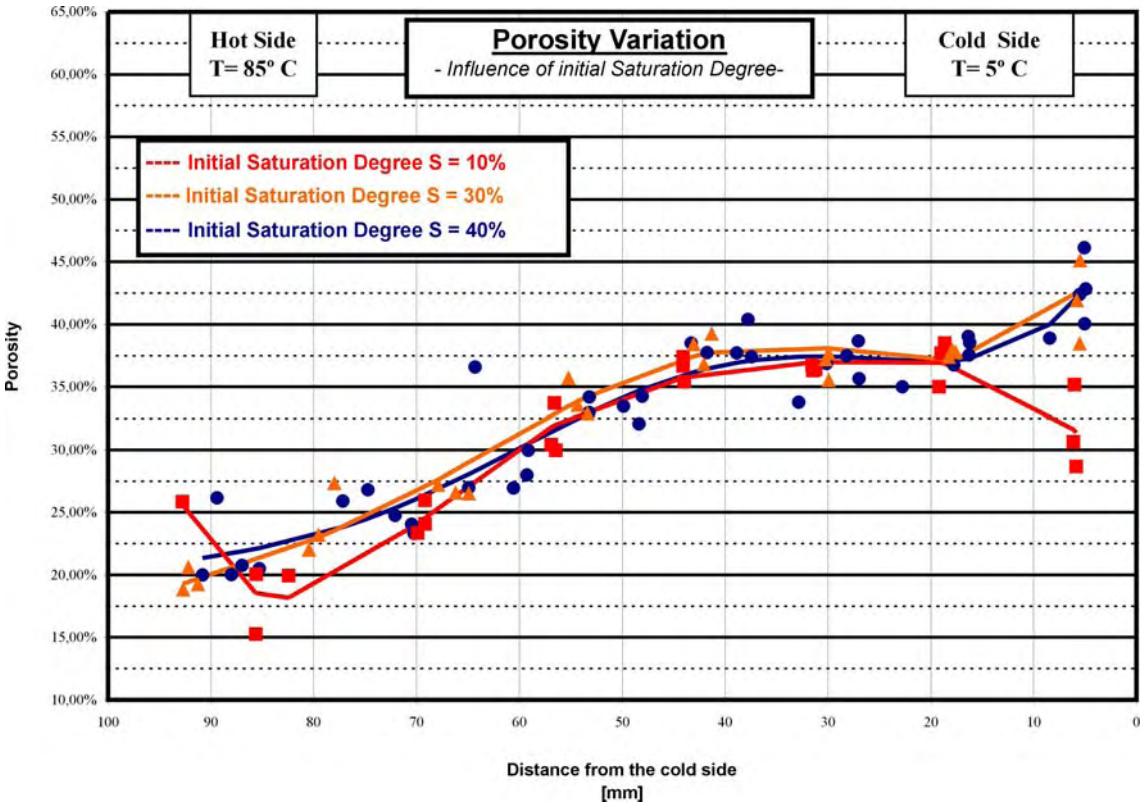


**Fig. 4.41** *Influence of the initial saturation degree.*

The comparison of the results in Figure 4.41 shows how close the results are from one another. The saturation degree does not affect the porosity variation due to the temperature difference when its value covers the range between S=10% and S=40%.

## Different sample length

The last effect studied was the influence of the sample length in the process. In this case a longer sample was tested. The length was 160 mm, 60 mm longer than the reference test. The other conditions were kept the same as in the reference test, including the time of application of the temperature difference: 15 days.

Figure 4.42 shows the results in terms of porosity.

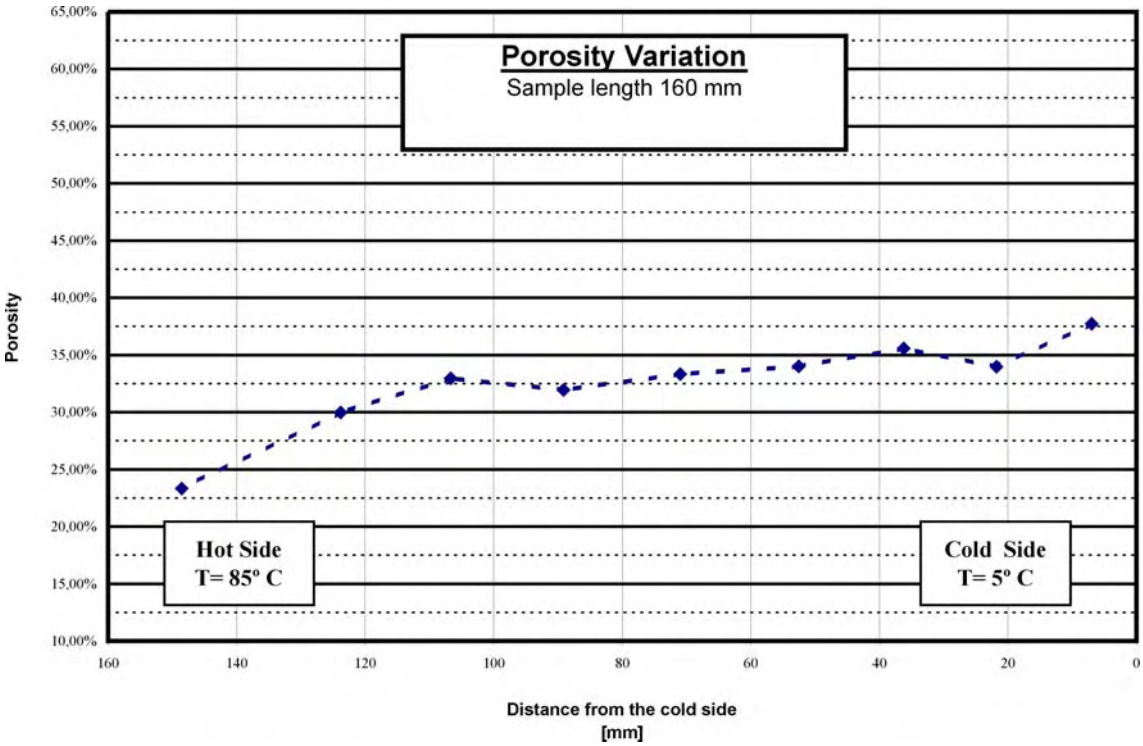


**Fig. 4.42** *The porosity variation of a 160-mm long sample.*

The variations in the sample are really small. In this case, fifteen days are not enough to appreciate the phenomena effects.

Considering the initial porosity variations from the ideal value, the phenomena are present only in the first 25 mm from the hot side.

This test can be compared to the 7-day test of 100-mm samples, with the important difference that, this time, it is possible to determine more points.

From this point of view the test is useful, because it confirms that there is an initial phase, in which the dissolution/precipitation phenomena involve only a little portion of the sample length.

Only one sample was tested because, once performed, the other two installations were busy with other type of tests and, due to the obtained results, it was decided to spend the time reserved to this tests to the study of the

influence of other parameters. It is clear that to get relevant results on this case, the time application of the temperature must be at least 30 days.

This aspect was already explained in the literature: Olivella (1995) studied a way to transform the solving equation in no-dimensional way and found out that the “characteristic time” is directly proportional to the square of the sample length:

$$t_o = x_0^2 \frac{1}{D} \tag{4.4}$$

where:
$x_0$ is the characteristic length
D is the diffusity

## 4.6 *Conclusions*

The phenomena of dissolution/precipitation of salt aggregates due to a temperature difference were presented in this chapter with a special attention to the use of crushed salt as sealing material for nuclear wastes.

The main objects of this chapter were: the phenomena presentation, the development of the testing laboratory apparatus and laboratory results.

The testing apparatus was entirely developed to fulfil this purpose and this task took a consistent part of the work. The test campaign demonstrated that the method and the apparatus are able to reproduce the wished condition.

The only way to improve the apparatus characteristics is to make an automatic control of temperature directly in the heat transmitters and use a system to save temperature data during the application of the temperature difference.

On the other hand, new equipment could be developed to reach such high temperatures as those of waste depositories.

The testing campaign is complete, the results are confirmed and, in a sense, they are better than expected.

The last point to be treated in this chapter is the engineering aspects of the problem. The results show that the variation of total density is a very important problem and to avoid it several conditions must be respected.

Once that these results are known, the next step of the investigation is the validation of these results by a numerical model. This will be the object of the next chapter in which the experimental tests will be reproduced by Olivella's Model for saline media (Olivella et al. 1993; Olivella et al. 1994 b). Then it will be possible to introduce in this numerical model the mechanical aspects and the real conditions of a deep nuclear waste deposit to study the development of the sealing condition during the centuries in which the nuclear wastes are a danger. A last step of this investigation will be the validation of the model results by a real scale test in an underground laboratory. If the importance of the dissolution/precipitation phenomena presented in this work is confirmed at the end of this process, the design of deep repositories will consider these aspects for a proper sealing.

Even if it is early to give some advices about repository design, the author thinks that:

- the best results for sealing can be obtained by the use of holes because a vertical installation uses the creep phenomenon and gravity force to keep the canisters closed. In this condition, the lower part where the wastes are located, could reduce its porosity and at the same time it could be easy to "refill" the cold side with new compacted material
- this system needs maintenance to keep its functionality for several centuries and the collocation of salt should be done with the

highest total density to reduce the effects of dissolution/precipitation

- the project must have the adequate systems to reduce the risks of seepage, especially of fresh water that could destroy the saline sealing system

# PART III

# NUMERICAL ANALYSIS

# CHAPTER 5

# NUMERICAL INVESTIGATION OF POROSITY VARIATIONS IN SALINE MEDIA INDUCED BY TEMPERATURE GRADIENTS

## 5.1 *Introduction*

The main objective of this chapter is the development of a numerical model to understand and analyse the results obtained in the laboratory.

In Chapter 4 the effects of temperature gradients on wet salt aggregates were presented and the entire laboratory campaign was explained. It was possible to observe the main characteristics of the phenomenon and its behaviour, but understanding of the processes was only intuitive.

A numerical approach allowed confirming the thermo-hydraulic processes in the laboratory tests. If the processes are confirmed then the effects of many parameters can be studied in depth through sensitivity calculations, if necessary.

The CODE_BRIGHT was used to develop the model because it is one of the most suitable tools in this context. In fact, it was developed for saline media to study coupled problems in thermo-hydro-mechanics (THM) involving dissolution and precipitation phenomena. The theoretical approach was developed by Olivella et al (1994), while the numerical approach was presented in Olivella et al (1996a). One of the capabilities of the code, shown in Olivella et al (1996b), was to predict the porosity variations caused by dissolution and precipitation in wet saline media induced by thermal gradients.

The main objective of the numerical work is to verify that the processes implemented in CODE_BRIGHT, regarding the problem presented in this thesis were sufficiently adequate to reproduce the phenomena identified during laboratory tests. It was already observed in Chapter 4 that the medium was not continuous and that the samples were affected by grain falls during the application of the temperature difference in laboratory. So, it is possible that there will be some differences between the laboratory results and the model ones in which these discontinuous features cannot be reproduced.

The chapter is organized as follows. First of all, the characteristics of the numerical tool (CODE_BRIGHT) are outlined; then, the numerical model is used to model a sample under a thermal gradient and the results are compared to laboratory tests measurements. The last part of the chapter focuses on drawing some conclusions on the numerical analysis performed.

## 5.2 *Description of CODE_BRIGHT*

CODE_BRIGHT (Olivella et al. 1996a) is a tool designed to handle coupled problems in geological media. The computer code, was originally developed on the basis of a general theory for saline media. Then the program was generalised to model thermo-hydro-mechanical (THM) processes in a coupled way in geological media. Basically, the code couples mechanical, hydraulic and thermal problems in geological media.

In porous media, subjected to thermal, hydraulic and mechanical conditions, relevant thermo-hydro-mechanical (THM) phenomena take place. In fact, there are a number of mutual and simultaneous interactions that must be taken into account.

For instance, the thermal expansion of the water in the pores themselves causes variations in the degree of saturation or, if the material is saturated or quasi-saturated, increases in water pressure. Thermal induced vapour diffusion and the dependence of water viscosity on temperature significantly affects the water transfer process. In case of deformation processes taking place, strains due to thermal loading will induce stress variations and changes in mass storage terms and hydraulic conductivity.

On the other hand, changes in hydraulic conditions affect the temperature field via variations of thermal conductivity, as well as the stress/strain field, due to pore water pressure and pore gas pressure changes. Gas pressure is affected by the increase in vapour pressure with temperature. This may lead to further changes in the pattern of gas and water flow.

Finally, porosity changes due to volumetric strain or dissolution/precipitation processes have an influence on pore pressure distributions because of associated variations in storage terms and hydraulic conductivity. Porosity variations also affect thermal conductivity.

The case under study is an example of some of the phenomena mentioned. Figure 5.1 shows a schematic representation of the phenomena involved in a horizontal sample subjected to a temperature gradient. Under these circumstances, the medium is assumed to be rigid to avoid the effect of the deformability on porosity changes. It is obvious that this is a clear example of a coupled phenomenon induced by thermo–hydraulic changes.

Solubility of salt in water is multivariable a function, one of the most important ones being temperature. In fact, the migration of brine inclusions in the solid phase may be caused by temperature gradients. Temperature gradients may induce significant phenomena in wet unsaturated saline media, as it was already shown in the laboratory tests that were carried out on these phenomena (Castagna et al., 2000)

Firstly, solubility dependence on temperature originates salt concentration gradients. Secondly, temperature vapour concentration originates gradients of vapour pressure and, consequently, migration of water vapour. The concentration of solute increases above solubility equilibrium when water evaporates from saturated brine, which leads to salt precipitation. Likewise

water condensation induces dissolution of salt. The vapour, transferred from a hot region to a cold one, generates a brine motion. The motion of salt in dissolution may be advective (liquid tends to flow in order to compensate for vapour migration) or nonadvective (diffusion plus dispersion, induced by gradients of salt concentration).

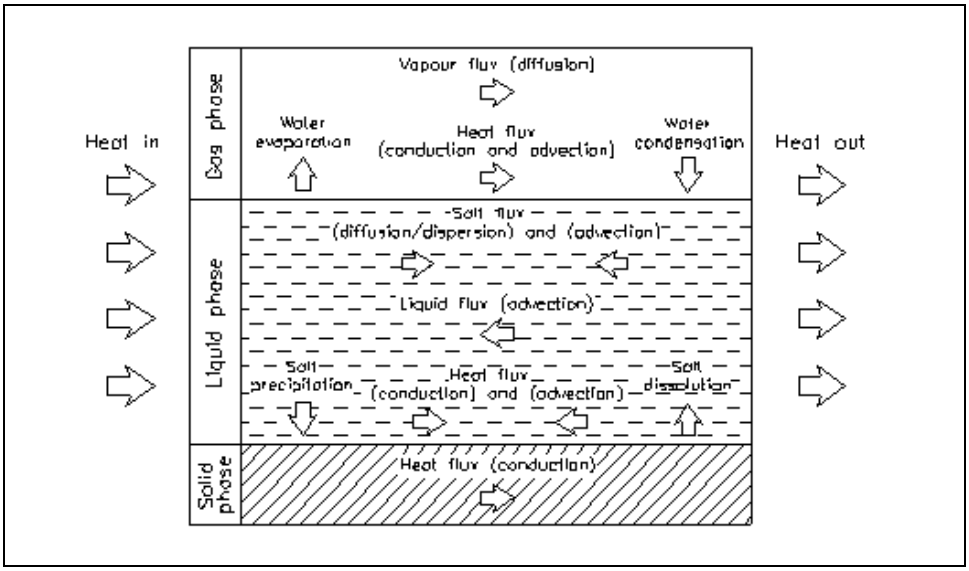


**Fig. 5.1** *Coupled phenomena induced by a temperature gradient (from Olivella, 1995).*

Under unsaturated conditions, it seems that the second mechanism of solute transfer (i.e. induced by vapour migration) will prevail with respect to the first one (i.e. induced by temperature-concentration differences). It is clear that, this relative importance of transport mechanisms depends on the transport properties of the medium, but it must be said that the diffusion of vapour in air is much more effective than the diffusion of salt in brine. The dominance of solute migration induced by concentration differences would take place under saturated conditions because vapour migration is not possible in this case.

A consequence of all those phenomena interacting simultaneously is the need to carry out coupled TH analyses in which all the main aspects of the problem can be considered in an integrated way.

The theoretical approach of CODE_BRIGHT consists in a set of governing equations, a set of constitutive laws and a special computational approach.

A formulation for the nonisothermal multiphase flow of brine and gas in deformable saline media was developed in Olivella (1995). In this paragraph, the approach to multiphase flow will be presented and the equations adapted to the experimental condition. As it has already been assumed for laboratory experiments, the stress-strain effects are negligible, and thus will not be taken into consideration for the development of the numerical model. Moreover, the brine inclusions migration phenomenon is considered negligible. For this

reason, the equations considered do not include all the terms in the general approach.

The equations can be divided into four main groups:

1. Balance equations;
2. Constitutive equations;
3. Equilibrium restrictions;
4. Definition constraints;

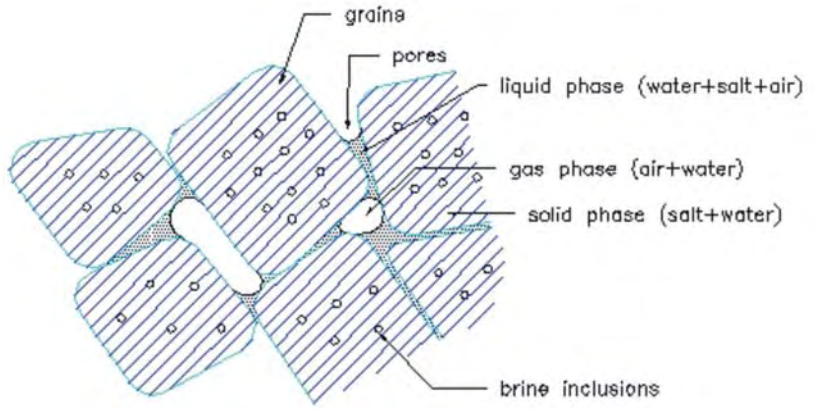


**Fig. 5.2** *Schematic representation of the salt medium*

Balance equations are written following the compositional approach (Panday and Corapcioglu, 1989), which takes into account the balance of the species and not that of the phases. In the case of salt material, this approach is better than the other because the species (salt, water and air) are present in several phases. For example, salt is present in the solid phase (grains), but it is also dissolved in the brine. Figure 5.2 shows a schematic representation of the material with the division into species and phases.

The three phases are:

- **Solid phase** : mineral, salt;
- **Liquid phase:** water + air dissolved + salt dissolved;
- **Gas phase**: mixture of dry air and water vapour;

The three species are:

- **Salt**, which forms the solid phase but it is also present as dissolved in liquids;
- **Water**, which is the main component of liquids and it is also present as evaporated in the gas phase;
- **Air**, that is dry air, as the main component of the gas phase (for low temperatures) or dissolved in the liquid phase;

The following assumptions and aspects are taken into account in the formulation of the problem:

- Dry air is considered as a single species and it is the main component of the gaseous phase. Henry's law is used to express equilibrium of dissolved air.
- Thermal equilibrium between phases is assumed. This means that the three phases are at the same temperature.
- Vapour concentration is in equilibrium with the liquid phase. The Psychrometric law expresses its concentration.
- State variables (also called unknowns) are: liquid pressure, $P_l$; gas pressure, $P_g$; and temperature, $T$.
- Balance of momentum for dissolved species and for fluid phases is reduced to constitutive equations (Fick's law and Darcy's law).
- Physical parameters in constitutive laws are a function of pressure, temperature and the presence of solutes. For example: concentration of vapour under a planar surface (psychrometric law), surface tension (in retention curve), dynamic viscosity (Darcy's law), strongly depend on temperature and the presence of solutes.

The unknowns are divided into two groups, independent variables or unknowns and dependent variables. The formulation of CODE_BRIGHT is done so that dependent variables are determined by constitutive equations and equilibrium restrictions. These values are then substituted in the balance equations.

The **balance equations** that must be considered in this case are:

I. Salt mass balance
II. Water mass balance
III. Air mass balance
IV. Internal energy

Constitutive equations describe the physical properties of the medium for the phenomena considered.

The **constitutive equations** are:

I. Retention Curve;
II. Darcy's law;
III. Fick's law;
IV. Fourier's law;
V. Ideal gases law;
VI. Phase law;

Finally, the **equilibrium restrictions** and **definition constraints** establish, as their names clearly state, the restrictions and constraints of the system.

In this case, the first group, equilibrium restrictions, includes:

I. Henry's law
II. Psychrometric law
III. Laws of solubility of species in phases.

while the definitions constraints consist in:

I. Mass fraction (3 equations, one for each species);
II. Volumetric fraction of voids;
III. Non-advective flux, species motion inside the phase (3 equations, one for each species);

The mathematical system must have the same number of variables and equations. The unknown variables are:

- Porosity
- Liquid pressure
- Gas pressure
- Temperature

## Balance Equations

The balance of the mass of salt for the porous medium is:

$$\frac{\partial}{\partial t}\left(\theta_s^h\left(1-\phi\right)+\theta_l^h S_l \phi\right)+\nabla\cdot\mathbf{j}_l^h=0 \qquad (5.1)$$

where:

$\theta^{i}_{\alpha}$ is $\omega^{i}_{\alpha}\,\rho^{i}_{\alpha}$ and the mass of i-species per unit volume of $\alpha$-phase;

$\omega^{i}_{\alpha}$ is the mass fraction, which is defined as: $\frac{\text{mass of component } \boldsymbol{i}}{\text{total mass of phase } \boldsymbol{\alpha}}$;

$\rho^{i}_{\alpha}$ is the mass of $\alpha$-phase per unit volume of $\alpha$-phase, i.e. the density of the $\alpha$-phase;

$\phi$ is the porosity;

$S_l$ is the volumetric fraction of pore volume occupied by $\alpha$-phase (gas or liquid), i.e. the degree of saturation;

$\mathbf{j}^h_l$ is the flux of salt species in the liquid phase.

The time derivative term represents the sum of the salt in solid phase (grains) and the salt dissolved in the liquid phase. Flux of salt in liquid ($\mathbf{j}^h_l$) is the sum of a non-advective counterpart (diffusion/dispersion) ($\mathbf{i}^h_l$) and an advective term caused by liquid motion:

$$\mathbf{j}_l^h=\mathbf{i}_l^h+\theta_l^h\mathbf{q}_l \qquad (5.2)$$

The balance of mass of water for the porous medium is:

$$\frac{\partial}{\partial t}\left(\theta_l^w S_l \phi + \theta_g^w S_g \phi\right) + \nabla \cdot \left(\mathbf{j}_l^w + \mathbf{j}_g^w\right) = 0 \tag{5.3}$$

The storage term includes water in liquid and in the gas phase. Consequently, motion of water is present in the liquid and in the gas phase. This motion can be divided into a non-advective counterpart (diffusion/dispersion) and an advective term.

The Balance of mass of air for the porous medium is:

$$\frac{\partial}{\partial t}\left(\theta_l^a S_l \phi + \theta_g^a S_g \phi\right) + \nabla \cdot \left(\mathbf{j}_l^a + \mathbf{j}_g^a\right) = 0 \tag{5.4}$$

Formally, this equation is identical to the former one. Air is considered a single species and the gaseous phase is a mixture of dry air and water vapour. The terms of motion are similar to the ones in the former equation.

In the case of temperature equilibrium between phases, the Energy balance for the porous medium is:

$$\frac{\partial}{\partial t}\left(E_s \rho_s (1-\phi) + E_l S_l \rho_l \phi + E_g S_g \rho_g \phi\right) + \nabla \cdot \left(\mathbf{i}_c + \mathbf{j}_{Es} + + \mathbf{j}_{El} + + \mathbf{j}_{Eg}\right) = f^E \tag{5.5}$$

where $E_\alpha$ is the specific internal energy corresponding to each phase and $f^E$ is an internal/external energy supply.

The internal energy of the gas phase can be divided into two terms: one for each species (water and air). Likewise the non-advective mass fluxes for the components are considered. This is necessary because in a phase each mass component transports different amounts of energy per unit mass. For instance, the latent heat in water vapour is important and should be considered for the vapour in the gas that flows in a different way as the air.

The most important processes of energy transfer in a porous medium are conduction, advection and phase change (Bear et al., 1991).

Heat conduction, $\mathbf{i}_c$, is computed by Fourier's law with an effective thermal conductivity coefficient to take into account the characteristics of the medium and heat dispersion (Faust and Mercer, 1979)

## Constitutive Equations

Constitutive equations define the physical properties of salt material by several laws. Some of them were included in this investigation (e.g. retention curves) and the results obtained have been presented in other chapters.

The first one to be listed here is the Ideal Gas Law. This law relates the magnitudes that govern the behaviour of ideal gases: temperature (*T*), pressure (*p*) and volume (*V*):

$$pV = nR(T + 273.15) \tag{5.6}$$

where *n* is the mole number and *R* is the universal gas constant.

This equation can be written regarding density, in the following way:

$$\rho_i = \frac{p_i M}{R(T + 273.15)} \tag{5.7}$$

The nonadvective flux of a species in a phase is formed of molecular diffusion and mechanical dispersion. Fick's Law is used to determine both of them. The expression of Fick's Law for molecular diffusion is:

$$\mathbf{i}_\alpha^i = -\left(\phi \rho_\alpha S_\alpha D_m^i \mathbf{I}\right) \nabla \omega_\alpha^i \tag{5.8}$$

where $\phi$ is porosity, $\rho_\alpha$ is density, $S_\alpha$ is saturation degree, $\omega$ is mass fraction and $D^i_m$ is the diffusion coefficient of species *i* in phase $\alpha$. The molecular diffusion of vapour is a function of temperature that can be calculated as:

$$D_m^{vap} = \tau D \left( \frac{(273 + T)^n}{P_g} \right) \tag{5.9}$$

where $P_g$ is the gas pressure in Pa and $\tau$ is the tortuosity. The values of D and n are 5.9 $10^{-6}$ $m^2/s/K^{-n}Pa$ and 2.3 respectively. *T* is the temperature in Celsius degrees. Tortuosity was studied in a sensitivity series of analyses that are not included for space reasons. The value adopted for tortuosity was 0.3. This parameter is constant in the present calculations. Dependencies on water content found in the literature are in fact a combination of both in a single function. Nevertheless, here the porosity variations induced by salt precipitation and dissolution, the changes in the retention curve induced by porosity variations, etc. would probably require a experimental program (for instance

diffusion experiments in samples with different porosity and degree of saturation), which is beyond the scope of this thesis.

The molecular diffusion of dissolved salt and dissolved air is:

$$D_m = \tau D \exp\left(\frac{-Q}{R(273+T)}\right) \tag{5.10}$$

where $Q$ is 24530 J/mol and $D$ is 1.1 $10^{-4}$ $m^2/s$.

The effect of tortuosity on the molecular diffusion of dissolved salt in the sample was not subject to study, an although this parameter varies between 0 and 1, it was fixed at $\tau$=1.

Mechanical dispersion mass flux is computed by means of Fick's law written as:

$$\mathbf{i}_\alpha^i = -\left(\rho_\alpha \mathbf{D'}_\alpha\right)\nabla\omega_\alpha^i \tag{5.11}$$

where the mechanical dispersion tensor is defined as:

$$\mathbf{D'}_\alpha = d_t\left|\mathbf{q}_\alpha\right|\mathbf{I} + (d_l - d_t)\frac{\mathbf{q}_\alpha \mathbf{q}_\alpha^t}{\left|\mathbf{q}_\alpha\right|} \tag{5.12}$$

and $d_l$ is the longitudinal dispersivity and $d_t$, transversal dispersivity. The values of $d_l$ and $d_t$ are 0.10 m and 0.05 m, respectively.

The conductive heat flux is computed through the Fourier's law:

$$\mathbf{i}_c = -\lambda(T, \phi, S_l)\nabla T \tag{5.13.a}$$

where:

$$\begin{aligned}
\lambda_{dry} &= \lambda_{solid}^{(1-\phi)}\lambda_{gas}^{\phi} \\
\lambda_{sat} &= \lambda_{solid}^{(1-\phi)}\lambda_{liquid}^{\phi} \\
\lambda_{solid} &= \left(\lambda_{solid}\right)_0 + a_1 T + a_2 T^2 + a_3 T^3
\end{aligned} \tag{5.13.b}$$

The law allows determining the conductive flux of heat as a function of porosity $\phi$, based on the conductivity of the phases of the solid, liquid and gas and three parameters, $a_1$, $a_2$ and $a_3$. The values of these parameters are:

| | |
|---|---|
| $(\lambda_{solid})_0$ | 5.734 W/mK |
| $\lambda_{gas}$ | 0.100 W/mK |
| $\lambda_{liq}$ | 0.600 W/mK |
| $a_1$ | $-1.830 \times 10^{-2}$ |
| $a_2$ | $2.860 \times 10^{-5}$ |
| $a_3$ | $-1.510 \times 10^{-8}$ |

The function for the solubility of NaCl in water is given by (Langer and Offermann,1982):

$$\omega_l^h = \frac{c}{c + 100} \tag{5.14}$$

where $c$ dependson temperature ($T$) by the following empirical relationship:

$$c = \frac{35.335 - 0.22947T}{1 - 0.0069059T} \tag{5.15}$$

Henry's Law evaluates the air fraction in the liquid phase:

$$\omega_l^a = \frac{p_a}{H}\frac{M_a}{M_w} \tag{5.16}$$

where $H$ is a constant and $M_i$ is the molar weight of the i-component.

The pressure of vapour in equilibrium with water is calculated by a curve that belongs to the phase diagram of water. This curve represents the points of equilibrium of the two phases for a fixed temperature value, and is expressed as:

$$P_v^o = 136075 \exp\left(\frac{-5239.7}{273.15 + T}\right) \text{[MPa]} \tag{5.17}$$

The pressure of vapour in equilibrium with pore water is inferior to the vapour in equilibrium with free water, because of the effects of capillarity. The vapour pressure is expressed by the Psychometric Law to take into account this effect (Edlefson and Anderson, 1943; Sprackling, 1985). Additionally, the effects of solute are taken considered by means of a coefficient that gives the relative humidity reduction caused by the solute:

$$
\begin{aligned}
&P_v = P_v^o F_{capillarity}\left(T, p_a - p_w\right) F_{solute}\left(T, \omega\right) \\
&F_{capillarity}\left(T, p_a - p_w\right) = \exp\left( -\frac{\left(p_a - p_w\right) V_l}{R\left(T + 273.15\right)} \right) \\
&F_{solute}\left(T, \omega\right) = [1 - ((m-3) + (1.977 \times 10^{-3} - 1.193 \times 10^{-5} T) + 0.035) m] \\
&m = \frac{\omega}{1-\omega} \times \frac{1000}{23 + 35.5} \left(\text{molality}\right)
\end{aligned}
\tag{5.18}
$$

where $F_{capillarity}$ and $F_{solute}$ are the relative humidity reductions induced by the capillarity forces and by the solute, respectively; $\omega$ is the mass fraction of solute;$m$ is the molality; $V_l$ is the molar volume of the brine; $R$ is the gas constant; and $T$ is the temperature.

Darcy's Law gives the specific discharges of liquid and gas. The generalised form of Darcy' s Law is expressed as follows (Nield & Bejan, 1999):

$$
\mathbf{q}_\alpha = -\frac{\mathbf{k} k_{r\alpha}}{\mu_\alpha} \left( \nabla P_\alpha - \rho_\alpha \mathbf{g} \right) \tag{5.19}
$$

where:

- **k** is the vector of intrinsic permeability
- $k_{r\alpha}$ is the relative permeability of the phase $\alpha$
- $\mu_\alpha$ is the fluid viscosity
- $z$ is the vertical coordinate

The permeability for gas flow is the result of intrinsic permeability and gas relative permeability, while permeability of a liquid is the product of intrinsic permeability and liquid relative permeability. In the study of multi-phase flow problems, it is accepted by the scientific community to separate the flow of each phase by introducing intrinsic and relative permeability.

Equation (5.20 a) is the Kozeny's model (Dullien, 1979; Baijal, 1982).

The intrinsic permeability is a property of the pore structure of the material. During the sensibility study for the numerical analysis of the laboratory tests, three expressions were considered for different cases (see equation (5.20)). In all the cases the intrinsic permeability is related to porosity and to a reference value of porosity ($\phi_0$),as well as to its correspondent intrinsic permeability ($k_0$).

$$\mathbf{k} = k_0 \frac{\phi^3}{(1-\phi)^2} \frac{(1-\phi_0)^2}{\phi_0^3} \mathbf{I} \qquad (5.20.a)$$

$$\mathrm{k} = k_o \exp\left[b_k \left(\phi - \phi_0\right)\right] \mathrm{I} \qquad (5.20.b)$$

$$\mathrm{k} = k_o \exp\left[b_k \left(\phi^c - \phi_0^c\right)\right] \mathrm{I} \qquad (5.20.c)$$

This equation was derived using the hydraulic radius to represent the flow passage and assuming the porous medium to be composed of a bundle of tortuous capillaries.

The second expression (5.20 b) is empirical. (Davidson et al., 1969), and consists in an exponential law. In order to use it, it is necessary to know a value of intrinsic permeability and its correspondent porosity value.

The last expression (5.20 c) was a review of equation 5.20.b modified for the purpose of this thesis. Expression (5.20 c) is an exponential model of variation of intrinsic permeability with porosity to fit the model to brine conditions.

The main difference between the three expressions is the degree of freedom:. Equation (5.20 a) has only one degree of freedom: the values of the vector of the intrinsic permeability $k_0$. These are experimental data, which can be determined by laboratory tests. On the other hand, expression (5.20 b) has two degrees of freedom because it also includes constant *b*.

Equation (5.20 b) is the one considered in the case presented in this chapter; where $k_0$ is equal to $10^{-12}$ $m^2$, the reference porosity is $\phi_o$=0.30 and $b_k$=2.

The relative permeability is the permeability of the medium for a specific fluid relative to the intrinsic permeability for a porous medium containing more than a single fluid phase (Sharp, 1999). Relative permeability depends on the saturation degree. There are two ways to obtain the relative permeability function: either by empiric methods or by experimental methods.

The expression used in this model is:

$$k_{rl} = A S_e^{\lambda} \qquad (5.21)$$

where *A* and $\lambda$ are two constants. The value of *A* is assumed to be 1 and $\lambda$ equals 3 in the presented model.

The retention curve is the constitutive law that describes the relationship between the matric suction and the degree of saturation. The determination of

these curves was subject to experimental work and the results were presented in Chapter 3.

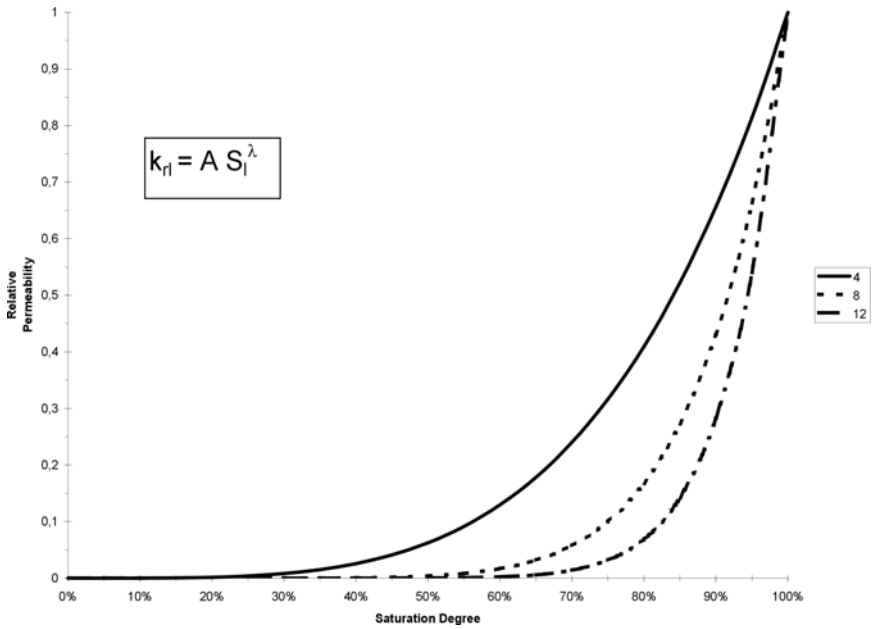


**Fig. 5.3** *Relative permeability function. Different* $\lambda$ *values are considered.*

The CODE_BRIGHT subroutines were improved to show more than one retention curve for the same material to take into account the variation of the retention curve regarding different values of porosity. The reasons for this choice were justified by the results of laboratory tests, which underlined the behaviour of matric suction and the high variation of porosity in salt samples when a change in temperature was applied.

Van Genuchten's (1980) Equation (5.22) can be used to describe the relationship between saturation degree and matric suction. This equation has two parameters:

$$S_e = \frac{S_l - S_{rl}}{S_{ls} - S_{rl}} = \left( 1 + \left( \frac{P_g - P_l}{P_o \dfrac{\sigma}{\sigma_0}} \right)^{\frac{1}{1-\lambda}} \right)^{\lambda} \qquad (5.22)$$

- $p_0$ represents the air entry value of the soil. In the graph this is represented by the lowest horizontal tangent and has the dimensions of pressure;
- $\lambda$ gives the shape to the retention curve;

The results of matric suction shown in Chapter 3 give the following values for the retention curve parameters:

| Porosity | $P_0$ [kPa] | $\lambda$ |
|---|---|---|
| 0.05 | 12 | 0.60 |
| 0.10 | 7 | 0.57 |

In model calculations, $\lambda$ was fixed equal to 0.65, due to the very low variation observed in the experimental results for this parameter.

The equation that was considered to define the variation of air entry value, $P_0$, as a function of the porosity, $\phi$, of a saline media is (Sanchez, M. 2004):

$$P = P_0 \exp\left(b_p \left(\phi_0 - \phi\right)\right) \tag{5.23}$$

where $b_p$ is a material parameter, and the reference porosity is equal to $\phi_o$=0.30.

Parameter $b_p$ was determined by the interpretation of laboratory tests on matric suction for retention curve determination. The $P_0$ value for porosity equal to 0.30 was determined by the interpolation of the known values of air entry for fixed porosity. $P_0$ was set equal to 0.0016 MPa and $b_p$ to 4.

Figure 5.4 shows the retention curves with the parameters presented above (there is a curve for each value of porosity and the air entry value is obtained by equation (5.23)).

From equations (5.20.b) and (5.23) it follows that for $b_p$=4=2x2:

$$\frac{P}{P_o} = \exp\left(b_p \left(\phi_o - \phi\right)\right) = \exp\left(2 \times 2 \left(\phi_o - \phi\right)\right) = \left(e^{2(\phi_o - \phi)}\right)^2 = \left(\frac{k_o}{k}\right)^{1/2} \tag{5.24}$$

This is a typical relationship that can be derived from Laplace equation, because capillary pressure is inversely proportional to pore size, while permeability is proportional to the square of pore size.

Consequently, the two parameters can be related as follows:

$$b_p = 2b_k \tag{5.25}$$

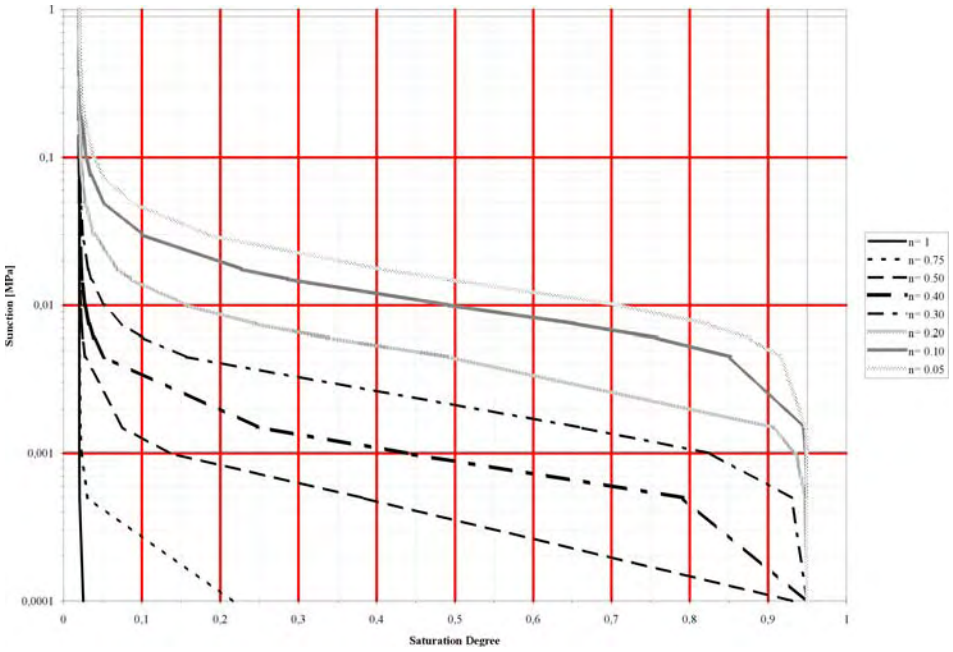


**Fig. 5.4** *Retention curves obtained using the interpolation process.*

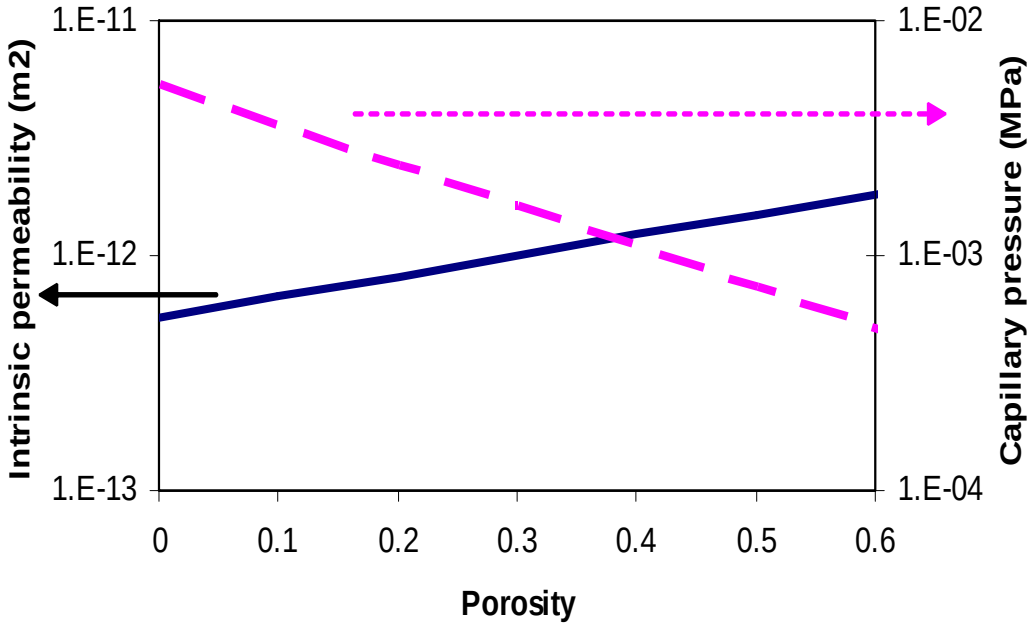


**Fig. 5.5** *Intrinsic permeability and capillary pressure functions of porosity.*

To complete the review of the theoretical basis that govern the code used to model the experimental test, it is necessary to introduce the last group of

equations to establish a sufficient number of equations and unknowns: that is, the definition constraints.

In this group we can recognize the following equations:

- mass fraction equation;
- volumetric fraction of voids;
- nonadvective flux equation that represents the species motion inside the phase;

Mass fraction equations are divided into three, one for each phase:

$$\begin{aligned} \omega_s^h + \omega_s^w &= 1 \\ \omega_l^h + \omega_l^w + \omega_l^a &= 1 \\ \omega_g^w + \omega_g^a &= 1 \end{aligned} \tag{5.26}$$

where $\omega_\alpha^i = \dfrac{\textbf{mass of component i}}{\textbf{total mass of phase } \alpha}$

Since we have reached the the hypothesis that the effect of brine inclusions is negligible, the first equation will not be considered in the case under study.

The volumetric fraction of voids is conditioned by these same voids being filled by either liquid or gas:

$$S_l + S_g = 1 \tag{5.27}$$

and nonadvective mass fluxes being equal to:

$$\sum \mathbf{i}_\alpha^i = 0 \tag{5.28}$$

which indicates that the sum of the species motion inside the phase is null.

## 5.3 *Application of FEM to laboratory tests on porosity variations induced by temperature gradients.*

The laboratory tests on saline media that were used to study porosity changes phenomena due to temperature differences were described in the previous chapter.

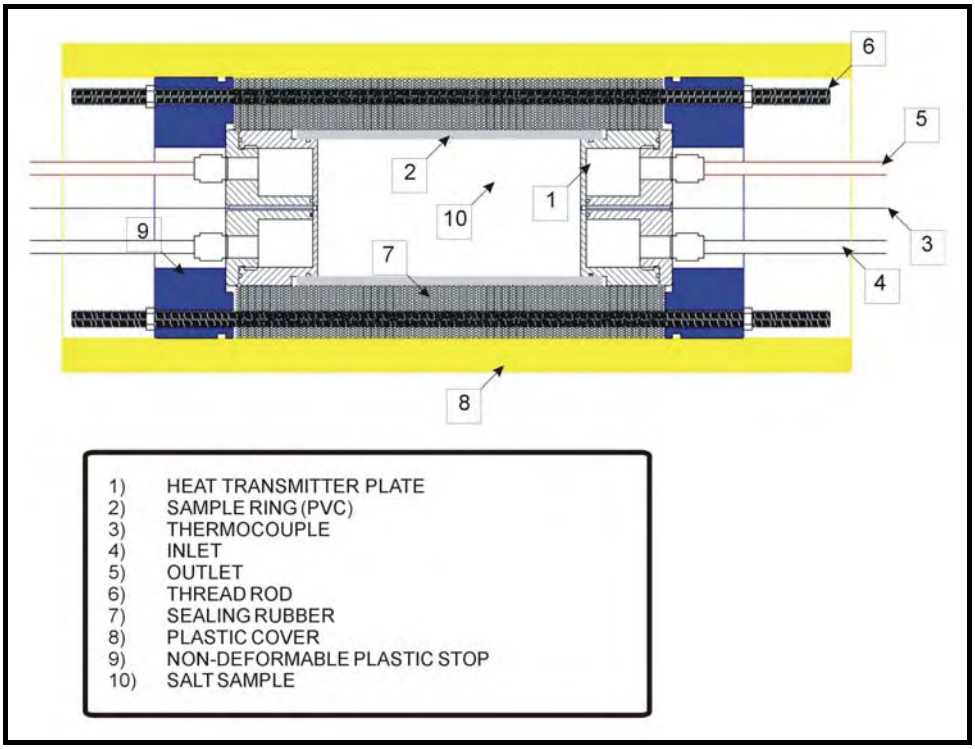


**Fig. 5.6** *Assembly of the salt sample used for the laboratory tests.*

Figure 5.6 shows the assembly of the salt sample that was used in the laboratory tests. The finite element model (FEM) was developed considering this scheme. This is one of the starting points to establish the materials characteristics, mesh and boundary conditions. The main characteristics of the model are as follows:

- The geometry of the sample is cylindrical
- Deformations are not allowed in the sample edges. In fact, there is a rigid sample ring and the heat transmitter plates are fixed in their position by three rods
- The sample was sealed laterally from heat exchange with the outside by three layers: the sample ring, a sealing rubber and a plastic cover
- The two heat-transmitter heads establish a fixed temperature value at each side of the sample during the test.

During the laboratory work a reference test was defined as:

| | |
|---|---|
| Sample | cylindrical with horizontal axis |
| Diameter | 50 mm |
| Length | 100 mm |
| Initial porosity | 30% |
| Initial saturation degree | 40% |
| Grain size | 1÷2 mm |
| Hot side temperature | 85º C |
| Cold side temperature | 5º C |
| Testing time | 15 days |

Several laboratory tests were performed with the same characteristics as the reference test and different testing times to dismantle the test. The chosen times were: 7, 15, 30 and 65 days. All these tests -including the reference one- represent 52% of the sample tested and 65% of the time spent on these laboratory tests. The rest of the tests were performed by changing the material properties: the initial degree of saturation (6 tests), the initial porosity of the sample before applying the temperature (7 tests) and different lengths (1 test).

The results of the laboratory tests show that porosity variations in saline media induced by a heat source are significant. For example, Figure 5.7 shows the effects on a sample tested for 65 days.

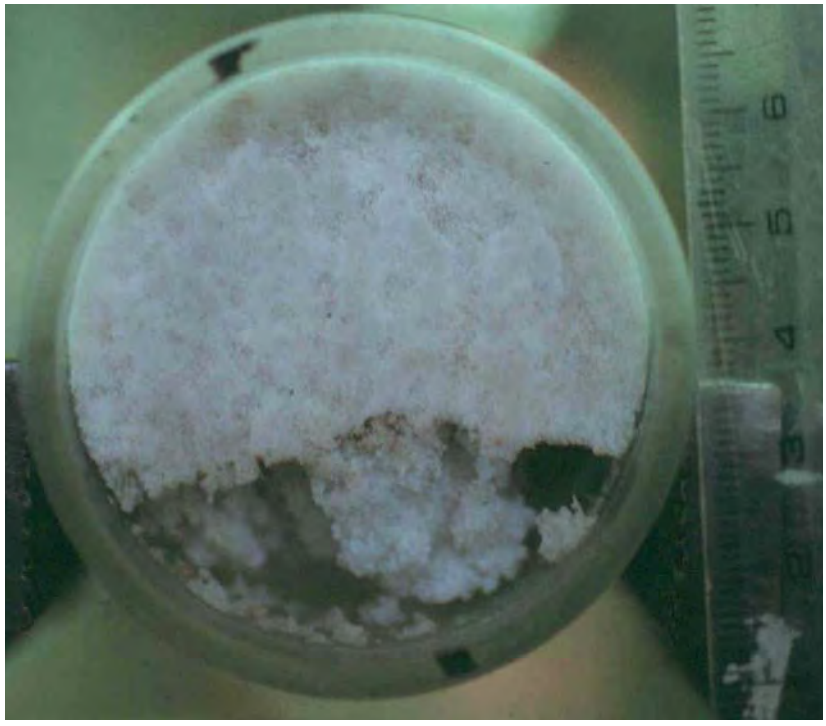

**Fig. 5.7** *Cold side of a sample tested for 65 days.*

The presence of macro voids is clear and the medium is not continuous but, it became a continuous porous media immediately after preparation of the sample. Moreover, grain fall phenomena occur and there are preferential paths for brine and vapour flux. All these aspects cannot be easily represented by a finite element program for continuous media, which is a limitation of the numerical model.

Even though a series of 3D and 2D calculations were performed, 1D calculations have shown sufficient approximation to the problem to be modelled and allowed doing the sensitivity calculations very rapidly.

The problem was analysed under hydrothermal conditions. The boundary conditions were easy to impose has only two fixed temperatures in the sample ends had to be imposed (5 and 85 C). All laboratory times (7, 15, 30 and 65 days) were selected as time steps of the analysis to compare directly the numerical results to the laboratory tests.

The sensibility study will not be presented here due to space reasons. In fact, taking into accopunt that there are only a series of calculations to reach a simulation close to the experimental results, the readers may refer for more information to Castagna & Olivella, 2001. The following parameters have strong influence on the results of the numerical simulation of the test:

- $\boldsymbol{k_0}$, $b_k$: for intrinsic permeability (see equations 5.20 a,b and c)
- A and $\lambda$: for relative permeability (see equation 5.21)
- $\tau$, tortuosity: for vapour diffusion (see Equation 5.9)

The vapour diffusion coupled to unsaturated flow is the driving force of the phenomena under study.

In the figures and text below, the comparison between experimental and numerical results for selected experimental results is presented.

Figure 5.8 shows the evolution of porosity in the sample, both for experimental and calculated results. It should be noted that results for different times can only be obtained by different samples dismantled at different times. A dissolution front forms in the hot side, but disappears as it reaches the cold side of the sample. Then, porosity tends to reduce near the hot side. The experimental results indicate that porosity reduction is limited and a minimum of 20% is reached. This is not accomplished by the model allowing porosity reduction through precipitation, even if porosity has reduced. The model does not take into account the size and the structure of the pores, it only considers the total amount of porosity.

The experimental behaviour seems to indicate that there must be a void size in which the gas and brine flows are not possible and the system reaches equilibrium partially in the sample. So, dissolution/precipitation phenomena are probably limited by the capacity of the fluids to move in porous media.

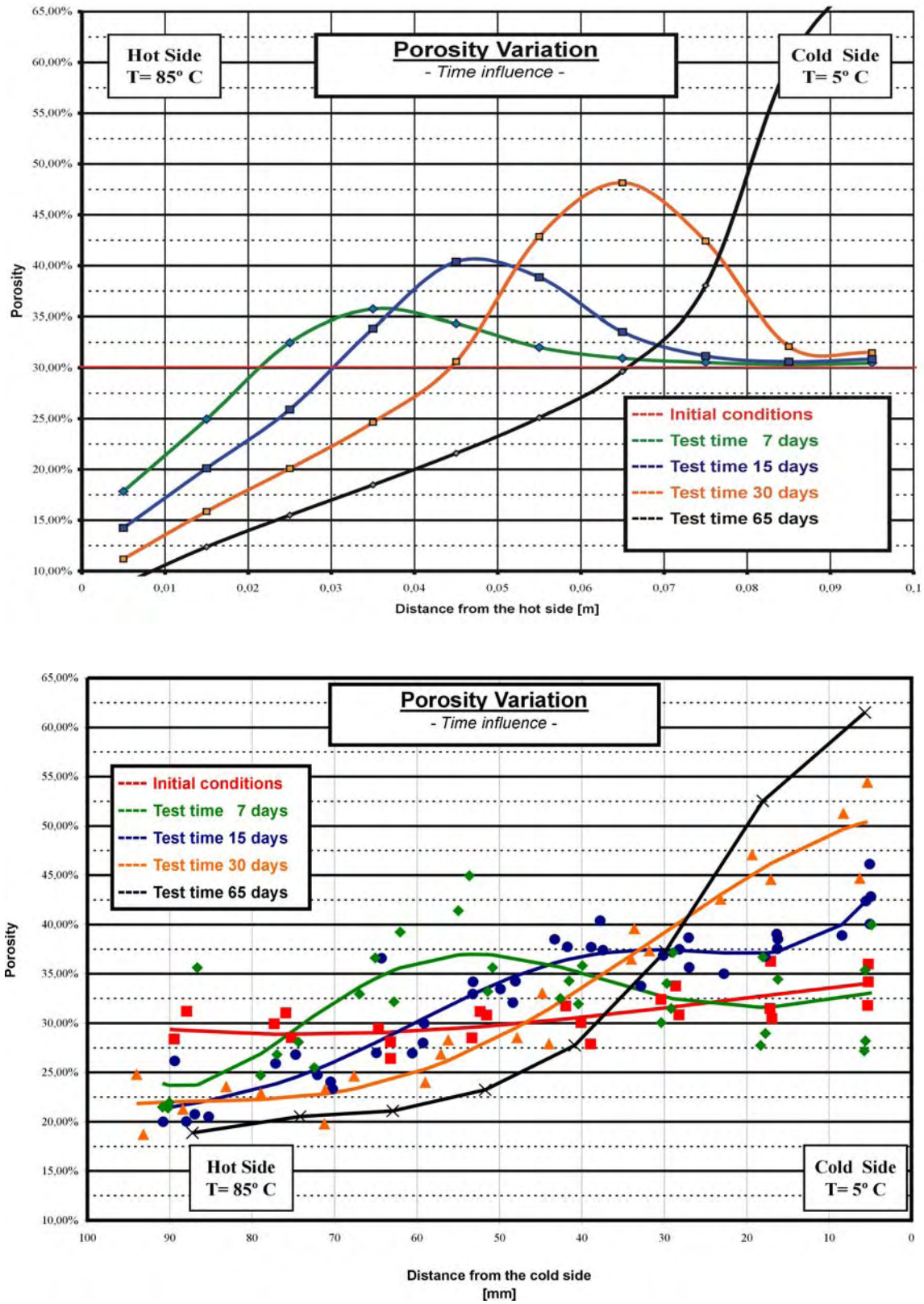


**Fig. 5.8** *Evolution of porosity in the sample regarding time. Numerical (above) and experimental results (below).*

Figure 5.9 shows the results for simulations at three initial porosities. The initial values are 20, 30 and 40%. The initial porosity in the sample implies different properties for the diffusion of vapour, liquid flow and heat flow. Moreover, the retention capacity is modified because the retention curve depends on porosity. In other words, model simulations for different porosities are carried out simply by altering the initial porosity. Consequently, the different functions modify the following parameters: vapour diffusivity, retention curve, thermal conductivity and hydraulic conductivity. Figure 5.9 shows that the model is able to capture the different behaviour at different porosities. It is clear from both experimental and numerical results, that the higher the porosity is, the higher the variations observed. This should be expected, as all the mass flows increase with porosity and hence there the system's capacity to transport salt increases. Vapour diffusivity changes by a factor of 2 from a porosity of 20% to 40%.

Figure 5.10 shows the influence of the initial degree of saturation in the sample. In this case, the flowing parameters, such as intrinsic permeability and thermal conductivity, do not changing with porosity as porosity remains the same in all cases. However, the variations on the degree of saturation have an influence on relative permeability, thermal conductivity and vapour diffusivity. Nevertheless, in this case the evolution is quite similar and the initial degree of saturation seems to have an almost negligible influence in the results. A possible interpretation could be that vapour diffusivity is not changing much, so the three cases are similar. Vapour diffusivity changes only by a factor of 1.5 between 10% (0.9) and 40% (0.6).

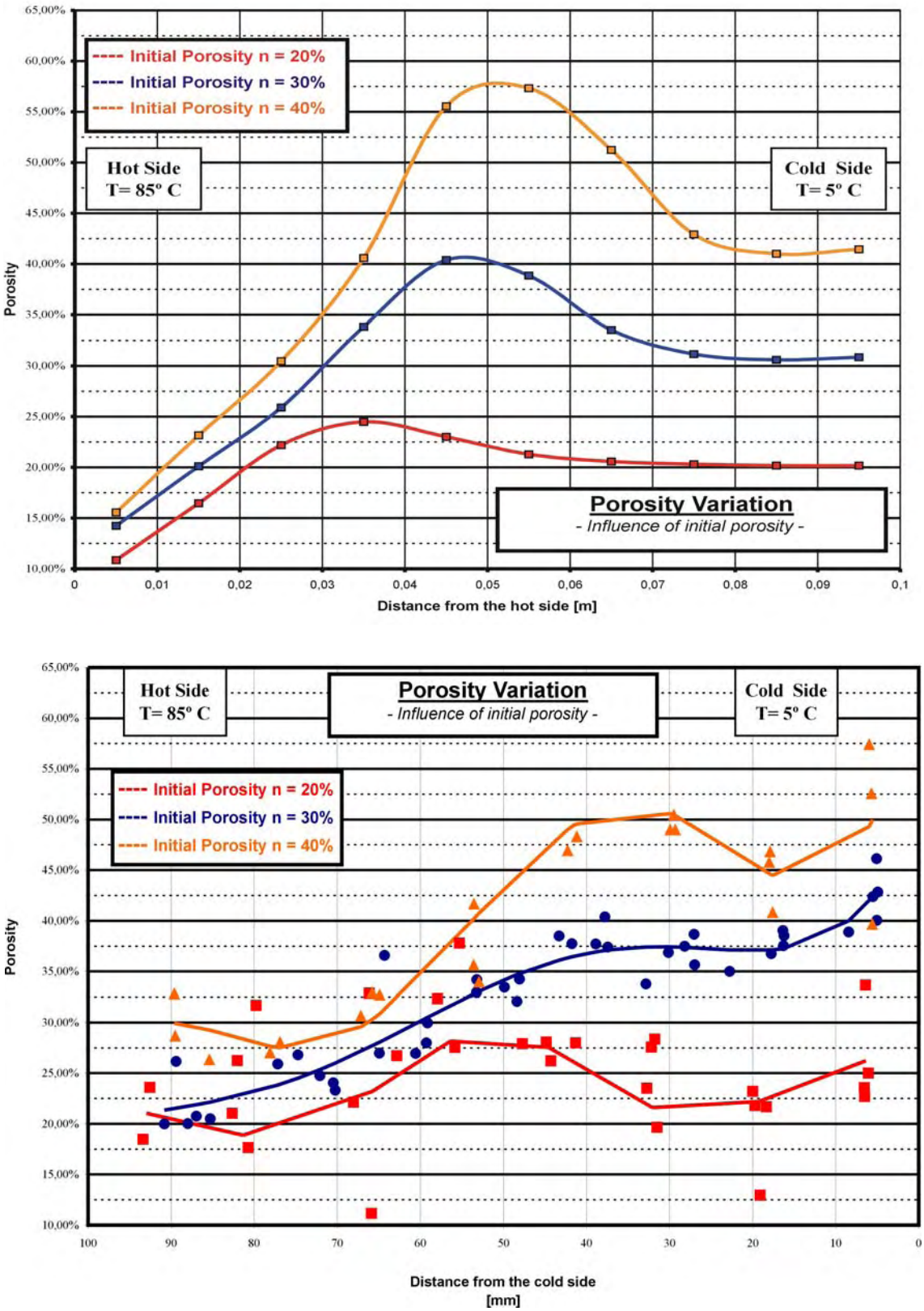


**Fig. 5.9** *Effect of initial porosity on porosity variation. Numerical (above) and experimental results (below).*

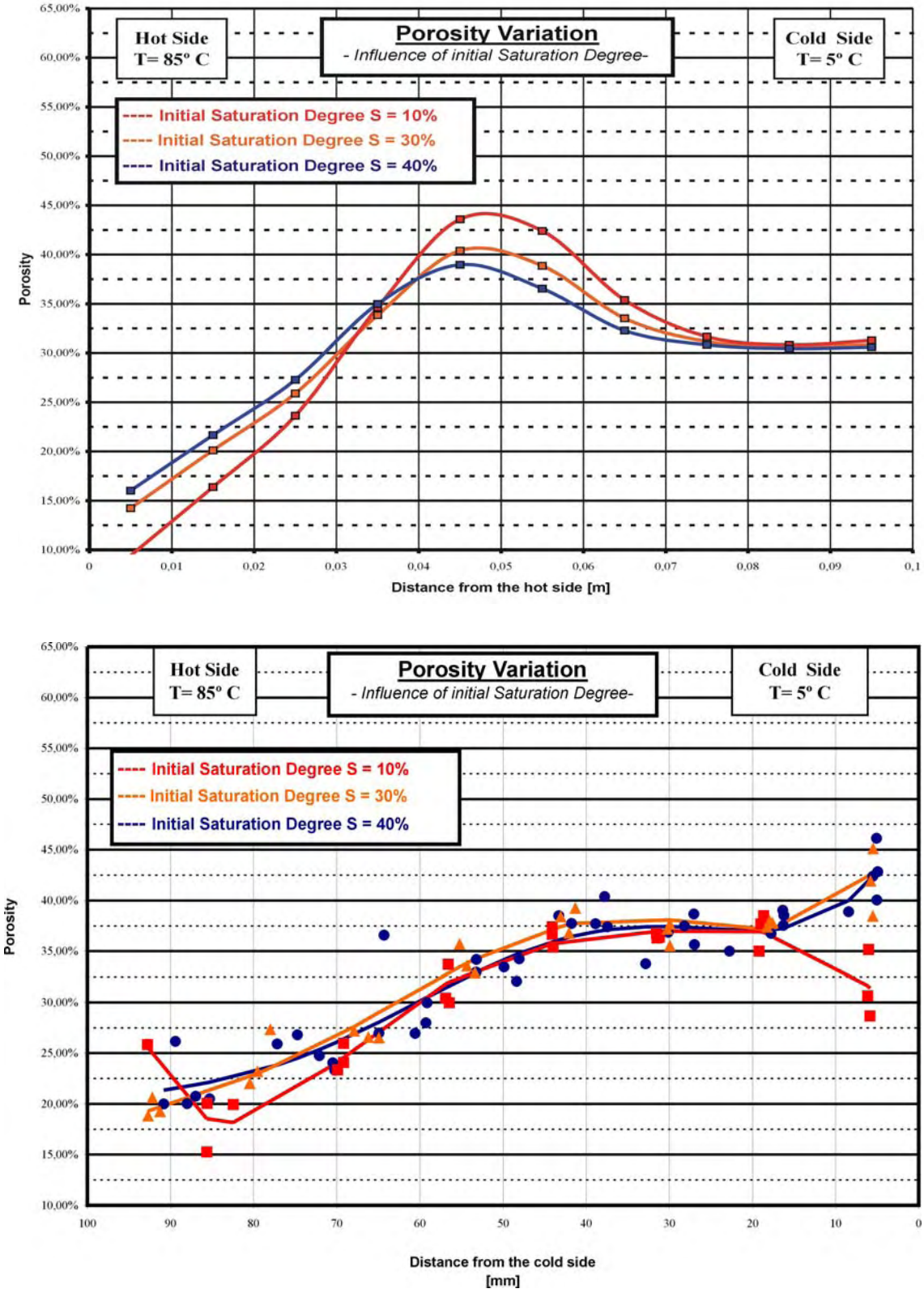


**Fig. 5.10** *Effect of initial degree of saturation on porosity variation. Numerical (above) and experimental results (below).*

## 5.4 *Concluding remarks*

As a conclusion, it can be said that modelling is well-done because the main tendencies have been caught in a qualitative and quantitative way. Of course, several improvements could be introduced. Some of these are related to the equilibrium assumed for phase change processes: water evaporation and salt precipitation. Considering these processes in transient would also allow introducing the effects of the medium structure through the specific surface, which may change as dissolution and precipitation of salt takes place. As indicated above, parameters depend on porosity, which is a value that does not reflect the possible variations related to the structure of the pores. And this may be different, for instance, if dissolution and precipitation takes place. Intrinsic permeability measurements in samples that have been subjected to dissolution/precipitation would allow improving the function that has been used in the present model. The same applies to thermal conductivity and vapour diffusivity. The retention curve was determined for different porosities, which were obtained by compaction and not by dissolution/precipitation. It is clear that the same porosity reached by different processes may imply different structure of the porous medium and hence, different evolution of the processes taking place.

The simulation of the different tests, and the range of initial conditions covered by the model as compared to the experiments, are certainly encouraging. A future research may be oriented to improve the shape of the dependencies that have been used in the present model.

# PART IV

# CONCLUSIONS

# CHAPTER 6

# CONCLUSIONS AND FURTHER TESTS

The main objective of this thesis was the study of compacted salt aggregates and its use as a sealing material in nuclear waste deposits.

The work was divided into two parts: laboratory investigation and numerical research.

The laboratory tests can be considered fully satisfactory, the aim of the laboratory campaign was attained and it was possible to determine the behaviour of salt aggregates in the cases studied, the results of the numerical part of the research allows fixing the first points to develop this new field of study.

The subject of the laboratory campaign had two main objectives: the determination of the matric suction for salt aggregates and the study of the phenomena of dissolution/precipitation, and its consequent variation of porosity (total density), which occurs when a temperature difference is applied onto a salt material.

In both cases the work was divided into the following three steps:

1. Development of the apparatus
2. Test campaign
3. Test result analysis

Since the subject of the research was new, the first and fundamental aim of the work was to study the type of test and to design the right apparatus that had to be developed to study the behaviour of salt aggregates.

Thus, in order to determine the retention curve, the first step was to design and check a suction plate properly prepared for salt material. The suction plate itself, and the results attained thanks to it, are the real innovation, because the test method and the analysis of results are already known, due to many researches developed for others materials.

Several matric suction application methods were analysed, and finally axis translation technique was reckoned the fittest to be modified and adapted to the study of salt aggregates.

This method gave satisfactory results and it was possible to determine two retention curves for heavily compacted salt aggregates.

The determination of these retention curves plays an important role in the deposit of nuclear waste, since, as shown in the previous chapters, matric suction is fundamental in hydro thermo mechanics of unsaturated porous materials and the knowledge of the magnitude of matric suction allows a better forecast of the behaviour of the salt material to seal nuclear waste deposits.

It must be pointed out that the values of matric suction observed are really small, but, as demonstrated in Chapter 5, one of the magnitudes that

affects dissolution/precipitation phenomena the most is matric suction and its variation regarding salt porosity.

That is the reason why the determination of the retention curve was the first test to be developed.

It can be argued that, in mechanics, this small variation of matric suction might not affect the phenomena involved, but it must be pointed out that, before this work, there were only predictions about salt suction. Moreover as this work shows, it is this small variation that significantly affects the hydro-thermo phenomena.

The matric suction measurement test achieves all the objectives fixed at the beginning of the test campaign, although a future line of investigation can be the study of further values of porosity. On the basis of the present research, it is foreseeable that those tests will give very low values of air entry, but they could also relate the air entry value and the sample porosity. Furthermore, the effect of grain size on matric suction for salt aggregates could be studied.

This new kind of campaign test could involve a new system for sample preparation; which could also study the sand retention curves. The comparison between sand and salt could provide with more information about the behaviour of such a peculiar material as salt, as it has been revealed during this investigation works.

In the second test a temperature difference was applied to a salt compacted sample. The aim of this test was to observe the porosity variation due to a phenomenon composed of dissolution/precipitation and transport whose main effect was the reduction on porosity near the hot side and an increase on porosity close to the cold side.

In this case the test reproduced the phenomena occurring in the salt sealing nuclear waste. These are very important phenomena and in Chapter 4 it was demonstrated how they must be considered in all the phases of the deposit’s life.

As mentioned above in this work, the test “was entirely built”, this means that a new test method was developed in order to reproduce the phenomena involved in a waste deposit.

The results are more than satisfactory: they go beyond all expectation. The development of the apparatus and the method were correct and the results of the tests confirm it: they are so homogeneous that they leave no significant doubts about the behaviour and the importance of the phenomena. Last but not least, the campaign is so wide that all the main aspects could be studied and the main parameters could be determined.

Finally, the porosity variations were bigger than expected.

Thus, the test clearly showed that there is a significant variation of porosity also with low saturation degree, and that the underestimation of the phenomenon could induce serious problem in the barrier. From this point of view to aspects must be underlined: the first one is that this is only a small scale laboratory test in a friendly environment and before reaching any definitive conclusions it is important to repeat the experimental campaign in one of the suggested environments for waste disposal at real scale and at service condition. It should be born in mind that there are more phenomena, such as

creep, affecting the barrier. The second aspect deals with the waste disposal deposit being an infrastructure that must work for centuries without man control, so any negligible phenomena in human life time scale (few years) can become an important problem in the decay time scale (many centuries). For example, a displacement of 1 mm per year, becomes 10 m in 10.000 years. In any case, the test developed shows clearly the presence of an important phenomenon of porosity variation that cannot be neglected.

If the small scale results were confirmed in a real scale investigation, the choice of the orientation of the deposit would be the first step for a correct use of salt as a sealing material, because this test shows that a gallery is the worst choice for the deposits and that a vertical storage is the most suitable and safest solution.

The reasons have been explained in Chapter 4 and all the practical aspects for the use of salt as the filling material have been considered in the conclusions of that chapter.

Likewise, in this case it is possible to indicate new lines of investigation. First of all, the effect of saturation degree should be further examined so to clear the few doubts left on this parameter.

Besides, it would be useful to improve the equipment used for the tests, providing the following:

1. An automatic system to record the temperature applied
2. A method to measure the matric suction during the application of the temperature in several points of a transverse section in order to record its distribution. In Chapter 5 the simulation by CODE_BRIGHT demonstrates the importance of matric suction in the phenomena
3. A system to accurately determine the saturation degree or water content
4. A new method to measure porosity, preferably a non-destructive one, that would allow accurately measuring porosity in the cold side where macro voids can be found. Consequently, it would be possible to apply the temperature difference for more than 65 days, where the results are very influenced by the macro voids.
5. A system to determine more data about porosity, which is not only the average porosity of slices but also the information about porosity distribution in several different planes.

The last part of this thesis is addressed to the simulation of the waste deposit phenomena due to the temperature difference by a numerical approach.

The numerical model was studied and the results were presented in Chapter 5.

It was possible to reproduce the phenomena and the numerical results confirm the laboratory tests.

It was already point out that the unsaturated flow has the main role in these phenomena. This flow must be reproduced taking into account the following physical properties:

1. Matric suction

2. Intrinsic permeability
3. Relative permeability

Some other remarkable circumstances could be determined in this numerical work, for example, the problem can be considered 1-D.

These results can be considered as a good starting point for a brand new research where, thanks to the laboratory tests and these first numerical data, it will be possible to develop a brand new formulation and, consequently, a new code that could take into account the presence of macro-voids and the collapse of grains in the medium. Nevertheless, for obvious problems of time, these improvements could not be developed in this study.

Finally, since the use of salt as a backfill material for nuclear waste repository promoted this research, what is now possible to say is that both numerical and experimental results confirm the presence of an important phenomenon of dissolution/precipitation, which must be taken into account in the design of waste repositories to ensure a safe sealing of nuclear waste.

The author of this thesis is satisfied of this result and reckons that an important step is done in the understanding of the main phenomena involved in the use of salt as a filling material in nuclear waste deposits. At the same time, it seems adequate to note that even if salt could possibly be used to seal waste deposits, other steps must be done before ensuring that salt is the right material for the purpose.

This work is to be considered another step to study and examine the potential and behaviour of salt as a filling material for waste deposits and further tests need to be carried out to reveal its sealing possibilities.

# REFERENCES


**Ahiström P.** (1996) *Progress Towards a Swedish Repository for Spent Fuel.* Second Worldwide Review in on Nuclear Waste. 213-221

**Aitchinson G.D.** (1965): *Moisture in soils beneath covered areas.* Symposium in print. Butterworths: Australia.

**Andersson J.** and **Hedin A.** (2005) *Preliminary Safety Evaluation of the host rock at Candidate Sites for the Swedish SNF Repository.* International High-Level Radioactive Waste Management Conference April 30 - May 4, 2006. Las Vegas, USA. On press

**Astudillo Pastor J.** (2002): *El almacenamiento geológico profundo de los residuos radiactivos de alta actividad Principios básicos y tecnología.* ENRESA.

**Baijal S.K.** (1982): *Flow behaviour of polymers in porous media.* Tulsa, OK: PennWell Books.

**Bear J.** (1979): *Hydraulic of the groundwater.* McGraw-Hill Editor.

**Bear J., Bensabat J.,** and **Nir A.** (1991): *Heat and Mass Transfer in Unsaturated Porous Media at a Hot Boundary*: *I. One-Dimensional Analytical Model*, Transport in Porous Media 6, 281-298.

**Bechthold W., Rothfuchs T., Poley A., Ghoreychi M., Heusermann S., Gens A., Olivella S.** (1999) *Backfilling and Sealing of Underground Repositories for Radioactive Waste in Salt.* (BAMBUS PROYECT) Final Report. European Commision. Nuclear Science and Technology

**Beghin C.** (1997) *European and international standards regarding radioactive waste disposal.* Nuclear Engineering and Design. Vol. 176 Issues 1-2. 121-139

**Cantlon J.E.** (1997) *Nuclear waste management in the US: The Nuclear Waste Technical Review Board's perspective*. Nuclear Engineering and Design. Vol. 176 Issues 1-2. 111-120

**Castagna S., Olivella S., Lloret A.** and **Alonso E.E.** (1998): *Experimental and Numerical Behaviour of Salt Aggregates due to Temperature Gradients*. Contribuciones 5th International Workshop on Key Issues in Waste Isolation Research. E. ALONSO, A. GENS, 100-110

**Castagna S., Olivella, S., Lloret, A.** and **Alonso, E.E**. (2000): *Experimental and Numerical Investigation of Porosity Variations in Saline Media Induced*

*by Temperature Gradients*. Theory and application of transport in porous media. Computational methods for flow and transport in porous media. J.M. Crolet editor Kluwer Academic Publisher, 327-338.

**Castagna S.** and **Olivella, S.** (2001): *Sensibility analysis of "parameters" in modelling the salt aggregates by CODE_BRIGHT for thermo hydraulic problems*. Internal Report, 1-20.

**Chumbe D.** (1996): *Rheological and fluid transport properties of compacted granular halite.* PhD Thesis. Department of Geotechnical Engineering and Geosciences. Universitat Politecnica de Catalunya

**Chumbe D., Lloret A.** and **Alonso E.E.** (1996) *Oedometric tests and permeability measurements on compacted granular salt.* International Symposium on Enviromental Geotechnology. IS-OSAKA.

*CODE-BRIGHT User's Manual.* (2004) Department of Geotechnical Engineering and Geosciences. Universitat Politecnica de Catalunya

**DBE** (1995): *Endlager und Deponienprojekte Weltweit",* DBE, Peine.

**Davison J.M., Stone L.R., Nielsen D.R.** and **Larue M.E.** (1969): *Field measurement and use of soil-water properties.* Water Resources Res. Vol nº5 1312-1321

**Delahaye C.** and **Alonso E.E.** (1998): *Soil heterogeneity and preferential paths for gas migration.* Proceedings of Progress meeting held in Naantali (PEGASUS Proyect) 227-2258

**Dyer J.R.** and **Voegele M.D.** (1996): *High-level Radioactive Waste Management in the United States Background and Status: 1996.* Second Worldwide Review in on Nuclear Waste. 259-270

**Droste J., Feddersen H.K., Rothfuchs T.** and **Zimmer U.** (1996): The TSS Project: *Thermal Simulation of Drift Emplacement*, GRS Report.

**Dublyansky Y.V., Smirnov S.Z.** and **Pashenko S.E.** (2003): *Identification of the deep-seated component in paleo fluidscirculated through a potential nuclear waste disposal site: Yucca Mountain, Nevada, USA.* Journal of Geochemical Exploration. Volume 78-79, 39-43.

**Dullien F.A.L.** (1979): *Porous media. Fluid transport and pore structure.* New York: Academic Press

**Edlefson N.E.** and **Anderson A.B.C.** (1943): *Thermodynamics of soil moisture*. Hilgardia, 15(2): 31-298.

**Ericsson L.O.** (1999) *Geoscientific R&D for high level radioactive waste disposal in Sweden current status and future plans.* Engineering Geology Volume 52 Issues 3-4 305-317

**Faust C.R.** and **Mercer J.W.** (1979): *Geothermal Reservoir Simulation: 1. Mathematical Models for Liquid and Vapour Dominated Hydrothermal* Systems, Water Resources Research, vol. 15, N° 1 23-30.

**Grahn P.G.** and **Skogsberg M.**.(2005) *The experience of interim storage of spent nuclear fuel and disposal of radioactive waste in Sweden.* European Nuclear Conference. Versailles December 2005. On press.

**Kaul A.** and **Röthemeyer H.** (1997) *Investigation and evaluation of the Gorleben site: a status report.* Nuclear Engineering and Design. Vol. 176 Issues 1-2. 83-88

**Kickmaier W., Vomvoris S., Mckinley I.G.** and **Alexander W.R.** (2005) *Grimsel Test Site: challenges for the 21$^{th}$ Century and beyond.* European Geologist nº 19. 19-22

**Korthaus E.** (1996): *Consolidation and Deviatoric Deformation Behaviour of Dry Crushed Salt at temperatures Up to 150 ºC*. Mechanical Behaviour of Salt IV, Trans Tech Publications, 365-379.

**Kovacs G.** (1981) *Seepage Hydraulics"* Elsevier Scientific Publishing Company.

**Lambe T.W.** and **Whitman R.V.,** (1969): *Soil Mechanics.* John Wiley and Sons Inc.

**Lange A.R.G.** (1967): *Osmotic coefficients and water potentials of Sodium Chloride solutions from 0 to 40 degree C* Australian Journal of Chemistry vol 20 2017-2023.

**Langer M.** and **Röthemeyer H.**, (1996): *Geoscientific and Rock Mechanical Activities for the Radioactive Waste Repositories in Germany: Key Issues, Status and Future Plans.* Second Worldwide Review in on Nuclear Waste. 105-112

**Langer H.** and **Offermann H.**, (1982): *On the solubility of Sodium Chloride in water*, Journal of Crystal Growth 60: 389-392. . Lewis, R.W.,.P.J. Roberts, B.A.

**Lloret A.** and **Alonso E.E.** (1980): *Consolidation of unsaturated soils including swelling and collapse behaviour* Geotechnique vol 30 nº4 449-477

**Lloret A.** (1993): *Métodos de medida y aplicación de succión en el laboratorio*. *La zona no saturada y la contaminación de las aguas subterráneas*. 1 ed.: CIMNE. 127-143.

**Matting A.** (1997) *Regulatory control of the German radioactive waste management system.* Nuclear Engineering and Design. Vol. 176 Issues 1-2. 141-144

**McEwen T.** and **Äikäs T.** (2000) *The site selection process for a spent fuel repository in Finland. Summary report.* POSIVA 2000-15 Report. 224 pages.

**McKinley I.G.** and **McCombie C.** (1996) *High Level Radioactive Waste Management in Switzerland: Background and Status 1995.* Second Worldwide Review in on Nuclear Waste. 223-231

**Nield D.A.** and **Bejan A.** (1999): *Convection in porous media.* (2nd edition). Springer.

**Oldecop, L. A.** and **Alonso E.E.** (2001): *A model for rockfill compressibility*. Géotechnique, Vol. 51 Nº 2 127-139

**Olivella S., Gens A., Carrera J.,** and **Alonso E.E.** (1993): *Behaviour of Porous Salt Aggregates. Constitutive and Field Equations for a Coupled Deformation, Brine, Gas and Heat Transport Model*. Mechanical Behaviour of Salt III, Trans Tech Publications, 269-284.

**Olivella S., Carrera J., Gens A.** and **Alonso E.E.** (1994a): *Non-isothermal Multiphase Flow of Brine and Gas through Saline Media*. Transport in Porous Media 15:271-293.

**Olivella S., Carrera J., Gens A., Alonso E.E.** (1994b): *Nonisothermal Multiphase Flow of Brine and Gas Thorough Saline Media*. Numerical aspects. Joumées Numériques de Besanon Computational Methods for Transport in Porous Media, Ed. by J .M. Crolet, 131-150.

**Olivella S.,** (1995): *Nonisothermal multiphase flow of brine and gas through saline media.* PhD Thesis. Department of Geotechnical Engineering and Geosciences. Universitat Politecnica de Catalunya.

**Olivella S., Carrera J., Gens A.** and **Alonso E. E.**, (1996a): *Numerical Formulation for a Simulator* (CODE_BRIGHT) *for the Coupled Analysis of Saline Media*. Engineering Computations, Vol 13, No 7, 87-112

**Olivella S., Carrera J., Gens A.** and **Alonso E. E.** (1996b): *Porosity Variations in Saline Media Caused by Temperature Gradients Coupled to Multiphase Flow and Dissolution/Precipitation* Transport in Porous Media, VOL 25: 1-25.

**Olivella S.** and **Gens A.** (2002) *A Constitutive Model for Crushed Salt.* International Journal for Numerical and Analytical Methods in Geomechanics nº 26 719-746.

**Ortí F., Busquets P., Pueyo J., Riba O., Rosell L., Saez A., Salas R., and Taberner C.,** "*Evaporite Deposition and Diagenesis in the Saline Catalan Basin, Upper Eocene*" Excursion Nº. 1, Faculty of Geology, University of Barcelona, Barcelona, 1990.

**Panday S**. and **Corapcioglu M. Y.** (1989): *Reservoir Transport Equations by Compositional Approach*, Transport in Porous Media 4, 369-393.

**POSIVA** (2005). *Olkiluoto Site Description 2004.* Posiva Report 2005-03. nº 3 volumes. 444 pages.

**Ridley A.M.** (1993): *The measurement of soil moisture suction.* PhD Thesis. University of London.

**Ridley A.M.** and **Burland J.B,** (1993): *A new instrument for the measurement of soil moisture suction.* Geotechnique Vol. Nº 43/2 321-324

**Ridley A.M.** and **Wray W.K.** (1996): *Suction measurement: A review of current theory and practices.* Unsaturated Soils, Alonso & Delange editors. Paris 1996. p. 1293-1322

**Ridley A.M.** (1995): *Discussion on "Laboratory filter paper suction measurement".* By Houston et al. Geotechnical Testing Jornal, 18 391-396.

**Romero E.,** (1999): *Characterisation and Thermo-hidro-mechanical behaviour of unsaturated boom clay: an experimental study.* PhD Thesis. Department of Geotechnical Engineering and Geosciences. Universitat Politecnica de Catalunya

**Sanchez M.,** (2004): *Thermo-Hydro-Mechanical coupled analysis in low permeability media.* PhD Thesis. Department of Geotechnical Engineering and Geosciences. Universitat Politecnica de Catalunya.

**Sattler P.** and **Fredlund D.G.** (1989): *Use of thermal conductivity sensors to measure matric suction in the laboratory.* Canadian Geotechnical Journal Vol. Nº 26 491-498.

**Schimidt M.W., Kolditz H.** and **Staupendahl G.** (1980) *Construction of a prototype-cavern in the decommissioned Asse salt-mine in support of research and development efforts in the field of storage of radioactive wastes* (In German). International Journal of Rock Mechanics and Mining Science Geomechanics Abstracts. Volume 17. Issue 5. 86

**Sharp J.M. Jr.** (1999): *A glossary of hydrogeological terms.* Department of Geological Sciences, The University of Texas, Austin, Texas.

**Sjöland K.A.** (2005) *Present Status of the Äspö Hard Rock Laboratory.* Internal Report from the SKB web site.

**Sjöland K.A.** and **Bockgärd N.** (2006) *Present Status of the Äspö Hard Rock Laboratory.* International High-Level Radioactive Waste Management Conference April 30 - May 4, 2006. Las Vegas, USA. On press.

**Slabaugh W.H.,** and **Parsons T.D.** (1966): *General Chemistry* John Wiley and Sons Inc.

**Soeiro F.** (1964) *Contribution à l'étude du mouvement de l'humidité dans les milieux poreux isothermes*. Cahier de la recherche, 18. Eyrolles, Paris.

**Spiers C.J., P.M.T.M. Schutjens, R.H. Brzesowsky, C.J. Peach, J.L Liezenberg,** and **H.J. Zwart (**1990): *Experimental determination of constitutive parameters governing creep of rocksalt by pressure solution, Deformation Mechanisms, Rheology and Tectonics.* Geological Society Special Publication nº 54; 215-228.

**Sprackling M. T.,** (1985): *Liquids and Solids*, Student Physics Series, King's College, University of London. Eds. Routledge and Kegan Paul.

**Thury M.** and **Bossart P.** (1999) *The Mont-Terri rock laboratory, a new international research project in a Mesozoic shale formation, in Switzerland.* Engineering Geology nº 52. 347-359

**Thury M.** (1997) *The Mont-Terri rock laboratory.* Nagra Report nº 31. 33-44

**Tonhauser W.** and **Jankowitsch-Prevor O.**, (2006): *The Joint Convention on the Safety of Spent Fuel Management and on the Safety of Radioactive Waste Management,* OECD. On press.

**van Genuchten R**., (1980): *Closed-form equation for predicting the hydraulic . conductivity of unsaturated soils*, Soil Sci. Soc. Am. J .: 892-898.

**Van Geet M., Swennen R.** and **Wersen M.** (2000) *Quantitative analysis of reservoir rocks by microfocus x-ray computerised tomography.* Sedimentary Geology vol. 132 25-36

**Vira J** (1996) *Disposal of High-Level Radioactive Waste in Finland.* Second Worldwide Review in on Nuclear Waste. 87-93

**Vomvoris S., Kickmaier W.** and **McKinley I.** (2004). *Grimsel Test Site: 20 years of research in fracturated crystalline rocks – experience gained and future needs.* Proceedings of the second international symposium on Dynamic of fluid in fracturated rock. Lawrence Berkeley National Laboratory. Witherspoon PA editors 14-18

**Woodburn J.A.** and **Lucas B.** (1995): *New approaches to the laboratory and field measurement of soil suction.* Unsaturated Soils, Alonso & Delange editors. Paris 1996